Forschungsbericht 2022-14

Flight Test Techniques and the Influence on Rotorcraft Handling Qualities during Isometric Failures of Active Sidesticks

Miles Philip Conrad Barnett

Deutsches Zentrum für Luft- und Raumfahrt
Institut für Flugsystemtechnik
Braunschweig

Deutsches Zentrum
DLR für Luft- und Raumfahrt

Forschungsbericht 2022-14

Flight Test Techniques and the Influence on Rotorcraft Handling Qualities during Isometric Failures of Active Sidesticks

Miles Philip Conrad Barnett

Deutsches Zentrum für Luft- und Raumfahrt
Institut für Flugsystemtechnik
Braunschweig

273 Seiten
129 Bilder
68 Tabellen
126 Literaturstellen

DLR Deutsches Zentrum für Luft- und Raumfahrt

Herausgeber:

Deutsches Zentrum
für Luft- und Raumfahrt e. V.
Wissenschaftliche Information
Linder Höhe
D-51147 Köln

ISSN 1434-8454
ISRN DLR-FB-2022-
Erscheinungsjahr 2022

DOI: https://doi.org/10.57676/06q9-fs05

Hubschrauber, aktive Steuerorgane, Isometrische Steuerungsfehler, Erprobungsmanöver, Flugregelung, Flugeigenschaften, ACT/FHS, aircraft-pilot coupling

Miles Philip Conrad BARNETT
DLR, Institut für Flugsystemtechnik, Braunschweig

Flugtesttechniken und die Auswirkungen auf die Flugeigenschaften von Hubschraubern bei isometrischen Ausfällen von aktiven Sidesticks

Dissertation, Technische Universität Carolo-Wilhelmina zu Braunschweig

Das Ziel dieser Arbeit war es, sowohl eine Methode zu entwickeln, um die HQs unmittelbar nach einem isometrischen AIS-Fehler zu quantifizieren als auch Lösungen zur Minderung potentieller Verschlechterungen zu identifizieren.

Mithilfe eines im Rahmen dieser Arbeit entwickelten Erprobungsmanövers (engl. Mission Task Element, MTE) in Kombination mit subjektiven und quantitativen Bewertungskriterien konnten die Flugeigenschaften und die Schwingungstendenzen, welche während eines isometrischen AIS-Fehlers auftreten, bewertet werden. Zukünftig könnte diese Bewertungsmethode für die Zertifizierung verwendet werden, um den Erfolg einer Fehlerminderungslösung zu bewerten. Die Bewertungsmethode aus MTE und Bewertungskriterien war darüber hinaus in der Lage, einen großen Bereich von HQ- und APC-Schweregraden aufzudecken und war sensibel gegenüber den erprobten Variationen. Diese Eigenschaften erleichterten die Verwendung der Bewertungsmethoden bei der Optimierung der Flugsteuerungsparameter, um die HQs nach einem Ausfall des AIS zu verbessern.

Nach Optimierung eines Filters der ersten Ordnung konnte eine große Verbesserung der Flugeigenschaften erreicht werden. Dagegen zeigten die getesteten Konfigurationen der zeitbasierten Rampenerhöhung weder Vorteile noch Nachteile. Vorteilhaft waren auch der Einsatz eines Flugreglers mit Lagestabilisierung (Attitude Command), als auch Training und Erfahrung. Beides führte zu einer erheblichen Minderung der HQ-Probleme nach einem AIS-Ausfall. Während die optimierten Filterparameter und Ergebnisse hubschrauberspezifisch sind, lässt sich die hier entwickelte Methode auch auf andere Hubschrauber anwenden.

Rotorcraft, Active Inceptor, Mission Task Element, Isometric Control Failure, Flight Control, Handling Qualities, ACT/FHS, Phase-aggression Criteria, Aircraft-Pilot Coupling

(Published in English)

Miles Philip Conrad BARNETT
German Aerospace Center (DLR), Institute of Fight Systems, Brunswick

Flight Test Techniques and the Influence on Rotorcraft Handling Qualities during Isometric Failures of Active Sidesticks

Doctoral Thesis, Technical University Carolo-Wilhelmina zu Braunschweig

The objective of this study has been to develop a method to quantify the handling qualities immediately after an isometric active inceptor failure and to identify solutions to mitigate the degradations.

Using a Mission Task Element (MTE) developed within this study in combination with the subjective Integrated Failure Evaluation Scale (IFES), the Aircraft-Pilot Coupling (APC) rating scale and the Phase-Aggression Criteria (PAC) analysis tool it was possible to assess the HQ and APC tendency during an isometric AIS failure. In its broadest function the application of this integrated assessment method could be used as a certification specification to establish the success of a failure mitigation solution. However, the structure of the MTE was also able to expose a wide range of HQ and APC severities and the fidelity of the rating scales was able to distinguish between the corresponding small HQ variations. These characteristics facilitated the use of the assessment methods in the optimisation of flight control parameters to improve the post-failure HQ.

An optimized configuration of a first order filter was identified that offered significant HQ benefits, however the tested configurations of a time based ramp attenuator presented neither benefit nor detritment. The employment of both the attitude command and previous isometric training and experience presented substantial mitigation to the post-failure HQ. Whilst these solutions have shown some success, the search of an optimum has neither been exhaustive nor would any identified solution be applicable to all helicopter and AIS permutations. However, the assessment method and optimisation process have both been proven to be effective and could by used directly in future more specific applications.

TU Braunschweig – Niedersächsisches

Forschungszentrum für Luftfahrt

Berichte aus der Luft- und Raumfahrttechnik

Forschungsbericht 2022-15

Flight Test Techniques and the Influence on Rotorcraft Handling Qualities during Isometric Failures of Active Sidesticks

Miles Philip Conrad Barnett

Deutsches Zentrum für Luft- und Raumfahrt

Institut für Flugsystemtechnik

Braunschweig

Diese Veröffentlichung wird gleichzeitig in der Berichtsreihe „NFL - Forschungsberichte“ geführt.

Diese Arbeit erscheint gleichzeitig als von der Fakultät für Maschinenbau der Technischen Universität Carolo-Wilhelmina zu Braunschweig zur Erlangung des akademischen Grades eines Doktor-Ingenieurs genehmigte Dissertation.

Flight Test Techniques and the Influence on Rotorcraft Handling Qualities during Isometric Failures of Active Sidesticks

Von der Fakultät für Maschinenbau
der Technischen Universität Carolo-Wilhelmina zu Braunschweig

zur Erlangung der Würde
eines Doktor-Ingenieurs (Dr.-Ing.)
genehmigte Dissertation

von:	Miles Philip Conrad Barnett
geboren in:	Harrogate, North Yorkshire, Vereinigtes Königreich

eingereicht am:	22.03.2021
mundliche Prufung am:	12.01.2022

Vorsitz:	Prof. Dr.-Ing C Rossow
Gutachter:	Prof. Dr.-Ing. S Levedag
	Prof. Dr.-Ing. P Hecker

2022

“When everything seems to be going against you, remember that the airplane takes off against the wind, not with it” –
Henry Ford

Abstract

The emerging presence of Active Inceptor Systems (AIS) in helicopter cockpits has brought many advantages in tactile cueing and adaptive mechanical characteristics that are capable of improving handling qualities (HQ). However, their expansion from research studies into the development of production aircraft, combined with their safety critical function has brought more attention to dealing with their failures. Previous research has identified two plausible AIS failure modes that cause either the force free isotonic state which utilises the position signal for aircraft control or the fixed position isometric state which uses the inceptor force signal for control. Whilst there have been investigations of both transient and long term effects of the isotonic as well as the long term effects of the isometric mode, until now there has been very little research into the transient and recovery phases of isometric failures.

The objective of this study has been to develop a method to quantify the HQ immediately after an isometric AIS failure and to identify solutions to mitigate the degradations.

Using a Mission Task Element (MTE) developed within this study in combination with the subjective Integrated Failure Evaluation Scale (IFES), the Aircraft-Pilot Coupling (APC) rating scale and the Phase-Aggression Criteria (PAC) analysis tool it was possible to assess the HQ and APC tendency during an isometric AIS failure. In its broadest function, the application of this integrated assessment method could be used as a certification specification to establish the success of a failure mitigation solution. However the structure of the MTE was also able to expose a wide range of HQ and APC severities and the fidelity of the rating scales was able to distinguish between the corresponding small HQ variations. These characteristics facilitated the use of the assessment methods in the optimisation of flight control parameters to improve the post-failure HQ.

A number of viable mitigation solutions were identified of which four were investigated further: a first order filter applied to the inceptor force signal; a ramp increase of gain with respect to time applied to the inceptor force signal; two alternative command types and substantial previous isometric training and experience. An optimised configuration of the first order filter was identified that offered significant HQ benefits, however the tested configurations of ramp attenuator presented neither benefit nor detriment. The employment of both the attitude command and previous isometric training and experience presented substantial mitigation to the post-failure HQ. Whilst these solutions have shown some success, the search for an optimum has neither been exhaustive nor would any identified solution be applicable to all helicopter and AIS permutations. However, the assessment method and optimisation process have both been proven to be effective and could be used directly in future more specific applications.

As the entirety of this study was conducted in the DLR AVES simulator, the appropriate next stage would be to validate the conclusions in flight. Recommended further research would be the adaptation of the ramp gain model; development of an automatic failure initiation system and the application of the isometric MTE in the isotonic failure mode.

Kurzfassung

Die zunehmende Präsenz von aktiven Steuerorganen (AIS) im Hubschrauber-Cockpit beinhaltet viele Vorteile, wie etwa haptisches Feedback (eng. tactile cueing) und der Optimierung der adaptiven mechanischen Eigenschaften zur Verbesserung der Flugeigenschaften (eng. Handling-Qualities, HQs). Der Übergang von der Forschung in die Verwendung im Serienhubschrauber hat jedoch die Aufmerksamkeit auf sicherheitskritische Funktionen des AIS und die Behandlung möglicher Ausfälle gelenkt. Frühere Untersuchungen haben die beiden plausiblen Fehlerfälle untersucht, bei dem das AIS durch den Ausfall des Antriebs entweder völlig kraftfrei (isotonisch) oder durch eine Blockade des Antriebs unbeweglich (isometrisch) ist. In letzterem Fall kann der Hubschrauber durch die gemessenen Steuerkräfte gesteuert werden. Bisher wurden jedoch nur sehr wenige Untersuchungen zur Transienten Phase unmittelbar nach Auftreten eines isometrischen Fehlers und der darauf folgenden Wiedererlangung der Steuerfähigkeit durchgeführt.

Das Ziel dieser Arbeit war es daher, sowohl eine Methode zu entwickeln, um die HQs unmittelbar nach einem isometrischen AIS-Fehler zu quantifizieren als auch Lösungen zur Minderung potentieller Verschlechterungen zu identifizieren.

Mithilfe eines im Rahmen dieser Arbeit entwickelten Erprobungsmanövers (eng. Mission Task Element, MTE) in Kombination mit subjektiven und quantitativen Bewertungskriterien konnten die Flugeigenschaften und die Schwingungstendenzen, welche während eines isometrischen AIS-Fehlers auftreten, bewertet werden. Zukünftig könnte diese Bewertungsmethode für die Zertifizierung verwendet werden, um den Erfolg einer Fehlerminderungslösung zu bewerten. Die Bewertungsmethode aus MTE und Bewertungskriterien war darüber hinaus in der Lage, einen großen Bereich von HQ- und APC-Schweregraden aufzudecken und war sensibel gegenüber den erprobten Variationen. Diese Eigenschaften erleichterten die Verwendung der Bewertungsmethoden bei der Optimierung der Flugsteuerungsparameter, um die HQs nach einem Ausfall des AIS zu verbessern.

Es wurden eine Anzahl von praktikablen Mitigationslösungen identifiziert, von denen vier weiter untersucht wurden: ein Filter erster Ordnung, mit dem das AIS-Kraftsignal gefiltert wurde; ein Rampenerhöhung der Verstärkung des AIS-Kraftsignals über Zeit; zwei alternative Reglermodi und umfangreiche Erfahrung durch vorheriges Training mit der isometrischen Steuerung. Nach Optimierung des Filters der ersten Ordnung konnte eine große Verbesserung der Flugeigenschaften erreicht werden. Dagegen zeigten die getesteten Konfigurationen der Rampenerhöhung weder Vorteile noch Nachteile. Vorteilhaft waren auch der Einsatz eines Flugreglers mit Lagestabilisierung (Attitude Command), als auch Training und Erfahrung. Beides führte zu einer erheblichen Minderung der HQ-Probleme nach einem AIS-Ausfall. Während die optimierten Filterparameter und Ergebnisse hubschrauberspezifisch sind, lässt sich die hier entwickelte Methode auch auf andere Hubschrauber anwenden.

Da alle Versuche dieser Studie im DLR-AVES-Simulator durchgeführt wurden, müssten die Schlussfolgerungen als nächstes im Flug validiert werden. Andere Erweiterungen dieser

Forschung könnten die Anpassung der Rampenerhöhung, die Entwicklung eines automatischen Fehlerinitiierungssystems und die Anwendung des isometrischen MTE im isotonischen Fehlermodus sein.

Acknowledgements

The journey of conducting this doctoral research and writing the dissertation involved the help and understanding of many people who gave their time and support generously. I take this opportunity here to acknowledge each of those who have helped me and had a positive influence on the outcome of this work.

Firstly, I wish to thank to Prof Dr Stefan Levedag, Prof Dr Peter Hecker, Prof Dr Christoph Keßler and Marc Höfinger for their individual knowledge, guidance and expert support as well as for facilitating the resources provided by the Institute of Flight Systems of the German Aerospace Centre (DLR).

There are numerous colleagues with whom I work within the Institute of Flight Systems and Flight Experiments that have directly or indirectly supported me and to whom I collectively wish to express my thanks. Specifically within the Institute of Flight Systems, Dr Mike Jones and Mario Müllhäuser contributed tremendously to my understanding of the subject and of the technical aspects of the research equipment. Our conversations were always insightful and the application of their knowledge proved invaluable for the completion of the study. Within Flight Experiments, I wish to thank Martin Gestwa, Sebastian Soffner, Uwe Göhmann and Elizabeth Buron who have all shown understanding and tolerance to the time that I have taken to write this dissertation.

Without any doubt this dissertation would not have been possible if it were not for my wife, Maike who was not only tirelessly supportive of my objective but also maintained normality within the rest of our lives during some long days. Her own PhD has been a constant source of admiration and motivation for me and our frequent discussions regarding research hurdles have always offered empathy, encouragement and solutions for progress.

I am also extremely grateful to my parents, Nigel and Christine who always supported and encouraged me in whatever I did, usually at their stressful, financial or emotional expense; and my children, Anna, Ben and Tom who showed absolutely no interest in this research but have kept me sufficiently distracted from it, bring fun to our lives and make me proud every single day.

Finally, I thank all of the test pilots that were involved with study: David Marsden, Rodolfo dos Santos Sampaio, Hamdy Sallam, Richard Pillans and Guy Butler. Their friendship and professionalism are valued in equal measure.

Contents

List of Figures

List of Tables

Nomenclature

A	Ramp attenuator gradient (s^{-1})
A_G	Inceptor Aggression ($°s^{-2}$ - Rate Command); ($°s^{-1}$- attitude Command)
AR	Amplitude Ratio (-)
D	Dimensionless damping, Damping Ratio, Relative Damping (-)
$\dot{F}$	Rate of Inceptor Force (Ns^{-1})
$F_{\theta 1C}$	Lateral Inceptor Force (N)
$F_{\theta 1S}$	Longitudinal Inceptor Force (N)
H_s	Displacement Control Power Factor ($°\%^{-1}s^{-1}$ - Rate Comd); ($°\%^{-1}$- Att. Comd)
H_{sF}	Force Control Power Factor ($°N^{-1}\ s^{-1}$ - Rate Comd); ($°N^{-1}$- Att. Comd)
j	Imaginary Unit $\sqrt{-1}$
k	Gain (-) or Force Gradient ($N\%^{-1}$)
K_D	Differential Gain
K_I	Integral Gain
K_P	Proportional Gain
m	Equivalent mass in a Mass-Spring-Damper System (kg)
p	Roll rate ($°s^{-1}$ or $rads^{-1}$)
q	Pitch rate ($°s^{-1}$ or $rads^{-1}$)
s	Laplace Operator (-)
t_1	Start Time of Current Oscillation (s)
t_2	End Time of Current Oscillation (s)
V_{NE}	Never Exceed Indicated Airspeed (kt)
V_{TOSS}	Take Off Safety Airspeed (kt)
V_{AUTO}	Maximum IAS in Autorotation (kt)
V_{MIN-IF}	Minimum IAS with Sole Reference to Cockpit Instruments (kt)
V_Y	Min power IAS or Lateral IAS (kt)
$\dot{\delta}$	Rate of Inceptor Displacement ($\%s^{-1}$)
δ_{1C}	Lateral Inceptor Displacement (%)
δ_{1S}	Longitudinal Inceptor Displacement (%)
δ_{1S-AC}	Longitudinal Inceptor Displacement with Attitude Command (%)
δ_{1s-RC}	Longitudinal Inceptor Displacement with Rate Command (%)
τ	Time Constant (s)
τ_P	Phase Delay (s)
ω	Forced Frequency ($rads^{-1}$ or Hz)
ω_0	Natural or Eigen Frequency ($rads^{-1}$ or Hz)
ω_{180}	Crossover Frequency ($rads^{-1}$ or Hz)
$\omega_{BW-Gain}$	Gain Limited Bandwidth ($rads^{-1}$ or Hz)
$\omega_{BW-Phase}$	Phase Limited Bandwidth ($rads^{-1}$ or Hz)
$\Delta\phi_{2\omega_{180}}$	Phase difference between ω_{180} and $2\omega_{180}$ (°)
θ	Pitch attitude (° or rad)
$\emptyset$	Roll attitude (° or rad)
Φ	Phase (rad or °)

Acronyms

AC	Attitude Command
ACS	Active Control System
ACT/FHS	Active Control Technology / Flying Helicopter Simulator
ADS	Aeronautical Design Standard
AFDD	Aeroflightdynamics Directorate (US Army)
AG	Apparent Gain
AGARD	Advisory Group for Aerospace and Development
AGL	Above Ground Level
AHRS	Attitude and Heading Reference System
AIS	Active Inceptor System
ANSV	Agencia Nazionale per la Sicurezza del Volo
APAS	Active Parallel Actuator Subsystem
APC	Aircraft Pilot Coupling
APCR	Aircraft Pilot Coupling Rating
AR	Amplitude Ratio
ASRA	Advanced Systems Research Aircraft
ATIC	Advanced Technology Institute of Commuter
AVES	Air Vehicle Simulator
CDU	Control and Display Unit
CHR	Cooper Harper Rating
COS	Core System / Cockpit-Schnittstellengerät (Cockpit Interface Control Unit)
CPU	Central Processing Unit
CS	Certification Standard
CS-27	Certification Specification for Small Rotorcraft
CS-29	Certification Specification for Large Rotorcraft
DC	Direct current
DLR	Deutsches Zentrum für Luft- und Raumfahrt (German Aerospace Centre)
DMC	Data Management Computer
DVE	Degraded Visual Environment
EASA	European Union Aviation Safety Agency
EC	Experimental Computer
FAA	Federal Aviation Administration (US)
FADEC	Full Authority Digital Engine Control
FBL	Fly-by-Light
FBW	Fly-by-Wire
FCMC	Flight Control Mechanical Characteristics
FCS	Flight Control System
FMEA	Failure Mode and Effects Analysis
FRP	Finger Reference Point
FRR	Failure Recovery Rating
FTE	Flight Test Engineer
FTI	Flight Test Instrumentation
FW	Fixed Wing

FWD	Forward
GSR	Global Success Rate
GUI	Graphical User Interface
GVE	Good Visual Environment
HQ	Handling Qualities
HQR	Handling Qualities Rating (equivalent to CHR)
IAS	Indicated Air Speed
IFES	Integrated Failure Evaluation Scale
IFR	Instrument Flight Rules
IR	Infra-Red
LHSS	Left Hand Sidestick
LIDAR	Light Detection and Ranging
MAA	Military Aviation Authority (UK); Military Airworthiness Authority (US)
MTE	Mission Task Element
NASA	National Aeronautics and Space Administration
NRC	National Research Council (Canada)
OFE	Operational Flight Envelope
OGE	Outside Ground Effect
OLOP	Open Loop Operating Point
OLP	Optical Line Pair
ONERA	l'Office National d'Ētudes et de Recherches Aérospatiales (The French Aerospace Lab)
PAC	Phase Aggression Criteria
PFR	Post Flight Report
PID	Proportional – Integral – Differential Controller
PIO(R)	Pilot Induced Oscillation (Rating)
PIS	Passive Inceptor System
PIW	Pilot Inceptor Workload
PRT	Pilot Response Time
RASCAL	Rotorcraft-Aircrew Systems Concepts Airborne Laboratory
RC	Rate Command
RFM	Rotorcraft Flight Manual
RHSS	Right Hand Sidestick
ROVER	Real Time Oscillation Verifier
RPM	Revolutions Per Minute
RRT	Rotorcraft Response Time
RW	Rotary Wing
SAE	Society of Automotive Engineers
SFE	Service Flight Envelope
SIMDUCE	Simulated Day Useable Cues Environment
SOIU	Statement of Operating Intent and Usage
TCDB	Trim Control Displacement Band
UCE	Useable Cue Environment
VCR	Visual Cue Rating
VFR	Visual Flight Rules

Chapter 1: Introduction

1.1 Context

Active inceptor systems (AIS) exploit the tactile sensory channel to assist the pilot with awareness and cueing. Unlike the Passive Inceptor Systems (PIS) commonly found in fly-by-wire aircraft, the inceptor control forces are generated by servo actuators and thus can be modified in real time. The potential uses of such a capability include pilot guidance in selecting a desired angle of bank [1], tactile cueing for obstacle avoidance [2, 3] and assistance in identifying engine torque limits [4]. It has also been demonstrated in various studies that the handling qualities (HQ) of a helicopter could be optimised by AIS through adaption of the flight control mechanical characteristics (FCMC) to the aircraft dynamics [5]. Until recently, AIS in aircraft have been limited to demonstrators, however their implementation has become more evident in a number of new helicopter programs, such as the Bell-525 [6] and CH-53K [7]; upgrade programmes, such as Chinook CH-47F [8] and fixed wing production programmes such as the F-35 and Korean Aerospace Industries T-50 fighter [9]. There is little doubt that the technology has many benefits including improved safety through the various uses of tactile cues; greater pilot comfort [10]; reduced pilot workload and increased capability [4]. However, with their greater complexity relative to pure mechanical inceptors, comes an increased range of failure possibilities, all of which must be assessed to ensure that in these events safety of flight can be maintained.

The potential benefits for implementing AIS technology into the core system design of new helicopters are attractive to both manufacturers and operators; hence commentators are expecting to see their appearance in most future helicopter cockpits [11, 12]. There is also scope for AIS upgrades to existing helicopter designs, such as the Chinook CH-47[1] to expand the capability and safety.

There is currently a scarcity[2] of information regarding the failure testing of AIS as there are only a small number of capable research aircraft[3]. The ongoing development activity at competing manufacturers[4] has meant that most research is not publicly disseminated. However, as a direct consequence that the AIS technology in helicopters is novel, the potential for a design oversight or safety critical omission is higher than for conventional controls.

1.2 Motivation

The Johari window principle [13] originally evolved from human relations psychology to categorise how a subject is viewed by themselves and by others. It has since been

[1] Chinook models CH-47F Block II and CH-47G upgrade programme to be fitted with Active Parallel Actuator Subsystem (APAS) [11, 8]

[2] Other than research activity already conducted at DLR [14, 15] and discussed in chapter 2

[3] DLR EC135 ACT/FHS [16]; NRC Bell 412 Advanced Systems Research Aircraft (ASRA) [17]; NASA/AFDD UH-60M Rotorcraft Aircrew Systems Concept Airborne Laboratory (RASCAL) [18]; Kawasaki Heavy Industries BK117 Advanced Technology Institute of Commuter (ATIC) [19, 20, 21]

[4] Sikorsky, Bell and Boeing

developed for alternative purposes and a variant of it was made famous by Donald Rumsfeld during a press briefing on the Iraq war [22]. Table 1-1(a) presents the familiar version of the Johari window where the concept of awareness and knowledge are categorised into four boxes. Table 1-1(b) presents a variation on this concept that can be used in the understanding of safety risks throughout the development and subsequent operation of aviation systems and new technologies.

Awareness	Knowledge	
	1. Known, Knowns	2. Known, Unknowns
	3. Unknown, knowns	4. Unknown, Unknowns

Awareness of Hazards	Mitigations of Hazard	
	1. Hazards known; Adequate mitigations exist	2. Hazards known; Adequate mitigations absent
	3. Hazards unknown or partially known; Adequate mitigations exist	4. Hazards unknown or partially known; Adequate mitigations absent

Table 1-1: (a) The Johari Window Principle, (b) Johari Principle applied to Risk Mitigation

The Johari window defines four groups of risks in terms of whether the hazard itself is fully understood and whether the risk has been adequately mitigated against. In the first group the hazards are known and adequate mitigation has been prepared, for example an engine failure in a twin engine helicopter where the risk is continuously mitigated by operating outside of the single engine avoid curve. The second group defines the hazards that are known but there are inadequate or no mitigations. An example in this group is a tail rotor drive failure for which it is impossible to mitigate through redundancy and throughout the required flight envelope of a helicopter. The third group contains hazards that can be subdivided into the unknown and those that may be expected through past experience but have not been observed or fully understood. The mitigation of this group is often a result of good general engineering practices or even good fortune but in the

case where the risk is not fully comprehended, the mitigation may be intentional but over-cautious and therefore present other disadvantageous consequences (for example weight, restriction of flight envelope, cost or development time). An example of this was the early adoption of flight data symbology in helmet mounted displays in military helicopters where the risk of its failure was unknown. So that aircrew training and limited operations could continue, the system was released with an interim operational capability in which its use was limited to VFR[5] operations only.

The final group defines the hazards that are either not known or have not been fully understood and there is no adequate mitigation in place. By definition, this group offers the most concerns to designers, engineers and test crews but despite best efforts, history has shown that the inadequate prediction of some hazards has had tragic consequences.

In June 2016 an example of this occurred as a developmental Bell 525 helicopter was conducting single engine failure certification flight tests [23]. During the last planned test point the engine failure was initiated and the rotor speed decayed as expected, but due to the high IAS[6] of 185kt an aggressive vertical 6Hz vibration developed. The intensity of the vibration was driven by both the AHRS[7] response and through biomechanical feedback[8] of the sidestick collective control. As the vibration continued, the main rotor began to flap out of plane until it struck the tail boom. The aircraft broke up in-flight resulting in the loss of aircraft and crew (figure 1-1). The hazard of the severity of vertical vibrations at low rotor speed and high IAS and the influence of the AHRS and biomechanical feedback had not been predicted and had therefore not been mitigated against. Consequently, the accident would be classified in table 1-1 as category 4 – hazards unknown or partially known and adequate mitigations absent.

Figure 1-1: Bell 525 Helicopter (source: Bell Helicopters); Accident Scene (NBC 5 News)

In the development and introduction to service of a new technology the understanding of the safety risks is essential. Various methods are used to identify unknown hazards

[5] Visual Flight Rules
[6] Indicated Air Speed
[7] Attitude and Heading Reference System
[8] Unintentional control inputs resulting from involuntary pilot limb motions caused by aircraft accelerations

continuously throughout the testing, implementation and full service life of the system and to minimise their effects [24, 25].

However two of the most effective solutions for realising the extent of the unknown hazards is to learn from accidents or to conduct research that is capable of predicting an accident before it occurs. As knowledge is expanded the hazards are matched with appropriate mitigations and they move from the categories three and four into the categories one and two.

Civilian and military aviation authorities take on a lot of the responsibilities of confirming that an aircraft or system is safe to operate through the initial airworthiness Certification Specifications (CS) [26, 27]. The CS reflects only the current known hazards, but as more evidence is gained, it is amended to encompass the safe design requirements that mitigate the hazards from categories three and four. Research is not a primary responsibility of aviation authorities however and they are inadequately resourced for the deep and comprehensive research required. Whilst they support some research, they predominantly rely on the input from external research organisations, the development by the manufacturer and the safety recommendations from relevant accidents and incident reports.

In general, the more novel the new aircraft or system, the more hazards are located in the 'unknown or partially known' categories of table 1-1. This statement can be validated by considering the data presented in table 1-2[9].

Cause	Pre-certification				Post-certification			
	Crashes		Fatalities		Crashes		Fatalities	
	V-22	S-92	V-22	S-92	V-22	S-92	V-22	S-92
Systems / Technology	4	0	11	0	1	1	2	17
Other	1	0	19	0	6	2	9	4

Table 1-2: Comparison of Accidents, during pre- and post-certification: S-92 and V-22

Both the Boeing V-22 Osprey[10] battlefield support aircraft and the Sikorsky 2-92A[11] civilian transport aircraft were developed at a similar time and currently have a similar number of airframes in service. However the technologies incorporated in the V-22 including tilt rotor, wing and rotor folding capabilities and fly-by-wire were far more

[9] Crashes constitute an accident in which the aircraft is categorised beyond economic repair.

[10] Bell-Boeing V-22 testing and development 1991 to 2006; approximately 400 built (including MV-22, CV-22 and HV-22 derivatives)

[11] Sikorsky S-92 testing and development 1998 to 2002 (FAA) and 2004 (EASA); approximately 300 built (including H-92 and VH-92 derivatives)

novel, advanced and complex than the predominantly conventional S-92A. The differences in their respective roles may have accounted for some of the post-certification crashes, in particular those with a cause other than systems or technology. However, during the pre-certification phases of both aircraft, the V-22 suffered 5 crashes of which 4 had a main causal factor of aircraft systems or new technologies [28]. The system or technology causes of these crashes were the flight control system (FCS) hardware; inadequate engine fire resilience; FCS software and engine control hardware and all constituted unknown hazards with inadequate mitigations. In comparison the S-92A suffered no crashes throughout its entire development and pre-certification programme [29, 30].

Figure 1-2: Bell-Boeing V-22 (source: Boeing); Sikorsky S-92 (source: Lockheed Martin)

It is therefore clear that failure modes and associated risks of new technology, such as AIS, must be thoroughly understood. Only when this research has been exhaustively completed will the engineers and test crews have confidence that the number of unknown hazards have been minimised.

1.3 AIS Technology and Generic System Architecture

Cockpit controllers, or inceptors, for fly-by wire (FBW) aircraft can be classified into two main types. Passive controllers or PIS that maintain a constant relationship between the force applied and its displacement, and active controllers or AIS that feature variable force-displacement characteristics.

The PIS use inherent, mechanically created forces of mass, damping, spring gradients and friction that provide tactile cues to the pilot and improve the handling of the aircraft. The characteristics are established by design and generally cannot be changed in-flight either automatically by an aircraft system or by the pilot[12]. As the control signal is transmitted to the FCS by wire (as opposed to mechanical linkages) the designer has the flexibility to fit the cyclic inceptor either in the conventional location between the pilot's knees or as a right hand sidestick. There are numerous examples of certified aircraft that use FBW technology with passive controllers, including Concorde, the airbus fixed wing fleet from A318 to A380 [31] and the NH90 helicopter [32].

[12] For some helicopters the friction of the cyclic and collective inceptors can be adjusted by the pilot.

The AIS simulate the force displacement characteristics of a passive system, including damping, spring gradients and friction but also have the capability to change these characteristics in flight and to generate more complex characteristics such as detents, gates, steps, shakers and knocks [33, 2]. The potential for tactile cueing is vast and has provided an additional channel to pass information to the pilot in a clear yet intuitive manner. Examples of the research activity that has been conducted in helicopter tactile cueing are described in the research review, section 2.4.

An example of a simple force-displacement relationship for an AIS is shown in figure 1-3 in which the trim system freeplay, breakout forces, spring gradients, dynamic friction, static friction, trim control dead band, detents and gates are annotated [34]. Dynamic effects associated with damping and mass can also be simulated by an AIS but are not indicated on the force-displacement plot.

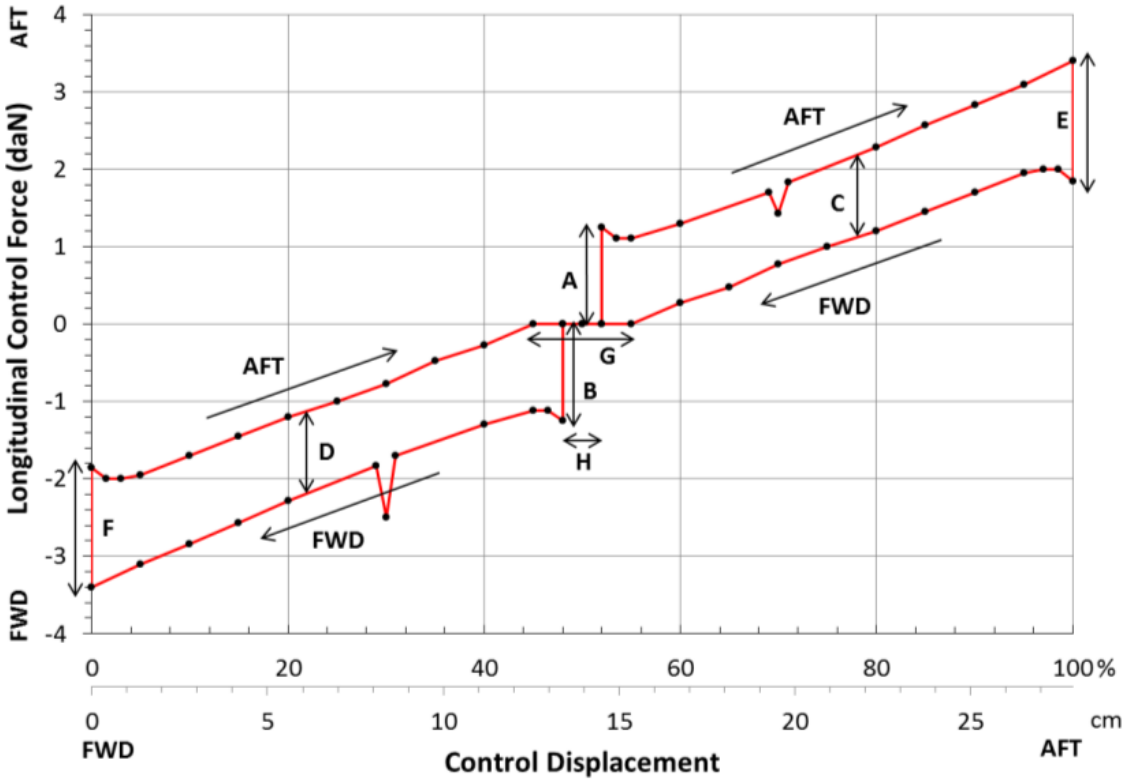

Legend			
A	Breakout + Static Friction Aft	B	Breakout + Static Friction Fwd
C	Twice Dynamic Friction Aft	D	Twice Dynamic Friction Fwd
E	Dynamic Friction Aft + Static Friction Forward (Fwd)	F	Dynamic Friction Fwd + Static Friction Aft
G	Trim Control Displacement Band	H	Trim System Freeplay
I	Gate Fwd	J	Detent Aft

Figure 1-3: Example of Force-Displacement Characteristics for a Compliant AIS

As with passive controllers, the cyclic inceptor can be fitted either in the conventional location or as a sidestick. A left sidestick can also be used either for the collective control alone or for both collective and pedal control axes.

The integral subsystems of an AIS are illustrated in Figure 1-4 [9]. The pilot force signal, measured by force sensors, is transmitted to an internal Central Processing Unit (CPU) which calculates the required stick deflections according to a control law. This law is a combination of a 'look up table' for direct force conversion that incorporates the characteristics of figure 1-3 and a mathematical second order transfer function that describes a mass, spring, damper system that simulate the dynamic characteristics. Any special features such as a stick shaker or knocker are also superimposed on to the position signal.

The stick's deflection is controlled by the motor drive electronics and electric servo actuators [9]. Position feedback sensors in each axis confirm that the actuators have functioned correctly and that the resulting deflection agrees with the demanded deflection. In the normal (compliant) mode of operation both position and force sensor signals are transmitted to the FCS via a digital bus, however it is usually the position sensor signal that is used for the FCS control input. The bus is also used as the conduit between the AIS and helicopter systems for other information such as real time initiation of special tactile cueing features, error and status messages, cyclic switches and buttons signals and in-flight modification of the AIS mechanical characteristics for research purposes.

A more detailed description of the cyclic AIS and its software laws that was used in this study can be found in chapter 3.

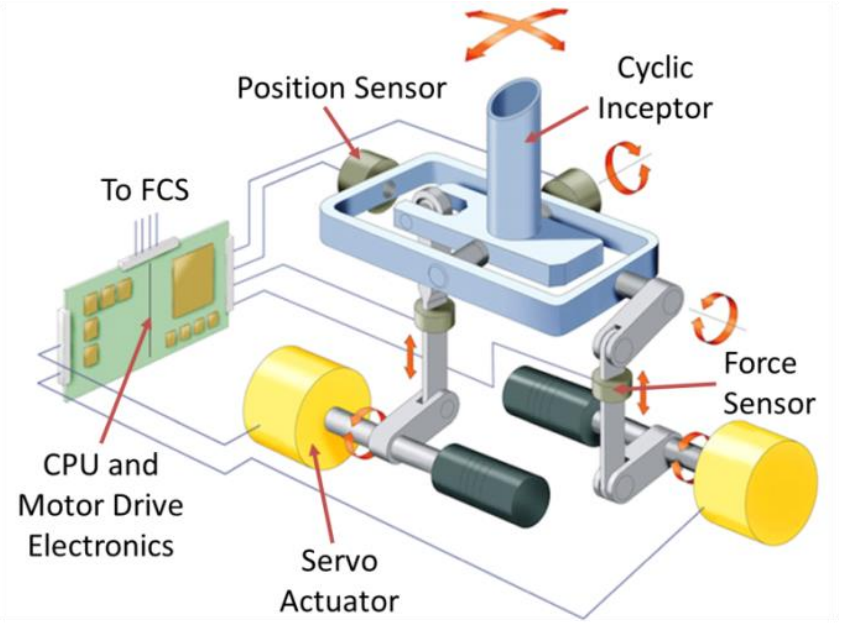

Figure 1-4: Typical Integral Components of an AIS (source: Taylor et al [9])

1.4 Mechanical AIS Failure Modes

The failure possibilities of an AIS are numerous and can be broadly classified into 3 categories: mechanical, electronic hardware and software code. Failures in each category

can be minimised by good engineering design and quality assurance, but the potential for failure remains and their causes and effects must be investigated. The two fundamental failure modes in the mechanical category[13] that will be investigated in this study are the isometric[14] and isotonic[15].

The isometric mode is characterised as a jammed stick and may be induced by a blockage in the control links; a blockage of the servo actuators or gearbox; or a failure in the control system that would fix the inceptor in one position. In this degraded mode the position signal would remain constant and could no longer be used by the FCS to control the helicopter. The force sensors however would still be functional and whilst the force signal could not be substituted directly for the position signal it could be modified to provide a suitable FCS input [15, 14]. Figure 1-5 (a) shows a simplified force displacement plot for an AIS in its compliant[16] mode. By comparison, figure 1-5 (b) shows the same plot in which an isometric failure has occurred in the pitch axis at 65% displacement and identifies its constant control deflection with variation of control force. In order to use the force signal as the FCS input a conversion factor could be used that approximates the average force gradient of the compliant mode as well as a first or second order filter to damp out signal noise and model the mass-spring-damper system of the compliant mode. More details of the isometric control system can be found in chapter 3.

The isotonic mode may be induced by a breakage in the control links; a failure of the servo actuators or gearbox; or a failure in the control system that would allow free movement of the inceptor with a very low constant force. In this degraded mode the position signal could still be used by the FCS as it would in the compliant mode, but the pilot would lose the tactile cueing assistance that the force model provided [35]. The forces that the pilot would then feel would only be a result of the inherent mass, damper and friction of the remaining load path. Furthermore, in order to reduce the contamination of the intentional tactile cueing in the compliant mode, most currently available AIS have been designed to minimise inherent force characteristics, and so in the isotonic mode, the remaining forces are likely to be only a result of very low friction. Figure 1-5 (c) shows the force displacement plot for an isotonic failure and indicates the low forces caused by inherent system friction that remain constant throughout the displacement envelope.

The practical manifestation of a mechanical failure may not actually result in a complete clinical operating state (one that is initiated instantly, fully, in all axes and without a signal runaway[17]). However, until the fundamental failure modes have been researched it would be impossible to investigate the more complex failures.

[13] These modes could also potentially be caused by failures in the electronic hardware and software.
[14] Constant position.
[15] Constant force.
[16] Normal mode of operation in which the inceptor incorporates both deflection and force.
[17] In the isometric mode the AIS could falsely send a maximum force signal to the FCS which would need to be opposed by the pilot with an equally high control force.

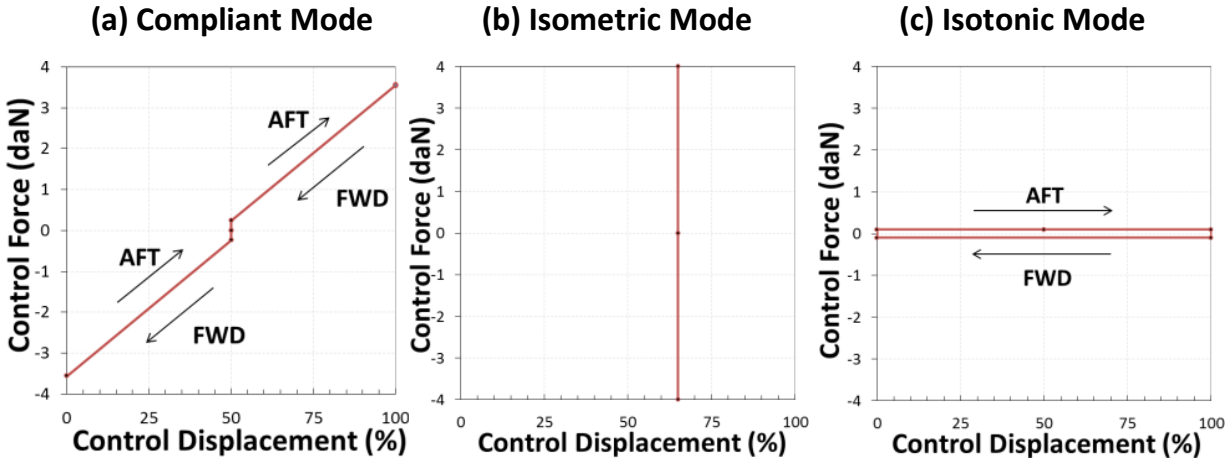

Figure 1-5: Force-Displacement Characteristics of an AIS in Various Operating Modes

1.5 The AIS Failure Problem

As flight control systems failures are considered 'specific failures'[18], they are required to demonstrate no dangerous or intolerable HQ during or after any single failure. After a mechanical failure, an AIS is designed to reconfigure to either an isometric or isotonic mode thus allowing the pilot to control the aircraft in a degraded manner. However, for compliance of airworthiness certification it must be demonstrated that the level of degradation allows acceptable accuracy, safe conduct and does not require excessive pilot skill or adaption of the control strategy.

In addition to demonstrating to the airworthiness authority that the AIS is safe, a design organisation must provide assurance to test crews for initial airborne testing; increase the confidence in the sales market (to justify continued developmental funding); and ensure that during post certification customer operations there is a low risk of an accident.

A statement of the AIS failure problem is therefore proposed:

In the event of an AIS failure the pilot must be able to recover the aircraft to stable flight and perform a landing appropriate to the aircraft's role.

The aircraft's role is an important consideration as the acceptable workload and HQ degradation for a civilian, multi-pilot, VFR transport helicopter would have very different requirements as that for a military, single-pilot, all-weather, small ship's helicopter.

1.6 Solving the AIS Failure Problem

Any solution to the AIS failure problem must not only offer a path to safe recovery of the aircraft but also minimise the impact on other development and through-life aspects. Relevant considerations are cost, weight, maintenance procedures, customer appeal and pilot training requirements. The following list proposes potentially viable solutions:

- **Redundancy of subsystem components.** It is feasible for an AIS to be designed with parallel duplication of many of its components either through an active or

[18] In accordance with Aeronautical Design Standard ADS-33E [36]

dormant philosophy[19]. Ideally the redundant components would be independent in design and production to avoid simultaneous common failures. Sensors, electronic control hardware, communication busses and software would be the most suitable components as they are small, light and easily brought into operation when required[20]. The use of one redundant sensor or communication path can also be used as an integrity monitor as Airbus proposes for its latest FBW architecture [37]. Mechanical components such as servo actuators and linkages can also be designed with redundant paths but are more difficult to integrate such that the redundant component is not compromised by the failed component. However, redundancy can cause greater weight and cost of the system and the greater complexity increases maintenance.

- **Redundancy of entire AIS for multi-pilot operations.** An adaptation to the redundancy of the individual components is to fit the helicopter with AISs for both the left and right cockpit seats. In the event of the failure of the handling pilot's AIS, the control of the helicopter could be immediately handed to the other pilot. The disadvantage of this solution is the greater operating cost of multi-pilot operations and the redundant workload burden in critical conditions where the non-handling pilot would need to be physically following the controls and be capable of taking over control instantaneously.
- **Automatic change of augmentation.** As the AIS incorporates force-position feedback validation, it is immediately aware of certain failure conditions. In cases where a failure causes a deterioration of the HQ and difficulties for the pilot to control the helicopter, the AIS could signal the FCS to immediately change the augmentation control laws (for example to increase stability and reduce agility until the pilot has adapted to the new control strategy). The disadvantage for this solution is that whilst it could be applied to entirely new helicopters, for an AIS upgrade to a previously certified helicopter it would require significant additional CS compliance activities.
- **Outer loop FCS.** With the capability that the AIS could immediately inform the FCS of a failure, it would be possible for a suitable higher order FCS to stabilise the aircraft in the pre-failure flight condition. Additional algorithms could maintain the aircraft clear of obstacles and dangerous flight regimes[21]. The pilot could then make appropriate FCS selections and without further direct pilot handling the aircraft could automatically fly to a suitable airfield and land safely. Whilst this solution is feasible with current technology no research or implementations have been identified. The greater disadvantage would be the unprecedented certification hurdles and associated expense of a system that would be authorised to take control from a pilot whilst in a safety critical

[19] Active redundancy components are in operation at all times, whereas dormant redundancy components remain available but are only brought into operation after a failure.

[20] The UH-60M FBW integrates a triplex-redundant system for control electronics, software, signal bus and inceptor force and displacement sensors [38].

[21] For example vortex ring, over-torque, retreating blade stall

situation close to obstructions. The autonomy of the take-over decision would require extremely high assurances of negligible false initiations and stabilisation of the aircraft with an appropriate level of aggression.

- **Shear pin for the isometric failure mode.** An AIS could be fitted with a shear pin that would break if the pilot applied an excessive force to the inceptor. After an isometric failure in which there was a control blockage the pilot would then be able to move the stick without tactile feedback in a similar condition to the isotonic mode. As the signal used by the FCS must in this case be the inceptor position, this option would only work if the position sensors were located between the shear pin and the pilot grip, and the blockage was not within these components. Additional disadvantages would be that there would likely be large transient inputs during the shear pin breakage and there would need to be shear pins in each axis (therefore potentially causing a mixed tactile feedback state between the axes).
- **Inherent spring gradient for isotonic failure mode.** The AIS could be designed with an inherent mechanical low spring gradient that in normal AIS operation could be compensated for by the servo actuators. If the active system then failed to an isotonic mode whilst maintaining the mechanical spring gradient, the pilot would be able to benefit from a reduced level of tactile feedback. A current SAE[22] Aerospace Recommended Practice suggested that all future AIS should be designed such that the inceptor retains some tactile cueing in the isotonic mode by integrating conventional mechanical characteristics [39]. The problems with this solution would be the complex implementation of a spring mechanism that during normal operation could constantly align its trim position with that of the active system yet could still be active during all isotonic failure causes.
- **Limitations.** A simple and low cost solution would be to apply limitations to the flight envelope, visual environment and type of operations so that the exposure to the known hazards are minimised. This option should only be selected as a last resort as it could reduce the capability of the helicopter below the intended expansion of capability created by the AIS. It would also require substantial flight testing to determine the limited envelope and confirm its suitability.
- **Training.** Increasing the initial and continuation training of the pilots to practice flight in the failure conditions, both in the simulator and through training modes in the real aircraft would be likely to improve their handling accuracy and performance in the event of a real malfunction. However, the increased training burden would be unpopular with operators due to the costs and loss revenue from the pilots. Furthermore, training may only partially compensate for the degraded HQ and its effects have varying strengths for the full spectrum of pilot abilities.
- **Automatic change of signal filter.** As discussed in the mechanical failure description, the signal used in the isometric mode by the FCS as a control input would be adapted from the inceptor force signal by a conversion law. As well as

[22] Society of Automotive Engineers

transient aircraft responses immediately after the failure, it has been identified by Jones and Barnett [15] that the change from the compliant to the isometric mode can cause Pilot Induced Oscillations (PIOs), alternatively known as Aircraft-Pilot Couplings (APCs). If the transient responses and tendency to APCs could be minimised by optimising the conversion law, then it could offer a low cost, negligible weight integral solution to the AIS failure problem.

Several of these solutions have been used in aviation design for other safety critical systems[23] and could be suitable for AIS. However, only the final proposed solution will be further investigated in this study as it presents an attractive proposal in terms of cost, weight and complexity. It can also be applied equally to AIS installations which have been fully integrated into a helicopter design as well as AIS modifications to previously certified helicopters.

However, no research has currently been published regarding this solution and so further research to assess its feasibility would be necessary. If it could be shown that safe recovery from these failures and subsequent continuation and completion of a flight is possible, the evidence could help to increase overall system safety and possibly even to avoid the need for some subsystem redundancy.

1.7 The Hazards of AIS Failures

With reference to the risk analysis model developed in section 1.2, the risk that must now be considered is not of the failure occurring, but of the pilots' ability to successfully control the helicopter during and after the failure. Table 1-3 identifies the hazards that may exist during an AIS failure and proposes some suitable mitigation measures. The hazards are categorised into the known, partially known and the unknown. The known hazards and their corresponding possible mitigations have been identified on the basis of experience, standard flight operations and current regulation [40, 26, 27, 41]. The partially known hazards had been observed through other research by Jones and Barnett [15] in which oscillatory APCs were intensified by the presence of rate limiters but the cause and mitigation had not been fully investigated. The unknown hazards are by definition yet to be identified and may be caused either as a consequence of the generic AIS technology or be more specific to the equipment and installation in a specific helicopter. By creating a structured method to analyse the HQ and APCs during an AIS failure, the unknown hazards may become exposed and hence appropriate mitigations can be formulated.

[23] For example integrated dormant-redundant pressure accumulator of hydraulic flight control systems in Westland Merlin EH101 [42]; requirement for redundant attitude indicator in all IFR aircraft [27]; automatic change of augmentation mode when trim actuator fails in EC135 [43]; pilot initiated disorientation recovery function (DRF) that automatically places the BAe Typhoon / Eurofighter in a defined safe attitude and speed [44]; shear pin in tailwheel assembly of Sikorsky Sea king to protect against overstress during ground operations [45].

Known Hazards	Proposed Mitigations
Surprise effect	• Initial and continuity training in Simulator; • Attentive Hands-on[24] during critical flight phases
Incorrect diagnosis of AIS failure mode	• Emergency procedure in RFM[25]; • Specific failure cause indicated on aircraft displays to pilot; • Multi-pilot operations to confirm diagnosis; • Initial and continuity training
Incorrect pilot actions to ameliorate failure	• Emergency Procedure in RFM; • Multi-pilot operations to confirm actions; • Initial and continuity training
Pilot disorientation	• Visual and aural warning systems • Stabilised flight recovery and guidance system initiated automatically after failure • Initial and continuity training
Mid-air collision during AIS failure	• Multi-pilot operations to help identify threats; • Electronic Awareness Aids
Collision with obstacles during AIS failure	• Minimum height and obstacle clearances • Electronic awareness aids (Radar altimeter, proximity warner)
Loss of tactile cueing	• Tactile cueing only allowed to be an aid for pilot awareness but not a necessity for safe flight
Partially Known Hazards	**Proposed Mitigations**
Oscillatory APCs induced at failure	• Failure mode specific stability augmentation; • Control signal adaptation; • Initial and continuity training
Unintentional transient control inputs	• Attenuation of initial control inputs; • Initial and continuity training
Unknown Hazards	**Proposed Mitigations**
To be identified	• Identify the factors that influence AIS failure hazards; • Develop a method of investigating, analysing and assuring the safety of AIS failures.

Table 1-3: AIS Failure Hazards and Proposed Mitigations

This hazard analysis was used to structure the formation of the objectives, scientific question and scope of the study.

[24] In accordance with definitions in DefStan 00-970, Part 7, Issue 2, Leaflet 604 [46]
[25] Rotorcraft Flight Manual [43]

1.8 Objectives and Scope of the Study

The purpose of this study is to answer the fundamental scientific question:

How can the degradation of handling qualities caused by an isometric failure of an active inceptor system in helicopters be quantified and mitigated?

The following objectives represent the scientific contributions of the study and define the path that will lead to an answer of the scientific question:

1.8.1 Identify the factors that influence the HQ of rotorcraft during the transient and recovery phases of isometric AIS failures.

A study of the factors affecting the degradation in HQ for *isotonic* failures has already been conducted to identify the worst case flight and environmental conditions so that an applicable failure Mission Task Element (MTE) could be created [35]. A similar investigation for *isometric* failures has not yet been carried out and must be conducted within this study for the same purpose of subsequently creating an assessment method. The investigation would also help in the preliminary understanding of the causes and potential mitigations of the observed APCs. Both subjective test pilot opinion and objective data analysis would provide strength to the conclusions.

1.8.2 Develop and validate methods for assessing the HQ and tendency of APCs during isometric failures of AIS.

There is currently no CS, design standard nor a generally accepted method for testing isometric failures of AIS. Indeed, ADS-33E [36] has a title at paragraph 3.6.2 for sidestick controllers with only "*This paragraph is reserved for future requirements*," stated beneath. An appropriate assessment method must expose an aircraft and AIS to role representative, specifically selected conditions that would indicate a broad spectrum of HQ degradation and APC tendency. Additionally, the method would need to be safe; structured; accurately defined so that it can be repeated the same by different test pilots; applicable to all rotorcraft (and potentially tilt rotor aircraft); and with defined clear performance requirements. Once validated it could be used in further research; the development and optimisation of new AIS installations and could be adopted by airworthiness authorities as a criterion basis for inclusion in certification specifications.

1.8.3 Identify, adapt and validate appropriate rating scales and analysis tools for the investigation of HQ during isometric failures.

Subjective rating scales such as the Integrated Failure Evaluation Scale (IFES) [47] have previously been developed for other control system failure modes and have already been validated by Müllhäuser and Barnett [35] for the isotonic failure mode. However, until now they have not been adapted or validated for an isometric AIS failure. Similarly, APC analysis tools such as the Phase Aggression Criteria (PAC) [48, 49], legacy PIO rating scale [50] and APC rating (APCR) scales [49] have previously been validated in the isometric failure mode by Jones and Barnett [15] but their use was limited to rate command helicopter controllers. Extension and validation of the APC to attitude command controllers would broaden the utilisation of an already useful analysis tool.

1.8.4 Identify an effective mitigation principle to improve the isometric post-failure HQ.

Section 1.6 selected the main mitigation to be investigated in this study, of an automatic adaptation of the inceptor force signal filter. The objective of this phase is not to discover the optimum parameter values of a first order filter for the specific experimental setup used, but to prove that the principle presents a viable solution for improving the post-failure HQ. Alternative solutions such as pilot training and helicopter augmentation command type will also be investigated to assess their effects on the HQ degradation.

1.8.5 Identify and discuss the causes of variations in HQ and APC tendency with modification of the first order filter and ramp attenuator parameters.

Analysis of trends in HQ and APC tendency with variation of filter and attenuator parameters would provide the basis for further development of the inceptor force signal filter solution in specific AIS installations. Whilst the first order filter and ramp attenuator represent the first directed research in this field, alternative signal processing solutions may develop from the results and analysis determined in this study.

1.9 Scope

The preceding discussion defined the objectives and structure of the study and already provided some of its boundaries. The following list combines both the scope previously discussed as well as new but essential limitations of the study:

- The analysis will be of the short (transient) and medium (recovery) term HQ degradation only. The long term HQ of the isometric mode has already been the subject of some subjective based research [14] and a method of quantifying the HQ exists in the Aeronautical Design Standard, ADS-33E [36] and accompanying Cooper-Harper Rating (CHR) [51].
- Only the cyclic axes of a right sidestick inceptor (not collective or yaw inceptors) will be investigated.
- The failure will be into the isometric mode that will be initiated instantly, fully, in both cyclic axes and without a signal runaway.
- The research is focussed on the post-failure recovery to a safe and stable flight condition without any requirement to make an approach and landing.
- The objective data will be gathered entirely in a ground based simulator due to no suitably equipped aircraft being currently available.

1.10 Test Participants

Data was gathered from a total of twelve test participants within the study. Both objective data and subjective opinion was recorded from the qualified helicopter test pilots but only objective data was recorded from the non-test qualified pilots. Table 1-4 presents a summary of the participants' qualifications[26] and isometric experience[27]. The

[26] FW – Qualified fixed wing pilot; RW – Qualified Helicopter Pilot.

[27] Isometric experience of greater than 2 hours.

table also states in which of the assessment they were employed and the relevant chapter. More information regarding the participants' qualifications and experience is detailed in Appendix A.

Test Participant	Qualified Pilot	Qualified Test Pilot (Category)	Isometric Experience	Assessment Involvement		
				Force-Displacement Investigation	Isometric MTE development	Main Investigation
				Ch 4	Ch 5	Ch 6 & 7
Pilot A	X	X	X	✓		
Pilot B	X	X	X	✓		
Pilot C	X	X	X	✓		
Pilot D	✓ (FW)	X	X	✓		
Pilot E	✓ (FW)	✓(2)	X	✓		
Pilot F	✓ (FW)	✓(2)	X	✓		
Pilot G	✓ (RW)	✓(1)	✓	✓	✓	
Pilot H	✓ (RW)	✓(1)	X	✓	✓	✓
Pilot I	✓ (RW)	✓(2)	✓	✓		
Pilot J	✓ (RW)	✓(1)	X			✓
Pilot K	✓ (RW)	✓(1)	✓			✓
Pilot L	✓ (RW)	✓(1)	X			✓

Table 1-4: Test Participants and Summary of Qualifications and Experience

1.11 Structure of Thesis

Chapter 1 presents an introduction to the area of research conducted in this study. The risks associated with implementing new technologies into aircraft designs are reviewed using a new analysis method. Technical details of AIS and their failures are described, the fundamental problem of controlling a helicopter after a failure is introduced and potential solutions are proposed. The scientific question for the study, the path to answer it and the scope boundaries are then presented.

Chapter 2 reviews the technology status of FBW helicopters and AIS, then reviews some of the research that has been conducted in the fields of HQ testing, Aircraft-Pilot couplings, AIS and their failures.

Chapter 3 details the facilities and equipment that were used within this study including the hardware capabilities and software configurations for the simulator, aircraft, control models and the AIS sidestick.

Chapter 4 examines the relationship between the application of a constant force and displacement in the compliant, isotonic and isometric modes. It identifies through a static analysis some potential causes of dynamic handling issues in degraded AIS modes. The conclusions from this chapter are subsequently used to offer explanation for some of the results analysed in chapter 7. Two investigations are presented: first of how a pilot varies the inceptor force and position from a specified datum over an extended period without visual reference to the inceptor values; and second of how accurately a pilot can repeat a force or displacement in a failed mode immediately after experiencing it in the compliant mode.

Chapter 5 introduces a new assessment method for the isometric failure mode that can be used to either confirm safety compliance or to modify an AIS configuration for optimisation of its HQ. It details the development of a new mission task element created specifically to expose the worst case HQ of isometric failures and uses previously developed, but slightly adapted, subjective rating scales for HQ and APC assessment.

Chapter 6 details the experimental setup used to assess the HQ and APC severity resulting from isometric failures. Different first order filter configurations are selected to convert the inceptor force signal into an equivalent position signal. A novel ramp attenuator that linearly increases the gain over a range of time periods is also defined. The extension and validation of the phase aggression criterion that offers objective identification of APC severity for use with attitude command controllers is presented. Predictions are then stated for APC tendency of the pre-failure compliant mode, and the post-failure isometric mode with some selected filter configurations, using frequency response analysis and the ADS-33E criteria. Finally, the specifics of the test conduct and conditions are detailed.

Chapter 7 presents and discusses the data from the investigation described in chapter 6. Firstly, the subjective test pilot opinion of the influential factors for APC severity is presented. This is followed by HQ and APC severity for variation of gain and time constant of the filter; time period of the ramp attenuator and augmentation command type. Frequency response analysis is also used to substantiate the analysis discussion. The effect of a test pilot's significant previous isometric training and experience is then analysed.

Chapter 8 outlines the conclusions identified and novel research contribution presented within this study and reflects on the scientific question. Recommendations for future research opportunities in the field of AIS failures in helicopters are also proposed.

Chapter 2: Technology Status and Research Review

2.1 Helicopters and Tiltrotor Aircraft with FBW and AIS

Fly-by-wire technology has been employed in commercial and military fixed wing aircraft for many years.[28] However, it only arrived in helicopters years later in 2003, with the NH-90 representing the first fully FBW production helicopter without mechanical backup. Around the same time Fly-by-Light (FBL) control made its debut in research helicopters with the DLR EC135 ACT/FHS aircraft in which main control signals were transmitted via fibre-optic cables but to reduce the risk, an emergency mechanical backup was also included [16]. This slow evolution has been partly due to the more complex rotary wing flight mechanics compared to fixed wing [37]. Table 2-1 summarises the current status of aircraft featuring FBW/FBL and PIS/AIS. The aircraft names in bold-text indicate that they continue to be operated or are involved in research or development activities.

In most cases AIS has been developed as an enhancement to FBW FCS designs and can be regarded as the next technology step. However, the BAe / Boeing APAS[29] currently in development for the Chinook and Apache helicopters is an AIS that is offered as an upgrade to conventional control systems, and therefore uses the legacy inceptors and integrates the AIS servo actuator units into the mechanical control runs [8].

Currently, the only non-research helicopter that is in development for full production with both FBW and AIS sidesticks, is the Sikorsky CH-53K military battlefield support helicopter[30], figure 2-1. As the replacement for the USMC CH-53E, the 33600kg aircraft features a triplex FBW system designed for level 1 HQ, active collective and cyclic inceptors and passive yaw pedals [52]. The right and left seat collective and cyclic inceptors are also electronically coupled so that when the handling pilot moves the controls, the non-handling pilot (or instructor) can monitor the inputs and, if necessary, take over control. A fundamental design philosophy was to encourage and support the pilot in spending more time looking out of the window in order to increase tactical and situational awareness. One element of this was the integration of tactile inceptor cueing for role-specific pilot information of control margin; power limits[31] and structural limits[32]. The proof of safety and certification requirements have predominantly been conducted in a purpose built simulator with only limited test points flown in the aircraft [53].

[28] BAe / Aerospatiele Concorde first commercially successful FBW aircraft, first flight 1969

[29] Active Parallel Actuation Subsystem (aka LinkEdge)

[30] Sikorsky has not yet announced the selected inceptor types for the S-97 Raider and SB>1 Defiant

[31] Constant collective force up to maximum continuous power, then a force gradient up to a 25% margin from maximum rated power, then a stick shaker up to the maximum rated power

[32] Retreating blade stall and g-limits

Aircraft Type	Operator	Role	Certified	FBW	Cyclic	PIS / AIS	Ref. Source
Chinook CH-47B	NASA / US Army	Research[33]	X	X	Side	PIS	54, 55
Sikorsky S-76B SHADOW	Boeing / Sikorsky	Research[33]	X	✓	Side	PIS	54
Bo105 ATTHeS	DLR	Research[33]	X	✓	Side	AIS	54
Comanche RAH-66	Boeing / Sikorsky	Development[34]	X	✓	Side	PIS	55
Dauphin 6001	Eurocopter	Research[33]	X	✓	Side	PIS	55, 56
EC135 ACT/FHS	DLR	Research	X	FBL	Side	AIS	16
Bell 412 ASRA	NRC	Research	X	✓	Side[35]	AIS	57, 17
Bell 205A	NRC	Research	X	✓	Side[35]	Isometric	57, 58
JUH-60A RASCAL	NASA / AFDD[36]	Research	X	✓	Centre	AIS	18, 38
BK117	Kawasaki	Research	X	✓	Side	AIS	19, 20, 21
Chinook CH-47F/G	Boeing	Development	X	X	Centre	AIS	11, 8
Apache AH-64	Boeing	Development	X	X	Centre	AIS	8
UH-60M FBW	Sikorsky	Development	X	✓	Centre	AIS	38
CH53K	Sikorsky	Development	X	✓	Side	AIS	53, 52
S-92F	Sikorsky	Development	X	✓	Centre	PIS[37]	19, 59
Bell 525	Bell	Development	X	✓	Side	PIS[37]	19, 6
NH-90	Military[38]	Utility	✓	✓	Centre	PIS	60
V-22	Military	Utility	✓	✓	Centre	PIS	55
AW609	Leonardo	Transport	X	✓	Centre	PIS	61

Table 2-1: Current State of FBW and AIS Equipped Helicopters and Tiltrotors

Whilst the aircraft is still under development (it is not expected to be released with full capability before mid-2024), much of the risk mitigation for AIS failures remain

[33] No longer in service
[34] Cancelled
[35] Additionally, active centre stick (and active collective and pedals for B412 ASRA)
[36] US Army Aeroflightdynamics Directorate
[37] AIS for collective axis only
[38] Italian, Belgian, Finnish, Greek, Dutch, New Zealand, Norwegian, Omani, Qatari, Spanish, Swedish, French, Australian and German Government Forces

confidential. It has been confirmed however that pilot training of the failure modes in a simulator will be a significant element to the management of their associated risks [53].

Figure 2-1: Sikorsky CH-53K FBW AIS Aircraft (source: Lockheed Martin)

2.2 FBW HQ Testing

During the development and certification phases of new rotorcraft with FBW FCS, the manufacturer is required to prove its safety and airworthiness through simulated and in-flight testing. The standards required for the fully operational FCS are specified by the relevant airworthiness authority and the primary customer in terms of stability and control performance and HQ specifications, within documents such as the EASA[39] Certification Standard for Large Rotorcraft (CS-29) [27] and the ADS-33E [36]. One of the greatest problems with HQ testing is that despite highly defined specifications, most of the conclusions depend upon pilot opinion. The universally accepted CHR [51] seeks to quantify these subjective comments into a relative scale[40] and comprehensive training at test pilot schools [62] teach pilots how to assess more consistently and accurately.

These rating scales and methods are not only used for certification but also in the development of new FCS. Amongst many examples of HQ optimisation of new FBW FCS [59, 6], two studies were published on the adaptation of the control laws of the UH-60M FBW helicopter to achieve level 1 HQ [38, 18]. The variable stability RASCAL JUH-60A in flight simulator was used as the test bed to prototype and modify the control laws, enabling their quick implementation in a low risk environment. Similar validations of control laws were conducted for the NH-90 in the Dauphin 6001 FBW [60, 56] and for the CH53K, again using the RASCAL[41] JUH-60A [52, 7]. All of these development campaigns have demonstrated that savings in time, cost and project risk as well as a reduction in flight risk can be realised through the selective use of more generic variable stability helicopters even if they possess different inherent flight characteristics to the development aircraft.

However, the identification of any handling anomalies or tendency to Aircraft-Pilot Couplings (APCs) can only be comprehensively done in-flight with the actual development

[39] European Union Aviation Safety Agency
[40] Scale of 1-10 and grouped into HQ levels of 1 (1-3); 2 (4-6) and 3 (7-8)
[41] Rotorcraft-Aircrew Systems Concepts Airborne Laboratory

aircraft in all representative configurations, flight conditions and final inceptor arrangements. These conditions are essential to identify the potential for APCs that pose the most dangerous of HQ deficiencies due to the difficulty in predicting the events that cause them [15]. This was demonstrated by two recent accidents of developmental FBW aircraft. In addition to the Bell 525 accident discussed in section 1.2 a tiltrotor AW609 suffered a similar fate during high speed boundary tests in which an unexpected lateral-directional oscillation developed. As the pilot attempted to damp the motion, the combination of his inputs and the FBW FCS control laws became out of phase with the aircraft response which led to large amplitude oscillations resulting in the right prop-rotor impacting the wing and a subsequent mid-air structural failure [63], figure 2-2.

The prediction and real-time detection of APCs in rotorcraft has produced a great deal of research [64, 65], notably from Jones et al who developed a subjective phase aggression criteria and a subjective APC rating, both of which are discussed later in chapter 6 [48, 49, 66].

Figure 2-2: Developmental AW609 Tiltrotor; Accident Scene (source: ANSV Final Report)

2.3 FBW Failures

Once the HQ has been optimised for flight with fully operational FBW FCS, all of its potential full or partial failure modes must be confirmed as safe following any single system failure regardless of its probability [36]. Furthermore, a more mulitplex or catastrophic failure resulting in casualties must be shown to occur at less than 10^{-9} failures per hour [67].

A comprehensive report was written during the early research of FBW technology by NASA regarding the dynamic response to flight control failures in fixed wing aircraft [68]. The ground and simulator based study identified that a hypothesis of 'graceful degradation' and reduced difference in control dynamics from the pre-failure state to the post-failure state improved the pilot's transition response and performance.

In 1994 the Advisory Group for Aerospace Research and Development (AGARD) produced a document that detailed principles for the development of flight test techniques for safety critical systems in helicopters [69]. As well as guidance for testing fully functional systems, it made several recommendations relevant to the work of failure testing within

this study. It introduced alternative methods of declaring acceptability of failed systems that are discussed in section 5.1. It also stated that the first task should be the investigation of the appearance and the mechanics of all potential failure modes and assignment of severity classifications. The importance of preliminary ground tests in simulators was emphasised to refine theory and to identify the worst cases of the failure. It also recommended that despite any positive conclusions made during rig and simulator testing, some flight tests must be conducted with an appropriate success criteria and role representative conditions.

Whilst the CHR was effective in assessing the HQ of consistent control configurations, it was not appropriate for the sudden changes experienced immediately after a control system failure. Hindson et al [47] devised and subsequently Kalinowski et al [70] adapted and validated a decision tree based rating scale that quantified test pilots opinions of the post-failure HQ. The short term transient phase was defined in terms of aircraft and control states and the medium term recovery phase was defined in terms of urgency and pilot effort. The scales and their development are discussed in detail in section 5.3.

During the development of the FBW / PIS equipped V-22 Osprey, a simulator test campaign was conducted to evaluate the long term HQ after various FBW and control failures [71]. A series of ten tightly defined flying tasks were consecutively flown in both the failed and non-failed states. The purpose of the assessment was to determine whether the residual HQ were adequate to permit a safe flight to a landing following a failure. Whilst the research focussed on the long term HQ of the aircraft, a limited assessment of the transient and recovery HQ was conducted using the IFES rating. In order to achieve consistent results across all test pilots and failure modes, the failures were initiated at pre-determined points. All failures were initiated in steady flight conditions but in order to maintain some element of surprise the assessing pilots were not aware at which point in the continuous cycle of tasks the failure would appear. The test philosophy attracted support from the test pilot and engineer community, and a number of useful recommendations[42] were adopted for this study.

2.4 Active Sidesticks and Haptic Cueing in Helicopters

Whilst haptic cueing had been available to fixed wing aircraft for some time, with stall warning stick shakers having been flight tested in 1953 [72], their arrival in helicopters has been more recent.

In 2000 Whalley, Hindson and Thiers investigated whether the active sidesticks (collective and cyclic) of a UH-60 simulator was able to warn the pilot of the proximity to flight envelope limits [10]. The cueing was generated in both active sidesticks as a combination of a soft stop, a force gradient and then a control shaker as the proximity to the limit approached. They concluded that the tactile cueing yielded significant HQ benefits and

[42] Use of the same MTEs and tolerances for failed and non-failed states so that a severity of degradation can be quantified; provide evaluation pilots with ample opportunity to practice the MTEs without failure; transients and ability to recover should be assessed with the IFES; a continuous cycle of tasks with an undisclosed failure initiation point assists in the pilot's surprise.

reduced exceedances of transmission torque, retreating blade stall and mast bending moment.

With the introduction into service of the DLR EC135 ACT/FHS[43] in 2001, [73] and subsequently the integration of the AIS in 2005, [33] the opportunities to investigate the potential for tactile cueing in flight increased. The aircraft supported a cyclic right hand sidestick (RHSS) and a combined collective and yaw, left hand sidestick (LHSS) for the experimental pilot who sits in the right seat. Both inceptors were active and their mechanical characteristics could be modified either off-line prior to flight or during the flight using a cockpit user interface. The AIS was integrated into the aircraft's Experimental Computer (EC) and therefore had the advantage that it could access a wide range of sensor signals and a highly flexible processor without any arduous certification requirements. The main risk mitigation of the simplex AIS and EC comes from the safety pilot who sits in the left seat and is able to immediately take control of the bare unaugmented aircraft through the certified quadruplex fly by light control system. An image of the aircraft and RHSS is shown in figure 2-3 and a full description of the EC135 ACT/FHS experimental system and the AIS is in chapter 3. Since 2013 the DLR has also operated a ground based motion simulator, the Air Vehicle Simulator (AVES) that mirrors the capabilities of the EC135 ACT/FHS [74].

Figure 2-3: DLR EC135 ACT/FHS, Sidestick and AVES Simulator (source: DLR)

[43] Active Control technology / Full Helicopter Simulator

A significant amount of haptic cueing research has been conducted both in-flight in the EC135 ACT/FHS and within the AVES simulator. Through a long-term collaboration, the French Aerospace Lab, ONERA[44] and the DLR have investigated the potential for haptic cueing in pilot's awareness of obstacles in the low speed environment. The study demonstrated that pulses or ticks induced onto the cyclic in the appropriate azimuth, which increased in amplitude and frequency with decreasing proximity to the obstacle increased the pilot's situational awareness and assisted collision avoidance without disturbing the helicopter control [3]. An extension of this study identified that the pulses were more effective than an increasing force gradient (where both were felt in the obstacles azimuth direction) [2].

Utilising both collective and cyclic active sidesticks the collaboration has also investigated the pilot awareness of the vortex ring state [75, 76]. As the airspeed was reduced towards the dangerous environment, either ticks or soft stops were created within the cyclic and similarly, as the rate of descent increased a soft stop was introduced onto the collective to warn the pilot not to lower it further. The main conclusion was that the pilots preferred the collective cueing above the cyclic cueing throughout the three relevant VRS prone tasks, but both cueing options increased the pilots' awareness of their proximity to VRS.

Collectively, Abildgaard, von Grünhagen, Müllhäuser et al demonstrated further examples of haptic cueing within both the simulator and in-flight for mast bending moment limits using soft stops in both cyclic axes; g-load limits using longitudinal cyclic soft stops; torque limit using collective soft stops and flight guidance of a rate 1 turn using lateral cyclic axis soft stops [1, 33, 4]. All of these studies confirmed that haptic cueing had been able to reduce the pilots' workload and, or increase their situational awareness.

More recently an area of research has emerged regarding the safe operation in a multi-pilot cockpit using AIS that are not mechanically coupled, such as designed in the CH-53K [52] and UH-60M FBW [38]. Dos Santos Sampaio identified that electronically coupled sidesticks increased the awareness of future helicopter states for an instructor pilot who was monitoring a student [19]. He also demonstrated that a time critical take-over of control from one pilot to another could either be conducted manually by a cyclic button or automatically by force sensors, and that the transient control overshoots could be mitigated by implementing a force fading logic.

2.5 AIS HQ Development and Testing

In 2004, Einthoven noted that whilst the benefits of AIS were becoming more widely appreciated, their implementation would be hindered without clear requirements and specifications. He proposed a set of performance requirements for the mechanical and inner loop software design (purposefully excluding the force feel model) that he envisaged would generate effective dynamic tactile cues [77]. The paper offered no specific objective success criteria definitions but identified general areas that needed to be considered in an implementation programme. These included force and displacement

[44] Utilising the PycsHel simulator at the ONERA Salon de Provence Facility

sensor accuracy and range; inherent mechanical characteristics; off-axis force sensitivity (effect of vertical force or twist on the cyclic axes); structural integrity; Inertia effects and model following performance.

In parallel to the research conducted on pilot awareness using the tactile cueing of AIS, the DLR also investigated how it could enhance the HQ of the aircraft. Von Grünhagen et al identified that by tailoring the mechanical characteristics of the AIS to the helicopter's control laws (for example attitude or translational rate commands) the HQ could be further improved [33]. A subsequent cooperation between the DLR, AFDD, NASA and ETPS studied the influence of the dynamic characteristics (damping and natural frequency) on the HQ of the aircraft [78, 79]. Flight testing was split between the DLR EC135 ACT/FHS for the active sidestick assessment and the AFDD JUH-60A RASCAL for the active centre stick assessment. Hover and slalom MTEs were flown in both rate command and attitude command response types and with a range of second order AIS characteristics. The results showed that the cyclic force characteristics had a significant impact on the HQ of the aircraft. Specifically, for the active sidesticks, higher natural frequency combined with higher damping ratio improved the HQ for both command types, but for the centre sticks only an increase in damping ratio improved the HQ significantly. It was also suggested however, that as there was a general preference towards high damping ratios greater than unity, a first order stick response with a time delay[45] may provide an optimal yet simpler solution to achieve harmony with the dynamic response of the augmented helicopter.

An extension of this study conducted the following year confirmed this hypothesis for the sidestick with an attitude command response type. It also asserted that the time delay of the first order response should be minimised [5].

2.6 Active Inceptor Failures

In Einthoven's AIS performance requirements paper [77] only two failure modes were identified: the loss of active force failure (akin to the isotonic mode) and the loss of coupling between the pilot stations. No mention was made of the isometric condition at this point; however he asserted that it was important to test the failures as opposed to just applying analysis to meet the given requirements.

In 2015 Barnett and Müllhäuser investigated the isotonic failure mode in the AVES simulator and identified the dominant factors that deteriorated the HQ [35]. Amongst 12 factors that were considered, the magnitude of inceptor displacement before failure and the pilot anticipation were shown to be the most influential. They proposed an MTE specifically designed to expose detrimental HQ during isotonic failures. A continuous series of sub-tasks were flown that included pull-up push-overs, flat figure of eight turns and wingovers. These were repeated until the failure was initiated at one of the pre-defined states that reflected the worst case conditions. The pilot was not aware of when the failure would occur and due to his focus on remaining within tightly defined

[45] A second order system with a damping ratio greater than unity can be modelled as a first order system with a small time delay [78]

tolerances of the sub-tasks, an element of surprise could be created. The study validated the IFES rating scale [47] against objective data and demonstrated that it could assess the relative HQ for different augmentation and AIS configurations. The MTE was subsequently flown without failures in a Gazelle SA341 [80] confirming that the pilot workload and tolerance definitions were appropriate, but a lack of funding prevented further investigations with failure initiations.

2.7 Isometric Condition

Due to the limited availability of applicable facilities, testing of the isometric condition in helicopters has predominantly been conducted by the NRC[46] and the DLR. In 1982 Morgan introduced the new NRC variable stability Bell 205A helicopter which had been fitted with isometric sidesticks [58]. Whilst previous fixed wing aircraft had utilised zero or very low compliance inceptors, notably the F-16 [81], the NRC represented the first helicopter with 4-axis isometric sidesticks (x, y and z axis forces, plus grip torque). The initial research showed that pilots could quickly and successfully adapt to the isometric mode. Even after only a short training period, the five test pilots awarded CHRs no worse than 4 during all of the transitions, hover and landing tasks with rate damped augmentation and 3-axis inceptor (z axis collective and conventional pedals).

The long term HQ of the isometric mode were also investigated within the EC135 ACT/FHS simulator. A paper by Müllhäuser and Schranz [14] presented qualitative data of the slalom and hover MTEs which rated the HQ as level two. The two pilots' had adapted to the new control strategy prior to the assessment and the CHRs were awarded only during the established isometric mode and did not relate to the failure period. However, they confirmed that the transient and recovery control immediately after the failure was challenging and recommended that pilots should be trained to deal with the sudden change of control behaviour during a failure.

A flight conducted by the author in the EC135 ACT/FHS during 2013 (described in the post flight report [82]) identified that whilst both AIS modes significantly deteriorated the HQ of the aircraft, the isometric condition possessed worse HQ than the isotonic. Considerable pilot attention and effort was required to suppress APCs immediately after the change to the isometric condition, but after a short period the pilot adapted his control strategy to reduce his gain and he was able to hover accurately with ease. Isometric single axis conditions showed only small detrimental effects to the overall HQ, potentially due to the retention of a counter force that felt harmonised between the axes (even though one axis couldn't move). Similarly, isometric failures at extremes of the control envelope were shown to expose specific hand and wrist anatomy and comfort related issues that in some cases required several minutes of adaptation to achieve adequate performance.

As part of the research within this study, Jones and Barnett used an initial version of the isometric MTE to investigate APCs caused by an isometric failure and their relationship to control limiters [15]. The modified IFES scale was used by the four test pilots to record

[46] National Research Council (Canada)

subjective data and the PAC tool was adapted for the isometric mode and used in the post-flight analysis of APCs. The results showed that for all cases in which limiters were activated, each pilot entered extreme oscillatory APCs. In contrast, no pilot experienced any APC during the manoeuvre without a failure. Furthermore, the isometric MTE received approval from the test pilot and engineering community and it demonstrated its ability to expose APCs and detrimental HQs specific to the isometric failure case.

2.8 Summary

The technology and research review confirmed that there has been a long history of FBW research in both fixed wing and rotary wing aircraft. The emerging AIS technology in helicopters has also seen published articles, in particular regarding the benefits of tactile cueing. However in most cases the fixed wing domain has taken the lead and rotary wing research has followed. Furthermore, there have been relatively few investigations published on the failure cases of the AIS and, other than the author's own work, they have focussed only on the long term considerations within the failed state.

A research gap has therefore been identified in the area of HQ and APCs caused by unannounced changes of AIS mode from the compliant to the isotonic or isometric.

The review generated the motivation to understand the influential factors and to develop a structured approach to assess the short term HQ and APC suppression during sudden changes of AIS mode which could then be adopted as a standard metric. This study aims to take the first generic steps into this area of research from which it can be further developed for more specific installations and solutions.

Chapter 3: Experimental Facilities, Configuration and Simulation Environment

3.0 Overview

With the exception of one flight that was flown in the DLR EC135 ACT/FHS and one flight in an ETPS Gazelle [80, 82], all of the testing and data gathering for this study was conducted in the DLR AVeS simulator facility. This chapter summarises the hardware capabilities and software configurations for the simulator, aircraft, control models and AIS sidestick.

3.1 Simulator

The AVES flight simulator centre, as shown in figure 3-1, features interchangeable EC135 ACT/FHS, figure 3-2, and Airbus A320 cockpits which can be installed in either the common motion platform or common fixed platform. The simulators are designed as research facilities with high levels of flexibility and are therefore not certified for flight training or licence revalidation in accordance with ICAO 9625-H [83]. However, the EC135 ACT/FHS cockpit has been accurately represented, the motion and visual characteristics exceed the requirements for a Type V [83, 84, 126] simulator and the experimental system hardware and software are maintained identical to the real aircraft. The fundamental visual and motion characteristics of the simulator are described in table 3-1 [74].

Figure 3-1: AVES, Motion-Based Centre and Fixed-Base Right of Picture (source: DLR)

Figure 3-2: Internal View of AVES EC135 ACT/FHS Cockpit, Left and Right Sidesticks Visible at Experimental Pilot (Right) Seat Position (source: DLR)

Visual System Characteristics	
Projection Type	Non-collimated (Real-Image Display)
Projection System	60Hz DLP-based LED System
Number of Projectors	15
Native Resolution	1920x1200
Screen Resolution (calculated)	5 arc-min / Optical Line Pair (OLP)
Brightness	13.5cd/m^2
Contrast Ratio	7:1
Field of View (horizontal)	+120° to -120°
Field of View (vertical)	+35° to -58°

Motion System Characteristics	
Motion Base	Hexapod
Actuators	60 inch Electric
Capacity	14 tons

Table 3-1: DLR AVES Simulator Characteristics

3.1.1 Useable Cueing Environment

The Simulated Day Useable Cueing Environment (SIMDUCE / UCE) was calculated for the isometric failure MTE[47] in the AVES Simulator in accordance with ADS-33E [36]. The simulator environment settings were selected to represent a Good Visual Environment (GVE - daylight; no cloud layers; no fog enabled; visibility 20km). Three test pilots each provided visual cue ratings (VCR) for pitch, roll, yaw, vertical translation and horizontal translation using the scale in figure 3-3. These ratings were then averaged across the three pilots and the worst attitude average and worst translation average were applied to figure 3-4. The ratings and calculation is summarised in table 3-2. The overall UCE for the Isometric Failure MTE in the AVES simulator was 1. With reference to table IV of ADS-33E, the minimum required response type for all MTEs is rate command.

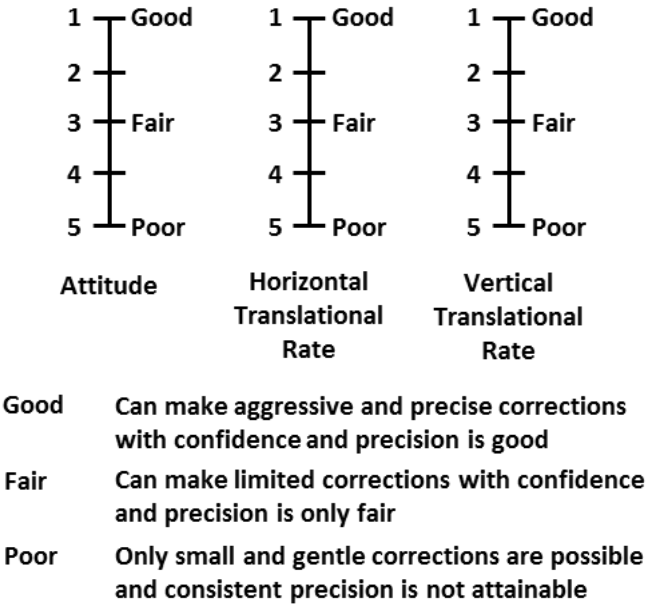

Figure 3-3: Visual Cue Rating Scale [36]

	Attitude			Translational	
	Pitch	Roll	Yaw	Vertical	Horizontal
Pilot G	1	2	3	2	2
Pilot H	1	1	1	2	1
Pilot L	2	2	2	3	2
Average	1.3	1.7	2	2.3	1.7
Worst		2		2.3	

Table 3-2: VCRs for AVeS Helicopter Configuration during Isometric Failure MTE

[47] Subsequently presented in chapter 5

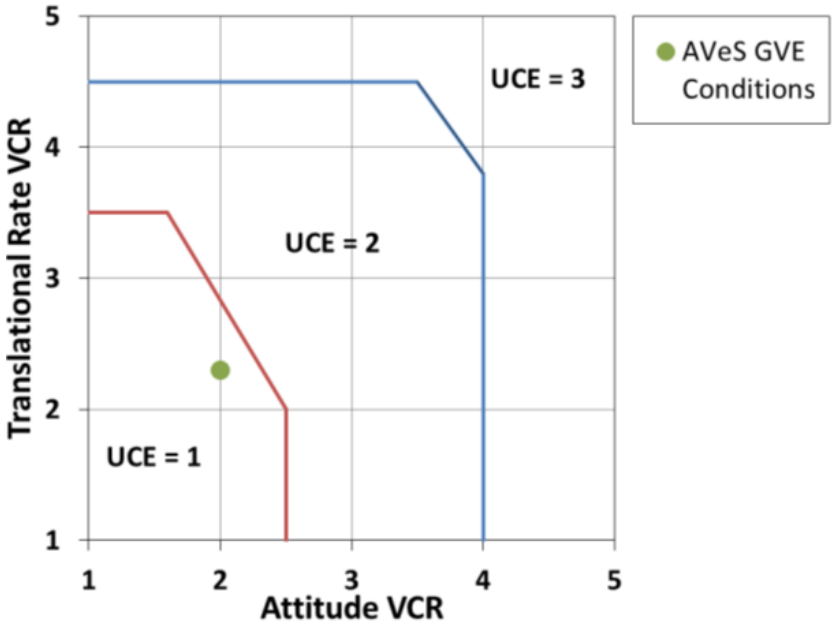

Figure 3-4: UCE for AVeS Helicopter Configuration during Isometric Failure MTE [36]

3.2 EC135 T2+ ACT/FHS

The simulated helicopter which was used in this study was based on the DLR operated EC135 ACT/FHS as shown in figure 3-5. The basic flight and physical characteristics of this aircraft and much of the mechanical components are consistent with the standard EC135T2+. A full description of the standard aircraft, limitations, procedures and performance is available in the Rotorcraft Flight Manual (RFM) [43] and the Type Certificate Data Sheet [85] and is summarised below:

- Light twin-engined helicopter with metal-composite fuselage structure and skid landing gear.
- Four-bladed bearingless main rotor rotates anti-clockwise when viewed from above and controlled by tandem dual hydraulic actuators.
- Anti-torque provided by a 'Fenestron' ducted fan 10-bladed tail rotor.
- Maximum seating for 8 passengers and 2 crew. Minimum crew one pilot.
- Dual 28v 200A DC gearbox driven generators and one 40Ah battery supplied electrical system.
- 680 Litre (544kg) fuel tank capacity with average fuel burn of 180kghr^{-1}
- Turbomeca Arrius 2B2 engines comprising one centrifugal compressor, reverse flow combustion chamber, one axial gas generator turbine and one axial free power turbine. Full Authority Digital Engine Control (FADEC).
- Standard aircraft fitted with pitch, roll and yaw stability augmentation and 3 axis autopilot.
- Certified for VFR day and night with optional certification for IFR[48] and category A flight.
- Helicopter dimensions shown in figure 3-6.

[48] Instrument Flight Rules

- Maximum take-off mass 2910kg; minimum take-off mass 1500kg.
- Maximum pressure altitude 20000ft
- Maximum V_{NE} 155KIAS; V_Y 65KIAS; V_{TOSS} 40KIAS; V_{AUTO} 75KIAS; $V_{MIN\ IF}$ 40KIAS

Figure 3-5: EC135 ACT/FHS Helicopter Operated by DLR (source: DLR)

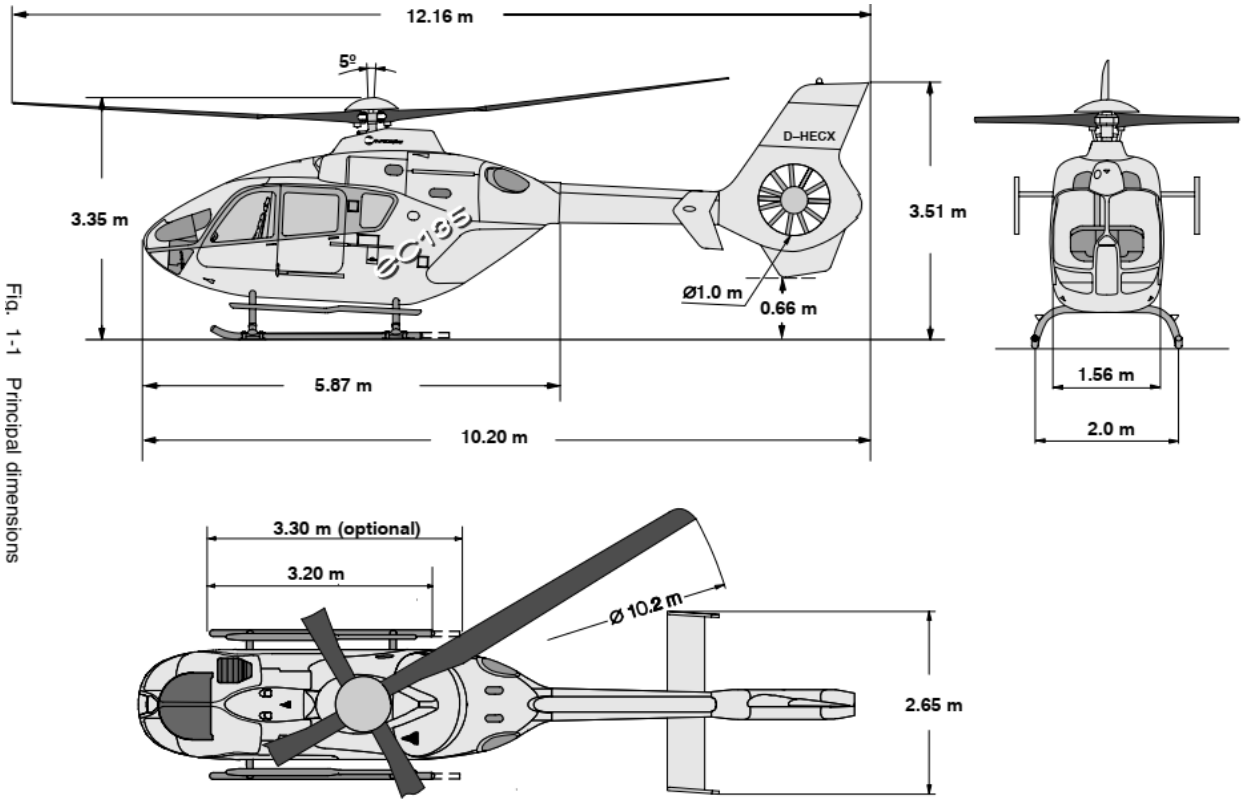

Figure 3-6: Dimensions of EC135T2+ (source: Airbus Helicopters)

The EC135 ACT/FHS that is operated by DLR has a number of differences from the standard helicopter which are detailed in the RFM ACT/FHS Appendix [16], the Experimental System Review [73] and are summarised below:

- Seating only for 2 pilots and one flight test engineer (no passenger accommodation).
- Certified for VFR day and night flight only (no IFR).
- Fly-by-light flight control system with backup mechanical control.
- Variable stability experimental control system manipulated in-flight through the Cockpit Display Unit (CDU).
- Experimental display for experimental pilot on the right side of the cockpit.
- High landing skids (711mm compared to standard 401mm)
- Optional sensor array (milimetric wave radar; IR sensor, visual camera, LIDAR[49] sensor).
- Optional helmet mounted display system.
- Optional left and right hand sidesticks.
- Minimum take-off mass 2150kg.
- Maximum V_{NE} 125KIAS.

3.3 Flight Control System Model

The Flight Control System (FCS) for both the pitch and roll systems are identical and are represented in figure 3-7 where the aircraft response is depicted as the FHS block. The proportional, integral and differential (PID) values of the settings for the rate command model and attitude command model are presented in tables 3-3 and 3-4 respectively. The naming convention of the feedback gains, K_P, K_I and K_D are taken from an assumption that the output of the system is an attitude. Hence the attitude command system includes a K_P term as well as a K_D term, whereas the rate command system includes only a K_D term. Despite this naming convention the output of the system is measured as both attitudes and rates by appropriate sensors and therefore, as the K_D term uses the rate signal, it does not require a differentiator, s.

The K_P parameter was implemented in the feed forward signal so that its value could be changed during FCS optimisation exercises without affecting the static pilot input response. If $K_P < 0.001$, then the attitude feedback loop and K_P gain are automatically removed and the system becomes that represented in figure 3-8.

The parameter values of both models were selected and optimised by successive Empire Test Pilots' School courses from 2008 to 2015 [86 and 87].

[49] Light Detection and Ranging

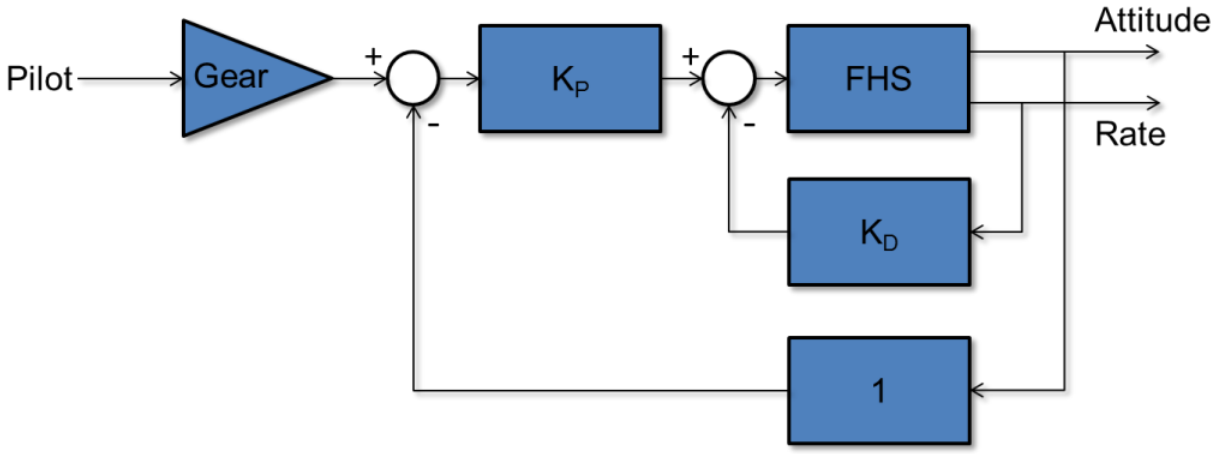

Figure 3-7: Simplified FCS System Model for Pitch and Roll Axes, $K_P \geq 0.001$

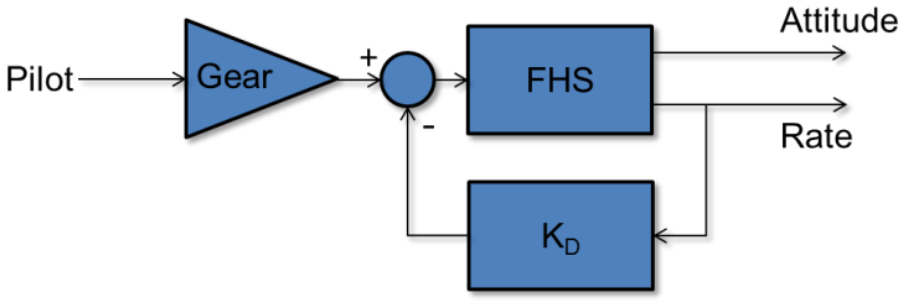

Figure 3-8: Simplified FCS System Model for Pitch and Roll Axes, $K_P < 0.001$

Characteristic	Value
FCS Scenario	AIS FAIL RC
COS[50] Limiters	Off
Actuator Limiters	Inhibited
Lead / Lag	Off

	Pitch	Roll	Yaw	Heave
Gear	1.2	2	1	1
K_P	0	0	0	0
K_I	0	0	0	0
K_D	40	30	45	5

Table 3-3: Rate Command FCS Configuration

[50] Core System / Cockpit-Schnittstellengerät (Cockpit Interface Control Unit)

Characteristic	Value
FCS Scenario	AIS FAIL AC
COS Limiters	Off
Actuator Limiters	Inhibited
Lead / Lag	Off

	Pitch	Roll	Yaw	Heave
Gear	1.83	2.01	1.2	1
K_P	50	60	0	0
K_I	0	0	0	0
K_D	60	50	45	5

Table 3-4: Attitude Command FCS Configuration

The short term response of the rate command configuration from a step input initially produced an almost constant attitude rate for both the pitch and roll axes, as shown in figure 3-9. However after the initial 1-1.5 seconds, the attitude rate begins to reduce in magnitude. As the inceptor inputs within an APC oscillation or those required for the Isometric MTE rarely last longer than this period, the approximation of the PID controller and its selected values remains valid as a rate command controller. Throughout this study, the term rate command has been used with respect to the short term response only and it is acknowledged that the available controller did not present a true rate command.

Similarly, the attitude command configuration short term response from a step input initially produced an almost constant attitude, as shown in figure 3-10 for both the pitch and roll axes. After the transient period, the attitudes remained reasonably constant for at least 1 second before beginning to reduce in magnitude. Throughout this thesis, the term attitude command has been used with respect to the short term response only and it is acknowledged that the available controller did not present a true attitude command.

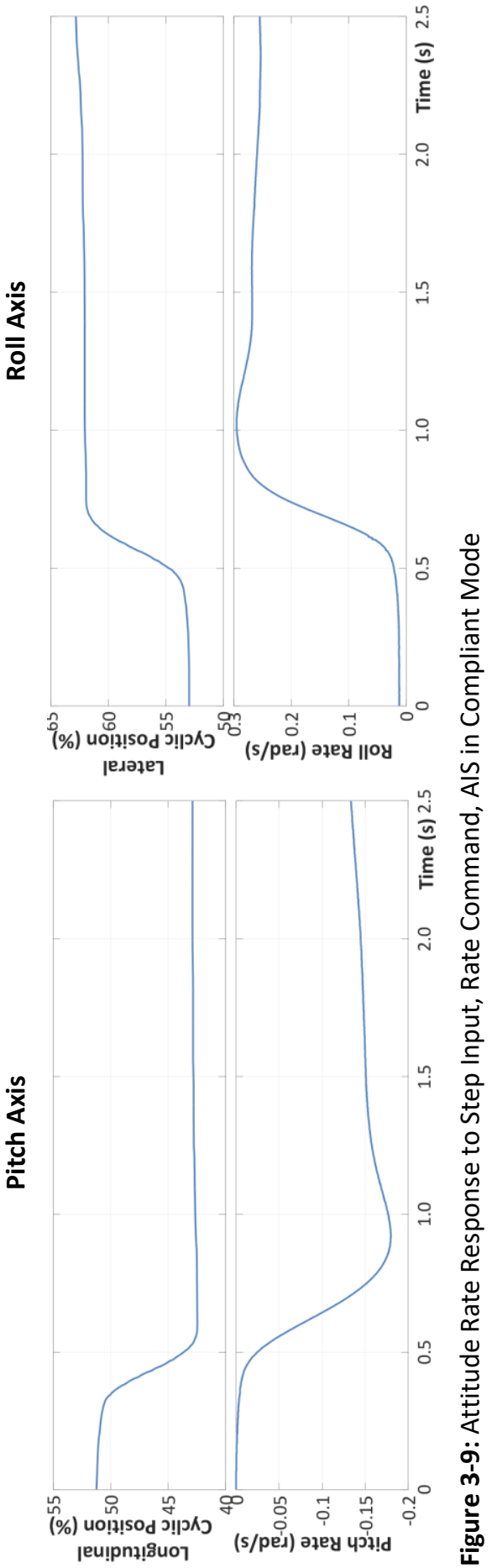

Figure 3-9: Attitude Rate Response to Step Input, Rate Command, AIS in Compliant Mode

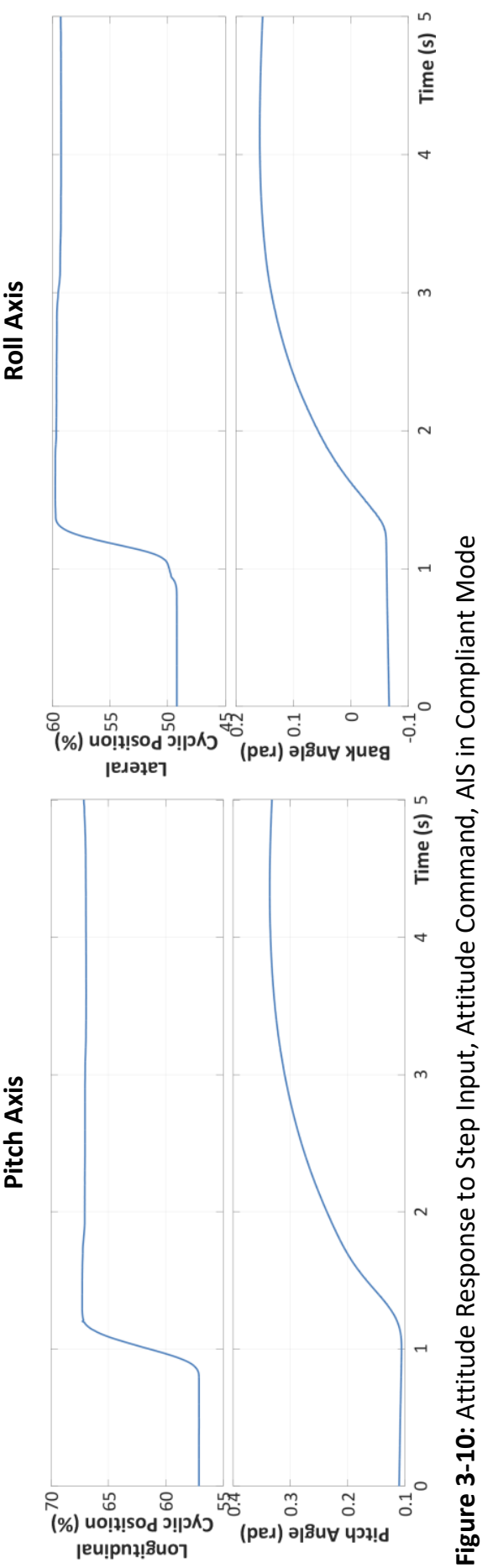

Figure 3-10: Attitude Response to Step Input, Attitude Command, AIS in Compliant Mode

3.4 Stirling Dynamics Right Hand Sidestick

The DLR EC135 ACT/FHS simulator was configured with the Stirling Dynamics Active Control System (ACS) right hand sidestick controlling the pitch and roll axes and the conventional collective and pedals controlling the heave and yaw axes respectively. The right sidestick is presented in figure 3-11. Whilst the conventional cyclic was fitted, it was not functional and was therefore not used. An optional left sidestick which was capable of controlling the heave and yaw axes was neither fitted nor used. The general hardware characteristics of the sidestick are presented in table 3-5 [33] with measurements taken from the Finger Reference Point (FRP), defined as the point where the middle finger touches the front of the grip.

Figure 3-11: Stirling Dynamics Right Sidestick Fitted in DLR EC135 ACT/FHS (source: DLR)

Sidestick Characteristics	
Manufacturer	Stirling Dynamics, Bristol, UK
Model	Goldstick
Max. Angular Displacement (both axes)	±25°
Max. Linear Displacement at FRP (both axes)	±0.07m
Maximum Force at FRP (both axes)	±150N

Table 3-5: Stirling Dynamics Cyclic AIS Hardware Characteristics

Figure 3-12 shows the block diagram of the active sidestick in the compliant mode. When the pilot applies a change of force to the stick, the force was sensed and compared with the force deflection look-up tables held internally. The resulting value was a cyclic position term but had only had a simple spring force gradient applied to it (which was not necessarily of a constant value). The simulated effect of the damping and mass (as well as a further spring term) of the stick was then applied through a second order filter. Equation 3-1 shows the generic transfer function for the second order filter in the frequency domain, where ω_0 is the Eigen frequency (also known as the natural frequency, ω_n), D is the dimensionless damping (also known as the damping ratio, ζ or relative damping) and s is the Laplace operator [88, 89]. The Eigen frequency and dimensionless damping could be set into the ACS configuration directly through the CDU. Equations 3-2 and 3-3 define the Eigen frequency and dimensionless damping in terms of familiar mechanical systems with mass m, damping b and constant force gradient k.

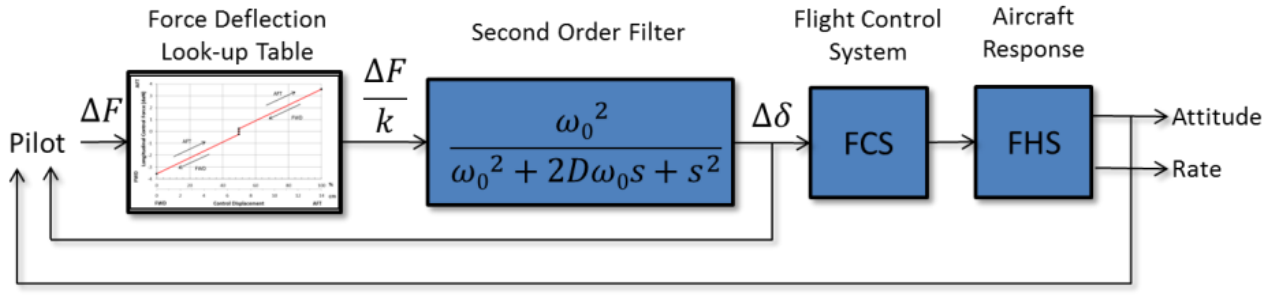

Figure 3-12: Simplified AIS Control System in Compliant Mode for Pitch and Roll Axes

$$G(s) = \frac{\omega_0^2}{\omega_0^2 + 2D\omega_0 s + s^2}$$

Equation 3-1

$$\omega_0 = \sqrt{\frac{k}{m}}$$

Equation 3-2

$$D = \frac{b}{\sqrt{4km}}$$

Equation 3-3

The output of the second order filter is termed the demanded cyclic position, δ. The actual cyclic position taken from internal sensors is then compared to the demanded cyclic position and the difference reduced to zero by the internal electrical motors moving the cyclic to the demanded position. The demanded cyclic position is also used as the input for the flight control system described in section 3.3.

The sidestick configuration that was used for all compliant mode test points is presented in table 3-6. The damping ratio was set at 1.0 and therefore presenting a critical damping

where a step input would create no overshoots of the steady state response. Each of the force characteristics were defined within tables held in the Experimental Computer and their values multiplied by the respective Q_{FEEL} prior to being transmitted to the sidestick processor. The consequential longitudinal and lateral force-displacement characteristics of the sidestick in compliant mode with the settings in table 3-6 are presented in figures 3-13 and 3-14 respectively.

Characteristic	ACS Reference CDU	Value
ACS Scenario	-	ETPS2014A01
Force-Deflection Gradient Table (Pitch)	MAINTBL PI	3 SM02 DEF
Force-Deflection Gradient Table (Roll)	MAINTBL RO	1 SM08 NLI
Force-Deflection Gradient Multiplier (Pitch & Roll)	MAINQFL (PI RO)	0.50
Breakout Force Table (Pitch & Roll)	BRKTBL (PI RO)	2 BUILTIN
Breakout Force Multiplier (Pitch & Roll)	BRKQFL (PI RO)	0.7
Eigen Frequency (Pitch & Roll)	FREQ (PI RO)	3.20 Hz
Dimensionless Damping (Pitch & Roll)	DAMP (PI RO)	1.0
Friction (Pitch & Roll)	FRIC (PI RO)	0.0

Table 3-6: Cyclic AIS Mechanical Characteristics User Defined Configuration

In accordance with the definitions of Cooke and Fitzpatrick in [90], there was no Trim Control Displacement Band (TCDB), trim system free-play, detents or friction incorporated into the system. A small breakout force can be seen in both axes of ±0.24daN which has been implemented to assist the pilot to identify the trim position and therefore improve the HQ of the aircraft. In the lateral axis a small increase in the force gradient was previously incorporated in the displacement area within 15% of the trim position in order to improve the HQ and was retained for this study.

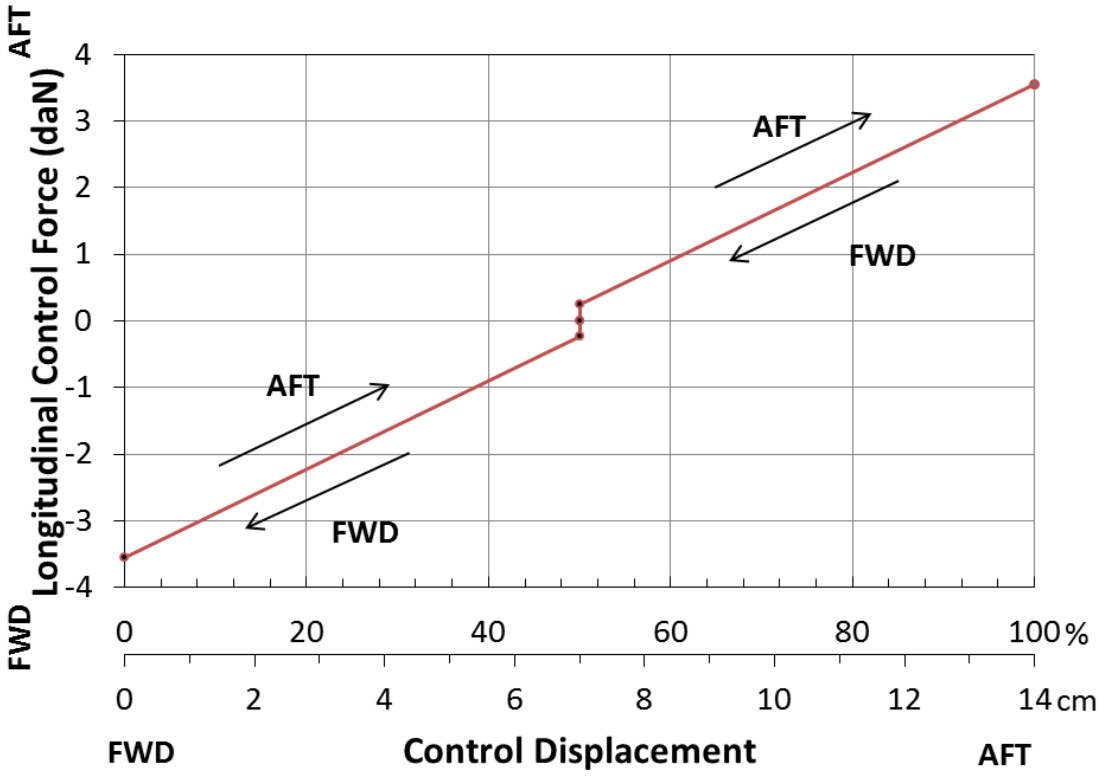

Figure 3-13: AIS Force-Displacement Characteristics, Longitudinal

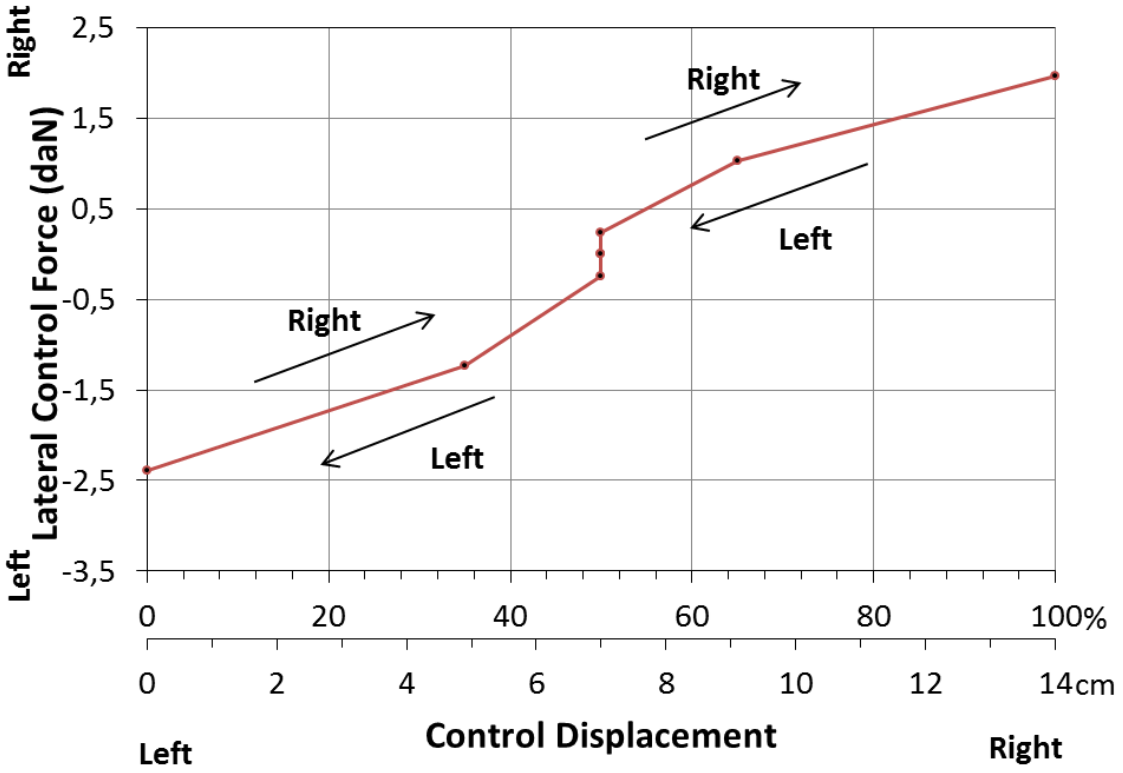

Figure 3-14: AIS Force-Displacement Characteristics, Lateral

Figure 3-15 shows the block diagram of the active sidestick in the isometric mode. When a pilot applies a change of force to the stick, it is sensed in the same way as in the compliant mode. However, the change of force is then converted to the demanded position in one stage through the first order filter defined in equation 3-4 where k is a constant force gradient, τ is a time constant and s is the Laplace operator. As the stick is not able to move, there is no position feedback to the pilot but similar to the compliant mode, the demanded position is used as the input to the FCS to control the aircraft. The first order filter is further discussed in section 6.1.

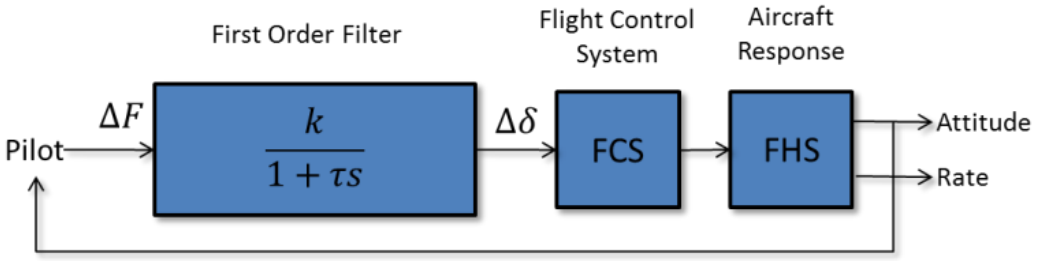

Figure 3-15: Simplified AIS Control System in Isometric Mode for Pitch and Roll Axes

$$G(s) = \frac{k}{1 + \tau s}$$

Equation 3-4

3.5 Sign Convention

The convention of signs for the sidestick signals is detailed in table 3-7.

Direction of Force or Position	Sign of Signal
Forward	-
Back	+
Left	-
Right	+

Table 3-7: Sign Convention of Stirling Dynamics Right Sidestick

Chapter 4: Force Displacement Investigation

4.0 Overview

The Flight test in the DLR EC135 ACT/FHS during 2013 identified that both the isometric and isotonic AIS modes were prone to oscillatory APCs and in some cases considerable suppression was needed to dampen the motions [82]. The test pilot commented that a number of factors influenced the suppression of the oscillations including the AIS failure mode, trim control strategy, pre-failure inceptor force / displacement, pre-failure inceptor direction, anatomic limitations as well as any need to maintain a prolonged out of trim control input. Furthermore, it was apparent that the participant's previous experience and training (helicopter and pilot qualifications, sidesticks and / or isometric AIS experience) would also influence the performance of the suppression. An initial focussed investigation of the relationship between the force and displacement of the active sidestick was therefore conducted to further understand the influence of some of the identified factors in the suppression of oscillatory APCs.

In order to specifically investigate these factors exclusively and to level the task complexity across pilots and non-pilots, the peripheral influences such as closed loop control of the helicopter, flight environment and aircraft limitations were minimised.

The specific objectives of the investigation were to analyse and identify consistent trends in the following relationships:

- The consistency of a participant to maintain a prolonged constant inceptor force or displacement input without reference to any AIS signal indications in relation to:
  - The inceptor mode (compliant, isometric and isotonic).
  - The participant's previous experience and training.
  - The direction of the inceptor input.
- The accuracy of a participant to repeat a previously held inceptor force or displacement input without reference to any AIS signal indications in relation to:
  - The inceptor mode (compliant, isometric and isotonic).
  - The participant's previous experience and training.
  - The direction of the inceptor input.
- The relative influence of inceptor displacement and force for making repeated, consistent and sustained control inputs.

4.1 Relevant Definitions

The following definitions are also presented graphically within the example data in figure 4-1[51]. With the exception of the Inceptor Trim Position, the same terms equally apply for inceptor force.

[51] Lateral control position in isotonic mode without reference to position values

Inceptor Trim Position	The initial position of the inceptor with no force applied. For all test points, this was set at 50% in both longitudinal and lateral axes.
Inceptor Datum	The position or force applied to the sidestick inceptor during the datum test points when reference to these values was available to the pilot on the experimental display. Throughout this investigation the Inceptor Datum for position reference was 35% (forward), 65% (aft), 35% (left), 65% (right) and for force reference was -10N (forward), +10N (aft), -10N (left), +10N (right).
Inceptor Datum Displacement	The relative displacement of the Inceptor Datum from the Inceptor Trim Position. Throughout this investigation the Inceptor Datum Displacement for position was -15% (forward), +15% (aft), -15% (left), +15% (right) and for force was -10N (forward), +10N (aft), -10N (left), +10N (right).
Pilot Variation	The difference in value of either the inceptor force or position between its maximum and minimum values recorded during the 60 seconds of each test point.
Inceptor Mean	The mean value of either the inceptor force or position recorded during the 60 seconds of each test point
Pilot Inaccuracy	The difference in value of the inceptor force or position between the inceptor mean and the inceptor datum values.
Pilot Inaccuracy Ratio	The ratio of Pilot Inaccuracy to Inceptor Datum Displacement. A positive ratio indicates that on the pilots displaced the inceptor with excessive magnitude.
Mean Pilot Inaccuracy Ratio	The mean of positive and negative values of the Pilot Inaccuracy Ratio across a sample group.
Mean Magnitude of Pilot Inaccuracy Ratio	The mean of the absolute values of each pilot inaccuracy ratio across a sample group. A larger ratio (which can only be positive) indicates that on average the pilots have been more inaccurate (either in an insufficient or excessive sense).

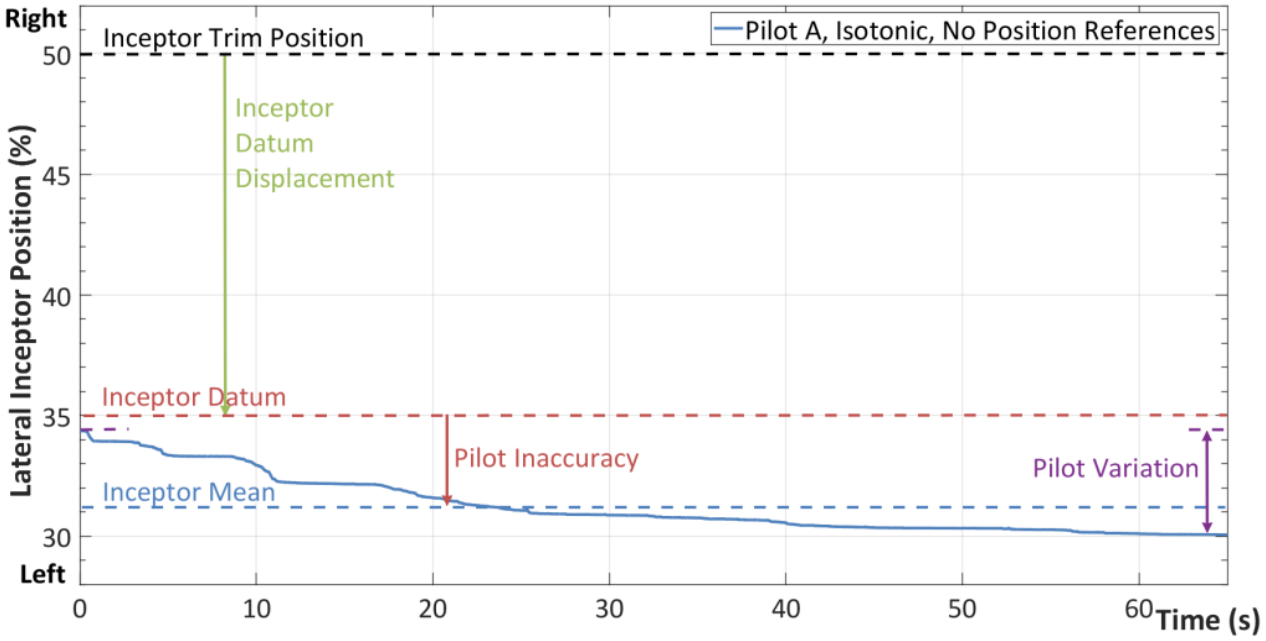

Figure 4-1: Example Time Plot with Annotations of Left 15% Inceptor Input in Isotonic Mode without Reference to Position Values

4.2 Assessment Method and Conditions

This assessment was conducted in the AVES EC135 ACT/FHS simulator situated at DLR Braunschweig. The right hand Stirling Dynamics sidestick was used with the experimental display and associated data management and experimental computers. As the assessment investigated only the relationship between the force and position of the sidestick with no relevance to actual flight, the simulator was set in a zero visibility external environment and the flight model remained at standby. Additionally, as the motion was not applicable to the assessment, the simulator was installed on the fixed base.

The assessment gathered data from 9 test participants across 3 subset groups: 3 non-pilots; 3 pilots with no active sidestick experience and 3 pilots with active sidestick experience. Details of the participants can be found in Appendix A, (pilots A, B, C, D, E, F, G, H, I). The conditions and preparation for each participant were identical. The assessment was split into 3 phases described below and summarised in table 4-1.

For each inceptor mode and for each cyclic direction the participants were required to conduct one test point in the compliant inceptor mode with a display available showing the inceptor position or force and then a subsequent test point in the compliant, isometric or isotonic mode without the display available. The purpose of the former test point was to provide the participant with a reference force or position to replicate during the subsequent test point when the displayed values were not available. When permitted, the displays were presented on a screen directly in front of the participant. The longitudinal and lateral inceptor positions were indicated with a yellow pointer on the grey bar at the right edge and top edge respectively on the display in figure 4-2. The participants agreed that the perceived combined error and inaccuracy of selecting an

inceptor position of 65% or 35% was ±0.5%. The longitudinal and lateral inceptor forces were indicated on a time trace on the display in figure 4-3. In order to make an inceptor force of +10N or -10N the participant was required to maintain the force trace (green for longitudinal, red for lateral) directly on top of the first grey grid line (±10N). The participants agreed that the perceived combined error and inaccuracy of selecting an inceptor force of +10N or -10N was ±0.5N.

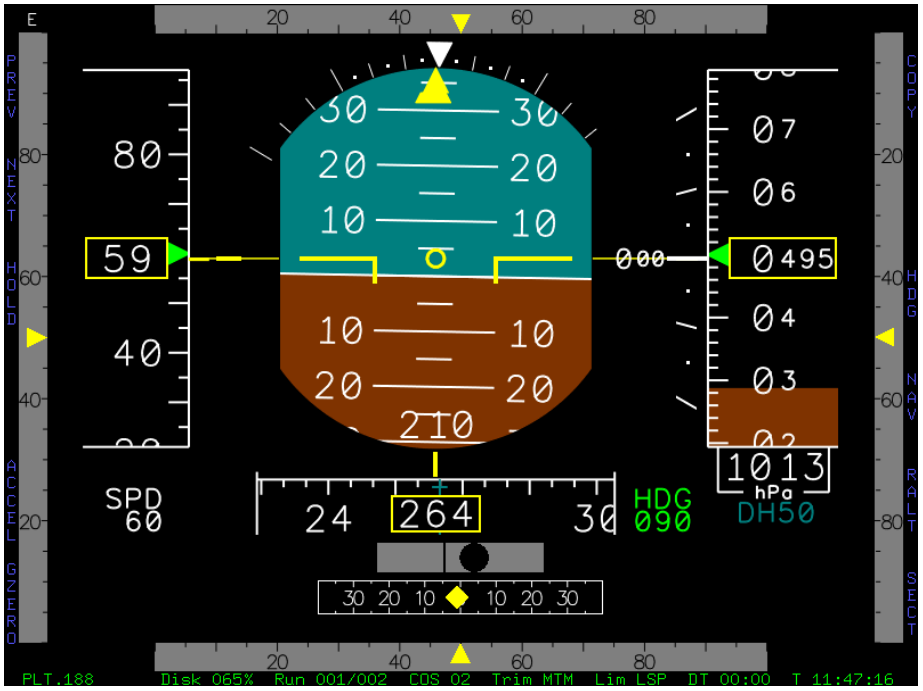

Figure 4-2: Experimental Display showing Inceptor Position Indicators (source: DLR)

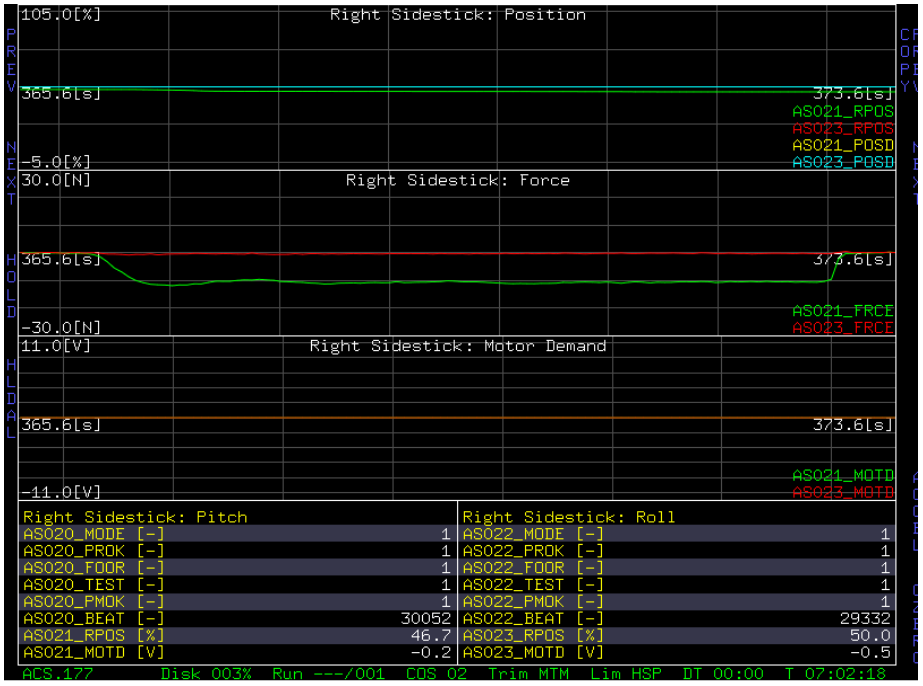

Figure 4-3: Experimental Display showing Inceptor Force Indicators (source: DLR)

Phase 1: Compliant Mode (Test points 1-8)

- With the sidestick operating in the compliant mode, the participant selected the Inceptor Datum Position (35% or 65%) and held it for 60 seconds whilst constantly watching the position indications of figure 4-2.
- The participant then returned the inceptor to the trim position and released the hand from the inceptor.
- With the sidestick still operating in the compliant mode, the participant again selected the Inceptor Datum Position but without any position indications visible, and therefore solely using their recollection of the position and force from the previous test point. The inceptor was held in position for 60 seconds.
- The participant then returned the inceptor to the trim position and released the hand from the inceptor.
- These 2 test points were then repeated for each cyclic axis direction.

Phase 2: Isometric Mode (Test points 9-16)

- With the sidestick operating in the compliant mode, the participant selected the Inceptor Datum Force (+10N or -10N) and held it for 60 seconds whilst constantly watching the force indications of figure 4-3.
- The participant then returned the inceptor to the trim position and released the hand from the inceptor.
- With the sidestick operating in the isometric mode, the participant again selected the Inceptor Datum Force but without any force indications visible, and therefore solely using their recollection of the force from the previous test point. The inceptor force was held for 60 seconds.
- The participant then returned the inceptor force to zero and released the hand from the inceptor.
- These 2 test points were then repeated for each cyclic axis direction.

Phase 3: Isotonic Mode (Test points 17-24)

- With the sidestick operating in the compliant mode, the participant selected the Inceptor Datum Position (35% or 65%) and held it for 60 seconds whilst constantly watching the position indications.
- The participant then returned the inceptor to the trim position and released the hand from the inceptor.
- With the sidestick operating in the isotonic mode, the participant again selected the Inceptor Datum Position but without any position indications visible, and therefore solely using their recollection of the position from the previous test point. The inceptor was held in position for 60 seconds.
- The participant then returned the inceptor to the trim position and released the hand from the inceptor.
- These 2 test points were then repeated for each cyclic axis direction.

Test Point	Inceptor Mode			Inceptor Datum Direction	Position or Force Indications Available
	Compliant	Isometric	Isotonic		
1	X			Forward	X
2	X			Forward	
3	X			Aft	X
4	X			Aft	
5	X			Left	X
6	X			Left	
7	X			Right	X
8	X			Right	
9	X			Forward	X
10		X		Forward	
11	X			Aft	X
12		X		Aft	
13	X			Left	X
14		X		Left	
15	X			Right	X
16		X		Right	
17	X			Forward	X
18			X	Forward	
19	X			Aft	X
20			X	Aft	
21	X			Left	X
22			X	Left	
23	X			Right	X
24			X	Right	

Table 4-1: Force Displacement Investigation Test Conditions

Prior to the assessment, the participants were given the opportunity to practice the test points and were given the following additional instructions:

- To predominantly concentrate on selecting the identical inceptor datum as previously made in the compliant mode preparation test point.

- To maintain as constant an inceptor force or position throughout the 60 seconds as possible, even if after the initial force or position selection, the participant felt that it was incorrect and wanted to change it.
- To use neither the beeper trim nor the trim release button.
- To make no inputs in the collective or yaw axes.
- To grip the inceptor in the 'as designed' method and not to use an alternative or novel grip method to improve accuracy or consistency.
- To ensure that the sidestick armrest was appropriately adjusted prior to the start of the assessment.
- To avoid looking at the inceptor to assess its position in lieu of the position indications.

4.3 Data Processing

After each assessment data from all test points were downloaded from the Data Management Computer (DMC) and uploaded into the FitLab Graphical User Interface (GUI) App [91] within MatLab. For the inceptor force signals, the 'remove spikes' function was used to remove spurious outlying data points. The data for both the inceptor force and positon signals were then manually interrogated to identify the maximum and minimum values whilst ignoring single data point spikes and effects of noise. The mean value was then automatically calculated by the FitLab GUI app. Microsoft Excel was subsequently used to present and analyse the maximum, minimum and mean values for each test point.

An annotated example of the raw data prepared by the Fitlab GUI app is shown at figure 4-1 with the defined terms presented graphically.

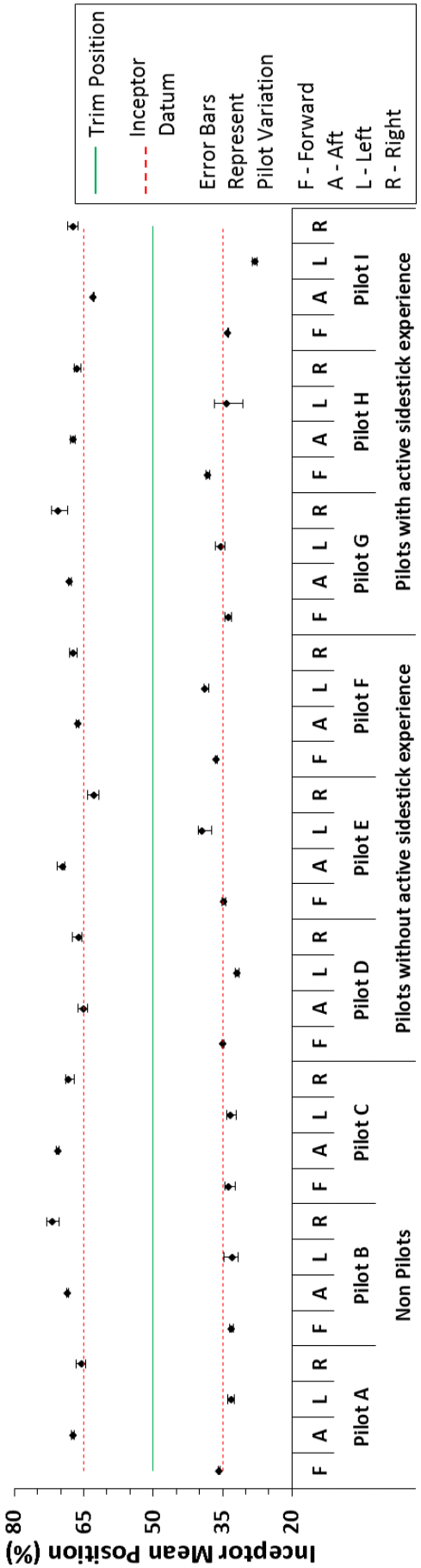

Figure 4-4: Inceptor Mean Position and Pilot Variation over 60 Seconds, without Reference to Inceptor Position, Compliant AIS Mode

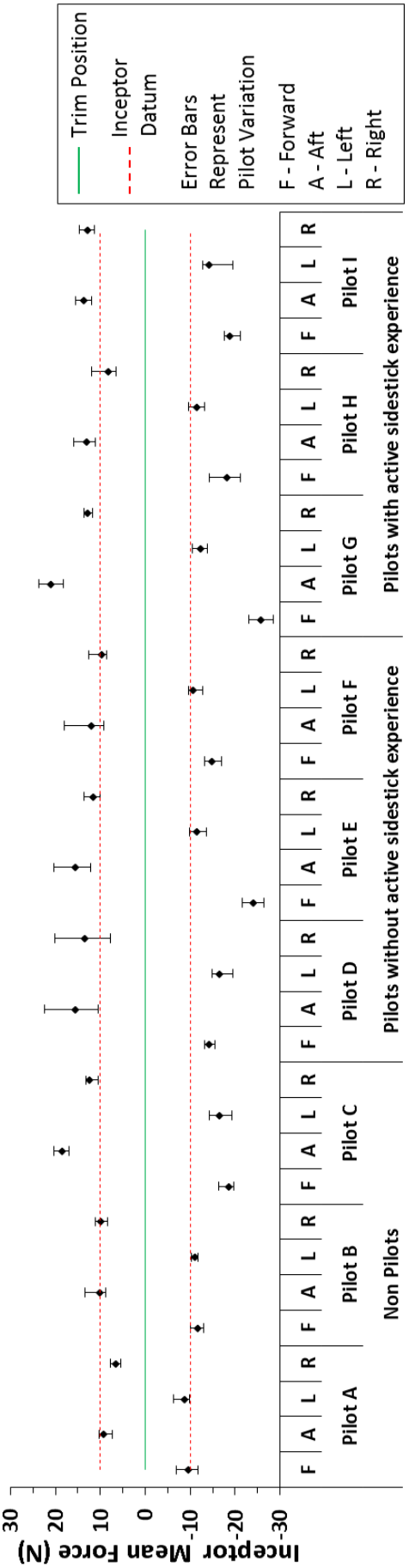

Figure 4-5: Inceptor Mean Force and Pilot Variation over 60 Seconds, without Reference to Inceptor Force, Isometric AIS Mode

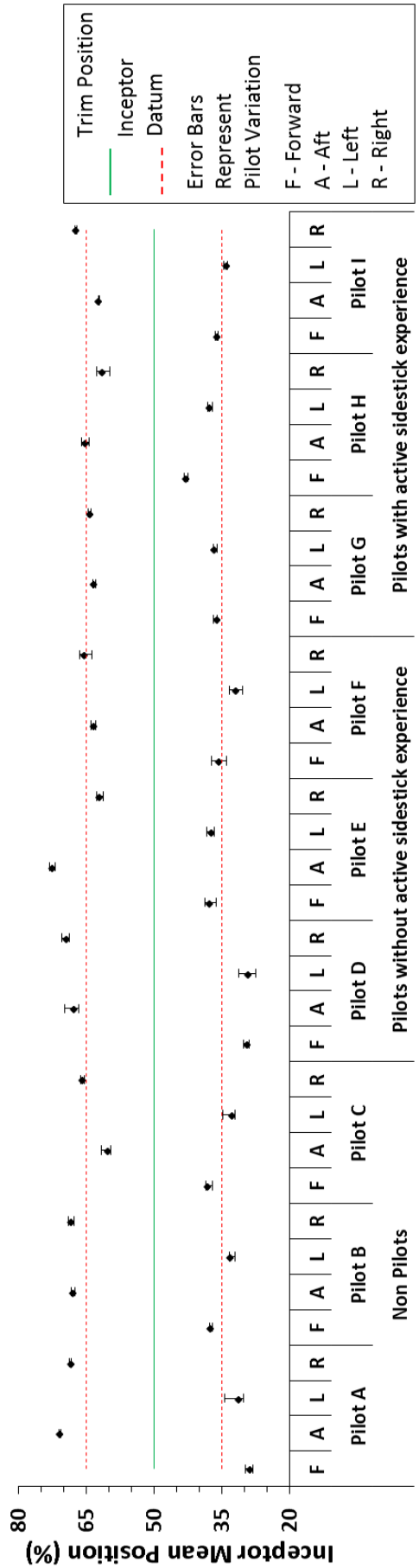

Figure 4-6: Inceptor Mean Position and Pilot Variation over 60 Seconds, without Reference to Inceptor Position, Isotonic AIS Mode

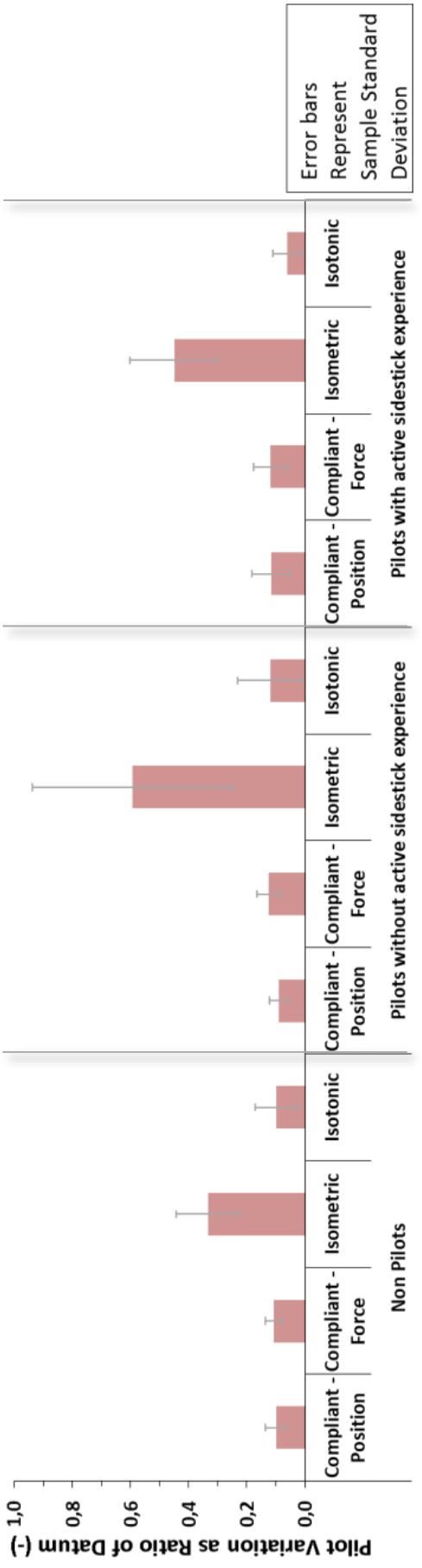

Figure 4-7: Pilot Variation of Input over 60 seconds as Ratio of Input Datum without Reference to Inceptor Values, All AIS Modes

4.4 Data Analysis and Discussion

Unless specifically stated, the following analysis refers to the test points during which the participants had no reference to the inceptor position or force.

Figures 4-4, 4-5 and 4-6 refer to the different AIS modes respectively: compliant, isometric and isotonic. They describe the Inceptor Mean values for each participant in each of the cyclic axes (F-forward, A-aft, L-left, R-right) during which the participant had no reference to the position or force indications. The Pilot Variation during the 60 seconds of the test point is indicated by the error bars on each individual data point. The Inceptor Trim Position is indicated by the solid green line at 50% inceptor position. The Inceptor Datum value is indicated by the dashed red line at ±35% inceptor position or ±10N inceptor force. The Pilot Inaccuracy is indicated by the difference between the data point and the Inceptor Datum value.

4.4.1 Pilot Variation of Sustained Inceptor Force or Positon over 60 Seconds without Reference to any Inceptor Signal Indications

Figure 4-7 shows the Pilot Variation of inceptor input as a ratio of the Inceptor Datum input (±15% or ±10N) during the 60 seconds of the test. The results are averaged across all inceptor directions and across each participant subset. The figure therefore shows a summary of the Pilot Variation identified by the error bars in figures 4-4, 4-5 and 4-6 as a function of AIS mode and participant sub-set. The error bars represent the sample standard deviation of the corresponding data set.

4.4.1.1 Comparison of Inceptor Modes

For the compliant mode, figure 4-7 identifies that all participants maintained a consistently stable inceptor position throughout each of the test points with a mean ratio of Pilot Variation to Inceptor Datum of 0.10 (sd 0.01) for the position signal and 0.12 (sd 0.01) for the force signal. Figure 4-4 confirms that the Pilot Variation was constant across each of the participant subsets. It also shows that the mean Pilot Variation across all participants for the position signal of 1.53% was relatively small in comparison to the assumed task and reading error of ±0.5% (estimated by all participants during the datum test points when the inceptor position displays were available).

Additionally and perhaps as expected by the design of the AIS, the Pilot Variation ratio from the position signal was consistent with that of the force signal across all participant subsets.

For the isometric mode, figure 4-7 shows that there was a larger ratio of Pilot Variation to Inceptor Datum in comparison to the compliant and isotonic modes. Whilst the error bars are large in comparison to the other two modes, it can be explained by the differing Pilot Variation values for the different cyclic directions that can be seen in figure 4-5 and which are further discussed in section 4.4.1.3.

Of the 36 test points recorded in the isometric inceptor mode, 4 had a Pilot Variation of less than 2.5N which was too low to identify a trend in the direction of the variation. In 28 of the remaining 32 test points, the participants consistently reduced the force applied as

the test point continued. The mean Pilot Variation of the Force across all participants was 4.6N which equated to a ratio of Pilot Variation to Inceptor Datum of 0.46 (sd 0.13) and was considered large (and significantly greater than the assumed task and reading error of ±0.5N). This result suggests that despite the participant consciously trying to maintain the force constant (with no other task to distract them during the test point) they were not able to overcome an unconscious tendency to relax the force. Furthermore, as the Inceptor Datum Force was only 10N it would be unlikely that the participants were becoming fatigued within the 60 seconds of holding the force.

In the isotonic mode, figure 4-7 shows that like the compliant mode, all participants maintained a consistently stable inceptor position throughout each of the 60 seconds test points, with a Mean Ratio of Pilot Variation to Inceptor Datum of only 0.09 (sd 0.03). Additionally, from figure 4-6 the mean Pilot Variation across all participants was 1.38% and was again relatively small in comparison to the assumed task and reading error of ±0.5%.

Comparing the data of Pilot Variation for all AIS modes shows that for all participants, the inceptor position for the compliant and isotonic modes varied by 0.10 and 0.09 of the datum value respectively and yet in the isometric mode the inceptor force varied on average by 0.46 of the datum value during each test point. This result confirms the subjective perception that the participants were much less able to retain the force constant throughout the 60 seconds of the test point in the isometric mode than in the compliant or isotonic modes. Furthermore, it can be surmised that for this test a lack of position feedback has a greater detrimental effect on the ability to maintain an inceptor input constant than the lack of a force feedback.

4.4.1.2 Comparison of Previous Experience and Training

Figure 4-7 indicates that the ratio of Pilot Variation (of control input during the 60 seconds of the test point) to the Inceptor Datum across all cyclic directions remained consistent across all participant subsets for the compliant and isotonic modes at 0.10 (sd 0.02). However, in the isometric mode it also shows that some participants were more susceptible than others to varying the inceptor force. Perhaps surprisingly, the non-pilots were the best subset at maintaining the force constant with a mean Pilot Variation Ratio of 0.33 (sd 0.11). The qualified pilots with active sidestick experience were slightly worse with a corresponding value of 0.45 (sd 0.15) and the qualified pilots without any active sidestick experience varied the inceptor force the most at 0.59 (sd 0.34).

From subjective assessment and discussions with the participants the result may be explained by the supposition that qualified pilots who are accustomed to conventional or compliant active inceptors find it easier to adapt to the isotonic inceptor mode, but if they maintain the same level of attention and effort have more difficulty in adapting to isometric inceptor modes. The non-pilots subset however is required to maintain a higher level of attention and effort during the compliant and isotonic modes than the pilot subset to achieve the same performance. Assuming that they maintain that same level for the isometric mode, they then possibly adapt quicker or make more effort to be accurate than the pilot cohort and therefore generate better results. Concurrent with this

supposition is the more appreciable result that a qualified pilot with AIS experience would be more consistent in maintaining a constant isometric force than a qualified pilot without AIS experience.

In summary, previous experience and training has a low influence on the variation of the input position throughout the 60 seconds of the test point for the compliant and isometric modes. However the training and experience has an adverse effect in the isometric mode for which non-pilots can apply a more consistent force than qualified pilots with AIS experience who in turn are more consistent than qualified pilots without AIS experience.

4.4.1.3 Comparison of Direction of Inceptor Input

With reference to figures 4-4 and 4-6 of the compliant and isotonic modes respectively, the error bars that represent the Pilot Variation of input position during the test point show only small values and no discernible correlation with any of the four cyclic directions.

Figure 4-5 shows the same data presentation for the isometric mode in which the following conclusions can be made:

- In the longitudinal cyclic axis, 7 out of the 9 participants demonstrated a lower variation of input force in the forward direction than the aft direction.
- In the lateral cyclic axis, 5 out of 9 participants demonstrated a lower variation of input force in the right direction than the left direction.
- Across both cyclic axes, 6 out of 9 participants demonstrated a lower variation of input force in the lateral axis than in the longitudinal axis.

The difference in a pilot's performance in maintaining a constant inceptor force with different cyclic direction caused a large spread of the Pilot Variation values within each pilot and AIS mode data set. In figure 4-7 the data for each pilot and AIS mode were averaged across all cyclic directions to make comparative analysis clearer, however it also resulted in the large sample standard deviations.

To surmise the influence of the cyclic input direction, there is a weak correlation that in the isometric mode a pilot can maintain a constant held input force without visual feedback reference of the values relative to the desired datum, better in the lateral axis than the longitudinal and within the axis, forward direction better than aft and right direction better than left. Furthermore, each individual participant subjectively stated that they had a preferred direction for best performance but there was a low blind agreement correlation with the other participants.

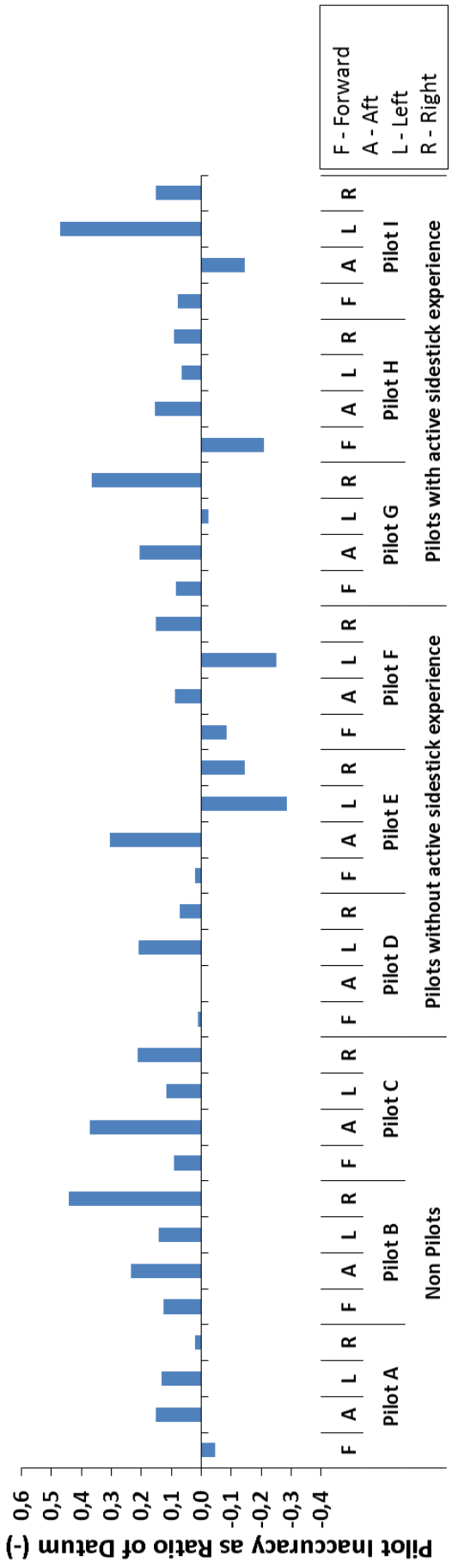

Figure 4-8: Pilot Inaccuracy as Ratio of Inceptor Datum Displacement, without Reference to Inceptor Positions, Compliant AIS Mode

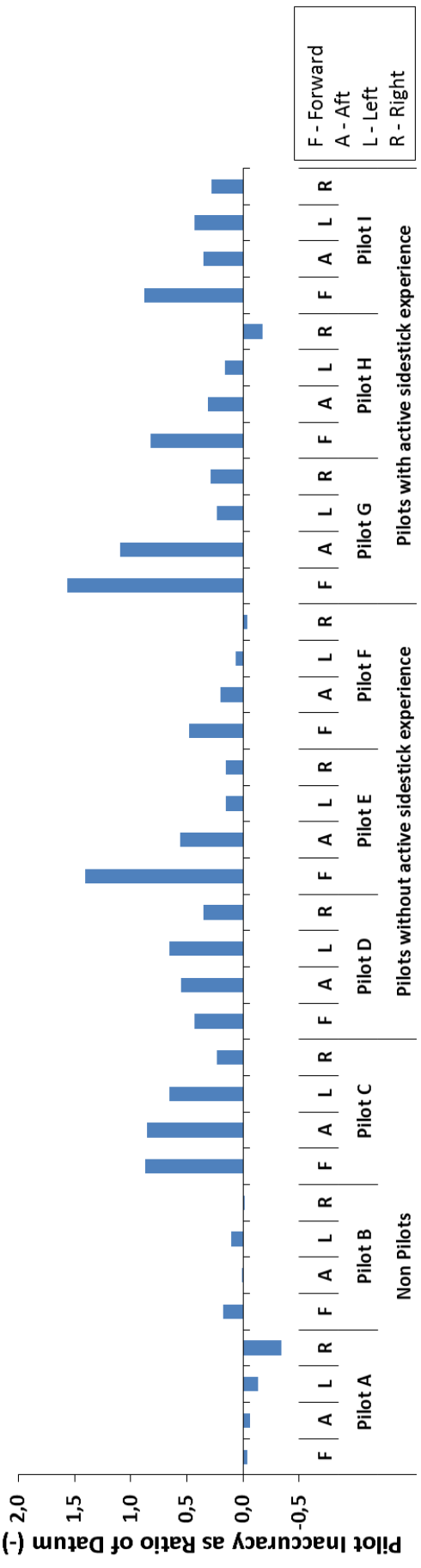

Figure 4-9: Pilot Inaccuracy as Ratio of Inceptor Datum Displacement, without Reference to Inceptor Positions, Isometric AIS Mode

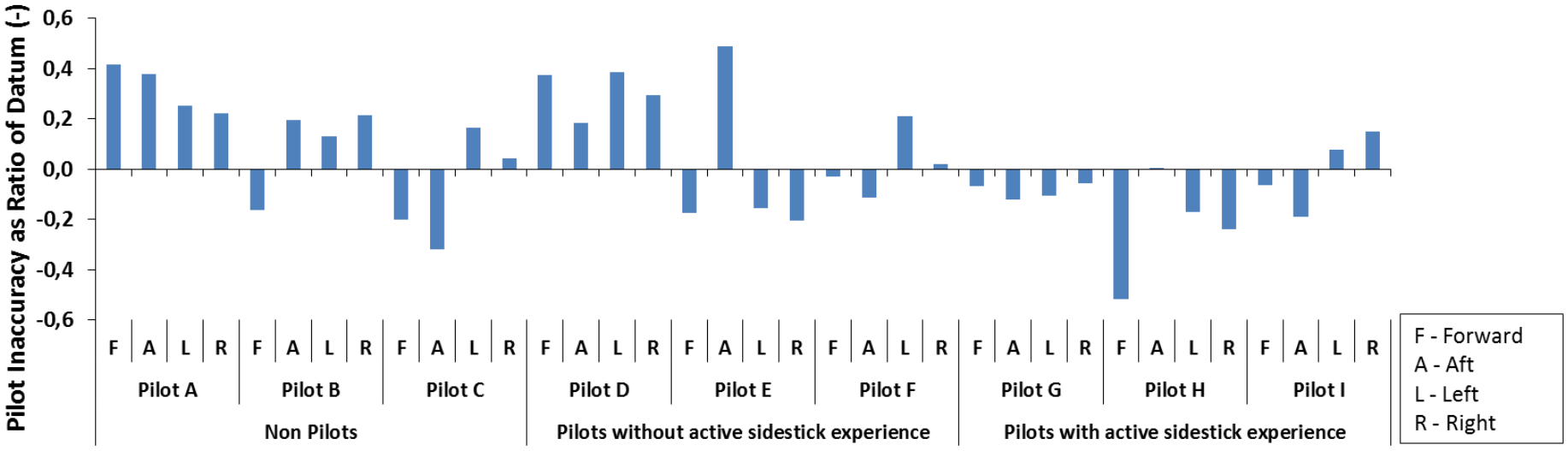

Figure 4-10: Pilot Inaccuracy as Ratio of Inceptor Datum Displacement, without Reference to Inceptor Positions, Isotonic AIS Mode

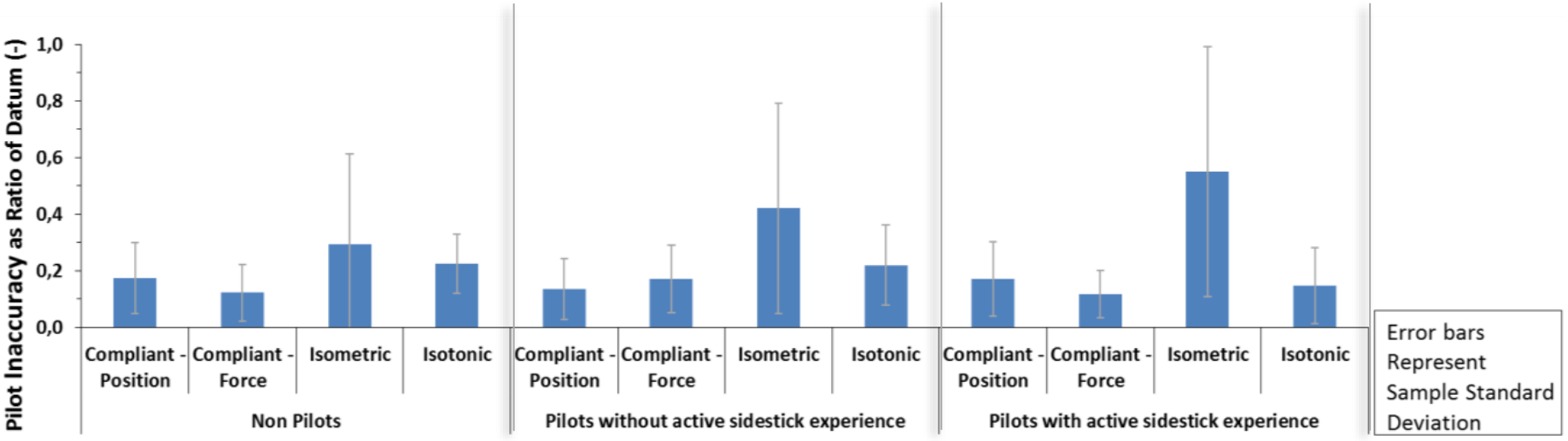

Figure 4-11: Pilot Inaccuracy of Repeating a Datum Input as Ratio of Datum without Reference to Inceptor Values, All AIS Modes

4.4.2 Pilot Inaccuracy of Repeating a Previously Held Inceptor Force or Displacement Input without Reference to any Inceptor Signal Indications

Figures 4-8, 4-9 and 4-10 describe the Pilot Inaccuracy as a ratio of the Inceptor Datum Displacement (Pilot Inaccuracy Ratio) for each participant in each of the cyclic axes (F-forward, A-aft, L-left, R-right). This ratio represents the pilot's inaccuracy in estimation of the inceptor position or force (without reference to relevant indications) relative to the previously experienced Datum Position or Force (with reference to relevant indications). A positive ratio indicates that the Pilot Inaccuracy was greater than the Inceptor Datum displacement (the participant had exceeded the required inceptor input in the given direction) and vice versa.

Figure 4-11 shows data of the Mean Magnitude of Pilot Inaccuracy Ratio. These results are averaged across all inceptor directions and across each participant subset. The figure therefore shows a summary of the Pilot Inaccuracy identified by the difference between the Inceptor Datum and the Inceptor Mean for each of the test points in figures 4-8, 4-9 and 4-10 as a function of AIS mode and participant sub-set. As the values were averaged from absolute values they do not indicate whether the participant over or under estimated the input required. The error bars represent the sample standard deviation of the corresponding data set. For all participant subsets in the isometric mode these standard deviations were large, which could be attributed to the data variation depending on the direction of cyclic input, as discussed in section 4.4.2.3.

4.4.2.1 Comparison of Inceptor Modes

Figure 4-11 shows that across all participant sub-sets the mean magnitudes of Pilot Inaccuracy Ratios were similar for the compliant and isotonic inceptor modes (0.14 and 0.16 respectively). This indicated that the participants were able to achieve similar accuracy of input for both of the modes that offered position feedback and the accuracy was independent of whether the mode offered a force feedback. Conversely, the Mean Magnitude of Pilot Inaccuracy Ratio across all participant sub-sets for the isometric mode (0.42) was over double that for the compliant mode, suggesting that the accuracy of input for the modes that offered only force feedback was far less than for the mode which offered any position feedback.

Furthermore, it is apparent that this result has even greater significance for both of the qualified pilots sub-sets (Pilot Inaccuracy Ratio compliant: 0.15, isotonic: 0.19 and isometric: 0.49) than for the non-pilot sub-set (Pilot Inaccuracy Ratio compliant: 0.15, isotonic: 0.22 and isometric: 0.29). A possible cause for this is considered in paragraph 4.4.2.2.

With reference to figure 4-9 it can be seen that for 78% of the isometric test points the Pilot Inaccuracy was positive, indicating that the participants exceeded the desired input force. This is shown as a potentially significant influence on the development of oscillatory APCs as discussed in section 4.5. The worst case of all test points was of pilot G applying a longitudinal force forward of 25.67N (2.57 times of that required).

Hence from these results, it can be surmised that the accuracy of a pilot to repeat a previously held inceptor force or position input without reference to any inceptor mode indications is worse for the isometric mode than for the compliant and isotonic modes. It can thus be concluded that the inceptor position is of greater influence to the pilot than inceptor force for making repeated and consistent control inputs

4.4.2.2 Comparison of Previous Experience and Training

With reference to figure 4-11, in the compliant mode it can be seen that the non-pilots were able to select the desired Datum Inceptor Position with a similar success as the qualified pilots. The Mean Magnitude of Pilot Inaccuracy Ratio across all axes for both the non-pilots and the qualified pilots was 0.15. All of the qualified pilots in this assessment had been trained and had acquired most of their flight experience from conventional inceptors which incorporated both position and force feedback cueing. During these hours of experience they had developed the skills to use these feedback cues to make small but accurate control inputs. This developed use of conventional inceptors had not been available to the non-pilots yet they were able to instinctively apply similar levels of accuracy.

The greatest difference however between the pilot and non-pilot subsets in the compliant mode can be seen in figure 4-8 where the Pilot Inaccuracy Ratios of the non-pilots were positive for 92% of the test points whereas for the qualified pilots they were positive for 71%. This indicates that whilst the overall inaccuracy was similar, the non-pilots had a stronger trend of consistently exceeding the required input than the qualified pilots who applied both too large and too small an input in a more inconsistent trend.

For the isometric mode, figure 4-11 shows that amongst all qualified pilots the Mean Magnitude of Pilot Inaccuracy Ratio was 0.49 and indicated a high level of inaccuracy. The corresponding Mean Magnitude of Pilot Inaccuracy ratio for the non-pilots was 0.29 which whilst it still represented a large error, was just 60% of the inaccuracy of the qualified pilots. More specifically, two of the three non-pilots were significantly more accurate than the qualified pilots at applying the required force with a Mean Magnitude of Pilot Inaccuracy Ratio of just 0.10 across all cyclic axes (the third non-pilot was of a similar accuracy to the qualified pilots).

As a result of training and the long exposure time to conventional inceptors in the compliant mode, the qualified pilots' psychomotor memory was more developed [125], specifically through the expected and limited range, rate and opposing force of the normal inceptor movement. This developed a predominantly sub-conscious skill that caused better recollection and higher accuracy in the selection of a position and force of the inceptor in the compliant mode. Conversely, the extensive pre-conditioning of the qualified pilots to the compliant inceptor mode caused worse performance in the isometric mode where they needed to adapt their control strategy away from long established psychomotor expectations. The non-pilots had not yet developed the psychomotor memory with regards to either compliant or isometric inceptors and were therefore more adaptable to both the conventional and unconventional control strategies.

In the Isotonic mode figure 4-11 shows that amongst all qualified pilots the Mean Pilot Inaccuracy Ratio was 0.19 which when compared to the same ratio of 0.22 for the non-pilots indicates that for the isotonic mode the qualified pilots were marginally more accurate than the non-pilots. Figure 4-10 also shows that the qualified pilots generated negative ratios on 14 of their 24 test points (58%), whereas the non-pilots generated negative ratios on 3 of their 12 test points (25%). This indicates that the qualified pilots underestimated the inceptor displacement on more than double the occasions than the non-pilots.

In summary, the previous experience and training of the qualified pilots had little effect on the Pilot Inaccuracy for either the compliant or isometric modes. In the isometric mode however, the qualified pilots had greater difficulty in adapting to the unconventional control strategy and were on average 60% less accurate than the non-pilots in repeating a defined control force input without visual feedback of the AIS values.

4.4.2.3 Comparison of Direction of Inceptor Input

From figure 4-8 in the compliant mode, the distribution of the Pilot Inaccuracy Ratios showed no discernible correlation with either axis or direction.

Figure 4-9 shows the same data presentation for the isometric mode in which the following conclusions can be made:

- In the longitudinal cyclic axis, 7 out of the 9 participants demonstrated a higher Pilot Inaccuracy Ratio in the forward direction than the aft direction. This result opposed that for the Pilot Variation identified in 4.4.1.3.
- In the lateral cyclic axis, 5 out of 9 participants demonstrated a higher Pilot Inaccuracy Ratio in the left direction than the right direction. This marginal result concurred with that identified in section 4.4.1.3 in that the Pilot Variation was also worse in the left direction.
- Across both cyclic axes, for 8 of the 9 participants the Pilot Inaccuracy Ratios were higher in the longitudinal axis than the lateral axis. Furthermore, a tendency to apply a greater force than required was over three times as severe in the longitudinal axis (Pilot Inaccuracy Ratio +0.58) as in the lateral axis (+0.17). This result concurred with that identified in section 4.4.1.3 in that the Pilot Variation was also worse in the longitudinal axis.

From figure 4-10 in the isotonic mode the distribution of the Pilot Inaccuracy Ratios showed no discernible correlation with either axis or direction.

The difference in a pilot's performance in accurately repeating the desired input with different cyclic direction caused a large spread of the Pilot Inaccuracy values within each pilot and AIS mode data set. In figure 4-11 the data for each pilot and AIS mode were averaged across all cyclic directions to make comparative analysis clearer, however it also resulted in the large sample standard deviations.

In summary, the direction or axis of the input had little effect on the Pilot Inaccuracy Ratio in either the compliant or isotonic modes but in the isometric mode there was a

weak correlation that the participants were able to repeat a datum force without visual feedback reference, with greater accuracy in the lateral than the longitudinal axis, aft greater than forward and right greater than left. Furthermore, and similar to the Pilot Variation opinion each individual participant subjectively stated that they had a preferred direction for best performance but there was a low blind agreement correlation with the other participants.

4.5 Effect of Pilot Inaccuracy on APC Excitation and Suppression in Isometric Mode

As previously identified from figure 4-9, for the isometric mode across all participant subsets (but most strongly across the qualified pilots subsets), there was a tendency to apply a greater force than required. The participants therefore overestimated the required force in the isometric mode that they recalled from the previous test in the compliant mode and with the inceptor force displayed.

This phenomenon is likely to be a contributing factor to the development and maintenance of the oscillatory APCs that will be identified in section 7.3.1 at higher apparent gains. This argument can be justified by considering the pilots response to an external disturbance. In the compliant inceptor mode, the pilot's control inputs are roughly proportional to and in opposition to the aircraft's translational or rotational rate. For pilots with even minimal flying experience, the magnitude of the required input is intuitive. In the isometric inceptor mode, the pilot is still conscious of the magnitude of the required control input to oppose the aircraft's motion, but until he/she adapts to the new control strategy he/she unconsciously applies a greater magnitude than that required. The result is an over-reaction of the aircraft beyond the desired stabilising flight condition, therefore causing a state which itself needs to be opposed in order to stabilise the aircraft.

A limitation of this argument is that it assumes that the pilot is controlling the aircraft in finite consecutive steps at a low pilot feedback rate through observing the disturbance, making a control input proportional to the disturbance and then observing the aircraft reaction to the control input. As the pilot feedback rate increases, the pilot may observe during the control input that the aircraft reaction is too aggressive and reduces the size of the initial control input thereby suppressing the APC (consistent with the control strategy adaptation process). However, certain conditions (high initial disturbance magnitude, degraded visual environment, inexperienced / under-performing pilot, pilot distraction or high pilot workload) may cause a low pilot feedback rate which would become one of the causal factors of the APC development.

These conscious and unconscious pilot reactions are similar to those witnessed during the recovery phase immediately after the initiation of the isometric inceptor mode that were previously identified during the qualitative AIS failure investigation flight [82]. The resulting excessive control input magnitudes (as well as the phase lag to the aircraft response) caused an oscillatory cycle which unless suppressed by determined pilot effort developed into an oscillatory APC.

In summary, for pilot-aircraft systems that are already APC prone, the sudden change of inceptor mode from compliant to isometric can present a trigger for APC development.

4.6 Summary

An investigation was conducted in the DLR AVES helicopter simulator to establish some pilot-machine interface characteristics of the active sidesticks in the compliant, isometric and isotonic modes. It was also hoped that the investigation could help to explain why the oscillatory APCs identified in earlier research were more likely in the isometric mode than in either the compliant or isotonic modes.

Initially, in the compliant mode the participants were tasked with selecting an inceptor force or displacement with the relevant values available on a cockpit display. The participants were then tasked with repeating the same inceptor force or position without the relevant values available and holding the condition for 60 seconds. The inaccuracy of the control input as well as its variation over the 60 seconds was recorded and analysed. Test points were conducted in each axis direction and in each AIS mode. In total, 9 participants were used as test subjects: 3 non-pilots; 3 qualified pilots without AIS experience and 3 qualified pilots with AIS experience.

The following analyses and conclusions were reached that reflected the objectives of the investigation:

- The consistency of a participant to maintain a prolonged constant inceptor input without reference to any inceptor signal indications was influenced by:
    - The inceptor mode. Only small variations were identified for both the compliant and isotonic modes. For the isometric mode however the variations were significantly worse with a mean force input range of 4.6N during the 60 seconds.
    - The participant's previous experience and training. A low influence on the variation was observed for the compliant and isotonic modes. However the training and experience had an adverse effect in the isometric mode for which non-pilots were able to apply a more consistent force than qualified pilots with AIS experience, who in turn were more consistent than qualified pilots without AIS experience.
    - The direction of the cyclic input. There was a weak correlation that in the isometric mode the variation was less in the lateral axis than the longitudinal axis and within the axes, forward direction was less than aft and right direction less than left.
    - Additionally, it was observed that in the isometric mode and without reference to any inceptor force indications, pilots had an unconscious tendency to reduce the force applied to the inceptor over time.

- The accuracy of a participant to repeat a previously held inceptor input without reference to any inceptor signal indications was influenced by:
    - The inceptor mode. The inaccuracy observed for both the compliant and isotonic modes, averaged across all participants, was small and essentially constant. The inaccuracy observed in the isometric mode however, was significantly higher at almost three times that of the compliant mode.

  - The participant's previous experience and training. This had little effect on the Pilot Inaccuracy for either the compliant or isometric modes. In the isometric mode however, the qualified pilots had greater difficulty in adapting to the unconventional control strategy and were on average 60% less accurate than the non-pilots
  - The direction of the cyclic input. There was a weak correlation that the participants were able to establish greater accuracy in the lateral axis than in the longitudinal axis, aft direction greater than forward and right direction greater than left.

- In terms of both the participant's ability to maintain a constant inceptor input and their ability to accurately repeat a previous input, the isometric mode created detrimental conditions. It can be concluded therefore that the inceptor position is of greater influence to the pilot than inceptor force for making repeated, consistent and sustained control inputs.

- With the information from both chapter 7 and this chapter, it was identified that for pilot-aircraft systems that are APC prone, the sudden change of inceptor mode from compliant to isometric presented a trigger for oscillatory APC development.

Chapter 5: Isometric Test Development

5.0 Overview

This chapter covers the progressive development of a flight test method and an analysis protocol for an isometric failure of an active sidestick controller. Together they are designed to be used either to confirm safety compliance as required by certification specifications or to modify system configuration for optimised HQ. The development process starts with the identification of the most appropriate failure test philosophy and an introduction to a modified version of the IFES that is used as the metric of HQ deterioration and perceived safety. A comparison with the previous development strategy of the isotonic MTE is made with a discussion of its limited suitability for the isometric case. The isometric MTE development is then described through 4 phases: investigation of the effect of different pre-failure conditions for a low gain task; identification of the most appropriate ADS-33E MTE for a high gain task; investigation of the effect of different pre-failure conditions for a high gain task with definition of the corresponding MTE parameters and tolerances and finally, the implementation and refinement of the defined MTE solution.

5.1 System Failure Testing Criteria

Failure testing of rotorcraft control systems generally use one, or a combination, of the following three classic test criteria:

- Failure Modes and Effects Analysis (FMEA);
- Response time analysis;
- Probability independent analysis.

5.1.1 Failure Modes and Effects Analysis

ADS-33E [36] and the AGARD [69] refer to FMEA within flight control systems as the analysis of allowable degradation of HQ based on probability. The process involves identifying all possible aircraft control failure states; determining the corresponding transient and long term effects on the aircraft's HQ level and determining the probability of each failure state per flight hour. The total probability of the aircraft's HQ degrading to HQ level 2, 3 or a loss of control is then calculated and compared to the specification in table 5-1. The definitions of Operational Flight Envelope (OFE) and the Service Flight Envelope (SFE) are stated in ADS-33E (repeated in section 5.3) and the HQ levels are measured in accordance with Cooper and Harper [51]. A design organisation[52] must demonstrate that the accumulated probability of all failures that lead to each level of degradation is less than in the specification.

The probabilities, acceptable degradation and definitions differ for various airworthiness authorities (EASA, FAA[53], MAA[54]) [26, 27, 46, 92, 93] and not all authorities follow the

[52] An organisation approved by a governing authority to design aircraft, components, repairs or modifications

[53] Federal Aviation Administration (US)

ADS-33E criteria. However in all cases, in order to achieve certification of a new control system, they are consistent that a design organisation must either demonstrate a low severity of the failure; a low probability of the failure or a combination of both (as defined by the applicable airworthiness authority). Generating a low probability of the failure is dependent on numerous factors, including design assurance, model predictions, parts and materials quality assurance, production quality management, bench, simulator and flight testing, through life monitoring, design life predictions, maintenance and expected risk exposure frequency sourced from the Statement of Operational Intent and Usage (SOIU). Gathering the evidence and calculating the failure probability is therefore a complicated process that remains a theoretical estimate and needs continuous updates during the system's lifetime. Fortunately, the analysis of failure probability is outside of the scope of this study.

Handling Qualities after Failure	Probability of Encountering Failure	
	Within Operational Flight Envelope	Within Service Flight Envelope
Level 2	$<2.5 \times 10^{-3}$ per flight hour	-
Level 3	$<2.5 \times 10^{-5}$ per flight hour	$<2.5 \times 10^{-3}$ per flight hour
Loss of Control	$<2.5 \times 10^{-7}$ per flight hour	-

Table 5-1: Levels and Probabilities of Rotorcraft Failure States (source: ADS-33E [36])

The certification specification found in ADS-33E has one major limitation for use in the isometric failure case, in that the failure degradation is only referenced to the Cooper Harper HQ levels. The use of these levels is appropriate for the long term control of an aircraft after the transient and recovery effects have subsided and whilst the mission is continued or a landing accomplished. Existing ADS-33E MTEs can easily be used with the Cooper Harper Rating (CHR) scale for this purpose. However the certification specification does not reflect the transient and recovery phases immediately after a failure which are often the dominant characteristics of the isometric failure and neither the extant ADS-33E MTEs nor the CHR scale are suitable to assess their severity.

5.1.2 Response Time Analysis

Response time analysis is used for failures associated with many safety critical systems including engine, gearbox and control components for which the effects can be ameliorated by pilot action. It is particularly relevant where the control failure affects the flight path of an aircraft and a time critical response is required from the pilot to avert a

[54] Military Aviation Authority (UK); Military Airworthiness Authority (US)

catastrophic outcome, for example after a cyclic trim motor runaway. The process, described in [94], involves incrementally increasing the intervention time taken from failure initiation to pilot response until either the recovery action would become unsafe or the time stated in a specification is reached. The determination of when the recovery action becomes unsafe may be identified by the trend towards a safety or SFE limit of a critical parameter (e.g. rotor RPM, load factor or height loss). The selection of one or more critical parameters is based upon test experience and analysis of the failure mode as well the necessity for their presentation to the test pilot in real time on a cockpit Flight Test Instrumentation (FTI) display. The time taken for the pilot to respond is referred to as the Pilot Response Time (PRT) and encompasses both the pilot decision time and the pilot reaction time. Specifications such as Defence Standards[55] [94] detail minimum PRTs that must be demonstrated of a successful recovery from a failure initiated from within the OFE.

The rotorcraft response time (RRT) is defined as that between the failure occurrence and the aircraft indicating or presenting its failure. The relationship between RRT, PRT and intervention time can be summarised by equation 5-1.

$$Intervention\ Time = RRT + PRT$$

Equation 5-1

The timing of the PRT requires a well-defined start point such as a warning light, audio alert or a clearly detectable uncommanded change of flight path. If there is no warning system or if the failure is initially benign, it would lead to an additional delay in the RRT therefore reduce the chance of a successful recovery after the corresponding minimum PRT.

Pilots control aircraft with different control attentiveness during different phases of flight depending upon the pilot feedback gain required and level of augmentation applied. Table 5-2 defines the pilot control attentiveness phases in accordance with Defence Standards and states the corresponding minimum PRT with which a safe recovery must be achievable in order to comply with the standard.

For the isometric failure, if there was no audio or visual warning (as for the test system used in this study) the RRT would depend on the pilot attentiveness level. For example, in an active phase the pilot would immediately feel the frozen control and so the RRT would be close to zero. However for a hands off phase, it could persist indefinitely or until the pilot changed to a hands on phase and attempted to control the aircraft. Therefore in the isometric failure case, a variation in pilot attentiveness phase causes a variation in both the RRT and the required PRT, which would hinder the effective use of this criterion.

Furthermore, the criterion assumes that it is possible to recover from a failure that has been initiated in any antecedent condition and configuration, and success is dependent only on the delay time in the pilot commencing the recovery action. Within the isometric failure case it will be seen that a successful recovery may in some conditions not be

[55] Defence Standard 00-970, Part 7, Issue 2, Leaflet 604

achieved even with negligible PRT and in other conditions may be more probable if the pilot delayed the initial response. For this reason, the response time analysis would be an ineffective criterion for the investigation and optimisation of the HQ during isometric failures.

Pilot Control Attentiveness Phases	Definition	Required Minimum PRT for safe recovery (s)
Active	Flight segment during which the pilot is using the flight controls to continuously maintain or change the flight path of the aircraft (e.g. landing)	0.5
Attentive – Hands On	Flight segment during which the pilot must pay particular attention and make occasional control inputs for short periods (e.g. manual instrument flight)	1.5
Attentive – Hands Off		2.5
Passive – Hands On	Flight segment during which the pilot need only give minimal amount of attention to controlling the flight path or monitoring an autopilot (e.g. cruise flight)	2.5
Passive – Hands Off		4.0

Table 5-2: Pilot Control Attentiveness Phases Definitions and Minimum PRTs [46, 94]

The response time analysis criterion does however provide some rationale for using an active flight phase within the subsequently developed isometric MTE, such that the pilot is immediately alerted to the failure and it provokes a control response. A hands off flight phase would stimulate no control inputs and the failure would remain dormant until the flight phase changes and the pilot increases his control involvement. This judgement is further supported in section 5.5.1.2 in which the requirement to expose oscillatory APCs by maintaining a high feedback gain task during and after the failure is discussed.

5.1.3 Probability Independent Analysis

ADS-33E [36] defines failures that must be assumed to occur regardless of their probability as ‘specific failures’ and provides an incomplete list of events that must be considered as such. Of particular relevance is the inclusion of ‘*Failure-induced transient motions and trim changes either immediately after failure or upon subsequent transfer to alternative control modes.*’ For all ‘specific failures’ evidence must be gathered to demonstrate that the occurrence of the failure throughout the OFE and SFE does not cause dangerous or intolerable flying qualities.

Probability independent failure testing investigates whether the pilot can recover the aircraft in different pre-failure conditions, ultimately reaching the worst case of all relevant parameters. If the transient response or recovery action exceeds the safe boundary, then prohibition of certain conditions must be recommended and the SFE limited.

It is apparent that the failures or partial failures of an active sidestick would constitute a 'specific failure' as defined by ADS-33E. Consequently, in order for an aircraft fitted with such a control system to be certified, it must demonstrate that, regardless of probability of the failure, the aircraft can be controlled safely and effectively in the transient and long term degraded state.

5.2 Isometric Test Philosophy

Analysis of the three identified testing criteria in the context of the isometric failure, identifies that the ADS-33E referenced FMEA criterion disregards the transient and recovery phases, and the response time criterion inappropriately assumes a better chance of a successful recovery with a quicker pilot response. The specific failures criterion however considers that as the sidestick is a safety critical system without redundancy, it must be safe for all stages of flight whilst in a degraded mode. A helicopter suffering a failure of such a system should be able to survive both the moment of failure and a subsequent period sufficiently to allow the flight to be completed [69]. The isometric test development therefore adopted the general philosophy of the specific failures criterion that focused on absolute safety in all circumstances and ignored failure probability and the initial recognition time of the failure.

In order to substantiate an argument for safe flight after a failure event, a demanding and applicable test profile with a complementary subjective rating scale was needed that was analogous to an ADS-33E [36] MTE and the HQ Rating scale of Cooper and Harper [51]. The subjective rating scale would be needed not just for the evaluation as part of the final MTE but also in the development of the MTE by helping the test pilots to identify the applicable conditions that would expose the worst handling deficiencies.

5.3 IFES Rating Scale

Whilst the generally accepted CHR scale [51] functions adequately for continuous or well blended control laws, it shows limitations for sudden discontinuities that are observed during hard-overs or active sidestick failures. During the transient phase of the discontinuities, the safety-of-fight concerns are more significant than maintaining desired or adequate tolerances and the pilot compensation metric used in the CHR proved inappropriate. Furthermore, the success of the recovery phase is highly dependent on the urgency and effort with which the pilot makes the corrective actions and these are also not reflected in the CHR scale.

The qualitative assessment of the safety-of-flight and deterioration in HQ immediately after the failure was therefore based on the IFES. This was first developed as the Extended Failure Rating Scale by Hindson, Eshow and Schroeder [47] and subsequently the Failure / Recovery Rating (FRR) scale by Kalinowski, Tucker, and Moralez III [70].

These scales were specifically developed for investigations of the transient effects and subsequent pilot recovery actions after sudden changes in helicopter flight control systems.

The FRR descriptors were established from the considerations that Hindson, Eshow and Schroeder understood to be most significant:

- The urgency required for recovery.
- The orderliness with which the several control phases of the failure event can be accomplished.
- The amplitude or coordination of the multi-axis control inputs required to recover.
- The compensation or adaptation required to stabilise the new dynamic characteristics.
- The additional compensation and workload that may result from the need to urgently and precisely control both inner attitude loops and outer position loops to avoid obstacles.

Similar to the CHR with its adequate and desired tolerances, the description of 'Safe Flight' in the IFES descriptors is dependent on the task, the aircraft and the environment. A high gain task such as an instrument approach would have safety-of-flight factors that would include engine, transmission and flight envelope limitations. These factors are considered in the IFES scale by comparing the aircraft's transient states to the OFE and SFE. ADS-33E [36] defines these envelopes:

- The Operational Flight Envelope shall define the boundaries within which the rotorcraft must be capable of operating in order to accomplish the operational missions detailed within ADS-33E (and the isometric MTE detailed in 5.5.4.4). These envelopes shall be defined in terms of combinations of airspeed, altitude, load factor, rate of climb, side-velocity and any other parameters specified by the system specifications, as necessary to accomplish the operational missions.

- The Service Flight Envelope shall be derived from the rotorcraft limits as distinguished from the mission requirements. These envelopes shall be expressed in terms of the parameters used to define the OFEs, plus any additional parameters deemed necessary to define the appropriate limits. The inner boundaries of the SFEs are defined as coincident with the outer boundaries of the OFEs. The outer boundaries of the SFEs are defined by one or more of the following: uncommanded rotorcraft motions or structural, engine / power train or rotor system limits.

Finally, Weakley et al [71] modified the FRR scale which used both the OFE and SFE as transient aircraft performance indicators by replacing all references of the OFE with the SFE. Their reasoning being that the purpose of the OFE was to maintain level 1 without failures, whereas the SFE was only to maintain level 2 flying qualities and was considered a more appropriate standard in a failed condition.

Padfield developed the ratings further by integrating the FRR with the CHR to produce a single scheme that reflected short term (defined as the transient phase), mid-term (defined as the recovery phase) and long term (defined as the continuation of flight phase) effects, which was then referred to as the IFES [95].

The IFES scale uses a decision tree based process, similar in construct to the CHR, in order to narrow down the possible ratings that may be assigned. The decision tree is entered at the bottom left and the pilot is asked first whether the recovery was possible and then whether the transitions were safe (or tolerable). The pilot must then assign a rating using the most appropriate descriptor permitted by the answers given to the previous 2 questions.

By definition of the IFES scale decision tree questions, assigned ratings of A-E for either the transient or recovery phases were regarded as tolerable and safe. Conversely, the ratings F-H were considered intolerable and unsafe.

Separate and independent ratings of the transient and recovery phases were allowed to be assigned that were not necessarily identical or even adjacent to one another's rating. An intermediate rating was permitted, providing that it didn't cross the tolerable / intolerable boundary at E/F.

Similar to the requirements of the CHR scale defined in ADS-33E [36], the IFES scale also had to be assessed by at least three test pilots. In accordance with the originators' instructions and whilst acknowledging the non-linear characteristics of subjective rating scales, the arithmetic average across all pilots was calculated and formed the overall rating for the specific MTE, environment and aircraft configuration [47].

The IFES scale assumes that the rotorcraft in its pre-failure state has level 1 HQ (Cooper Harper Rating 1 to 3.5). This prerequisite is in order to assert that any identified poor HQ or reduction in safety margins are attributed to the degradation of the system and not the rotorcraft or MTE itself.

The initial validation of the scale was conducted with respect to hard-over signals during the development of a UH-60 variable stability experimental helicopter (RASCAL) both in a simulator and subsequently in the aircraft during its monitor performance assessment. It was also successfully used in flight trials of a variable stability CH47B during the initial validation of the scale [47] and a variable stability Bell 206 during an APC investigation using active inceptors [96]. In the DLR AVES simulator, the IFES scale has been used in specifically relevant active sidestick scenarios to investigate APCs during isometric failures with different signal limiters [15] and to investigate transient recovery handling during isotonic failures [35].

As stated in chapter 1 the specific interest of this study was to research only the transient and recovery phases of the isometric failure. The long term phase was not investigated and so whilst the format of the IFES has been used, the long term section has been omitted.

Additionally, as a result of test pilot feedback within this study, the four descriptors in table 5-3 were changed from the original wording by Hindson et al [47] to provide more

clearly defined pilot effort (changes shown in italics). The test pilots suggested that including the additional 'effort' reference for recovery ratings B and C would help to increase the linearity of the severity and be less ambiguous to individual pilot's interpretation. In its previous form, there was no reference to 'pilot effort' for ratings B and C and so an assumption would have to be made by the pilot whether that meant there was negligible effort required or whether the level of effort reflected the level of urgency.

Recovery Rating	Original Descriptor [47]	Amended Descriptor
B	Corrective inputs with minimal urgency	Corrective inputs with minimal urgency *and / or low pilot effort*
C	Corrective inputs with moderate urgency	Corrective inputs with moderate urgency *and / or moderate pilot effort*
D	Corrective action requires immediate and considerable pilot effort	Corrective action requires immediate and */ or* considerable pilot effort
E	Corrective action requires immediate and extensive pilot effort	Corrective action requires immediate and */ or* extensive pilot effort

Table 5-3: Modified IFES Recovery Rating Descriptors

The change of the logic in each recovery rating from 'urgency *and* pilot effort' to 'urgency *and / or* pilot effort' also sought to reduce ambiguity. In some early preliminary subjective investigations by pilots G and H, situations were observed in which the effort was extensive in suppressing an APC, but the urgency required was not immediate. In fact in most cases reacting later caused the APC to develop slower, weaker and was consequently easier to suppress. It was therefore more appropriate that the severity of the recovery should be described by the most severe factor of either the urgency or the pilot effort.

The original and modified versions of the IFES scale were explained to the test pilots H, J, L and K during the practice sessions prior to their assessments for the first order filter investigation (chapters 6 and 7). During these sessions the test pilots were able to fly the isometric MTE (detailed later in this chapter) and to practice using the scales without recording the data. Unanimously, the test pilots were in favour of the modifications due to the reduction in potential ambiguity. They confirmed that the modified IFES scale was applicable to the isometric failure and that it contained appropriate decision processes and descriptions for the HQ and APCs that were encountered. Furthermore, three of the pilots particularly stressed the importance of the accompanying instructions that the ratings should be awarded in relation to the most severe factor of either urgency or pilot effort. The final version of the modified IFES rating scale that has been used throughout this study is presented in figure 5-1.

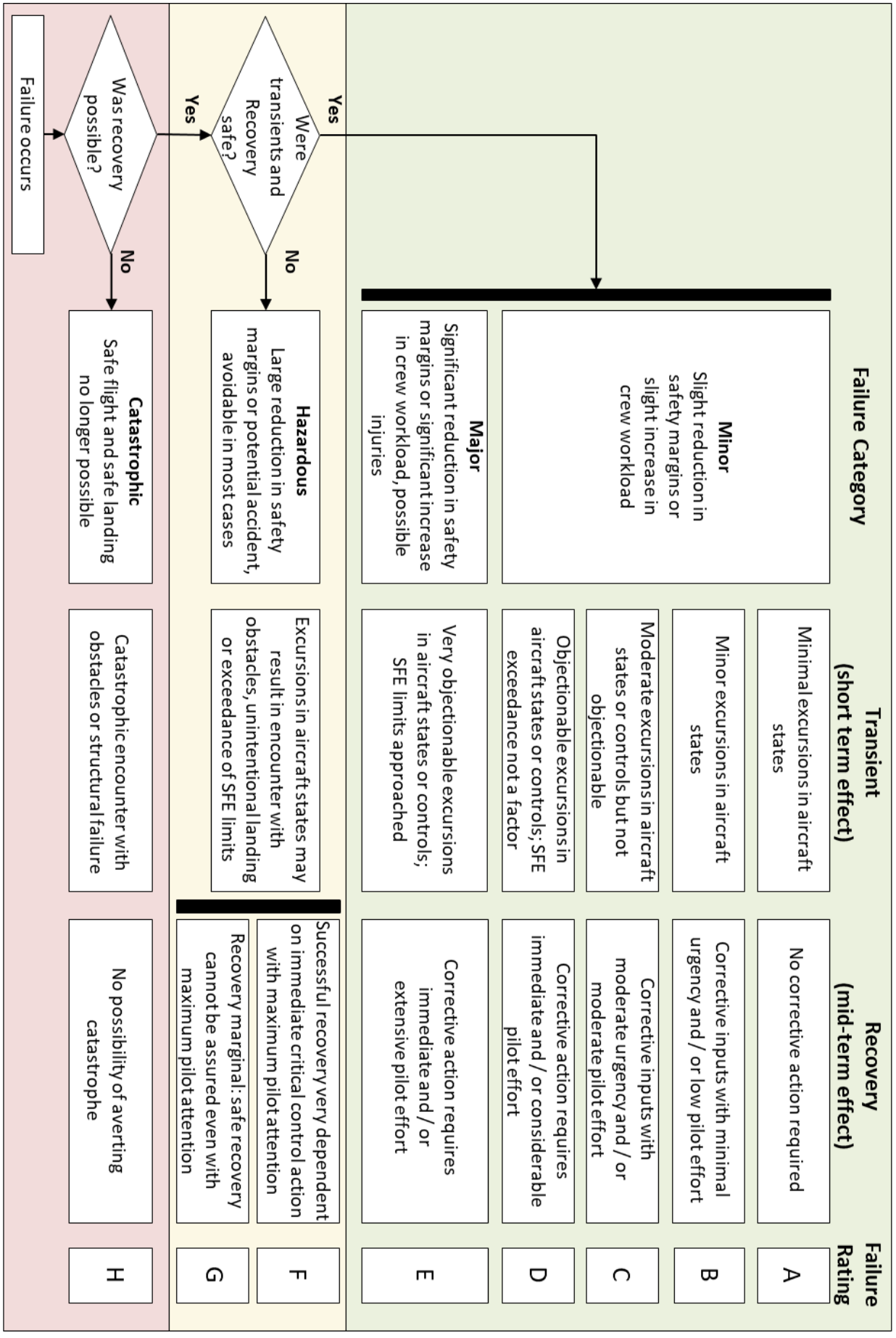

Figure 5-1: Modified Integrated Failure Evaluation Scheme

5.4 Isotonic 'Free Stick' Failure MTE Approach and Development

As already mentioned in chapter 2 and detailed in [35], a suitable MTE had already been developed for the isotonic or 'free stick' failure case. Despite the isotonic failure case being outside of the scope of this study, a review of the development of its MTE was useful in establishing an approach for the development of the isometric MTE.

The isotonic MTE constituted a pseudo-random failure input during a continuous and repetitive series of manoeuvres and was designed such that it exposed the aircraft and pilot to the flight conditions that would cause the worst HQ after an isotonic failure. During its development it was apparent that the MTE must fulfil all of the following essential characteristics:

- Safety – conducted at a sufficient height for safe recovery from transiently high attitudes and attitude rates. Conducted in forward flight to avoid inadvertent entry into vortex ring states aggravated by hover Outside Ground Effect (OGE) with poor external height references.
- Repeatability – simple, but well defined manoeuvres on specific flight parameters, within defined tolerances and in a series that was easy to remember.
- Universality – applicable, or at least adaptable, to all rotary aircraft to ensure that the test was truly generic.
- Utility – encompass all 'worst case' scenarios for isotonic failure modes defined during previous testing. The manoeuvres should be sufficiently challenging to reduce the pilot's capacity to anticipate when a failure may be initiated.
- Ubiquity – available at any location without the need for specific infrastructure or course markings.

The 'utility' of the MTE was achieved by identifying all test conditions that could possibly have an influence on the severity of the failure and then investigate each characteristic in turn to assess the strength of influence and appropriate parameter values. Each test point was conducted at a specific test condition (variation of one characteristic whilst maintaining all of the others at a standard value or condition). The aircraft was then flown from the trim condition (hover or 60KIAS straight and level) into the desired test condition. Once at the specific condition, the isotonic failure was initiated and the pilot was required to return the aircraft to the initial stabilised trim condition. After each test point the assessing pilot awarded two IFES ratings the first for the transient aircraft response and the second for the recovery handling. The pilots were instructed to award ratings that reflected the increase of the 'pilot urgency and effort' from the same conditions without the failure. The assessments were repeated for different levels of each characteristic to enable an analysis of parameter sensitivity.

Parameter Varied (Pre-Failure)	Effects on IFES	Strength of Influence
Stable Inceptor Force / Displacement	Higher with increased force / displacement	High
Attitude	Neutral	Low
Axis of Stable Inceptor Displacement	Higher for lateral than longitudinal axis	Med
Flight Condition	Marginally higher for forward flight than hover	Med
Inceptor Displacement Direction	Neutral but subjectively considered relevant	Med
Inceptor Oscillation Frequency	Neutral	Low
Phase of Inceptor Oscillation	Neutral	Low
Attitude Rate	Higher for dynamic manoeuvre but independent of rate	Med
Command Type (AC and RC[56])	Neutral with comparable inceptor Forces Higher for AC with comparable attitudes or attitude rates	Low
Anticipation	Higher with less anticipation	High
Pilot Attentiveness	Higher with lower pilot feedback	Med
Multiple Axis Inceptor Displacements	Adverse with multiple axis manoeuvres	Med

Table 5-4: Summary of Dependent Factors for the Isotonic Failure

Table 5-4 shows the characteristics that were investigated and a summary of the effects and the corresponding strength of influence on the IFES rating. The strength of influence was qualitatively identified from analysis of the IFES ratings; post-failure aircraft states and the test pilots' subjective opinion. Using these results with the aforementioned principles of safety, repeatability, universality and ubiquity an MTE was developed as graphically defined in figure 5-2. The sequence of manoeuvres was repetitively flown until an isotonic failure was initiated at one of the conditions represented by a red letter and defined in table 5-5. After the failure, the pilot was required to recover the aircraft to straight and level flight at 60KIAS and then award IFES ratings for the transient and recovery phases. A more detailed description of the isotonic MTE development and its validation is detailed in [35].

[56] AC – Attitude Command; RC – Rate Command

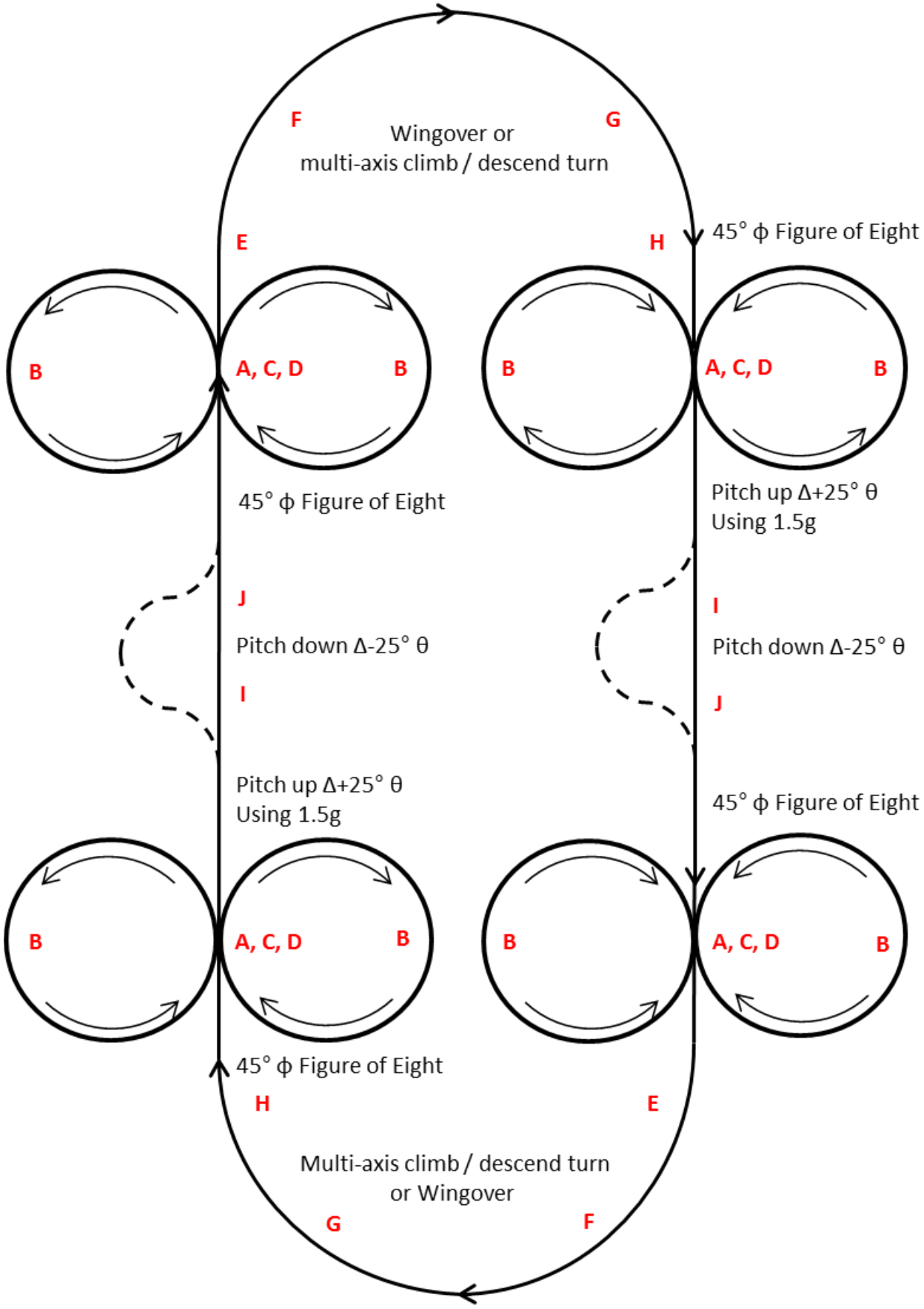

Figure 5-2: Course Definition of the Isotonic MTE

Serial	Failure Initiation Position Description
A	Entry into 45° ϕ figure of eight at maximum roll rate / lateral cyclic displacement
B	At any point within figure of eight >5seconds after achieving constant 45°ϕ
C	Roll reversal within 45° ϕ figure of eight at maximum roll rate / lateral cyclic displacement
D	Exit from 45° ϕ figure of eight at maximum roll rate / lateral cyclic displacement
E	Entry to wingover at max pitch rate / longitudinal cyclic displacement
F	Point of max roll rate / lateral cyclic displacement into wingover (multi-axis)
G	Point of max roll rate / lateral cyclic displacement out of wingover
H	Exit from wingover to level flight at max pitch rate / longitudinal cyclic displacement
I	Point of maximum pitch rate / longitudinal cyclic displacement during entry to pull up
J	Point of maximum pitch rate / longitudinal cyclic displacement during push over

Table 5-5: Isotonic MTE Failure Input Conditions

5.5 Isometric 'Fixed Stick' Failure MTE Approach and Development

The initial intention had been to use the same approach to develop the MTE for the isometric failure case and so a full assessment of all of the characteristics within table 5-4 was repeated in the isometric condition (subsequently referred to as the phase 1 development). Whilst mild oscillatory APCs had occasionally been observed in the isotonic testing, their influence on the overall HQ of the post-failure condition was significantly lower than for the isometric testing. Furthermore, the overwhelming factor affecting the HQ post-failure was considered to be the presence of oscillatory APCs. A statement from pilot G within Post Flight Report (PFR) 5 [97] confirms: '*For most of the test conditions, on recovering back to the hover / straight and level position the pilot had to reduce his gain or smoothly reduce the rate of inceptor force to avoid a PIO.*' Pilot G additionally states in PFR 7 [98]: '*Suppression of PIO was the most significant factor affecting the recovery rating and was evident in most cases'*.

The presence of oscillatory APCs was not always physically evident, but was dependent upon the pilot's control strategy and his pilot gain. As the APCs were more identifiable or more severe with increasing pilot gain, it was surmised that in order for the MTE to highlight the worst case HQ, the task had to demand a high pilot gain post-failure.

The very high influence of the pilot gain post-failure often masked the influence of the weaker characteristics and so the MTE required a profile that would maintain a consistent

pilot control strategy across different test conditions, configurations and pilots. The chosen solution was to develop a task structure and set of tolerances that was sufficiently demanding such that the pilot was forced to remain actively in the control loop after the failure, during both selection and maintenance sub-tasks. A comprehensively described task and high accuracy tolerances would also keep the control strategy consistent across different test pilots who have varying strengths of inherent pilot gain.

The development of the isometric failure MTE was divided into 4 iterative phases:

- Phase 1: Investigation of effects of flight conditions and aircraft configuration without defined high gain task after failure. Conducted to mirror the previous assessment for the isotonic failure mode.
- Phase 2: Selection of most appropriate MTE format for further development (based on ADS-33E MTE options).
- Phase 3: Investigation of effects of flight conditions and aircraft configuration with defined high gain task after failure. Development of isometric MTE course definition and task tolerances.
- Phase 4: Implementation and refinement of isometric MTE

5.5.1 Phase 1: Effects of Pre-failure Conditions without Defined Post-failure High Gain Task

The Phase 1 series of test points was only intended to be used for evidence gathering for the subsequent development of the MTE and not as an embryonic version of the isometric failure MTE itself. The objective was to identify the most adverse conditions that created the highest severity transient and recovery characteristics during the failure [69]. Data was gathered in a similar protocol as for the previous isotonic assessment by varying the values of the following parameters in the pre-failure condition.

- Lateral and longitudinal displacement
- Pitch and roll attitude and rates
- Pitch and roll oscillation frequency and phase
- Initial trim condition (Hover and forward flight)
- Attitude command and rate command
- Good and degraded visual environments

During each test point the sidestick was failed to the isometric condition, after which the pilot was required to recover the aircraft to the safe, stable initial trim condition (hover or wings level 60KIAS) without attempting to constrain the flight parameters within any position, height or heading tolerances. The test pilot then awarded IFES transient and recovery ratings (described in section 5.3) as well as a legacy PIO rating (described in section 6.4.1). Post flight analysis was also conducted using the cyclic force and position signals and the aircraft's attitude and attitude rates.

Figures 5-3, 5-4 and 5-5 show time traces of phase 1 test points flown in a GVE (visibility 10km, no cloud and no precipitation) in both rate and attitude command as annotated.

Figures 5-6 and 5-7 show the similar test points flown in a Degraded Visual Environment (DVE - visibility 100m, no cloud and heavy precipitation) also in both of the two command types. The timing point of the failure initiation is represented by the change of background colour from green to red and the aircraft attitudes are indicated in pitch by theta, θ and in roll by phi, ϕ.

The pre-failure condition of the test point shown in figure 5-3 was a trimmed hover and therefore there were only very low or no control forces applied at the failure initiation point. For the remaining time traces, the pilot applied a near constant input (position and force) immediately prior to the failure which resulted in a near constant attitude (for the attitude command configuration) or attitude rate (for the rate command configuration).

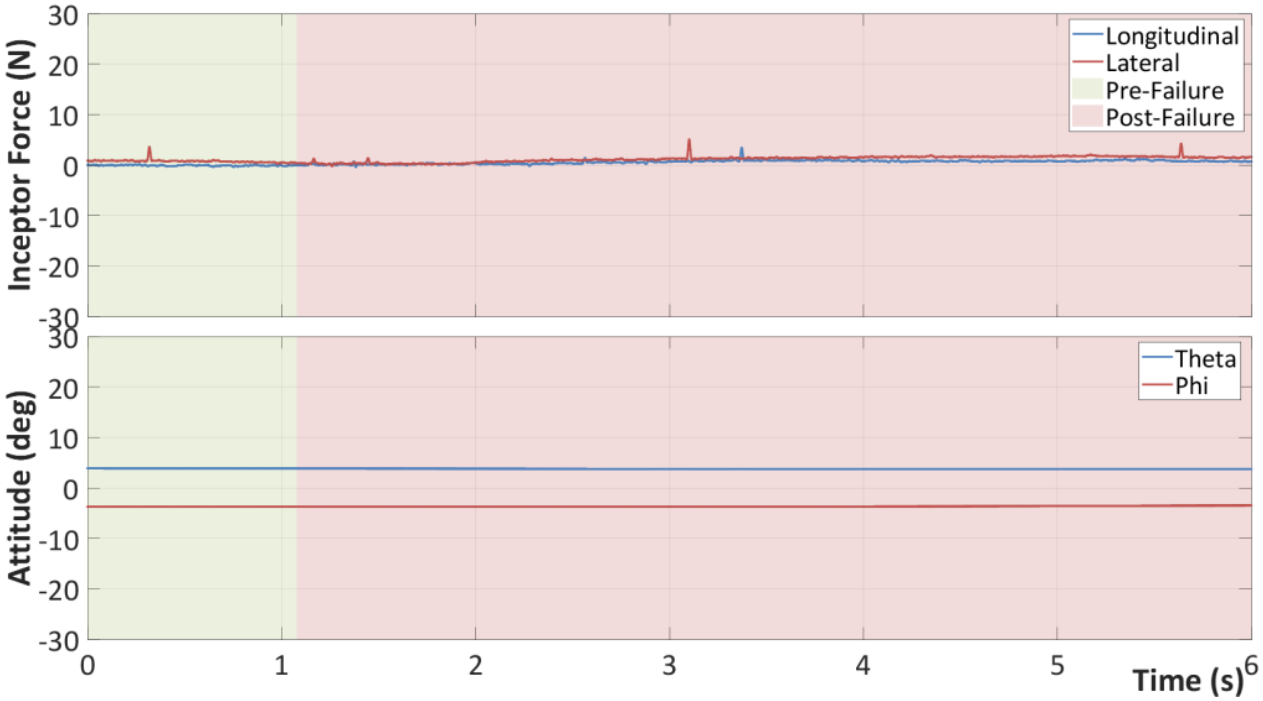

Figure 5-3: Isometric Failure, No Displacement from Trim, Rate Command, GVE

Whilst the phase 1 investigations did not fulfil initial expectations in identifying the worst case conditions for the design of the MTE, it did contribute the following information that became useful in mapping the MTE's development within phases 2 and 3:

5.5.1.1 Pre-failure Sidestick Position / Applied Force

The results showed that if the failure occurred with a very low out of trim force, the pilot was able to retract out of the feedback loop and in some circumstances become open loop. As shown in figure 5-3 in which the failure occurred in the hover with inceptor forces trimmed to zero, the subsequent post-failure applied forces were less than ±2N in maintaining the attitude within 1 degree. The smaller magnitudes of required control inputs caused a natural suppression of any oscillatory APC tendency and therefore resulted in low IFES recovery ratings (IFES transient: A and IFES recovery: A).

Conversely, for test points in which the failure occurred whilst a substantial cyclic input was being applied, the sidestick became fixed in a position which also became the new

zero-force trim position (no input force would be required to maintain it at this failed position and attitude). Consequently, in order to recover the aircraft to the stable initial condition, the pilot was required to apply a force to *select* the attitude but also thereafter to apply a constant out of trim force (as well as superimposed small corrective forces) to *maintain* the attitude. Figure 5-4 shows the pilot and aircraft response to an isometric failure with a pre-failure cyclic input of approximately 5N held in the aft and left directions. The aircraft was configured with a rate command controller and the environment was GVE.

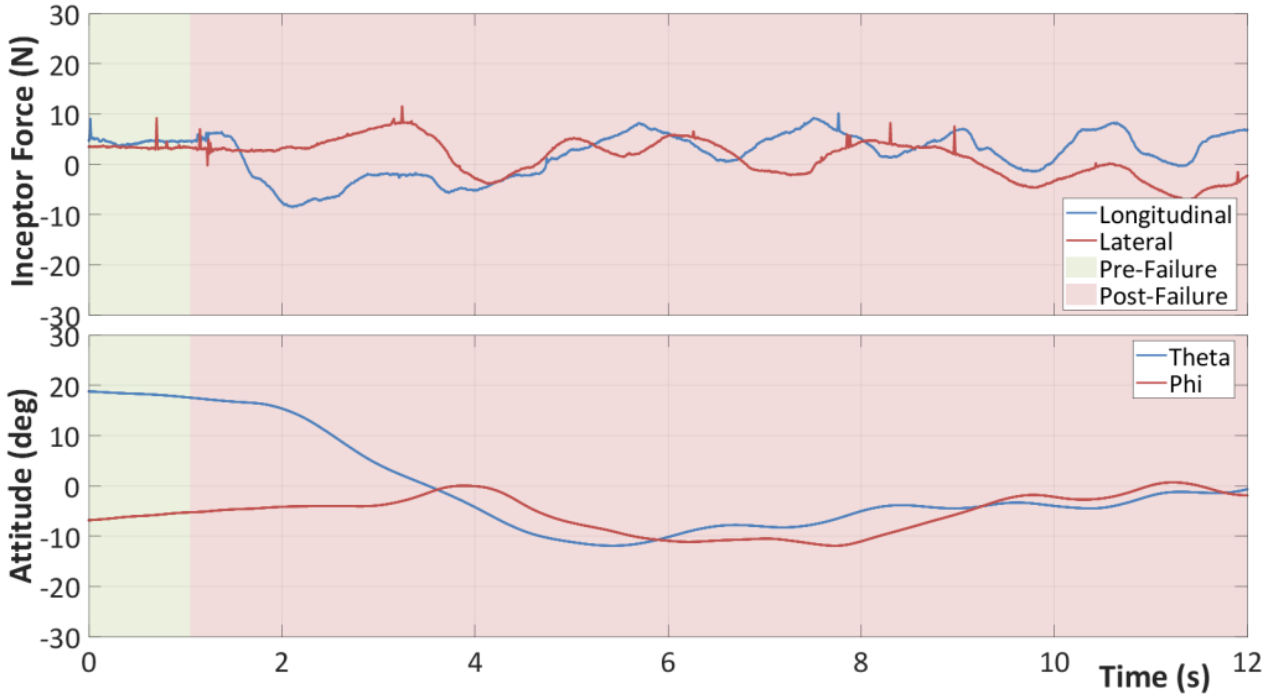

Figure 5-4: Isometric Failure, Longitudinal Displacement from Trim, Rate Command, GVE

The consequence of the sustained control force was a greater difficulty in achieving a stable flight condition and a greater susceptibility to APC. This tendency occurred in many of the phase 1 test points but rarely developed into an observable oscillatory APC unless forced by an increase in pilot gain or degradation of visual environment.

Consistent application of an off trim control force was dependent on magnitude and direction. A deeper investigation of the factors that influence a pilot's ability to maintain a control force is described in chapter 7.

5.5.1.2 Gain of Task

As the pilot's mission within phase 1 after recognising the failure was only to stabilise the aircraft and not to complete a further higher gain task, oscillatory APCs were only seen in the degraded visual environment or with a large pre-failure control force. APC suppression was often reported but as the pilot had no precision task, he was able to reduce his gain and accept a reduction in flying accuracy. With this 'lazy' control strategy the suppression was always quick, easy and effective. However, it was apparent that in most cases, as soon as the pilot entered the loop to conduct a hover task or landing, the

APC was exposed. The tighter the requirements of the post-failure task, the more severe were the oscillations, leading to the conclusion that the isometric test had to include a high gain task after the failure with appropriate performance tolerances of position, height and heading that exposed oscillatory APC tendency even for pilots with isometric experience.

5.5.1.3 Height

As previously detailed, the IFES requires an assessment of the safety margin experienced during the transient and recovery phases after the failure. When the test points were flown above 500ft the pilot noted that it was very difficult to assess both absolute safety margins and the relative difference in safety between different test points, PFR 6 [99]. It would be reasonable to expect the pilot to have greater safety margin awareness in the real aircraft than in a simulator, but the designed MTE had to be applicable in both environments. Importantly, the design of the MTE could not prioritise the requirement for the pilot to accurately assess safety over any significant encroachment on real safety margins.

5.5.1.4 Rate Command / Attitude Command

Comparison of the time traces in GVE for the two command types shows that the rate command configuration (figure 5-4) developed a stronger APC with longitudinal and lateral inceptor force oscillations of amplitude ±5N, than the attitude command configuration (figure 5-5) which developed negligible inceptor force oscillations. The IFES recovery rating concurred with this evidence with a rating of C for rate command and B for attitude command.

A similar comparison of the DVE test points shows that with poorer external visual references the rate command configuration (figure 5-6) also developed stronger oscillatory APCs with longitudinal and lateral inceptor force oscillations of amplitude ±6 to ±10N than the attitude command configuration (figure 5-7) which had irregular non-oscillatory APCs of up to ±3N. Again, the IFES recovery rating concurred with this evidence with a rating of D for rate command and C for attitude command.

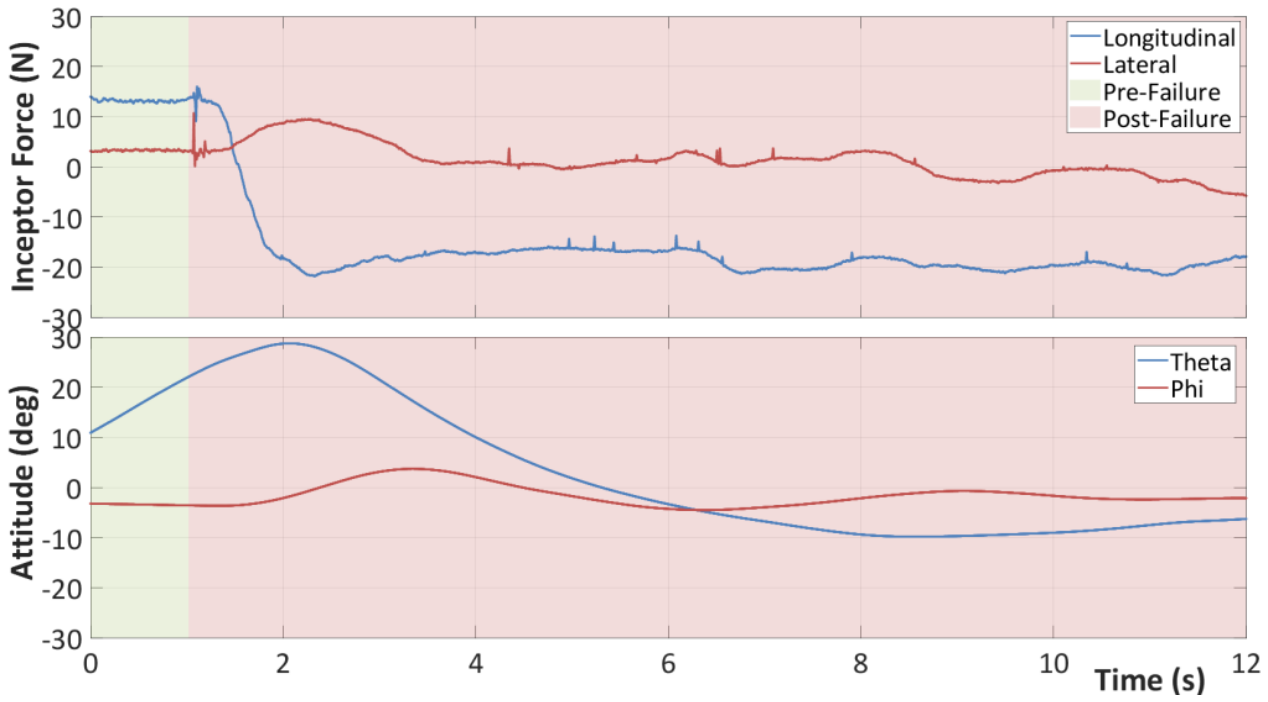

Figure 5-5: Isometric Failure, Longitudinal Displacement from Trim, Attitude Command, GVE

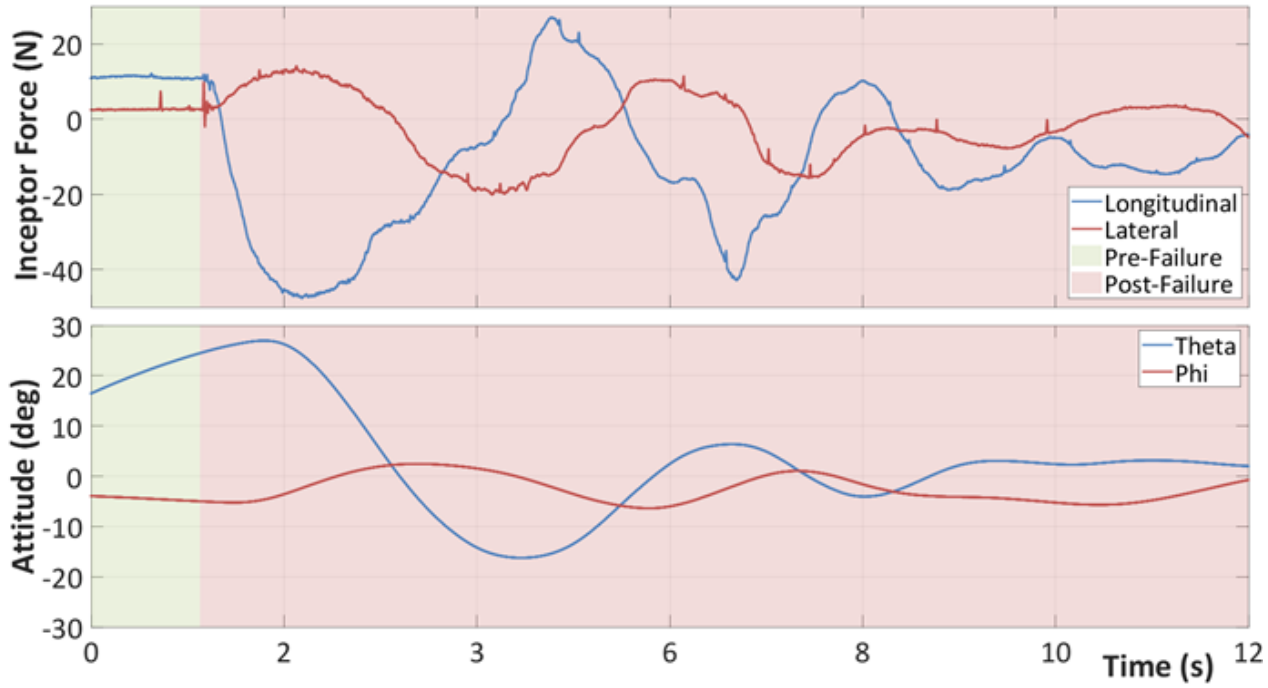

Figure 5-6: Isometric Failure, Longitudinal Displacement from Trim, Rate Command, DVE

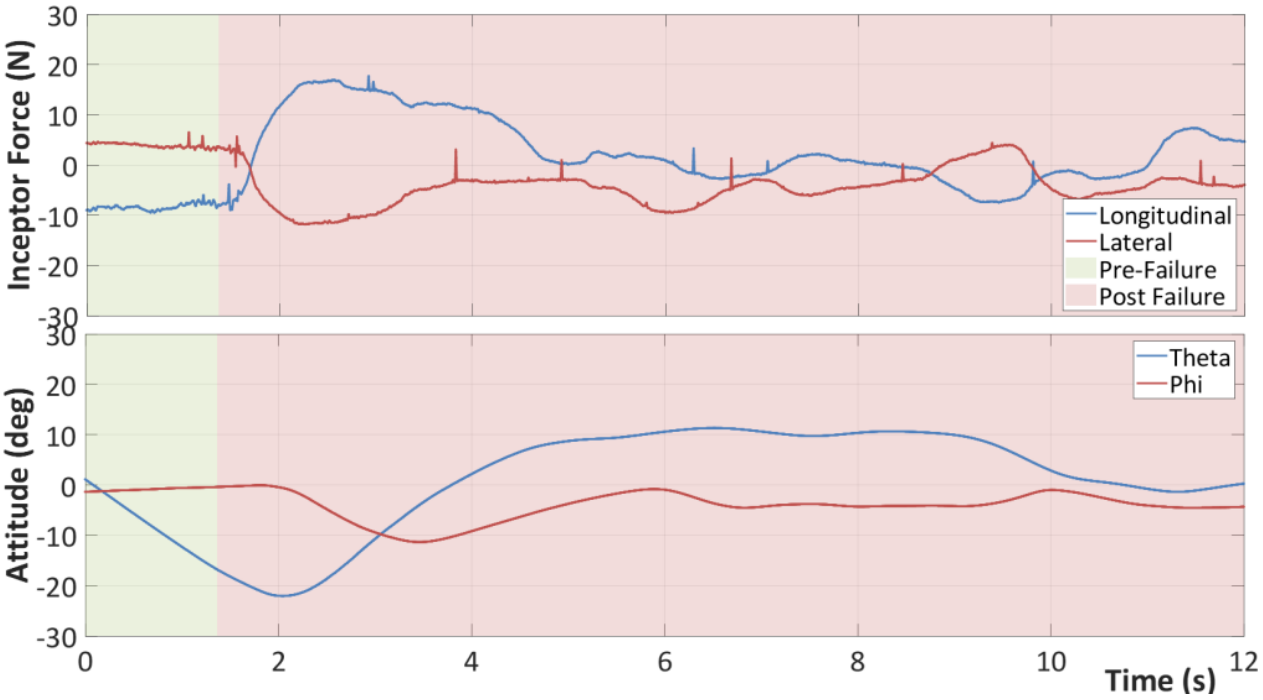

Figure 5-7: Isometric Failure, Longitudinal Displacement from Trim, Attitude Command, DVE

The data agreed with an antecedent expectation that an attitude command controller would present a lower APC severity than a rate command controller. The cause was considered to be due to the pilot using less pilot gain (lower level of in-the-loop involvement) to maintain the stable attitude whilst using the attitude command controller as opposed to whilst using a rate command controller. As the excitation of an oscillatory APC requires a high level of in-the-loop pilot involvement to drive the oscillations, the attitude command controller would theoretically expose less severe APCs than the rate command controller.

5.5.1.5 Visual Environment

A pilot would always use external references, if acceptable, in preference to cockpit flight instruments to recover from a non-stabilised aircraft condition [100]. Throughout phase 1, the test pilot solely used external references regardless of the useable cueing environment (UCE) as defined by ADS-33E [36]. The DVE conditions were assessed as UCE 2 and even with only the limited external references they were more compelling in facilitating the recovery and suppression of APCs than using cockpit instruments. The test pilot noted in PFR 6 [99] that "*Even a partial horizontal reference (such as the simulator clouds that are always horizontal or a part of the buildings, fence or two trees) vastly improve the ease of recovery*". Furthermore, it was noted that generally the IFES transient rating was independent of the visual environment whereas the IFES Recovery rating appeared to be directly dependent on the degradation level of the visual environment.

Despite the pilots' strong and consistent preference to use external visual cues in all conditions, the DVE test points exposed oscillatory APCs more than for the same test conditions in GVE. Figure 5-4 and 5-6 show the variation of control force and aircraft

attitudes after an isometric failure with a rate command controller in the GVE and DVE respectively. Both test points contained oscillations in the force input and aircraft attitudes of both axes, however the DVE test point maintained a larger longitudinal amplitude force oscillation of approximately ±6 to 10N in comparison to the GVE test point of approximately ±4N. The IFES transient rating remained constant at B within both environments, thereby agreeing with the pilot's subjective opinion that the transient rating appeared to be independent of the visual cueing. The IFES recovery rating reflected both the subjective opinion and the objective graphical evidence with deterioration from C in the GVE to D in the DVE.

5.5.2 Phase 2: Selection of Most Appropriate MTE Format for Further Development

From the phase 1 investigation it was apparent that a MTE needed to be selected which could be used in phase 3 to analyse the effects of the pre-failure flight conditions and aircraft configuration on the APC severity. The essential characteristics of the phase 3 MTE would encompass initial aggressive manoeuvring with large and sustained control inputs during which the failure could be initiated and then for it to drive a high pilot feedback immediately after the failure. The following MTEs from ADS-33E [36] were considered, using the cargo/utility performance tolerances and assessed in simulated flight for their appropriateness in exposing oscillatory APC activity.

- Landing: high risk of aircraft damage and crew injury during peak transient attitudes or oscillatory APCs whilst manoeuvring in very close proximity to the ground. Unsuitable solution.
- Slalom: the nature of the continuous, smooth, low frequency and high amplitude lateral oscillatory control inputs that were required to meet the course tolerances did not force the pilot into a high gain feedback loop. The highly aggressive manoeuvring (±50ft from centreline every 500ft at 60KIAS) was coupled with low or undefined accuracy tolerances which meant that only transient effects were observed immediately after the failure but oscillatory APCs were not exposed. Unsuitable solution.
- ILS approach: the manoeuvring was very benign with only small unpredictable control inputs meaning that not all APCs would be triggered and the precise timing of the failure would cause inconsistent results. Unsuitable solution.
- Acceleration – deceleration: sufficiently tight tolerances to maintain the required pilot gain during translational sub-tasks (±10ft lateral position; ±10° heading) and adequate aggression (accelerate laterally to 50kt using 95% max power whilst maintaining below 50ft then decelerate to hover using less than 5% max power), but insufficiently tight tolerances on completion of the deceleration. Potential solution for adaptation.
- Lateral reposition: sufficiently tight tolerances to maintain the required pilot gain during translational sub-tasks (±10ft longitudinal position; ±10ft height; ±10° heading) and adequate aggression (accelerate laterally to 35kt and back to

hover within 18s and 400ft) but insufficiently tight tolerances on completion of the deceleration (±10ft position). Potential solution for adaptation.

- Precision Hover: sufficiently tight tolerances to maintain the required pilot gain during translational (±10ft position; ±10ft height; ±10° heading) and hover (±3ft position; ±2ft height; ±5° heading) sub-tasks. The moderate multi-axis aggression (deceleration from 6-10kt groundspeed to hover in 5s) created suitable attitude rates and large control inputs that were capable of triggering oscillatory APCs. Desirable solution.

The precision hover was therefore selected as the most suitable MTE for further development in phase 3 as it required the pilot to manoeuvre with moderate multi-axis aggression to establish the hover and thereafter maintain it within tight performance tolerances in all axes for 30 seconds. The failure would be initiated during the deceleration manoeuvre, and so any oscillatory APC would be exposed in the subsequent hover selection and maintenance sub-tasks. The ADS-33E hover task is presented in appendix C.

5.5.3 Phase 3: Investigation of the Effect of Different Pre-failure Conditions for a High Gain Task and Definition of the Corresponding MTE Parameters and Tolerances

5.5.3.1 MTE Sub-tasks

The phase 2 investigation identified that the hover MTE was considered the most appropriate for phase 3 investigations into the effects of the pre-failure conditions. However, it was concurrently noted that the hover MTE was also appropriate as a basis for the isometric MTE providing that the hover selection and maintenance sub-tasks could be adapted to demand greater pilot gain after the deceleration manoeuvre. It was therefore concluded that the following MTE sub-tasks, that were present in all 3 of the suitable or partially suitable MTEs, would present a combined optimal solution:

- Sub-task 1: Acceleration to transit groundspeed whilst maintaining constant height and heading. Required to establish the pre-failure flight condition and so not critical in the assignment of IFES ratings.
- Sub-task 2: Maintenance of transit groundspeed whilst maintaining constant height and heading. Required to establish the pre-failure flight condition and so not critical in the assignment of IFES ratings.
- Sub-task 3: Deceleration and selection of hover at defined location within position tolerances whilst maintaining constant height and heading. Directly related to the failure transient and recovery actions and therefore critical to the IFES rating assignment.
- Sub-task 4: Maintenance of hover at defined location within position tolerances whilst maintaining constant height and heading. Directly related to the failure transient and recovery actions and therefore critical to the IFES rating assignment.

5.5.3.2 Position Tolerances

Whilst all of the hover MTE performance tolerances have an effect on the pilot workload and compensation, the tolerances that directly affect the HQ and pilot gain in the cyclic axes were the longitudinal and lateral position tolerances. As already identified, the required gain for the post-failure sub-task needed to be sufficient to expose any oscillatory APCs. The hover MTE of ADS-33E had been designed such that it should identify an oscillatory tendency and the corresponding desired performance requires that 'there shall be no objectionable oscillations in any axis either during the transition to hover or the stabilised hover'. Therefore the hover MTE tolerances were adopted as the first iteration to assess their suitability for use in the isometric MTE. From PFR 14 [101] it was confirmed that the position tolerances taken from the hover MTE of desired ±3ft and adequate ±6ft were appropriate for the isometric failure MTE.

5.5.3.3 Failure Timing

As well as the tight position tolerances, in order to expose any oscillatory APCs there would need to be a suitable APC trigger [65]. The primary trigger would normally be the instantaneous change to isometric mode during the failure, which may be sufficient to initiate an oscillation on its own. However a catalyst or secondary trigger to the APC could strengthen its effects or, if not already evident, could expose it. As identified in phase 1, a high off-trim control force, large attitude or large attitude rate at the time of failure could fulfil this worst-case condition. For both rate command and attitude command controllers, selection of a hover from a high attitude needs a large control input force to create the required attitude rate or attitude change. Consequently, a high attitude at the point of failure offered not just the high attitude, but also a subsequent high attitude rate and high control force. In order to consistently achieve the high attitude at the point of failure, the following objectives were identified.

- The deceleration element of sub-task 3 must be of at least moderate aggression. A more aggressive deceleration develops a greater decelerative attitude. The deceleration is maximised by high translational groundspeed and low time to stabilise.
- In order to accurately and repeatedly decelerate from the translation speed to the precise hover point at zero groundspeed the deceleration must be predictable and regular (no sudden or significant changes in value or sign). This is achieved by the pilot gradually and progressively increasing the attitude to a point where the peak occurs just prior to the hover (peaking early will cause a sudden change in the deceleration just after the peak and during the continued deceleration) [102]. The pilot must be directed to conduct the deceleration with this profile and so it would not be permissible to decelerate aggressively initially and then reduce the deceleration in order to improve hover position accuracy. The statement in the acceleration – deceleration MTE within ADS-33E [36]: "*The peak attitude should occur just before reaching the final stabilised hover*" should be copied to the course description of the isometric MTE.

- Manual initiation of the failure should occur at the point of maximum attitude and as the pilot initiates the hover selection with a large control input.
- As described in PFR 13 [103]: "*In achieving the hover at each corner it was acceptable to make a small overshoot providing that the time to stabilise was still achieved (similar to that permitted in the Hover MTE). If no overshoots would be allowed, it would cause the pilot to avoid using a peak decelerative attitude immediately before the hover as he would have to decelerate earlier and then moderate the decelerative attitude to achieve the hover at the exact desired hover point.*"

5.5.3.4 Groundspeed

The translational groundspeed is one of the factors that affect the aggression of the hover selection sub-task.

A series of lateral repositions were flown from left to right in the AVES simulator at varying groundspeeds and subjective levels of aggression as detailed in PFR 12 [104] and summarised in appendix F.

It was expected and observed that with a constant time to stabilise, a higher groundspeed would cause a greater aggression. Achieving a greater decelerative aggression through increasing the groundspeed, as opposed to reducing the time to stabilise brought two main advantages. Firstly, at airspeeds above 12kt [105] the power margin was affected much less by ground effect or translational lift, which led to fewer collective inputs to maintain height and therefore lower pilot workload for the non-critical sub-task 2. Secondly, a higher groundspeed for a given level of aggression would require the pilot to maintain the decelerative attitude for longer and therefore present a slightly longer period for the Flight Test Engineer (FTE) to target the failure initiation.

Whilst it was considered beneficial to use a higher translational groundspeed for the isometric MTE it was also considered that each helicopter would have a limit of sidewards and rearwards airspeed that would limit the maximum groundspeed. A helicopter's airspeed limits depend on the structural strength, available power margin, control authority, HQ and vibration and so are specific to each helicopter type. In order to make the isometric MTE applicable to all helicopters a translational groundspeed was required that was as high as possible but was within the respective limits of all helicopters. The EASA issued certification specifications CS-27 for small rotorcraft [26] and CS-29 for large rotorcraft [27] both state that for all helicopters "*Wind velocities from zero to at least 31 km/h (17 knots), from all azimuths, must be established in which the rotorcraft can be operated without loss of control on or near the ground in any manoeuvre appropriate to the type (such as crosswind take-offs, sideward flight, and rearward flight)*". Therefore, using the interpretation that wind speed in the hover is the equivalent to sidewards and rearwards airspeed in still wind conditions, it has been assumed that all helicopters are capable of manoeuvring with at least 17kt in any direction.

The range of groundspeed permitted for the hover MTE was 8 ±2kt. This has often been considered to be too broad, as the deceleration from 6kt to the hover over 5 seconds was

considerably less aggressive than decelerating from 10kt over the same time period. Whilst both extremes were permitted, they often caused a wide spread of data. For the purposes of the isometric MTE, a higher groundspeed was used and if using the same tolerance, the extremes of groundspeed would be 13 to 17kt. During isometric MTE simulator testing, the test pilot assessed that the difference in aggression between the groundspeed extremes was not greatly significant and was balanced with an acceptable workload in maintaining the accuracy in what was acknowledged as a non-critical sub-task, PFR 12 [104].

Compliance with the maximum groundspeed of 17kt and the range of ±2kt resulted in the isometric MTE translational groundspeed being defined as 13-17kt.

5.5.3.5 Time to Stabilise

The time to stabilise is the other factor that affects the aggression of the hover selection sub-task. As the translational groundspeed had been set at 13-17kt, the time to stabilise needed to be chosen such that it defined the appropriate level of aggression and standardised the manoeuvre across all pilots.

To assess an appropriate stabilisation time for the isometric MTE the test points detailed in PFR 14 [101] and repeated in appendix F were conducted in the left to right translational direction both with and without failure. Both the hover MTE groundspeed (8kt) and the proposed isometric MTE groundspeed (15kt) were used. Whilst these test points were all conducted with an attitude command controller, the MTE solution must also work for a rate command controller. As already identified in section 5.5.1.4, rate command controllers are more prone to oscillatory APCs than attitude command controllers and so for all test conditions in which APCs were observed, it is reasonable to also expect at least as severe APCs for the rate command controllers.

The criterion for selecting the stabilisation time was based on an attitude command controller flown from 15kt to a stabilised hover without failure, such that within the adequate performance standard there were no observed sustained oscillatory APCs. In the same conditions for the desired standard, an oscillatory APC could be observed with only mild severity or low intensity suppression.

Figures 5-8 and 5-9 show 2 separate test points each comprising a translation flown from left to right at a groundspeed of 15-16kt and height of 10-20ft followed by a deceleration to the hover. The time for stabilisation was measured from the point of first decelerative control input until the attitude was stabilised with a groundspeed of less than 1kt. The test point in figure 5-8 had no failure initiated and after a stabilisation time of 5.6s (from 17.5s to 23.1s) no attitude oscillations were observed and the control force inputs indicated only very small variation. This supported the pilot's subjective opinion that a very mild APC was suppressed. A further test point was flown under the same conditions (not shown) but with a stabilisation time of 4s which was reported subjectively in PFR14 [101] as very difficult to fly accurately and caused a moderate APC. The results of these test points were compared with the proposed criterion and the desired performance tolerance for stabilisation time was therefore set at 6s.

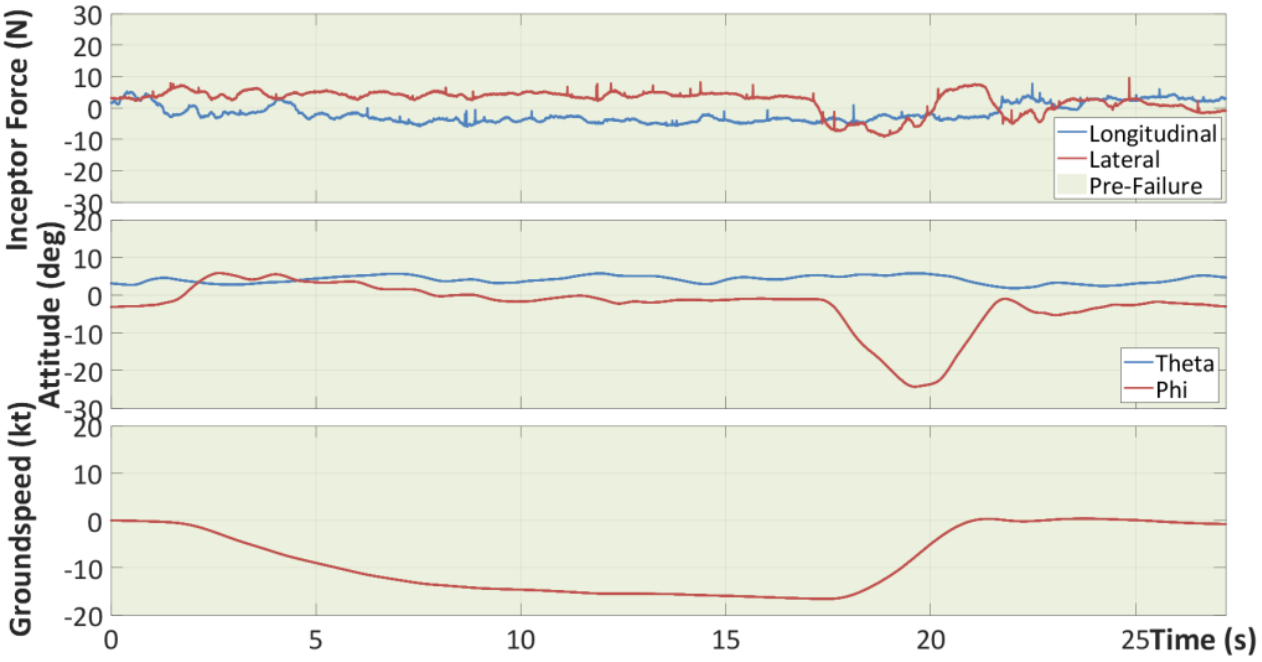

Figure 5-8: Isometric MTE no Failure, Right, Attitude Command, 5.6s Stabilisation time

The hover MTE performance requirements in ADS-33E [36] define the time to attain a stabilised hover after the initiation of the deceleration from 6-10kt as 5s for desired and 8s for adequate (cargo / utility). The ratio of the adequate to desired stabilisation times for the hover MTE was used as a guideline for calculating the equivalent adequate performance stabilisation time of 10s for the isometric MTE. This adequate performance was also tested and confirmed in PFR 14 [101] as appropriate with no signs of APC during the entire manoeuvre.

The test point in figure 5-9 however, had a failure initiated at the point indicated by the change in background colour from green to red which coincided with the peak decelerative roll attitude. The time to stabilise was 5.3s (from 21s to 26.3s) and whilst the time period is similar to the non-failure case, a severe oscillatory APC was observed in both axes that was partially suppressed after a further 5s. This test point confirmed that a desired stabilisation time of 6s would expose oscillatory APCs for attitude command controllers if a failure was initiated.

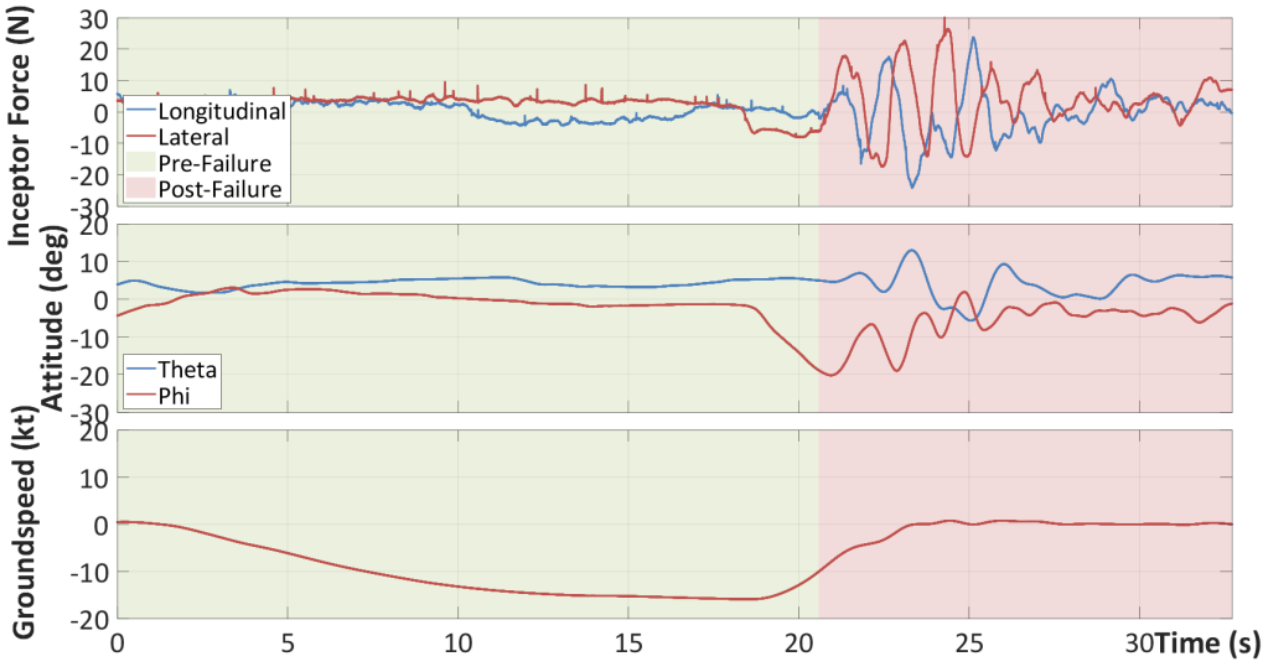

Figure 5-9: Isometric MTE with Failure, Right, Attitude Command, 5.3s Stabilisation time

Whilst performance standards of desired 6s and adequate 10s demanded moderate aggression for a 3 tonne, rigid rotor head helicopter, further testing may be required for larger aircraft with different flight characteristics.

5.5.3.6 Directions

In order to maintain some element of surprise to the pilot the intention was to develop a pattern that could be repeated, either independently from pilot memory or under the direction of a FTE until the failure was initiated. This characteristic had already been used successfully for the isotonic failure MTE [35] in which the pilot was required to fly a series of manoeuvres within defined tolerances and in a specified order. At one of the pre-defined 'worst-case' conditions the FTE would initiate the failure without warning. Due to the combination of moderate workload and level of pilot involvement in maintaining the required flight parameters, the pilot was not able to devote all of his attention to anticipating the failure.

Consequently, the adoption of a similar approach for the isometric failure MTE would require a continuous pattern of the previously defined 4 sub-tasks which was sufficiently engaging and with an uninterrupted workload such that failure anticipation was minimised. This was achieved through the transition towards and then selection and maintenance of a hover at a corner of a square, followed by the same repeated procedure to different corners of the square as directed by the FTE.

The evidence from the phase 2 testing suggested that the transit direction could be either in the lateral direction (lateral reposition MTE), longitudinal direction (acceleration – deceleration MTE) or a compound forward-right or forward-left direction (hover MTE). During phase 3 testing all pre-failure transit directions were assessed (forward; back; left; right; forward-right; forward-left; back-right; back-left) as described in the PFR 13 [101].

Whilst it was desirable to be able to initiate failures from all directions; the cockpit field of view to the left and forward left, from the right seat (experimental pilot seat in the EC135 ACT/FHS) was very poor. Furthermore, all directions with a backwards component were very difficult to fly accurately due to the pilot not being able to see the hover point until it had been passed. Therefore, whilst all directions were permissible during non-failure manoeuvres, due to the degradation in flight accuracy and assessment quality, only the data from the forward; right and forward / right directions were used for analysis of the failure condition.

5.5.3.7 Height

Due to obstruction clearance requirements and the intention to permit translation towards and hovering at any of the four corners of a square, it would be impossible to use an external visual height reference (as used for the hover MTE). The only effective alternative reference for height indication would be the radar altimeter and whilst it is not always a standard fit for new helicopters, it could be reasonably expected that a helicopter with an advanced fly-by-wire active sidestick system would also be fitted with a rather less advanced radar altimeter system. A significant advantage in using the radar altimeter over an external visual reference is that it induces divided attention into the task by forcing the pilot to use both internal and external references. This further deepens the level of involvement of the pilot in the pre-failure task, leading to less anticipation of the failure.

The selection of the height datum (15ft) and tolerances (±5ft desired / ±10ft adequate) was influenced by the following factors that were identified in PFR 15 [106]:

- Safe conduct is paramount in the development of an MTE, and the greatest hazard during low speed, inside ground effect testing is the potential impact with the ground or obstructions. The minimum height should be a balance between remaining outside of the single engine failure avoid curve, and maintaining an adequate clearance over the ground and obstacles. As a standard guideline when manoeuvring at low speed (below 40kt), pilots normally adopt a minimum height in feet, that equates to the groundspeed in knots. As the groundspeed had already been set at 15kt, it was appropriate that the datum height be set at 15ft.
- Other previously identified suitable or partially suitable MTEs from ADS-33E [36] offered some initial guidance for the height datum and tolerances.
    - Hover MTE (8kt): Datum 8ft, desired ±2ft, adequate ±4ft
    - Acceleration – Deceleration (50kt): desired <50ft, adequate <70ft
    - Lateral reposition (35kt): Datum 35ft, desired ±10ft, adequate ±15ft

    For clarity, ADS-33E actually specifies that for the hover MTE, the datum height should be less than 20ft, however 8ft is most commonly used (for example the AVES simulator hover MTE course uses an 8ft datum). As is apparent from this information, the datum height of these MTEs is fundamentally linked to the maximum groundspeeds which concurs with the safety guideline stated

previously. With increased datum height, the performance tolerances are also increased and so for a datum of 15ft (between the hover 8ft and lateral reposition 35ft), tolerances of desired ±5ft, adequate ±10ft would be appropriate.

- According to the comments of the test pilot in PFR 15 [106], the pilot required significantly more compensation to maintain the height within the desired tolerances of ±2ft for the developing isometric MTE than for the hover MTE. This was considered to be due to both the greater decelerative aggression and worse height references in the developing isometric MTE. In order to retain a similar pilot workload for the isometric MTE, the desired height tolerances of ±5ft were considered appropriate.

- So that the MTE did not become unnecessarily complicated or too challenging to fly it was essential that there was a continuity of datum height between the translation sub-tasks and the hover sub-tasks.

- Some consideration must be given to a test pilot's ability to remember all of the course definition and performance parameters. An unnecessarily complicated task with a lot of numbers to remember can become more of an assessment of the test pilot's memory than of the characteristics of the helicopter. The test pilot must be afforded the spare mental capacity to not only fly the manoeuvre accurately but also to analyse his actions and performance whilst doing so. Given the selected datum groundspeed of 15kt, a height datum of the same 15ft would pose no additional cognitive workload that could detract from him developing a critical opinion.

5.5.4 Phase 4: Implementation and Refinement of Isometric MTE

Within the phase 2 testing it was considered that whilst an adapted hover MTE was the most appropriate for the phase 3, high gain testing, the final isometric MTE solution, developed in phase 4 would encompass elements of the acceleration-deceleration and lateral reposition in addition to the hover MTE.

Phase 3 testing further identified that the MTE course would be a square with hover points and corresponding position tolerances at each corner and there would be no external height references as the pilot would use the aircraft's radar altimeter.

5.5.4.1 Trim Strategy

The EC135 ACT/FHS has the following 2 cyclic trim functions [16]:

- Pitch and roll trim release: sets the current equivalent control position signal as the datum for a zero force input (applies for both compliant and isometric modes).

- Pitch and roll beep trim: adjusts the datum (zero force) equivalent control position signal progressively in one cyclic direction (forward, aft, left, right) (applies for both compliant and isometric modes).

A defined trim strategy within the isometric MTE was required so that the test pilots all used a consistent approach and the consequent data could be legitimately compared. The simple trim strategy of prohibiting the use of all trim functions was adopted for the following reasons:

- Use of the trim release functions causes transient responses. These are of varying magnitude and characteristics and depend on the grip with which the pilot holds the cyclic, the magnitude of the pre-trim control force and the inherent flight control mechanical characteristics of the inceptor (specifically, friction, damping and mass). Due to the breadth and complexity of these variables it would be difficult to extract from the transient effects of the trim release from the subjective and objective data.
- ADS-33E [36] specifies in paragraph 3.8.2 that during a transfer between response types '*the heading, altitude, rate of climb or descent and speed shall be maintained without use of the trimmer controls'*. Whilst the statement refers to changes of controller response types, for example rate command to attitude command, it is analogous to the requirement for a stable transfer of control mechanism without use of trim functions.
- The trim strategy would be consistent with the isotonic MTE description.
- In order to encompass the 'worst case' conditions into the MTE, a large pre-failure control force was required such that a large post-failure force could trigger the initiation of an oscillatory APC [section 5.5.3.3]. Effective use of the trim functions could reduce the cyclic forces required to maintain a stabilised hover during the transient and recovery phases after an isometric failure and therefore not fulfil the 'worst case' criterion.
- The critical component of the previous argument is that the use of the trim function would have to be effective for it to have a positive influence. Unless the pilot is well prepared for isometric failures and therefore accustomed to taking the best course of action, in a truly surprise situation it would be expected that the pilot would prioritise safe stabilisation ahead of using trim functions. The incorrect or inappropriate timing of the trim functions would likely exacerbate the emergency situation.

Whilst not investigated within this study, the trim functions however would be relevant to assessing the HQ in the post-failure long term.

5.5.4.2 Overall Course Dimensions and Markings

The requirement for the overall dimensions of the square course was such that the acceleration to the transit speed of 13-17kt would not be too aggressive. Neither the transit speed selection nor speed maintenance were critical sub-tasks for the award of the IFES ratings and so the pilot effort to achieve these sub-tasks should be low. Furthermore, the course must also be applicable to the largest helicopters as well as a 3 tonne EC135. Whilst a 20 tonne cargo / transport helicopter model was not available in

the AVES simulator, further analysis should be completed to confirm the course dimensions are still appropriate.

An equally important influence on the course size was that most test centres are limited by suitable available areas to create such ADS-33E and bespoke courses. The defined size should therefore be the smallest that fulfils all other requirements. After consideration of similar courses described in ADS-33E and flying the proposed isometric MTE with various course dimensions, the selected optimum size was a square of dimensions 400x400ft.

The ground markings depicted in figure 5-10 of the square course were implemented into the AVES simulated environment as shown in figure 5-11. Each hover position was labelled with a letter so that the FTE could easily direct the pilot in a continuous pattern of manoeuvres before the failure event. The hover tolerances were represented as 2 groupings of red and white 3-dimensional traffic cones (ahead of the hover point and forward-right of the hover point). Each grouping consisted of 5 rows of cones such that when the pilot could see the centre row in line, he was in the exact hover position as shown in figure 5-12. When the pilot maintained his position such that the rows 2 and 4 did not come into line he was within desired tolerance and similarly for rows 1 and 5 he was within adequate tolerance.

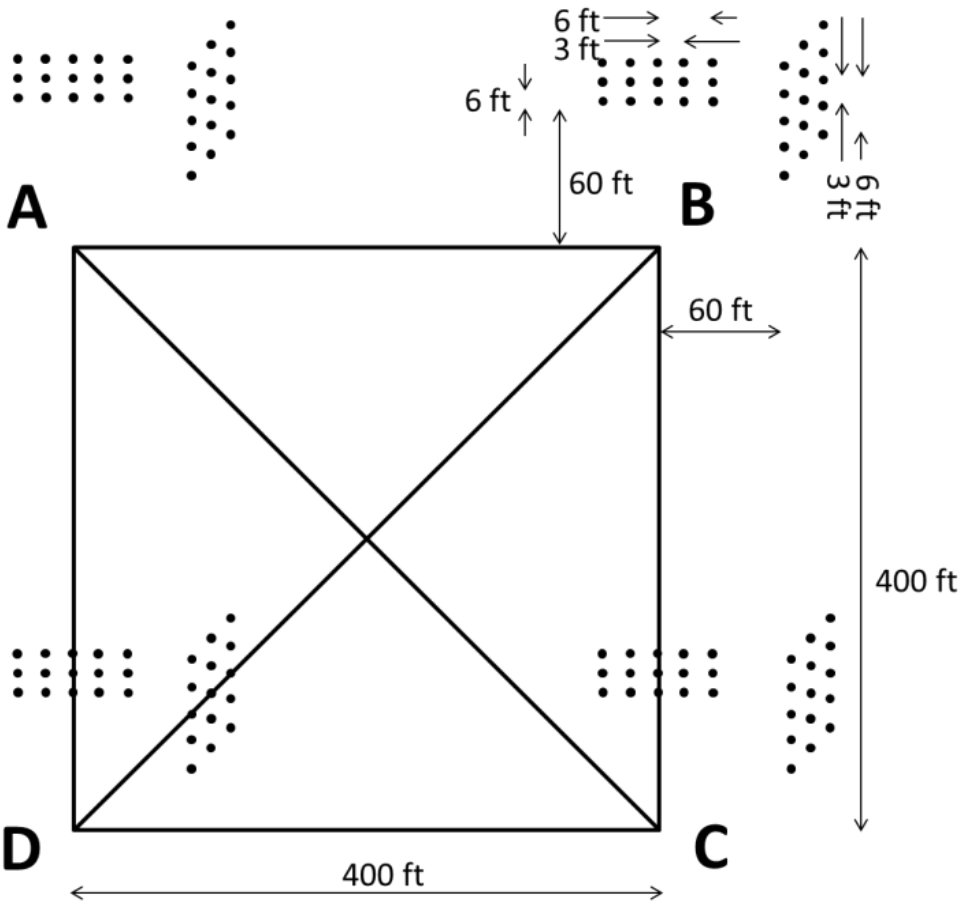

Figure 5-10: Course Layout and Dimensions, Isometric Failure MTE

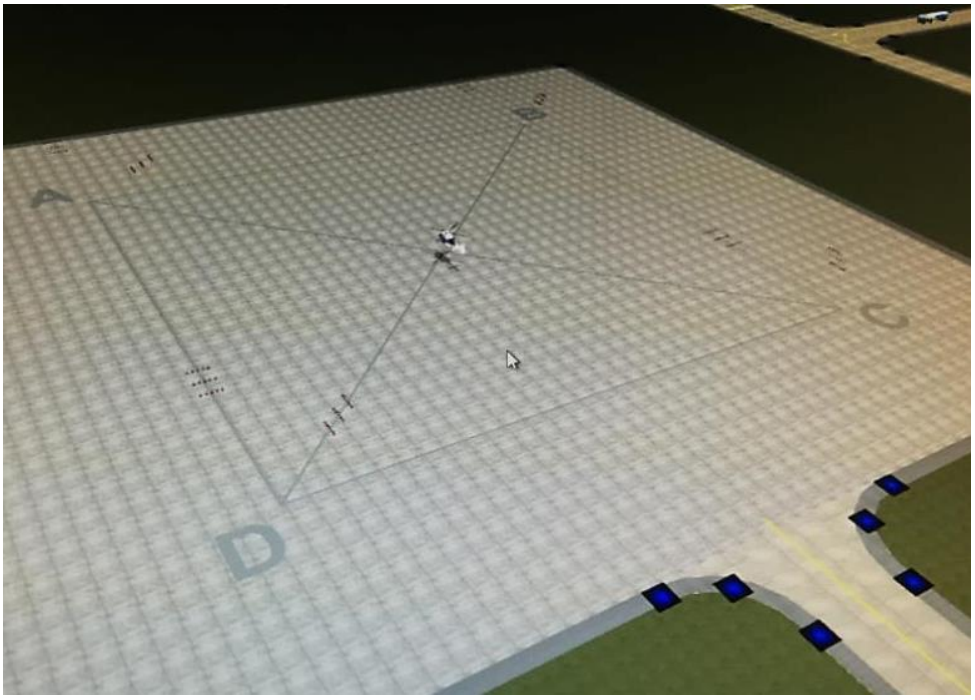

Figure 5-11: Isometric MTE Course with Helicopter at Initial Hover Position (source: DLR)

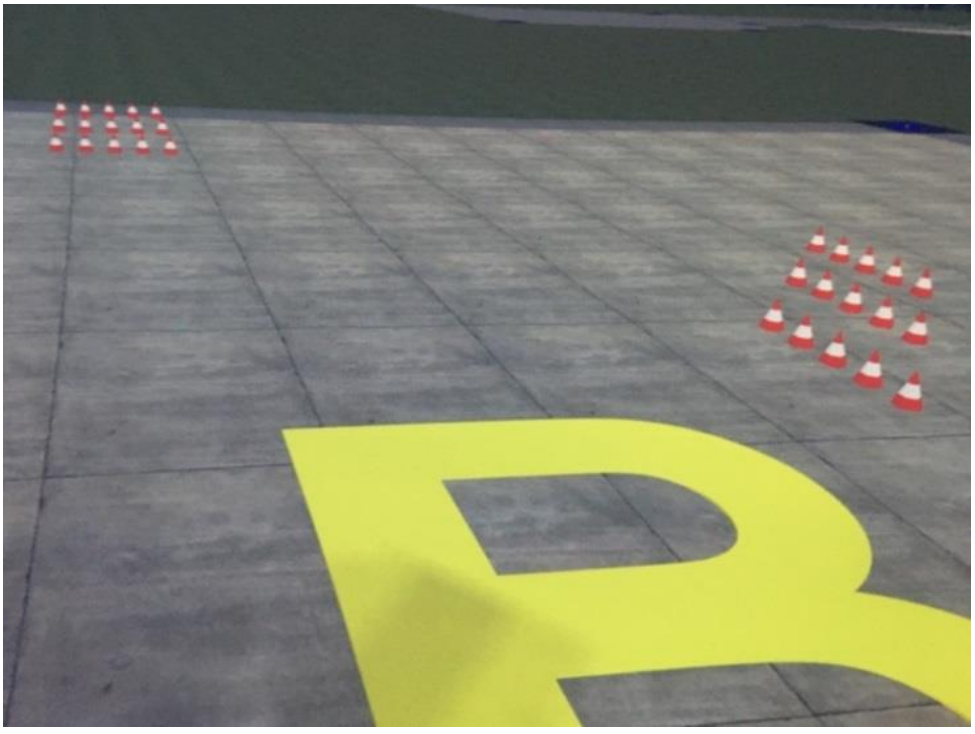

Figure 5-12: Pilot Eye View in Hover Position B of Isometric Failure MTE (source: DLR)

5.5.4.3 Definitions of 'Safe Recovery' for IFES Rating Scale

From the definitions in section 5.3 it is apparent that the SFE definitions do not consider other important safety-of-flight factors such as collision with obstructions or flight into

terrain. In some failure circumstances these could be highly relevant and so must also be included in the considerations in assigning the IFES recovery rating. For the isometric MTE the definition of both 'safe flight' and the outer boundary of the SFE were identical and were as detailed in table 5-6.

Safe Recovery Performance / Outer Boundary of SFE	Boundary
Attain a stabilised hover within X seconds of initiation of deceleration or sidestick failure, whichever comes latest.	10s
Maintain a stabilised hover for at least X seconds.	20s
Maintain the longitudinal and lateral position within ±Xft of a point on the ground	6ft
Maintain height within ±Xft	10ft
Maintain heading within ±X°	10°

Table 5-6: Safe Recovery and SFE Boundaries for Isometric MTE

As a consequence of the assessment having been conducted in a simulator (instead of a real life helicopter), in which the flying experience is not fully immersive, the pilots felt no real concern for safety. In such conditions the concept of safety-of-flight can sometimes become arbitrary or at least open to a large variation of opinion across different pilots. Hence the safe recovery definition was critical to the integrity of the subjective data. It was therefore emphasised to each test pilot that any excursion of these boundaries must be considered unsafe or intolerable.

5.5.4.4 Isometric MTE Functional Testing

Once the course was implemented in the AVES, the safety, functionality and comprehension of the extant MTE course, tasks, assessment methods and accompanying instructions were assessed by pilot H. He made the following comments and recommendations that have been taken from PFR 17 [107].

- Without a failure the manoeuvre could be flown accurately in the forward, right and combined forward-right directions resulting in CHRs of 3.0 for all attitude command test points and 4.0 for all rate command test points (see appendix D for more details). It was noted however that the yaw axis augmentation required more rate damping so that the less significant yaw axis did not require a disproportionate pilot workload.
- The failure could be consistently initiated by the FTE at the point of maximum decelerative attitude just as the cyclic was being moved to select the hover attitude.
- When using the rate command controller, once the failure had been initiated an oscillatory APC was immediately observed. The natural response from the pilot was to reduce his feedback gain by accepting the adequate tolerances and

therefore suppress the oscillations. However, this posed the risk that 2 pilots with different control strategies would assign very different IFES and APC ratings for the same test conditions. One pilot could induce a high gain response by prioritising the position accuracy at the expense of the APC suppression and another pilot could adopt a low gain strategy, thereby improving the attitude stability but accepting a lesser position accuracy. For consistency, it needed to be stressed (similar to ADS-33E [36]) that the pilot must always strive for desired tolerances even above the objective to suppress an APC.

- The hover selection (sub-task 3) and hover maintenance (sub-task 4) sub-tasks were the most critical to the observation of oscillatory APCs. The acceleration and maintenance of the translational groundspeed sub-tasks (1 and 2) were insignificant in affecting the severity of the APC.
- The definition for 'loss of control' within the APCR was required to be able to differentiate between an IFES recovery rating of 8 and 9. The definition was agreed as 'a safe landing is not possible even outside of the safe area (for example on any flat ground)'.
- There was a learning process that constituted at least 3 attempts before the performance plateaued and so the pilots should be offered adequate opportunity to practice the manoeuvres with and without failure before the representative data is recorded.
- The SIMDUCE was calculated with pilot H, and subsequently pilots G and L to be a combined UCE=1. For more details see chapter 3.
- Using the radar altimeter as the height reference increased workload slightly and divided the pilot's attention between external and cockpit references.
- The indeterminate repetition of tasks directed by the FTE prior to the failure caused the pilot to be less aware or prepared for the failure and therefore presented a more characteristic startle or surprise.
- The dimensions of the course, ground markings, position of the cones and the performance standards for groundspeed, height, stabilisation time and hover position were all appropriate for the task using either the attitude or rate command controller.
- The methodology of the IFES and APCR scales was logical and the scales were appropriate for the assessment task. However, as they are both novel to the test pilot community, pilot H suggested that the scales need to be introduced and discussed before flight and then their use practiced before representative data is recorded.

After taking into account these comments the MTE was amended and a conclusive solution was presented in the same familiar format found within ADS-33E and shown in table 5-7.

Objectives

- Check that a rotorcraft is controllable after a sidestick failure to an isometric mode.
- Check that the rotorcraft has no APC tendency during a high gain task in an isometric sidestick mode.

Description of manoeuvre Initiate the manoeuvre from a ground referenced hover at a Radar Altimeter height of 15ft agl at one of the corners of the course. Accelerate to 13-17kt ground speed towards another corner as directed by the FTE. The ground track should be along one of the lines as illustrated in figure 5-10 and be such that the rotorcraft will arrive over the target hover point. The transition to the hover must be achieved in one smooth manoeuvre with the maximum decelerative attitude achieved immediately prior to the hover. It is not acceptable to accomplish most of the deceleration well before the target hover point and then to creep up to the final position. The trim release button shall not be used during the manoeuvre. After 10 seconds the FTE will select the next target hover point which the pilot must then manoeuvre to. The process is repeated until the FTE initiates the isometric failure during the deceleration to a hover point. After identifying the failure, the pilot must recover the aircraft and achieve the hover at the nominated target hover point. The manoeuvre shall be accomplished in calm winds. The recovery of the aircraft within 'safe parameters' as defined must be of greater importance than suppressing the APC. Loss of control means that a safe landing is not possible even outside of the safe area (ie on any flat ground)

Description of test course The suggested course for this manoeuvre is presented in figures 5-10, 5-11 and 5-12. Note that the height is maintained by reference to the radar altimeter on the cockpit displays.

Performance standards. The CHR performance standards are presented below. It is acceptable for the pilot to overshoot the target hover point slightly providing that he is still able to achieve the stabilised hover time.

	Cargo/Utility GVE	
	Desired Performance	Adequate Performance
Attain a stabilised hover within X seconds of initiation of deceleration or sidestick failure, whichever comes latest	6 sec	10 sec
Maintain a stabilised hover for at least	20 sec	20 sec

Maintain the longitudinal and lateral position within ±Xft of a point on the ground	3ft	6ft
Maintain height within ±Xft	5ft	10ft
Maintain heading within ±X°	5°	10°
There shall be no objectionable oscillations in any axis either during the transition to hover or the stabilised hover	√	

The IFES safe recovery performance standards and SFE definitions are presented below:

Safe Recovery Performance / SFE	Cargo/Utility GVE
Attain a stabilised hover within X seconds of initiation of deceleration or sidestick failure, whichever comes latest	10 sec
Maintain a stabilised hover for at least	20 sec
Maintain the longitudinal and lateral position within ±Xft of a point on the ground	6ft
Maintain height within ±Xft	10ft
Maintain heading within ±X°	10°

Table 5-7: ADS-33E Format of Isometric Failure MTE

5.6 Characteristic Oscillation Frequency

For the subsequent theoretical analysis and parameter value selection described in chapter 6 a characteristic frequency was required for a typical post-failure oscillatory APC. Figure 5-13 shows a representative post isometric failure oscillatory APC that was recorded during a left to right translation at 15kt groundspeed, in GVE, using an attitude command and with a target stabilisation time of 8s. The time periods of the longitudinal and lateral inceptor forces were averaged over at least 3 cycles and were recorded at 3.01s and 1.29s respectively. The corresponding time periods of the pitch and roll attitudes were also averaged over at least 3 cycles and were recorded as 3.13s and 1.27s respectively. Table 5-8 shows the averaged frequencies for the test point shown in figure 5-13 (denoted as serial 1) and an additional 2 test points with the same conditions and configuration but with different pilots. As the longitudinal oscillation was dominant throughout all of the oscillatory APCs (see further discussion in section 6.8) the characteristic oscillation frequency was taken as the average of the inceptor force frequencies (2.63rads^{-1} or 0.42Hz).

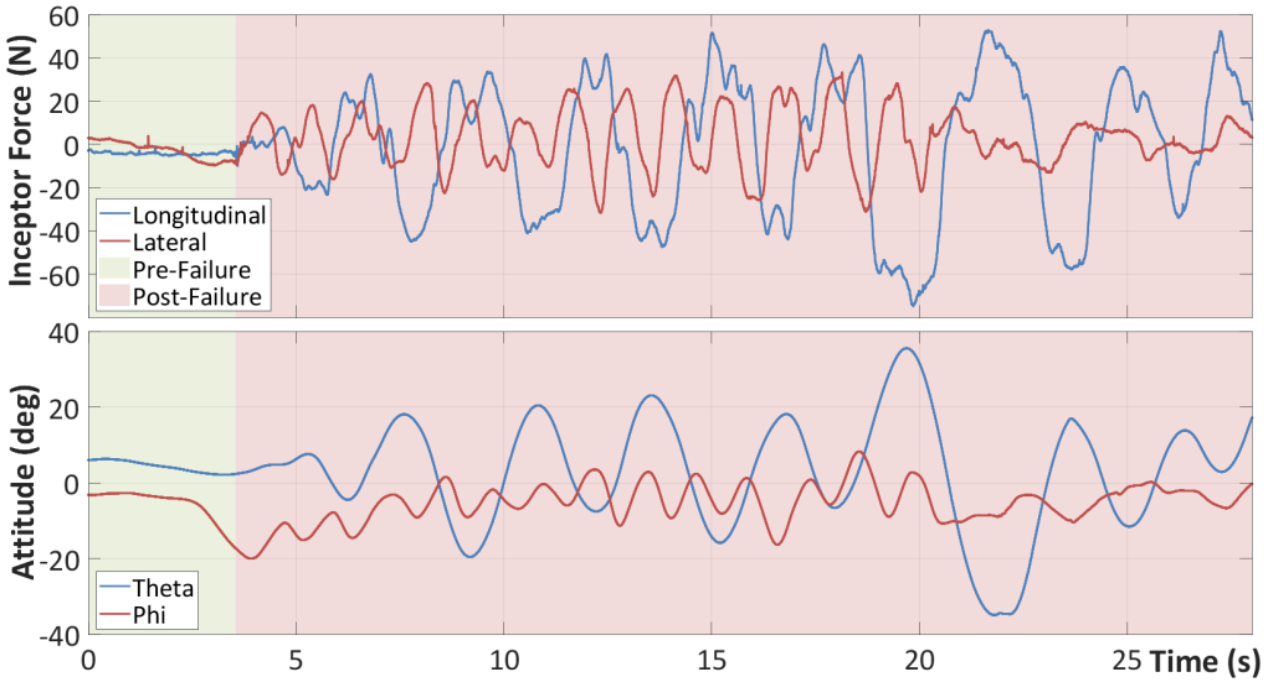

Figure 5-13: Isometric MTE with Failure, Right, Attitude Command, 15kt Groundspeed

Serial	Inceptor Force Frequency ($rads^{-1}$)		Attitude Frequency ($rads^{-1}$)	
	Longitudinal	Lateral	Longitudinal	Lateral
1	2.07	4.84	2.01	4.96
2	2.70	3.58	2.51	2.70
3	3.14	4.84	2.95	4.34
Average	2.63	4.40	2.51	4.02

Table 5-8: Characteristic Oscillation Frequencies of a Post Isometric Failure APC

5.7 Summary

A MTE was required to assess the HQ and pilot workload during and immediately after an isometric sidestick failure. The course definition and performance tolerances were developed in an iterative process with consideration of all parameters. During the development phases of the MTE, the IFES rating scale was used (with minor adaptation) to help identify worst case conditions and to substantiate subjective decisions. The final definition of the MTE also used the IFES rating scale, as well as the APC rating scale in order to support subjective evidence. The essential characteristics of the MTE were initially identified as Safety, Repeatability, Universality, Utility and Ubiquity and were reflected in the developed solution as follows:

- **Safety:** Whilst the course was designed for the higher risk low speed environment and inside the ground effect, it would be located in a clear area and free of all obstructions or structures. The defined height of 15ft would preclude the possibility of entering vortex ring and provide sufficient space to recover from transient attitudes generated from the failure. An absolute minimum height of 5ft would constitute a test point termination criterion.

- **Repeatability:** The course definition was easy to remember (15kt groundspeed, 15ft height and tolerances identical to the hover MTE that all test pilots are familiar with). Pilot H confirmed that the acceleration and translational sub-tasks were easy to fly accurately and the hover selection and hover maintenance sub-tasks without failure were also easy in both command types. The ground markings provided adequate visual cues for accurate flying and the description and definition according to pilot H were clear and unambiguous.

- **Universality:** Most of the course definition and tolerances would be suitable for all types and sizes of helicopter. However the time to stabilise the hover may require reassessment for larger helicopters. With reference to the hover MTE time to stabilise, a longer time period is permitted for cargo/utility as for scout/attack and so for the isometric MTE it could be expected that a graceless transport helicopter of 20 tonnes would require more than 6s.

- **Utility:** The MTE encompassed the most critical conditions of groundspeed, height, aggression, stabilisation time and position tolerances that had been identified in phase 3. Furthermore the course definition and performance tolerances were applicable in both GVE and DVE and with either rate or attitude command controllers. The sub-tasks were sufficiently demanding to reduce the pilot's capacity and the pilot's uncertainty of when the failure would occur provided a limited element of surprise for the failure. The IFES transient, IFES recovery and APC rating scales were capable of assessing the severity and safety as well as describing the pilot's compensation throughout the failure.

- **Ubiquity:** Whilst not as readily available as the isotonic MTE, the isometric MTE requires only ground markings and traffic cones. No bespoke ground structure or aircraft instrumentation is required.

Chapter 6: First Order Filter Experimental Provision, Conditions and Theoretical Prediction

6.0 Overview

An investigation was conducted of the function of a first order filter and ramp attenuator implemented within the conversion process of the sidestick force signal into an equivalent position signal. The overall objective was to reduce the effect of any oscillatory APCs.

The filter and attenuator were activated only after the failure had been initiated and the sidestick had degraded to the isometric failure mode. Prior to the failure, the sidestick signal used a second order filter and conversion table that simulated the sidestick mechanical characteristics as depicted in figure 3-12.

This chapter starts with an overview of the first order theory and conventions used. Justification for using a first order filter, instead of a simple gain or higher order filter is then discussed, followed by selection of appropriate filter parameter values for inclusion in the test programme. The theory, development and function of both the subjective APCR and objective PAC are then described. As the PAC had only been used with rate command controllers, the development for its use with attitude command controllers is then described and verified. The results from frequency response analyses of selected configurations are then used to predict the proneness to oscillatory APCs using the ADS-33E criteria [36]. An argument to limit the subsequent results analysis to only the pitch axis is presented followed by a description and HQ assessment of the baseline aircraft. Finally, the specifics of the test investigation is described regarding the test pilot selection, general conduct of the tests, assessment of data quality and the test conditions.

6.1 First Order Filter Theory and Conventions

In this study the first order filter transfer function has been used in Bode form where k is the gain, s is the Laplace operator and τ is the time constant:

$$G(s) = \frac{k}{1 + \tau s}$$

Equation 6-1

The specific effect of a first order filter in the time domain for variation of k and τ are shown for a unit step input, figure 6-1(a) and a unit ramp input, figure 6-1(b). The red line represents the input and the green and blue lines represent the output of first order filters k=0.8, τ=0.3s and k=0.8, τ=0.1s respectively.

For the step input, the gain simply multiplies the input by k. The effect of increasing τ slows the response but the steady state amplitude remains the same subject to the gain. The time to reach 63.2% of the steady state value is τ and time to reach 95% is 3τ. For the ramp input, the gain multiplies the gradient by k and the effect of increasing τ slows the response to reach the constant gradient.

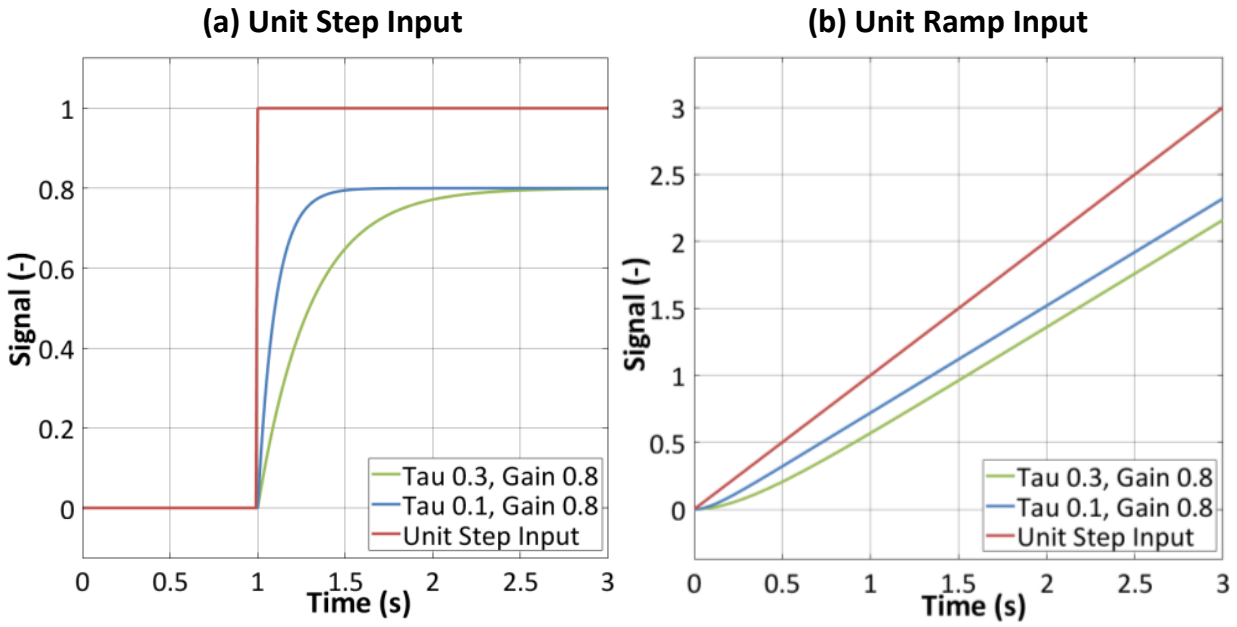

Figure 6-1: Standard First Order Filter Time Domain Response to Step and Ramp Inputs

With an oscillatory input the effect of variation of k and τ are shown in figure 6-2 using an input indicated by the red line with frequency of 2.5rads^{-1} and amplitude of unity. The blue line represents the output of a first order filter k=0.62, τ=0.1s. Similar to the step input, the gain has an effect on the amplitude of the output and τ affects the speed of response. However the frequency of the input now also has an influence on the strength of these effects.

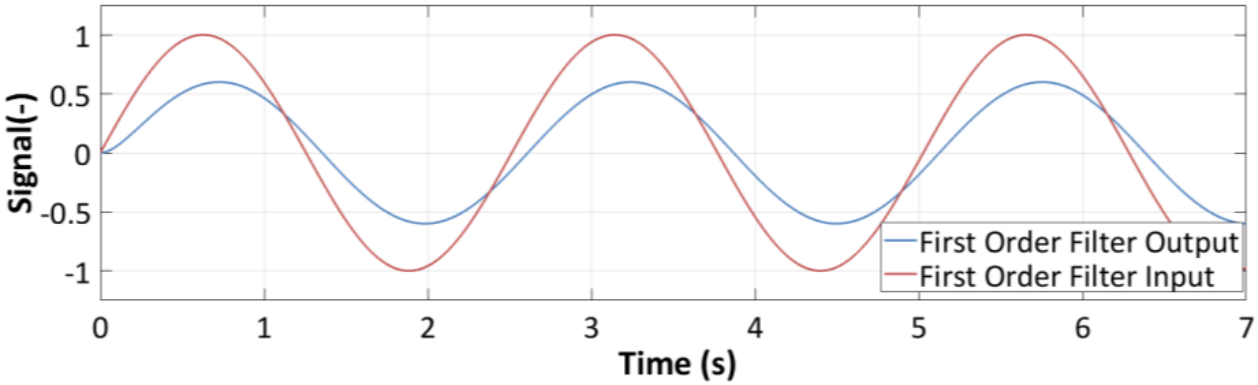

Figure 6-2: First Order Filter Response to 2.5 rads^{-1} Oscillatory Input, AG=0.6, τ=0.1s

Figure 6-3 shows a theoretical Bode plot for a first order system. At low frequencies (and for example the unit step input), the output is simply multiplied by k, but at frequencies greater than 1/τ the Amplitude Ratio (AR) in dB reduces at a rate of 20dB/dec. Whilst the red lines show the asymptotes of the expected frequency response, the difference between the asymptotic intersection and the true curve would be -3dB.

The phase of the output remains at zero for low frequencies but starts to lag from a frequency of 0.1/τ at a rate of 45°/dec until it reaches 90° at 10/τ and thereafter remains constant.

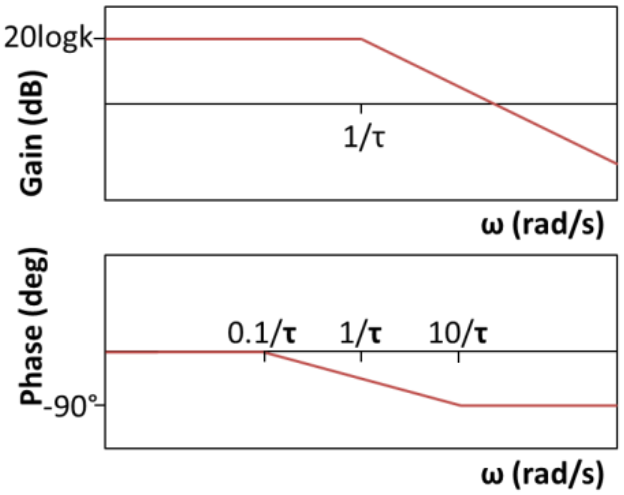

Figure 6-3: Theoretical Bode Diagram for First Order Filter

The corresponding equations for first order filter frequency responses are given in equations 6-2 and 6-3. It is therefore apparent that as τ is increased, the AR is reduced. Whilst τ must be small for a quick response, any noise is passed directly to the output. In order to filter out input noise, τ may be increased but at the expense of increasing the first order lag [88].

$$AR(dB) = 20logk - 20log\sqrt{1 + (\omega\tau)^2}$$

Equation 6-2

$$\Phi = tan^{-1}(-\omega\tau)$$

Equation 6-3

6.2 Justification for First Order Filter Selection

In the compliant condition a second order transfer function is used to convert the inceptor force into a corresponding position. This position signal is then used both as an input to the FCS and also to correctly position the sidestick using the position motors (as detailed in chapter 3). However, Grünhagen et al identified that as the optimal configuration of the second order transfer function for best HQ entailed a high damping ratio above unity; a first order filter could alternatively be used [78]. Despite this subsequently having been confirmed in a flight trial [5], the standard compliant second order filter had been retained within the DLR EC135 ACT/FHS but with an increased damping ratio of 1.

Initially a second order filter as shown in equation 6-4 had also been used for the same task in the isometric condition, where ω_0 is the Eigen frequency, D is the dimensionless damping, k is the force gradient and s is the Laplace operator. The parameters used in the isometric condition, ω_0=3.2Hz, D=1.0, k=1.0N/% had been selected to match those used in the compliant condition. The isometric condition was then flown in the AVES simulator and in the EC135 ACT/FHS using these parameters which were initially approved [108].

$$G(s) = \frac{{\omega_0^2}/{k}}{{\omega_0}^2 + 2D\omega_0 s + s^2}$$

Equation 6-4

However, it was subsequently determined during a simulator campaign [15] that this second order filter for the isometric mode, with the parameters set by theoretical analysis was prone to exposing oscillatory APCs in the isometric mode. Further optimisation of the parameters or the filter structure through practical HQ analysis was therefore required to reduce or eliminate this undesirable tendency.

Figure 6-4 shows the Bode plots of the first order filter shown in equation 6-1 (with k=1.03 and τ=0.1s, subsequently defined as the datum configuration) and the second order filter shown in equation 6-4 (with ω_0=3.2Hz, D=1.0 and k=1.0N/% from the legacy configuration). As is expected, the first order filter creates a negligible lag at low frequencies below 0.1Hz and tends to a 90° lag at high frequencies above 10Hz. The second order filter has a similar negligible lag at low frequencies but tends to 180° lag at high frequencies.

This lag is applied in addition to the lead or lag of the other system components throughout the control path. It is therefore apparent that the lower lag of the first order system throughout the pilot control frequency spectrum would be likely to reduce the overall lag of the control path in comparison to the second order filter. This would ultimately increase its bandwidth and decrease the phase delay (described subsequently in section 6.6), therefore reducing its tendency to oscillatory APCs.

It was also considered that the increased complexity of optimising the three variables of a second order filter (compared with 2 variables in a first order filter) could potentially extend a design process unnecessarily. Consequently, a thorough analysis of a first order filter was planned with the intention of investigating a second order filter as a contingency if it became necessary.

The first order filter was required to translate the force signal into an equivalent position signal during isometric sidestick operation with the following characteristics:

- Proportionally convert a force signal into a position signal that could be used by the flight control system to control the aircraft.
- Reduce the effect of signal noise that is inherent in the force signal.
- Provide some damping to reduce the effect of over-controlling which could lead to APCs.

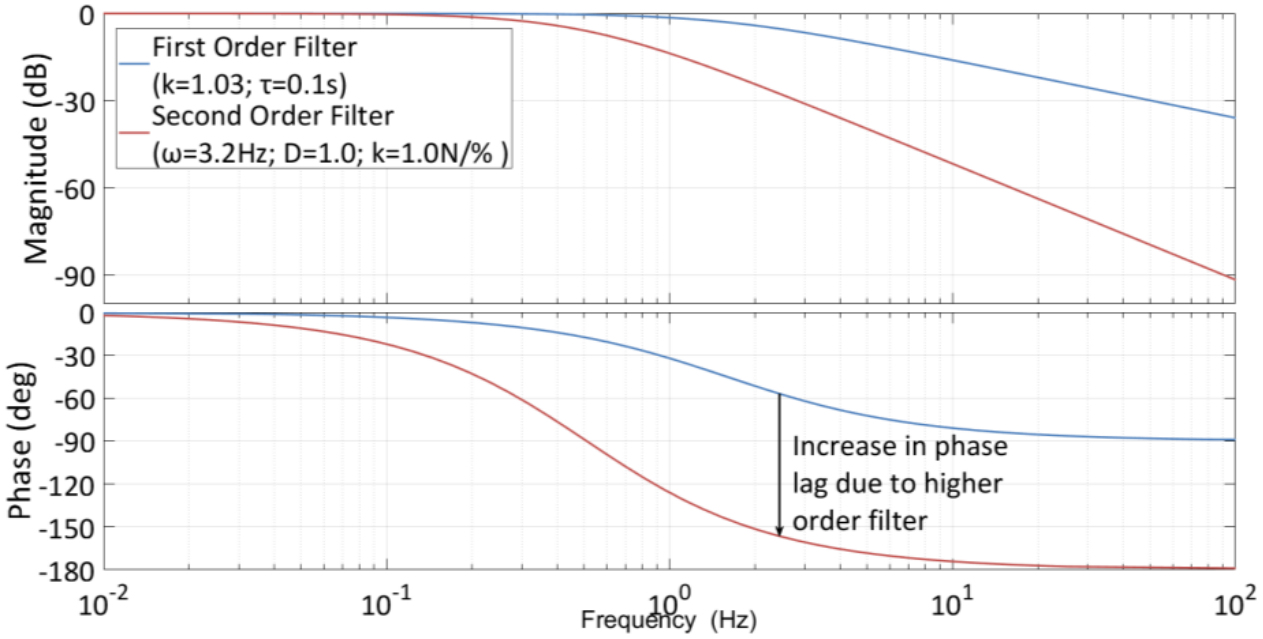

Figure 6-4: Theoretical Bode Plot of Representative First and Second Order Filters

6.3 Selection of Test Parameters

The selection of the transfer function parameters, τ and k that were used in the practical investigation was conducted using the MatLab Simulink model shown in Figure 6-5. The intention of this theoretical analysis was to identify datum values that presented the probable best solution as well as a range of values which presented extreme plausible solutions.

Each of the 4 test pilots were available for one day and were therefore able to support 5 hours of testing in the simulator (plus initial familiarisation training, compliant sidestick CHR assessments and time for breaks). On the assumption that a test point rate of 12-15 per hour was achievable, the expected number of test points was 60-75 for each test pilot.

As the subjective differences of the HQ and APC suppression could be very small for the different test configurations, it was important for the pilot to be able to regularly refer back to a datum configuration for 'qualitative calibration'. It was initially assumed that a cycle of four consecutive non-datum configuration test points followed by one datum configuration test point was adequate to maintain the pilot's 'qualitative calibration'. This was subsequently confirmed as appropriate during the practical investigation by all of the test pilots. Each test configuration would be assessed twice with different approach directions. The entire assessment would also be conducted with both attitude and rate command stability augmentation laws. The result of this calculation was an expectation that 12-15 different test configurations could be investigated in the time available.

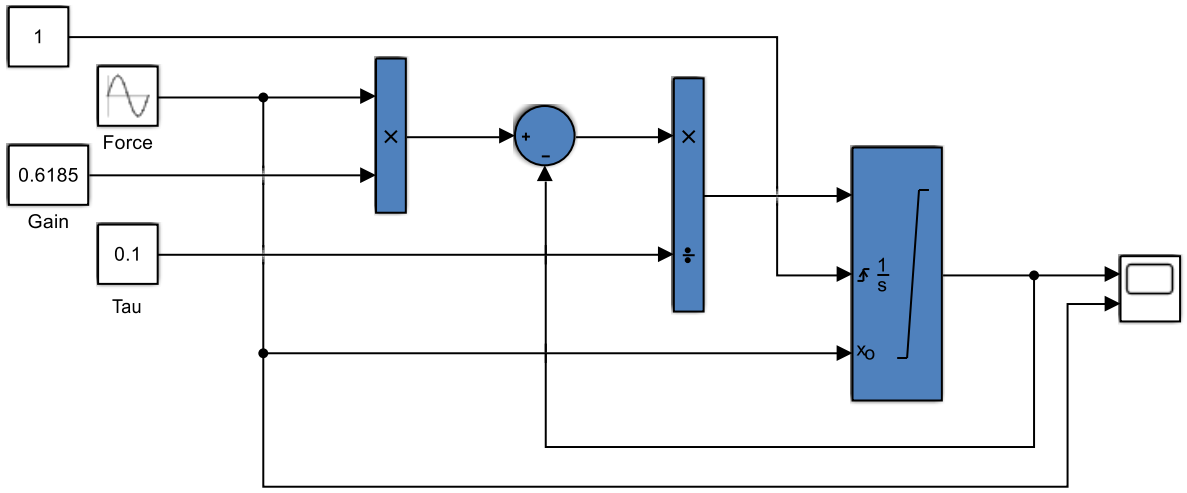

Figure 6-5: Simulink Model of First Order Filter

The control parameters used for the investigation were τ and the amplitude ratio that resulted from a 2.6rads^{-1} oscillation (henceforth referred to as the apparent gain or AG). As previously identified in section 5.6, the most common longitudinal oscillatory APC frequency observed in the representative experimental configuration was 2.6rads^{-1}. The decision to use the apparent gain instead of the value of k from the transfer function was because of how the pilot observed the gain whilst in the APC. As discussed in the previous section, for a system with first order characteristics and low frequency (below 1/τ) or aperiodic control inputs, the pilot observes an apparent gain identical to k, however as the frequency of the inputs increases, the apparent gain reduces. As the purpose of the investigation was to observe the effects of triggered APCs, it was considered that the value of apparent gain would be a more appropriate control parameter instead of k as it specifies the amplitude ratio at the expected APC frequency.

In order to segregate the effects of apparent gain and τ, a variation of τ would require a variation in k to keep the apparent gain constant. Furthermore, in order to vary the apparent gain whilst maintaining τ constant, the value of k required a proportional variation to create a change only in the apparent gain.

The selection of the datum, maximum and minimum values of τ and apparent gain was conducted with the following conclusions:

6.3.1 Minimum Apparent Gain (0.4)

The minimum apparent gain was derived from the ADS-33E [36] defined minimum requirements for large attitude changes and from the gathered control response test data. It was acknowledged that this approach would assume a linearity of the control response with increasing input size and so could only provide very approximate guidance for the selection of an appropriate minimum apparent gain. The corresponding data and calculations are shown in table 6-1. The ratios of steady state responses to step inputs were gathered during testing for both command types and axes. These were multiplied by the maximum available inceptor force which could be applied to and sensed by the sidestick (from the flight control mechanical characteristics detailed in chapter 3) which

produced the theoretical maximum available control response with full control deflection.

The ADS-33E defines minimum rates (rate command) or attitudes (attitude command) that must be achievable with full control deflection, separately defined for limited, moderate and aggressive agility task. The isometric MTE was considered a limited agility task as it shared many of the elements of the hover MTE which had also been categorised as limited agility by ADS-33E. The corresponding minimum rates or attitudes that were required to meet level 1 HQ were then divided by the previously calculated theoretical maximum available control responses to create a theoretical minimum apparent gain. As the minimum apparent gain that was selected had to be applicable to both axes and both command types, the highest value of all 'theoretical minimum apparent gains' was used for the overall minimum (0.42, rounded to 0.4).

	Rate Command		Attitude Command	
	Pitch	Roll	Pitch	Roll
Steady state control response	$1.2875°s^{-1}N^{-1}$	$2.0539°s^{-1}N^{-1}$	$1.7375°N^{-1}$	$2.0964°N^{-1}$
Maximum available control force from 50% trim position	35.6N	23.9N	35.6N	23.9N
Theoretical maximum available control response with full control deflection	$45.84°s^{-1}$	$49.09°s^{-1}$	61.86°	50.10°
Minimum control response in accordance with ADS-33E [36 Table VI]	$6°s^{-1}$	$21°s^{-1}$	15°	15°
Theoretical minimum apparent gain	0.17	0.42	0.24	0.30

Table 6-1: Calculation of Minimum Apparent Gain

6.3.2 Maximum Apparent Gain (1.2)

As the APC previously identified in figure 5-13 had characteristics of over-controlling, that is, the pilot exceeding the required control inputs, it was considered unlikely that a gain much greater than unity would improve the HQ. Nevertheless, an apparent gain of 1.2 was chosen in case a small increase of gain offered improvements for other reasons.

6.3.3 Datum Apparent Gain (1.0)

The selected value of apparent gain for the datum test configuration was unity. It was assumed that an apparent gain in compliant mode should be the same as the apparent

gain in isometric mode, such that the transient effects would be minimised and the control power would be as close to the pre-failure aircraft as possible.

6.3.4 Maximum Time Constant, τ (0.3s)

A larger time constant increased the damping of high frequency inputs and signal noise but created a phase lag between the force input and the equivalent position signal output. An example phase Bode plot of the recorded frequency response using the compliant cyclic position as an input and aircraft attitude as the output for attitude command in the roll axis is shown in figure 6-6. The equivalent Bode plots of both axes in rate command and attitude command are shown in appendix D. These frequency responses represent all components of the helicopter control system, flight dynamics model and simulator model other than the conversion function of the pilot's input force signal into a position signal. In order to establish the phase lag of the entire system of pilot force input to attitude output at a specific frequency, the phase lag of the isometric first order filter (or second order filter in the compliant mode) would need to be summed to the lag observed in the bode plots of pilot position input to attitude output.

The phase margin is defined as the difference between the phase lag at any specified frequency and a phase of -180°. The phase bandwidth is the measure of the range of frequencies over which a pilot can exert good closed loop control without having to compensate excessively [64] and in accordance with ADS-33E [36] is defined as the frequency at which there is a 45° phase margin (phase lag at -135°).

The phase lags at 2.6rads^{-1} were taken from the corresponding Bode plots, converted into their respective phase margins and are detailed in table 6-2. The highest phase margin identified was 79° (for the roll axis in attitude command). In this case the phase margin could be reduced by 34° through the effect of the filter, before the phase bandwidth at 45° margin would be reached and at which point the aircraft may display instability [15]. The time constant that would create the additional phase lag for the system to have a phase bandwidth of 2.6rads^{-1} was then calculated using equation 6-3 and is shown for all cases in table 6-2. Similar to the argument for the selection of maximum apparent gain, the maximum time constant that was selected had to be applicable to both axes and both command types, therefore the highest value of time constant was used for the overall maximum (0.27 rounded to 0.30).

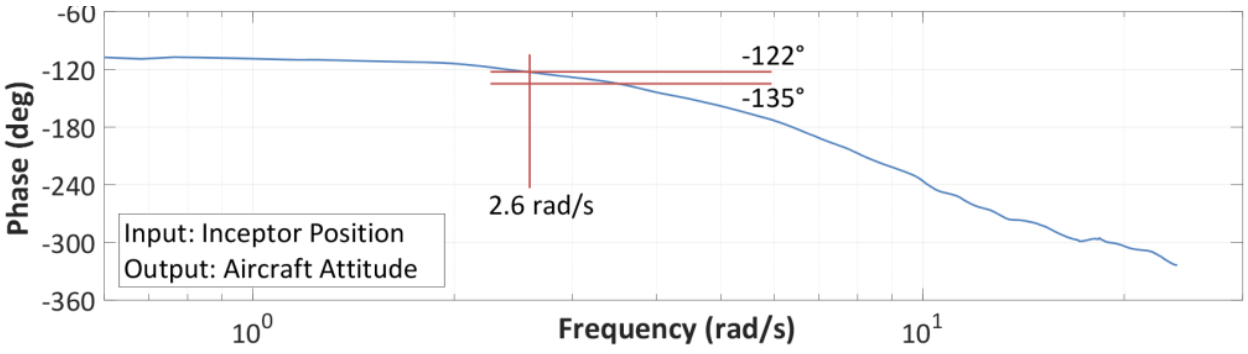

Figure 6-6: Phase Bode Plot, Attitude Command, Roll Axis, Compliant AIS Mode

	Rate Command		Attitude Command	
	Pitch	Roll	Pitch	Roll
Phase Lag at 2.6rads^{-1}	-122°	-122°	-104	-101
Phase Margin at 2.6rads^{-1}	58°	58	76°	79°
Time Constant required to generate $\omega_{BW\text{-}GAIN}$ of 2.6rads^{-1}	0.092s	0.093s	0.244s	0.271s

Table 6-2: Phase characteristics of Combined First Order Filter and Aircraft at 2.6rads^{-1}

An additional and equally important factor on selecting the maximum value of τ was the requirement to keep the value of H_{SF} constant. With reference to the first order filter theory described earlier in this chapter and the relevance of and calculation of H_{SF} described subsequently, if τ was greater than 1/ω of the forcing frequency, the AR would start to reduce and would have an effect on the H_{SF}. In theory a variable H_{SF} would be possible but has not yet been tested nor validated. Whilst this was a problem only for the PAC tool and would not affect the tendency of an APC, it was a limitation for the use of the PAC in its current form. With an expected APC frequency of 2.6rads^{-1} (0.4Hz), the maximum τ that could be used with the PAC tool would be 0.4s.

6.3.5 Minimum Time Constant, τ (0.01s)

A wide variety of time constants were investigated using the MatLab Simulink model of the first order filter in figure 6-4 with a pure sinusoidal input frequency of 2.6rads^{-1}. The figures 6-7, 6-8 and 6-9 depict the comparisons of the input inceptor force to the equivalent output position of the first order filters in the time domain for variation of time constant. The filter parameter configurations in the figure titles cross reference to the full list of all configurations used in this study that are defined in table 6-3. In these plots the output has not been modified by the appropriate conversion factor that is required to convert the force signal into a position signal for the specific aircraft and control system. The output is therefore referred to as the *normalised* equivalent inceptor position and is not a true equivalent inceptor position. As expected, an increase in τ caused an increase in phase lag and if reduced to a very low value of 0.01s, produced a phase lag of just 1.43° as shown by the almost identical traces in figure 6-7. However, as the sidestick force signal was inherently 'noisy', the modelled pure sinusoidal input was summed with a random noise signal to investigate the effect of τ in more realistic conditions. Figure 6-10 shows the output position equivalent for the 'noisy' input signal. Due to the very low τ value of 0.01s, virtually all of the noise on the input signal was passed through to the output signal. Whilst not ideal from the noise perspective, a zero value of τ would have eliminated any phase lag caused by the filter, but for practical purposes and to maintain a consistent experimental approach, the non-zero value of 0.01s was selected as the minimum value.

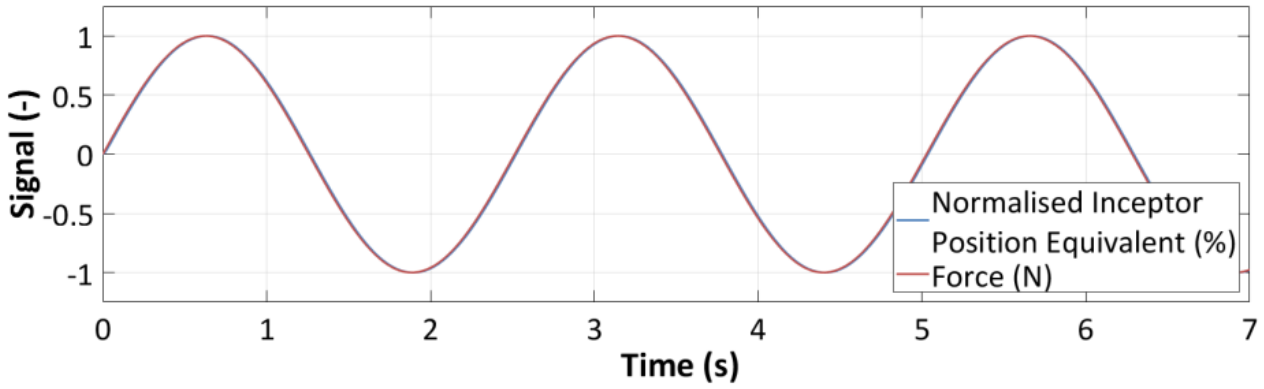

Figure 6-7: Time Response of First Order Filter, AG=1.0, τ=0.01s, Config. 6

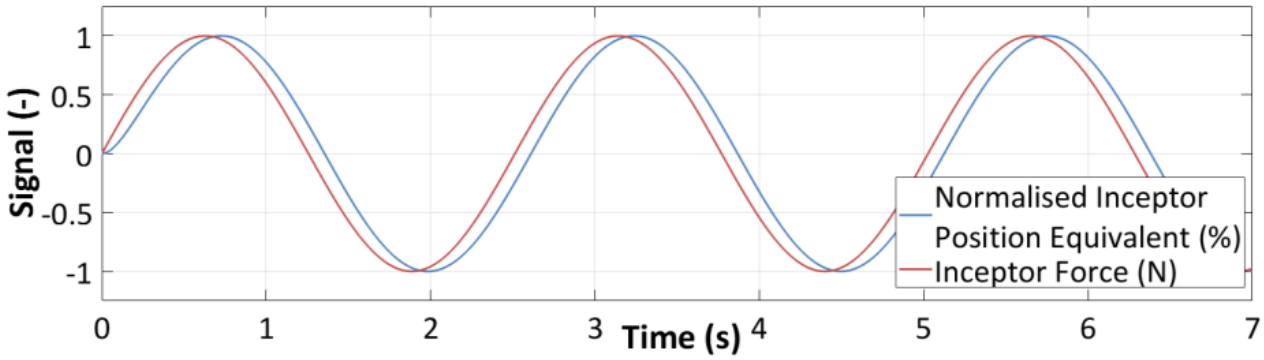

Figure 6-8: Time Response of Datum First Order Filter, AG=1.0, τ=0.1s, Config. 1

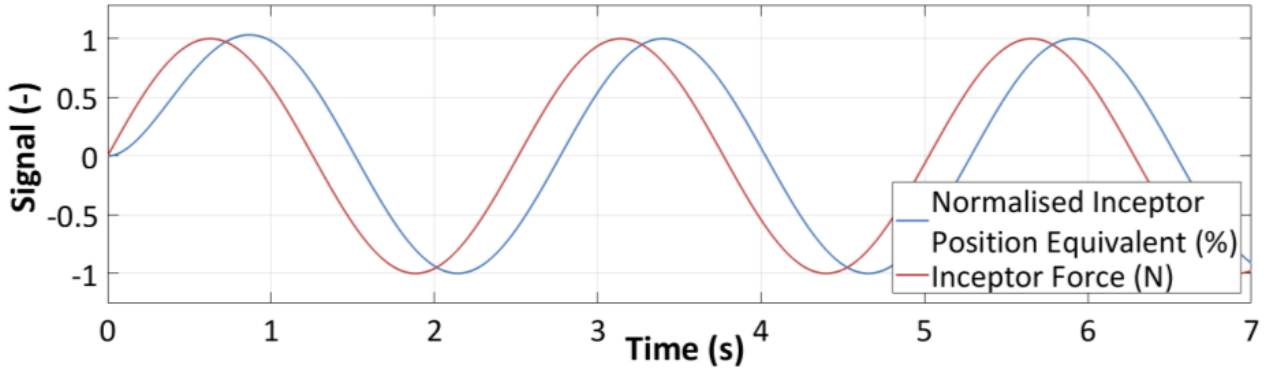

Figure 6-9: Time Response of First Order Filter, AG=1.0, τ=0.3s, Config. 8

6.3.6 Datum Time Constant, τ (0.1s)

As τ was increased, so was the damping effect on the signal. This led to less of the input noise being observed in the output signal, but at the disadvantage of increasing the phase lag. A compromise between noise transmission and phase lag was found at a τ of 0.1s, as shown in figure 6-11. This kept the phase lag as low as possible (14.3°) without the noise significantly affecting the aircraft response.

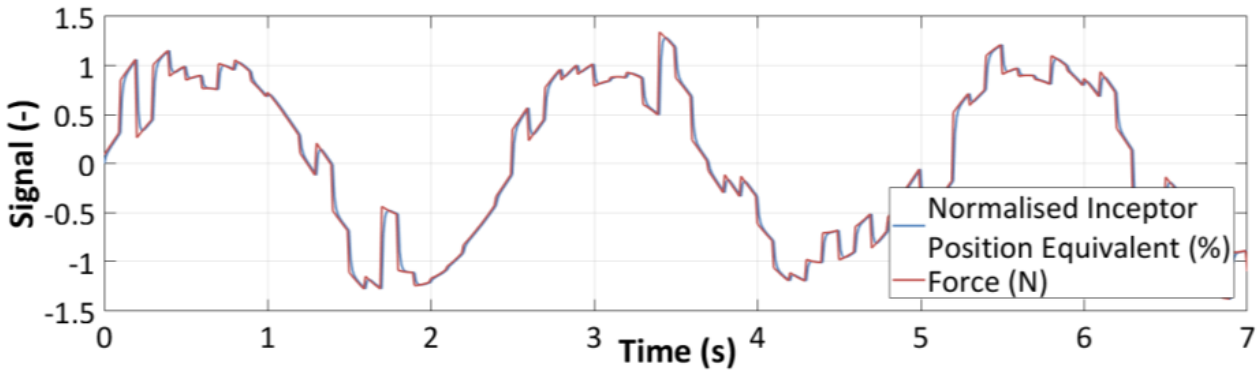

Figure 6-10: Time Response of First Order Filter with Noise, AG=1.0, τ=0.01s, Config. 6

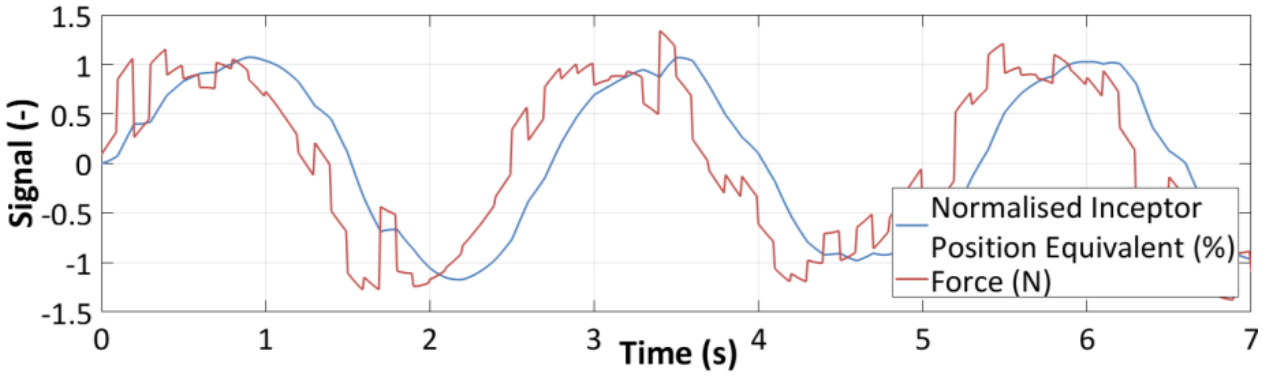

Figure 6-11: Time Response of First Order Filter with Noise, AG=1.0, τ=0.1s, Config. 1

6.3.7 Ramp Attenuator

In order to investigate the potential of reducing the effect of the initial high amplitude pilot's reaction that was experienced immediately after the failure (previously discussed in section 4.5), an optional ramp attenuator was added to the datum first order filter configuration. The purpose of the attenuator was to multiply the gain of the transfer function from 0 to 1 over a specified time period. The characteristic of the ramp attenuator was a proportional linear ramp generator as defined by the transfer function in equation 6-5, with a gradient A and limited between 0 and +1. The ramp attenuator gradients for both longitudinal and lateral axes were always set to the same value.

$$K(s) = \frac{A}{s}$$

Equation 6-5

For the Simulink model that was used within the AVES Experimental System, the ramp attenuator was modelled as a rising integrator with a saturation limit of 1, an initial condition of 0 and a user defined gradient. The trigger to start the integrator slope was provided by the isometric failure signal. Figure 6-12 shows the Simulink model of the ramp attenuator added to the first order filter.

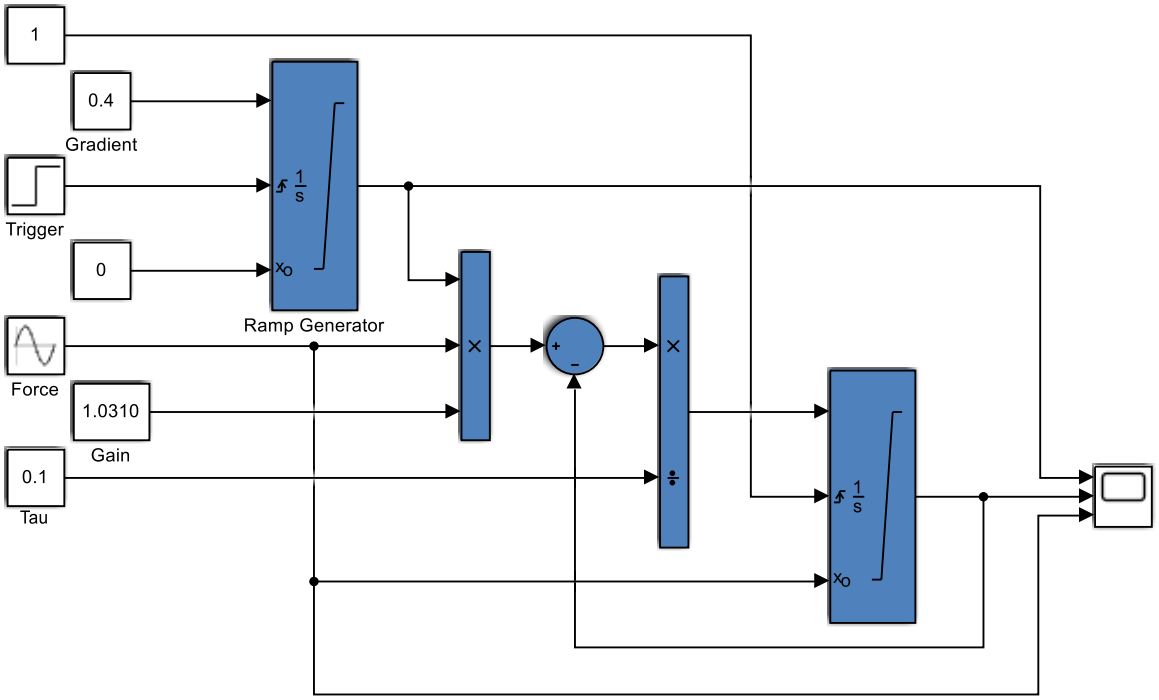

Figure 6-12: Simulink Model of First Order Filter with Ramp Attenuator

The ramp attenuation periods that were selected for the investigation were derived from the time period of the typical APC frequency (2.6rads^{-1}) observed during initial MTE definition testing (section 5.6). Hence, the output signal would increase from zero to its full value over the period of 0.5, 1.0 or 1.5 of a typical APC cycle. Table 6-3 presents the ramp attenuation periods selected.

Fraction of Typical APC Time Period (-)	Ramp Attenuation Time Period (s)	Ramp Attenuation Gradient (s^{-1})
~0	0.01	100
0.5	1.25	0.80
1.0	2.50	0.40
1.5	3.75	0.27

Table 6-3: Ramp Attenuator Periods selected for First Order Filter Investigation

Figure 6-13 presents the combined output of the first order filter and ramp attenuator for test configuration 10 (AG=1.0; τ=0.1s; ramp attenuation period 1.0 cycle or 2.5s). The first order filter parameters of configuration 10 are identical to those of the datum configuration (configuration 1). The input force (red trace) oscillates at 2.6rads^{-1} and has amplitude of unity. The multiplication of the ramp (green trace) with the input force can be seen in the output of the combined filter and ramp, as indicated by the normalised inceptor position equivalent signal (blue trace). The amplitude of the output can be seen

to increase relative to the input until it reaches parity at 2.5s. As would be expected, the phase lag and steady state gain are unaffected by the ramp attenuator.

When the ramp attenuator was not required, the ramp slope was set to 100s^{-1} thereby reducing the ramp period to 0.01s. With such a short ramp period, the effect of the attenuation was effectively removed.

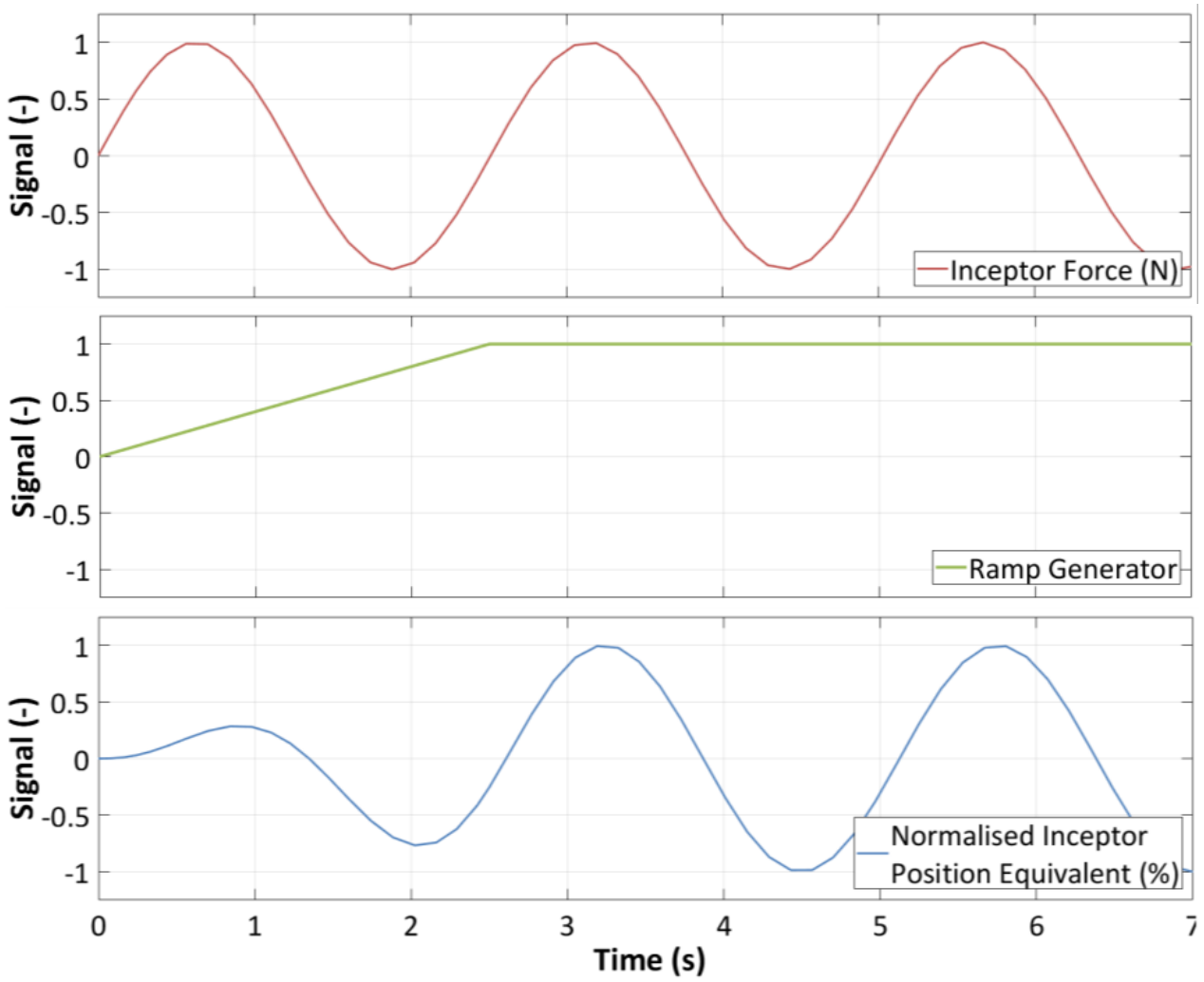

Figure 6-13: Time Response of Datum First Order Filter with 2.5s Ramp Attenuator

6.3.8 Configuration Matrix

The specific test configurations were selected to include the datum, the extreme values and some intermediate values of each of the three control parameters, apparent gain, time constant and attenuation gradient. The test configurations that investigated independent variation of the parameters were classified as high priority. Test configurations that varied both apparent gain and time constant simultaneously were also identified, but only classified as medium or low priority and would therefore only be completed if time and facilities allowed. The full list of all test configurations is presented in table 6-4 showing the first order parameter settings of k and τ as well as the corresponding apparent gain and phase lag at 2.6$rads^{-1}$. Three test configurations which

incorporated a ramp attenuator combined with the datum first order filter settings are also presented with their independent configuration reference. All test configurations are also presented graphically with the relative priorities in figure 6-14.

Test Configuration	Low Frequency Gain, k (-)	Time Constant, τ (s)	Ramp Period (s)	Apparent Gain (-)	2.6rads^{-1} Phase Lag (°)	Test Configuration Priority
1 (Datum)	1.0310	0.10	0	1.0	14.32	High
2	1.2375	0.10	0	1.2	14.32	High
3	0.8247	0.10	0	0.8	14.32	High
4	0.6185	0.10	0	0.6	14.32	High
5	0.4123	0.10	0	0.4	14.32	High
6	1.0005	0.01	0	1.0	1.43	High
7	1.1180	0.20	0	1.0	27.20	High
8	1.2500	0.30	0	1.0	37.25	High
9	1.0310	0.10	1.25	1.0	14.32	High
10	1.0310	0.10	2.50	1.0	14.32	High
11	1.0310	0.10	3.75	1.0	14.32	High
12	1.2000	0.01	0	1.2	1.43	Med
13	0.6002	0.01	0	0.6	1.43	Med
14	0.6708	0.20	0	0.6	27.20	Med
15	1.3420	0.20	0	1.2	27.20	Med
16	1.4145	0.40	0	1.0	45.80	Low
17	0.8002	0.01	0	0.8	1.43	Low
18	0.8945	0.20	0	0.8	27.20	Low

Table 6-4: Selected First Order Filter and Ramp Attenuator Configurations

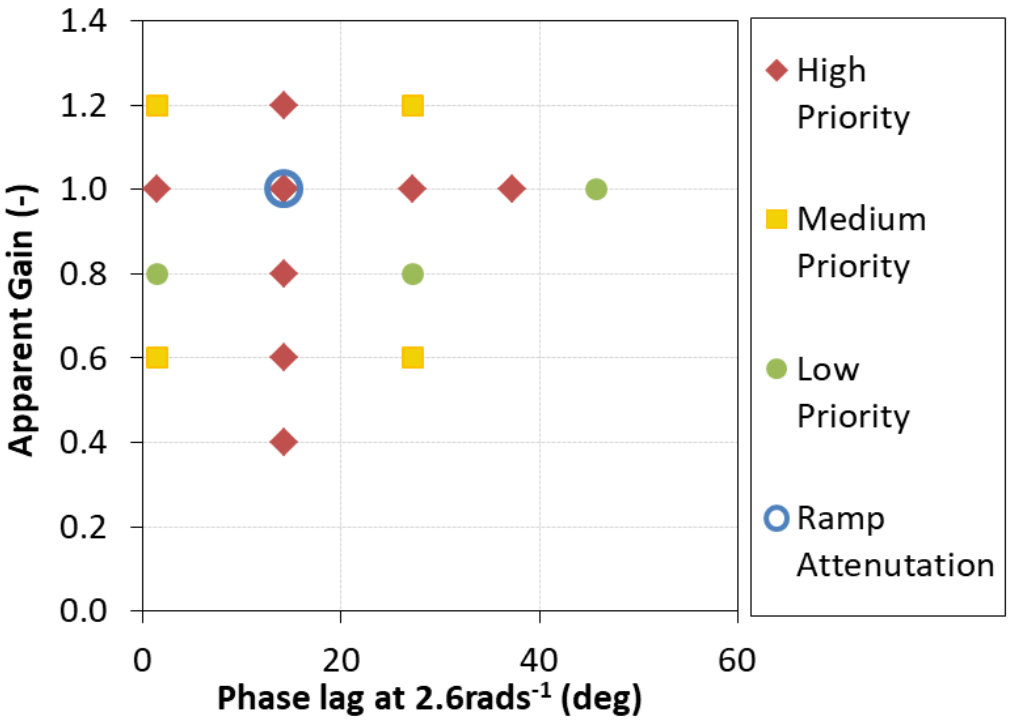

Figure 6-14: Relative Priority of Selected First Order Filter Test Configurations

The values of the time constant and attenuation ramp gradient could be set directly in the ACS experimental system using the CDU. However, because the first order transfer function converted the force signal to an equivalent position signal, the value of gain also had to encompass the conversion factor of force to position. From the flight control mechanical characteristics of the sidestick in compliant mode, presented in the standard graphical format in figures 3-13 and 3-14 and detailed further in chapter 3, the average ratio of position to force taken over the full cyclic envelope was 1.41%N^{-1} for the longitudinal axis and 2.29%N^{-1} for the lateral axis. The gain value that was then set in the CDU was the product of the position to force gradient for the respective axis and the configuration specific value of k.

6.4 Adverse Pilot Coupling Rating

6.4.1 Development and Description of APCR

Within this study, the Adverse Pilot Coupling Rating (APCR) was used for subjective analysis of the APC susceptibility and severity. The APCR was developed by Jones and Jump [48, 49] in order to resolve issues with the legacy PIO rating scales.

The US Aviation Safety Council [64] defines APC events as “rare, unintended, and unexpected oscillations or divergences of the pilot-aircraft system. Adverse APC events are fundamentally interactive and occur during highly demanding tasks when environmental, pilot, or aircraft dynamic changes create or trigger mismatches between actual and expected aircraft responses.” It further defines two major types of APC events: oscillatory events commonly referred to as PIOs and non-oscillatory events.

For oscillatory APCs to occur the following three conditions must be met [96]:

- An active pilot attempting to control the aircraft within the control loop,
- Unfavourable and undesirable response of the vehicle,
- An event or 'trigger' which causes oscillations to occur.

The very first pilot rating scale that was used to assign a numerical rating to the severity of an APC was presented in 1963 [109]. This 'Pilot Opinion Rating Scale' was developed further by DiFranco [50] and, in its form detailed in table 6-5, has been used extensively since. Whilst this scale is simple and intuitive, it provides no guidance to the pilot in bracketing the possible ratings and therefore is prone to large variations of results between pilots experiencing the same APCs. Further iterations of APC scales have continued to be developed by various research organisations, notably Calspan in 1981 [110] which introduced a decision tree and the US Military in the Mil-HDBK-1797A [111] which drew the decision tree concept together with the descriptors of the DiFranco scale. A combined scale of the decision tree and the descriptors is presented in the Test Guide for ADS-33E [112] and copied in figure 6-15. This combined scale is hereafter referred to as the legacy PIO rating scale (PIOR) and is used in this study only for the purpose of validating the APCR.

Rating	PIO Description
1	No tendency for pilot to induce undesirable motion.
2	Undesirable motions tend to occur when pilot initiates abrupt manoeuvres or attempts tight control. These motions can be prevented or eliminated by pilot technique.
3	Undesirable motions easily induced when pilot initiates abrupt manoeuvres or attempts tight control. These motions can be prevented or eliminated, but only at sacrifice to task performance or through considerable pilot attention and effort.
4	Oscillations tend to develop when pilot initiates abrupt manoeuvres or attempts tight control. Pilot must reduce gain or abandon task to recover.
5	Divergent oscillations tend to develop when pilot initiates abrupt manoeuvres or attempts tight control. Pilot must open loop by releasing or freezing the stick.
6	Disturbance or normal pilot control may cause divergent oscillation. Pilot must open control loop by releasing or freezing the stick.

Table 6-5: Pilot Opinion Rating Scale, DiFranco, 1967

The limitations with all of the preceding APC rating scales were noted by Jones and Jump [48] as:

- They did not contain sufficient 'subjectivity' for the pilots to adequately provide a rating that they felt accurately described the situations encountered. Each path of decision branch led to only one rating option.
- There was insufficient consideration given to what happened after the onset of the oscillatory behaviour, or how this was linked to 'task performance'.
- There was little consideration for the impact of or on the task itself.
- There was always difficulty in being able to distinguish between 'undesirable motions' and 'oscillations'.

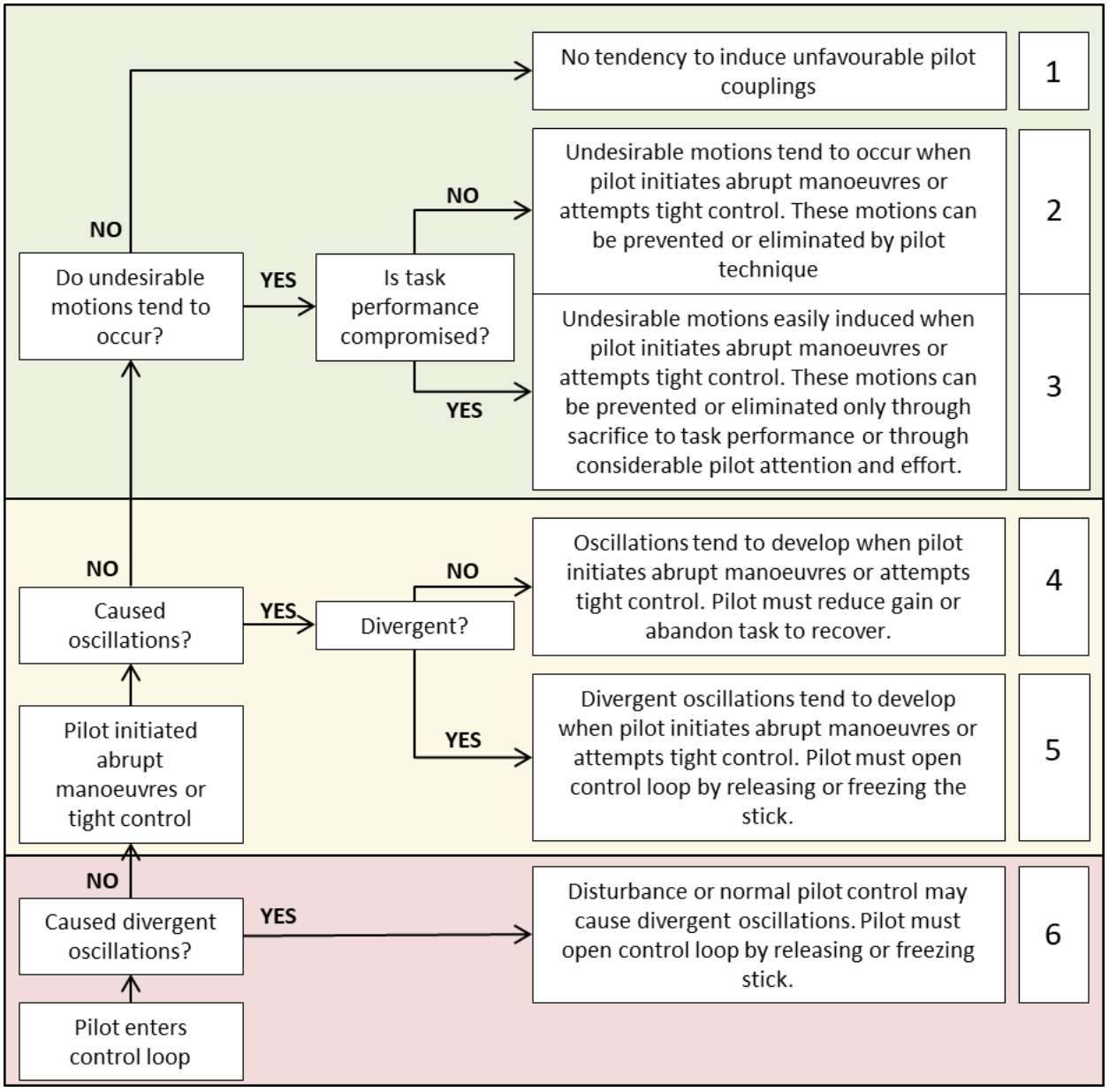

Figure 6-15: Combined (or Legacy) PIO Rating Scale

In order to address these issues the APCR scale depicted in figure 6-16 was developed. The APCR demanded more information to describe the characteristic of the APC; integrated the decision tree directly with the task performance; and introduced comparison of the oscillation to pilot adaptation and workload. Most importantly, it provided greater fidelity within the more significant circumstances where oscillations were suppressed in order to remain within the task (APCR 4-7 / PIOR 2-3). The accompanying definitions also provided the clarity between undesirable motions and oscillations:

- Unintentional: Vehicle response that the pilot did not intend to induce through their control strategy.
- Undesirable: Vehicle motions that are unwanted and adversely affected task performance.
- Motions: Vehicle translational or rotational response due to pilot control.
- Oscillations: Periodic control and vehicle motions exhibited during close-loop flying tasks.

The APCR is split into 3 assigned regions: the desired region (APCR 1) for which no undesirable motions or unintentional vehicle responses were observed; the closed-loop suppression region (APCR 2-7) for which the pilot was required to adapt their control strategy or increase workload in order to continue with task; and the task failure region (APCR 8-9) for which the pilot was unable to commence or continue with the task due to the severity of motions. The structure of the decision tree is similar to the familiar CHR scale [51] and the IFES scale, in that the pilot enters the scale at the bottom left and answers the vertical path questions. The vertical progress continues until a positive response is selected and then the pilot enters one of the three regions. Within the closed loop suppression region the pilot must further select whether the motions were unintentional oscillatory or unintentional non-oscillatory. Unintentional non-oscillatory motion (APCR 2-3) implies that the vehicle has incipient APC qualities but the task did not force the motion to become oscillatory [48]. The pilot must then select the most appropriate descriptor from the limited options available. If the pilot entered the closed-loop task but was not able to maintain the task-defined performance standard or was no longer engaged in the task due to suppression of the APC, a rating of no lower than 8 must be assigned. If a rating of APCR 4-7 has been assigned (or the task was abandoned after an initial closed loop attempt), the pilot must also assign a characteristic letter A-E describing the nature of the oscillations.

For consistency across all of the test pilots involved and because for many, it was a new scale for which they had received no formal training (unlike for example the CHR), it was essential that they used the APCR scale within clearly defined ‘rules’:

- The definitions of *Unintentional, Undesirable, Motions,* and *Oscillations* were reviewed and understood prior to the test flight.

- The pilot had to assign a rating based upon what actually happened and not what he/she felt had been the tendency to occur (which presented a difference from the legacy rating scale).

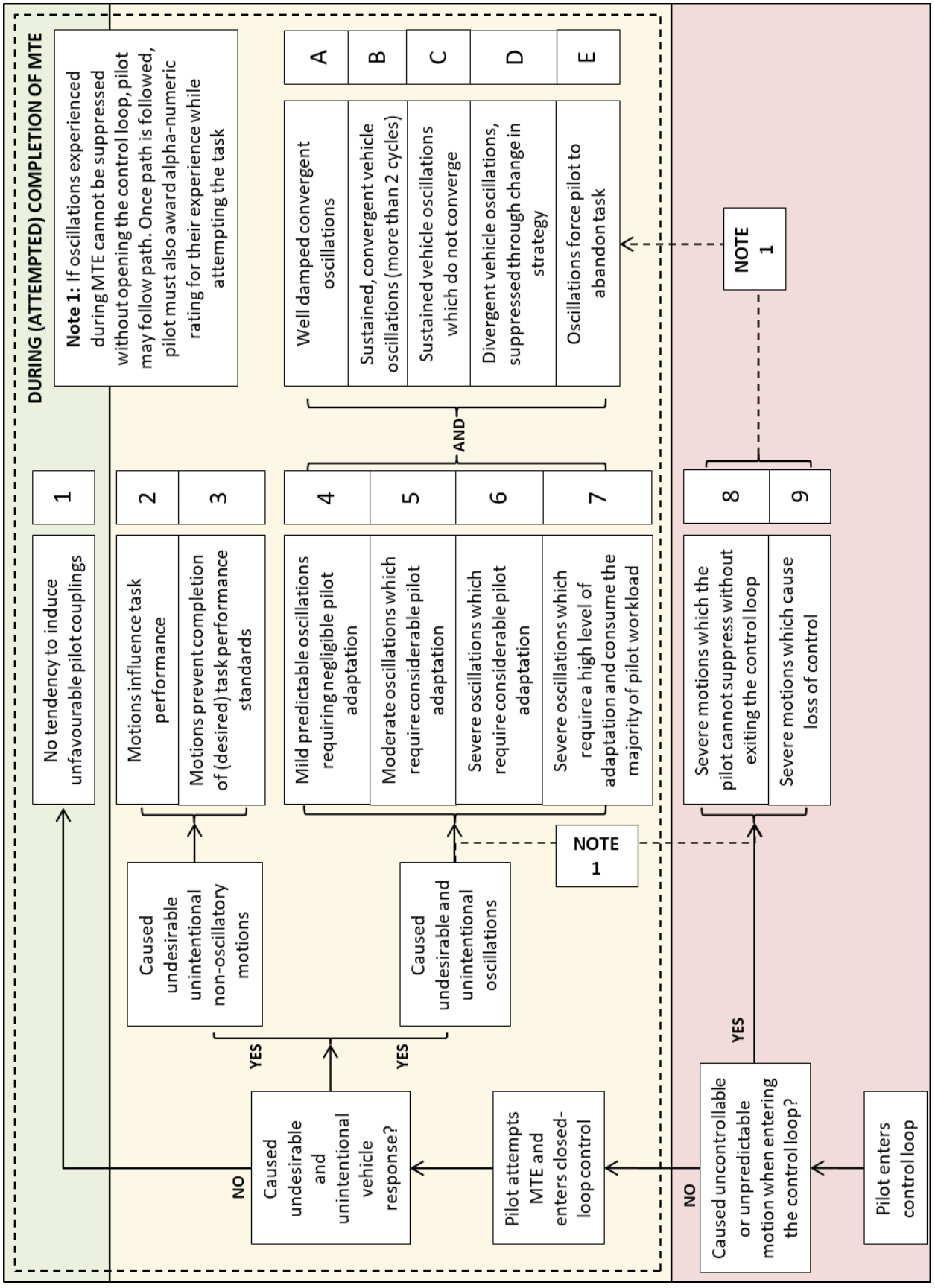

Figure 6-16: Adverse Pilot Coupling Rating Scale

- For each rating assignment the pilot had to enter the decision tree from the start and answer each question and not jump straight to the descriptors.
- For the purposes of establishing a datum for pilot adaptation, ‘considerable’ inferred that the pilot had to consciously act to suppress oscillation but still retained some spare capacity for ancillary tasks.
- The term ‘loss of control’ in the descriptor for APCR 9 inferred that the pilot was unable to retain control of the aircraft sufficiently to execute a safe landing on clear, flat ground within the structural limits of the aircraft and without concern for accuracy.
- ‘Safe‘ and accurate flying had to be given a higher priority than APC suppression.
- The pilot had to always attempt to achieve ‘desired’ tolerances and not accept ‘adequate’ in order to suppress the APC.

6.4.2 Validation of APCR

Validation of the APCR scale has been conducted both in simulators [48, 49, 15] and in flight [96] using the legacy PIO scale as a comparator.

During the original research and development of the APCR, its initial validation was flown by four test pilots in the University of Liverpool Simulator [48]. The precision hover MTE was selected as a suitable high gain task that could expose an APC. ADS-33E [36] describes the task as a translation at 6-10kt in the forward-right direction followed by a deceleration to select and maintain a hover within defined performance standards assisted by specific external references. Appendix C describes the MTE and performance standards in full. The external visual height reference consisted of a white board with a thick black border located 150ft from the hover position and a spherical marker mounted on a pole located at 75ft from the hover position. In order to maintain the desired height, the pilot had to keep the marker within the white area of the board (the black border represented adequate performance) from his/her point of view. The aircraft model was a Bo105 that was reportedly not APC prone. In order to progressively increase the APC tendency and severity, a range of time delays and rate limits were introduced into both the pitch and roll control axes, resulting in four vehicle configurations. Additionally, in order to improve the consistency of the required pilot feedback gain, the task was adapted to reduce the performance tolerances by moving the pole towards the aircraft (75, 40 and 20ft), whilst leaving the board at the standard position.

The comparative results are presented in figure 6-17 as a plot of the APCR against the PIOR for each of the 58 test points. The numbers displayed on the plot represent the number of times each specific correlation was assigned.

Whilst it is acknowledged that a number of limitations exist with the PIOR, it has had a long established history in flight testing and can be used effectively to determine the severity of an APC. Any new rating scale must resolve these limitations whilst still retaining some correlation with the legacy scale. The results demonstrated a correlation

between the APCR and the PIOR; however they also highlighted some of the deficiencies of the PIOR. As an example, of the 13 test points that were awarded PIOR 3, the spread of APCR varied from 2 to 7. This was due to the broad spectrum of APC that fulfilled the definition of PIOR 3:

> *Undesirable motions easily induced when pilot initiates abrupt manoeuvres or attempts tight control. These motions can be prevented or eliminated, but only at sacrifice to task performance or through considerable pilot attention and effort.*

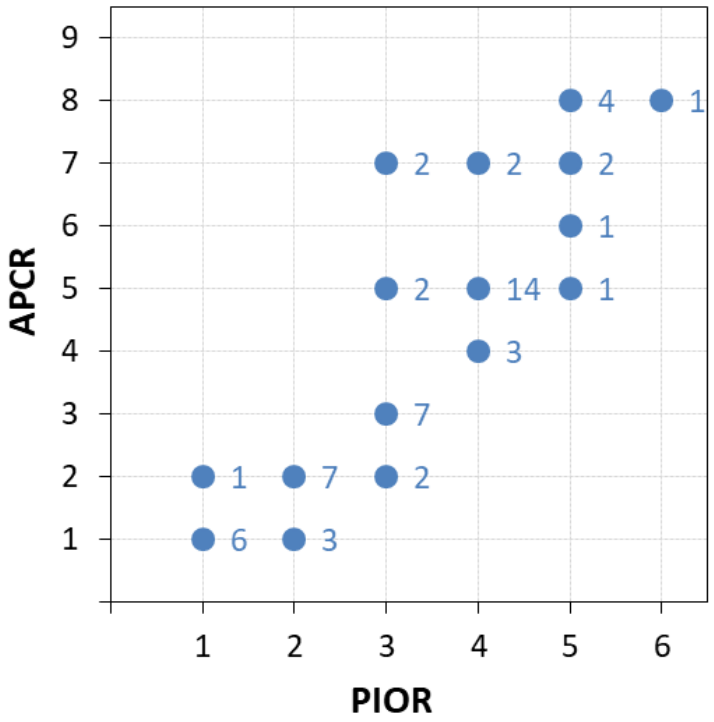

Figure 6-17: Comparison of APCR and PIOR Results from Simulator Validation

This descriptor includes non-oscillatory and oscillatory motions and covers a broad range of pilot workload and adaptation. In contrast, the APCR descriptors define the type of oscillation and pilot compensation more distinctly and offer the test pilot broader options to accurately reflect the APC that was experienced.

Furthermore, test pilot opinion within this validation exercise of the APCR was favourable and it was considered a major improvement over the legacy PIOR scale.

A second validation of the APCR was conducted during a simulator investigation at DLR into APCs caused by an isometric sidestick failure of an aircraft with artificial time delays and rate limiters [15]. The MTE described in chapter 5 was used with both APCR and PIOR assigned for each test point to characterise the APCs. Four test pilots were used, of whom all had previous experience of the PIOR scale but no previous experience of the APCR scale. Comparison of the results of the two scales demonstrated similar conclusions to the original validation, that the APCR was more suitable but still provided correlation with the PIOR.

The investigation also highlighted the benefit that the APCR scale provided more information describing any oscillations within the supplementary assigned letters A to E (defining whether they were sustained, convergent or divergent which was not always apparent in the PIOR scale). General pilot opinion of the APCR was that it provided more detail of the severity and nature of an APC in direct relation to the completion of the MTE.

Most recently, an in-flight validation of the APCR was conducted in the NRC variable stability Bell-205A as part of a DLR-NRC collaboration [96]. The purpose of the research was to explore novel methods and techniques that expose rotorcraft APCs. Therefore as well as using the objective analysis of the PAC as described in section 6.5, subjective analysis using both the APCR and the legacy PIOR was performed. The NRC Bell-205A was configured with various flight control settings that affected how prone the aircraft was to APCs (standard rate damped; strongly rate damped; weakly rate damped, attitude command). Four MTEs were selected (Pirouette, Precision hover, Lateral reposition, Depart abort) and were conducted using the ADS-33E course at Ottawa International airport. The precision hover MTE was flown in 3 formats: standard as described in ADS-33E; position tolerances for both desired and adequate reduced by 50%; and translational speed increased from the standard 6-10kt to 13-17kt. All test points were flown by one test pilot who had extensive previous experience of both the APCR and PIOR scales.

The comparative results are presented in figure 6-18 as a plot of the APCR against the PIOR for each of the 20 test points. The numbers displayed on the plot represent the number of times each specific correlation was assigned.

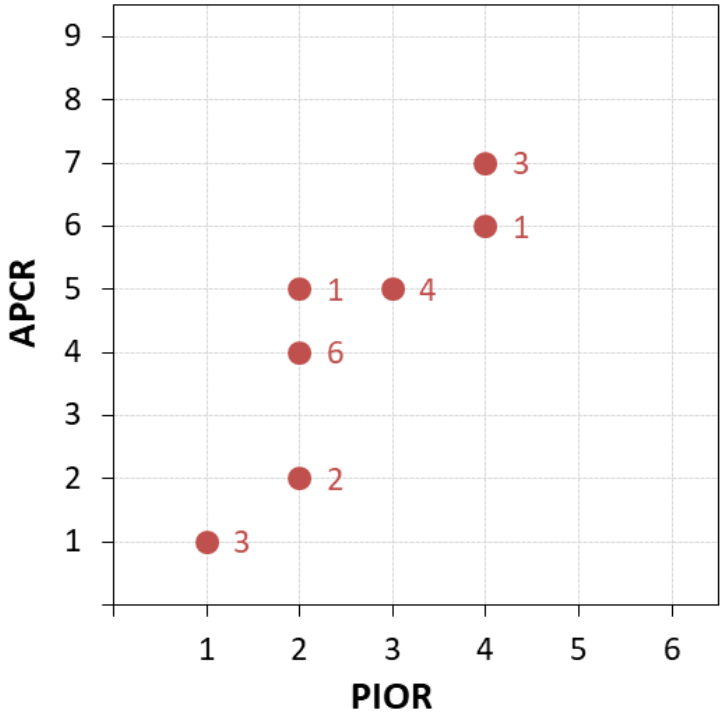

Figure 6-18: Comparison of APCR and PIOR Results from Flight Validation

Similar to the initial validation conducted in the University of Liverpool simulator, the validation from the flight results show a correlation between the assigned APCRs and PIORs. A condition in which PIOR 1 was assigned was consistently also assigned APCR 1. Whilst the PIOR assigned ratings were confined to just 1 to 4, the APCR assigned ratings varied between 1 and 7, demonstrating the broader descriptors that the test pilot assigned to match the APCs observed.

In order to demonstrate an advantage of the APCR scale, two test points may be considered, for which the pilot assigned PIOR 4 and APCR 7C. The PIOR descriptor for a rating of 4 and 5 both state that an oscillation developed, but the rating 5 further states that the oscillation was divergent. As it was not divergent in these example test points, the assigned rating was therefore 4. This highlights the limitation of the PIOR scale in that the oscillation was severe, sustained but not divergent so was still assigned a PIOR of 4, whereas with the APCR scale they were assigned a more appropriate 7 relating to the severity and C relating to its sustained, non-divergence. Thus, in comparison with the legacy PIOR, the APCR was shown to provide a more linear reflection of the severity whilst also conveying a broader description of the oscillations.

After completion of all test points, the test pilot commented that the decision tree construct of the APCR held an advantage over the PIOR in reducing the scope of interpretation and therefore variation across different test pilots, leading to better data quality and reliability. However he emphasised that due to the inherent relationship between the severity of the APC and the required feedback gain of the pilot, the APCR could only function with a suitable MTE with a specific course description and defined performance tolerances. The test pilot also recommended that due to a large jump in pilot adaptation from APCR 4 to 5, the wording of the APCR 5 descriptor should be changed to '…moderate pilot adaptation'. Unfortunately, this recommendation was only noted after the test phase of this PhD study had been completed.

6.5 Phase Aggression Criterion (PAC)

6.5.1 Objective APC Analysis Tools

The objective analysis of the APCs was conducted using the Phase Aggression Criterion (PAC) that was developed by Jones, Jump and Lu [66]. The PAC is an analysis tool that can be used for either near real time or post flight APC identification and provides a continuous graphical representation of the severity of the APC throughout a given time period.

The decision to use the PAC was taken after a review of alternative tools which included the Real Time Oscillation Verifier (ROVER) developed by the US Air Force [113] and subsequently by the NASA Dryden Flight Research Centre [114], the Open Loop Operating Point (OLOP) developed by Duda [15, 115, 116] and the Pilot Inceptor Workload (PIW) developed by Gray [117; 62].

6.5.1.1 Real Time Oscillation Verifier (ROVER)

The ROVER detection tool takes data from control inputs and aircraft states to calculate the phase, frequency and magnitude of the oscillations. These signals are compared

against threshold values and if they exceed these values a binary flag is set to one. The thresholds are set at values which are likely to cause APCs and are dependent on the aircraft's characteristics and configuration. There are four binary flags, one for each of the selected parameters (APC frequency; APC phase; control input magnitude; aircraft rate magnitude). The number of flags that are set to one indicates whether an APC has been experienced and so the overall result can vary between zero flags (no APC detected) and four flags (APC detected). The tool has been successfully validated during multiple research and development test programmes. Notably, it was used within an investigation of the roll APCs of a C-17 Globemaster observed during approach and landing [118], and subsequently for an investigation of APCs experienced during in-flight refuelling of a F-14 [119]. In both studies the tool was capable of identifying the presence of APCs and correlated with the pilot subjective opinion.

Whilst the ROVER tool is simple to use and the analysis of results are clear, the threshold values of the four defined parameters must be set for each configuration and are reliant on subjective opinion. The subjective nature of the threshold selection can greatly affect the results obtained [120] and so must be very carefully chosen. For the C17 study, 10 test flights were conducted in order to set these threshold values. In a study where there are a large number of configurations, the definition of the parameter thresholds would involve a lengthy analysis of subjective pilot opinions and manual interrogation of the parameter signals for each configuration and over a number of APC severities. The subsequent ROVER results would therefore offer little more information about the APC than would have already been analysed. Furthermore, the subjective selection of the thresholds for each configuration prohibits effective comparison of the ROVER results between the configurations.

Finally, the ROVER tool is not able to distinguish the severity of an APC beyond its mere presence. An increase in the number of binary flags indicates the confidence in the presence of the APC but not the severity. For example any increase in the phase angle between the control input and the vehicle attitude rate would indicate a stronger, more developed APC; however the ROVER tool records this value only in binary terms of whether a threshold has been exceeded.

6.5.1.2 Open Loop Operating Point (OLOP)

The OLOP criterion was developed by Duda [115, 116] to predict the stability issues of rate-saturated closed loop systems. It has proved valuable in the prediction and detection of Category 2 APCs resulting from non-linearities in the feedback loop (discussed later in this section). However, as the rate limiters within the aircraft model used in this study were inhibited and few non-linearities were expected, the employment of this criterion was considered less appropriate.

6.5.1.3 Pilot Inceptor Workload (PIW)

The PIW tool has also been used to assess APC activity [62]. The criterion uses two parameters within the analysis that are gathered in real time from the aircraft inceptors: Duty Cycle and Aggression. The duty cycle describes the pilot activity in terms of a minimum inceptor displacement and a minimum rate of displacement as a percentage of

time that the pilot is actively moving the respective control [66]. The aggression describes the pilot activity in terms of the magnitude of inceptor displacement and rate of displacement. All of the data required to use the PIW tool is derived from the inceptor movement and so it can be effectively used either subjectively (pilot's opinion on how much, and how aggressively the inceptor was moved), or objectively (using instrumentation to record and analyse the inceptor movements).

A low duty cycle with low aggression implies an open loop or very low workload task is being flown. Conversely, a high duty cycle and high aggression indicates that the pilot is moving the inceptor constantly and aggressively. Whilst this condition is consistent with an APC (if bandwidth or rate limiters are reached), without phase information between the inceptor and the aircraft response, it cannot be confirmed that the control activity is indicative of an APC. There is a possibility that the task being flown requires a high gain from the pilot, requiring constant aggressive inputs (for example fixed wing carrier landing) that has no APC tendency. Therefore whilst the PIW tool is useful in assessing the workload of the pilot, and may indicate situations in which APCs may arise or are being suppressed, it is also likely to identify other high workload activity that is not APC related.

6.5.2 Development and Description of PAC

The PAC was developed in order to address the limitations of the ROVER and PIW tools by making it more objectively adaptable across different aircraft and configurations, as well as being capable of assessing the severity of an APC [66]. It was initially considered for rate command helicopter controllers but its extension into an attitude command application is discussed further in section 6.5.4. The PAC develops the PIW principle further, using inceptor aggression but instead of the duty cycle it uses the phase between the inceptor and aircraft response as its second parameter. The inceptor aggression in the pitch axis is defined by the equation 6-6 and represents the magnitude of rate of inceptor displacement $\dot{\delta}(t)$ averaged over a time period between t_1 and t_2. The respective equation for the roll axis is similar but is not shown. The sample rate which defined the time steps between t_1 and t_2 was selected as the duration of one complete inceptor oscillation. The factor H_S originally represented the control sensitivity (ratio of control surface output to pilot inceptor input), however in subsequent research, due to the difficulty in recording swash plate angles, this was modified to represent the control power (ratio of aircraft response to pilot inceptor input) [15]. Despite H_S being a function of a number of flight and control characteristics which make it non-linear, within all previous PAC studies its value has been approximated to be constant. For the rate command helicopter controller, H_S has been represented by equation 6-7 for pitch and roll axes respectively, where Δp and Δq are the changes in pitch and roll rates, and $\Delta\delta_{1C}$ and $\Delta\delta_{1s}$ are the changes in inceptor displacements.

$$A_G = H_s . \frac{1}{(t_2 - t_1)} \int_{t_1}^{t_2} \left|\dot{\delta}(t)\right| dt$$

Equation 6-6

$$H_s = \frac{\Delta q}{\Delta \delta_{1S}} \; or \; \frac{\Delta p}{\Delta \delta_{1C}}$$

Equation 6-7

The phase between the inceptor input and the aircraft response in the pitch axis was calculated using equation 6-8 (the respective roll axis equation is not shown). T_{qPK2} and $T_{\delta PK2}$ represent the time of the most recent peak values of pitch rate and inceptor input, whilst $T_{\delta PK1}$ represents the time of the previous peak value of inceptor input.

$$\Phi = 360\left(\frac{T_{qPK2} - T_{\delta PK2}}{T_{\delta PK2} - T_{\delta PK1}}\right)$$

Equation 6-8

However, as the APCs in this study were analysed in an isometric condition the equations 6-6, 6-7 and 6-8 were modified to reflect that the inceptor input would be a force and not a displacement. The amended isometric equations are shown in equations 6-9, 6-10 and 6-11 where $\dot{F}(t)$ is the rate of inceptor force; H_{SF} is the ratio of aircraft attitude rates to inceptor force; $\Delta F_{\theta 1C}$ and $\Delta F_{\theta 1S}$ are changes in inceptor forces. T_{FPK1} and T_{FPK2} represent the time of the most recent and the previous peak values of inceptor force.

$$A_G = H_{sF}.\frac{1}{(t_2 - t_1)}\int_{t_1}^{t_2}\left|\dot{F}(t)\right|dt$$

Equation 6-9

$$H_{sF} = \frac{\Delta q}{\Delta F_{\theta 1S}} \; or \; \frac{\Delta p}{\Delta F_{\theta 1C}}$$

Equation 6-10

$$\Phi = 360\left(\frac{T_{qPK2} - T_{FPK2}}{T_{FPK2} - T_{FPK1}}\right)$$

Equation 6-11

For any time period or test point the aggression can be plotted against the phase with a discrete data point for each time step (or oscillation). The data points are linked with a continuous line indicating the chronological order of the time steps. The schematic diagram of such a plot is reproduced from Jones and Barnett [15] in figure 6-19. With low aggression and low phase, the pilot is nearing an open loop condition and all control inputs are reflected in representative and predictable slow aircraft responses. As the Aggression increases but without an increase in phase, the gain of the pilot has increased, perhaps due to a higher gain task or a deterioration of HQ, but the aircraft is still responding representatively and all vehicular motion and oscillations are commanded and intentional. With a low aggression and high phase difference the HQ of the aircraft have deteriorated, but the pilot is flying with low gain and therefore a divergent oscillation is not observed. If the aggression was increased whilst maintaining the high

phase difference then a divergent oscillatory APC would certainly ensue and must be detected by the PAC tool.

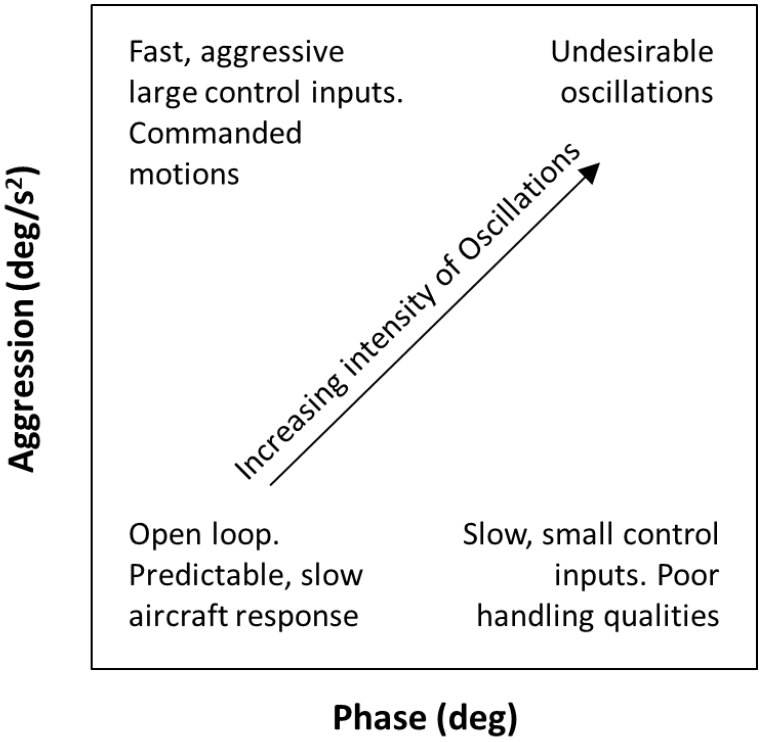

Figure 6-19: Schematic Plot of Phase Aggression Criteria

Due to the employment of the H_S or H_{SF} factor in scaling the aircraft response to control inputs, the severity regions for APCs located on a phase-aggression plot should be consistent irrespective of the aircraft (providing that the aircraft uses a rate command controller). However, the nature of the APCs was initially considered to have an effect. McRuer defined PIOs into 3 categories [64, 65]:

- Category 1 PIOs linear oscillations. The dynamic characteristics of the aircraft as well as the pilot's behavioural dynamics could be assumed to be linear. The APCs were caused by excessive time delays or phase lags.
- Category 2 PIOs quasi-linear oscillations. The control system typically contained some non-linearities in the feedback loop such as rate or position limiters. The dynamic characteristics were considered to be linear until the onset of the limiters.
- Category 3 PIOs non-linear oscillations. The control system features some non-linearities from one state to another for example flaps, gear, non-linear aerodynamics or non-linear pilot behaviour.

Whilst a failure of the sidestick to an isometric mode clearly provides a non-linearity to the control system, the post-failure condition remains in a linear condition. For this study both the simulated actuator limiters and the self-protection experimental computer limiters (required for protection of the real aircraft only) were deselected. It was

therefore surmised that within the limited scope of this study the oscillations would be considered category 1.

As part of the validation process, boundaries were determined for both category 1 and category 2 aircraft systems. However for category 2 systems, when the aggression was above that required to activate rate limiters, the phase would also increase. The argument presented in a very recent study [15] suggested that in these circumstances, the phase of the oscillations could also be classified by the category 1 boundaries.

The PAC boundaries in pitch and roll for a rate command controller are shown in figure 6-20.

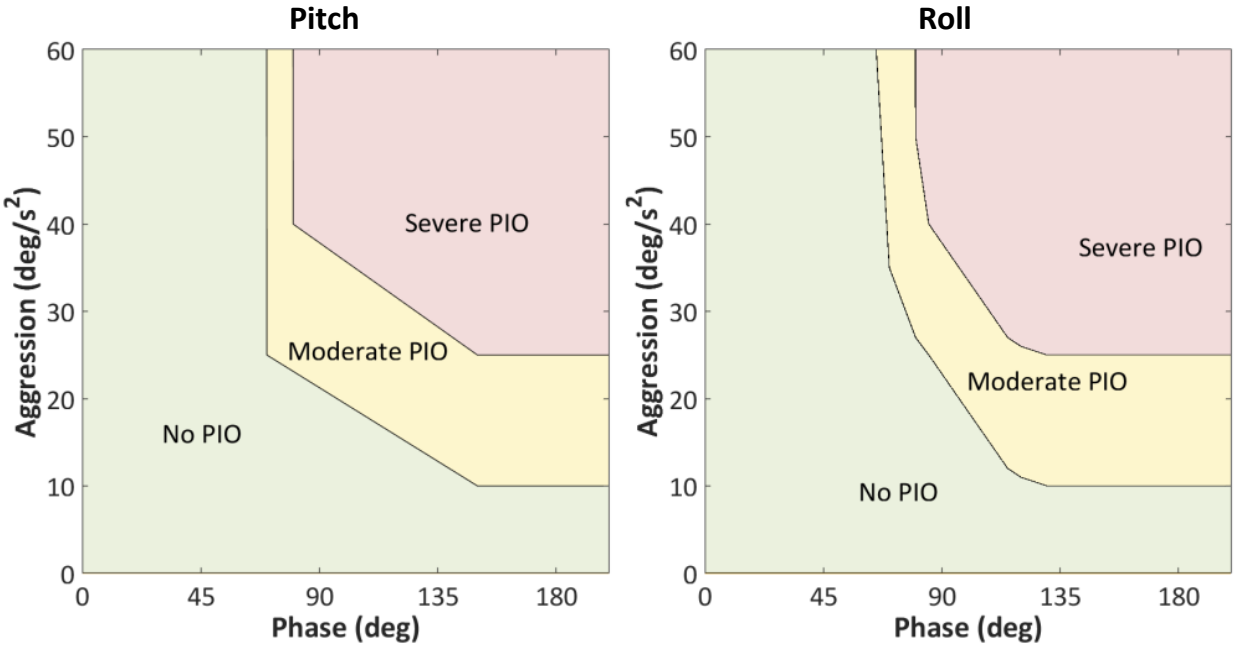

Figure 6-20: PAC Boundaries for Rate Command, Pitch and Roll Axes

After flight all PAC analysis was conducted using MatLab/Simulink. In order to avoid the effects of noise on the phase calculation PAC points were automatically only calculated if:

- $F_{\theta 1S}$ or $F_{\theta 1C}$ respectively were greater than 4N, below which the inputs were considered to be very close to open loop.
- The calculated frequency of the oscillation was within 1-10rad/s which is the generally accepted frequency range for traditional APCs.
- PAC points with a phase of greater than 200° were calculated but not plotted.

Once the PAC points were plotted, the assignment of the APC severity (None, Moderate or Severe) was conducted manually in relation to the boundaries defined in figure 6-20. So that spurious or unsustained PAC points did not affect the results, a test point was awarded the highest severity that fulfilled the following protocol:

- Two or more consecutive PAC points (linked directly by a continuous line)
- Three non-consecutive PAC points

Figures 6-21 shows the time trace of the isometric MTE with pilot J in configuration 8 and a rate command controller. Figure 6-22 presents the PAC chart for the same test point. The analysis of the data can be broken down into 3 chronological phases: transition (sub-tasks 1 and 2), hover selection (sub-task 3) and hover maintenance (sub-task 4).

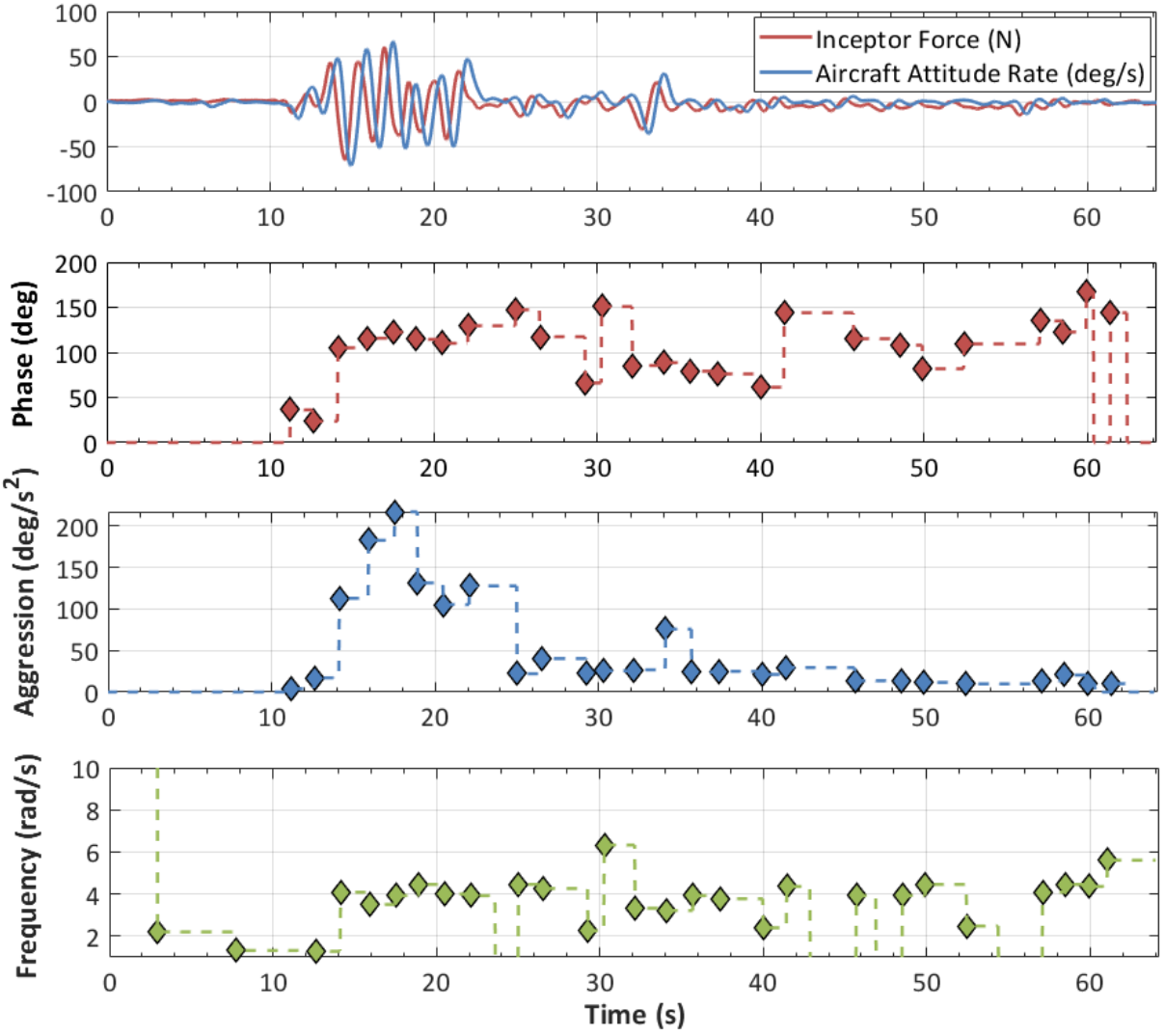

Figure 6-21: Isometric MTE with Failure, Configuration 8, Rate Command, Pilot J Pitch Axis

The period up to 11.5s was the transition phase in which the aircraft was flown in compliant mode with constant speed towards the hover point. The control inputs were of very low aggression and in phase with the aircraft response. As they were below the 4N threshold they were not registered by the PAC tool.

The pilot then manoeuvred the aircraft to select the hover with small inputs between 11.5 and 12.5s. At 12.5s the sidestick was failed to an isometric mode. Immediately, the aggression and phase increased, resulting in six large inceptor and aircraft pitch oscillations. These oscillations can be seen on both the time trace and as PAC points in the severe region of the PAC chart.

At around 23s the pilot entered the hover maintenance phase. He has established the hover position, albeit not stabilised and consciously reduces his gain to suppress the APC.

The amplitude and aggression of the inceptor inputs were reduced and the APC diminished in severity. This is observed in both the reduction in oscillations in the input/output time trace and the PAC points occupying the 'No PIO' region of the PAC chart. Throughout this phase and until the end of the test point the phase remained consistently around 80-100°. On occasion the pilot's suppression becomes less effective in contending with the phase (notably at 34s), resulting in an increase in aggression and a single oscillation, causing a further incursion into the severe region of the PAC chart.

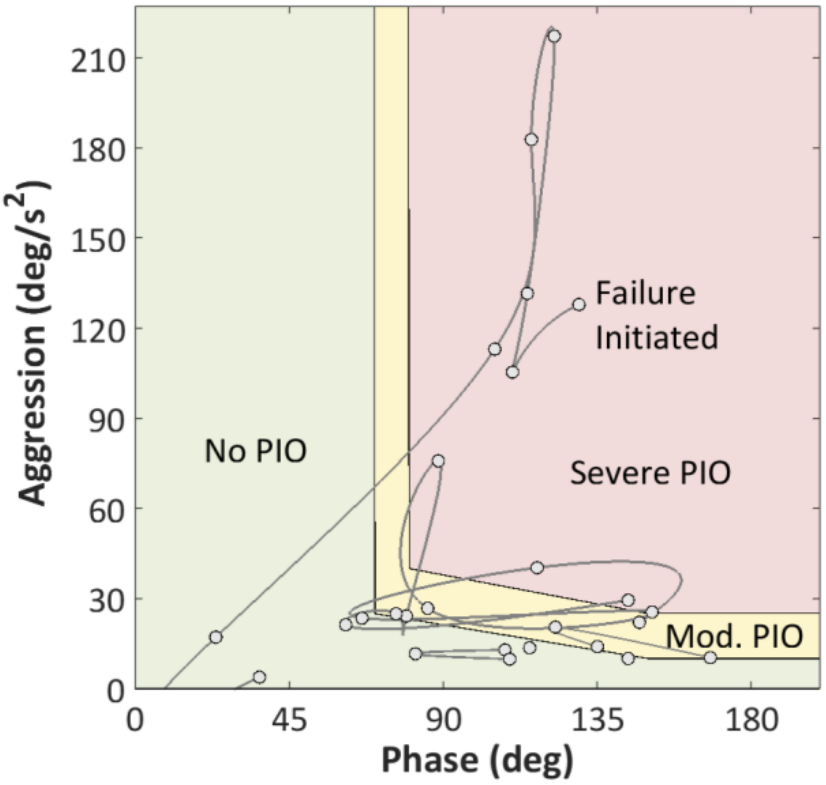

Figure 6-22: PAC Chart, Isometric MTE with Failure, Configuration 8, Rate Command, Pilot J, Pitch Axis

6.5.3 Calculation of H_{SF}

A major advantage of the PAC tool over the ROVER is its parity across different helicopter types, command types and configurations. This is achieved objectively by calculating a value of H_s for compliant inceptors or H_{sF} for isometric inceptors for each of the tested configurations.

The PAC tool therefore required a value of H_{sF} for each of the configurations detailed in table 6-4 in both the pitch and roll axes. These values were calculated using equation 6-10 for a rate command controller. The extension of the PAC for use with attitude command controllers is explained in section 6.5.4 for which specific values of H_S and H_{SF} were also required. These were calculated using equations 6-12 and 6-13 for isometric and compliant inceptor modes respectively.

The data of inceptor force, steady state aircraft attitude and steady state aircraft rate were gathered from manually flown step inputs. As the time constant, τ has no effect on

the value of H_{sF} below the frequency 1/τ (see section 6.1) the number of different configurations could be reduced to those that only varied the apparent gain (steady state gain at 2.6rads^{-1}).

$$H_{sF} = \frac{\Delta\theta}{\Delta F_{\theta 1S}} \; or \; \frac{\Delta\emptyset}{\Delta F_{\theta 1C}}$$

Equation 6-12

$$H_{s} = \frac{\Delta\theta}{\Delta \delta_{1S}} \; or \; \frac{\Delta\emptyset}{\Delta \delta_{1C}}$$

Equation 6-13

The apparent gain has a linear effect on the value of H_{sF} in accordance with the equation 6-14, where the $H_{sF\ Datum}$ is the value of H_{sF} with an apparent gain of unity.

$$H_{sF\ Configuration} = H_{sF\ Datum} . Apparent\ gain$$

Equation 6-14

H_{sF} was calculated from two test points in each cyclic axis direction for each of the configurations 1 to 6 (8 test points per configuration). Each H_{sF} value was then divided by the apparent gain in order to determine an equivalent $H_{sF\ Datum}$. The averaged values of $H_{sF\ Datum}$ for each axis and for each command type across 24 test points are presented in table 6-6. The value of H_{sF} that was then used within the PAC tool was the averaged $H_{sFDatum}$ multiplied by the apparent gain for the specific configuration being analysed, again using equation 6-14.

		$H_{sF\ Datum}$	
		Pitch	Roll
Rate Command	degs^{-1}N^{-1}	1,2875	2,0539
Attitude Command	degN^{-1}	1,7375	2,0964

Table 6-6: Calculated $H_{sF\ Datum}$ values

H_s and H_{sF} were also calculated for the normal compliant sidestick mode using the equations 6-7, 6-10, 6-12 and 6-13. The full calculations and results for the compliant mode H_S and H_{SF} as well as the isometric mode H_{SF} are presented in Appendix E.

6.5.4 PAC Tool for Attitude Command Helicopters

Whilst the PAC tool has been verified with rate command helicopters during numerous simulator campaigns [15, 48, 49, 66] and one flight campaign [96], it has not previously been validated for use with attitude command helicopters. The adaptation of H_s to H_{sF} for the isometric mode has already been considered in section 6.5.2 and has been calculated using equations 6-7 and 6-10. All other calculations and processes within the PAC tool

remain consistent between the attitude command and rate command and so providing the appropriate H_s or H_{sF} are used from equations 6-12 and 6-13, the theory would expect representative results of APC severity on a PAC chart. It must be noted however that the aggression axis (y-axis) of the PAC chart would have units of $degs^{-1}$ for the attitude command and $degs^{-2}$ for the rate command. It was surmised that the boundaries between severity regions on the plot would not be consistent between the command types and so an analysis of the appropriate boundaries for attitude command was required. As subsequently discussed in section 6.8, the tendency and severity of APCs are generally greater in the pitch axis than in the roll axis and hence the attitude command PAC boundaries have only been identified for the pitch axis.

The process that was used for determining the severity boundaries is outlined below:

- Each of the available attitude command test points was processed by the MatLab PAC tool with an appropriate attitude command H_{sF}, each producing a chart similar to that shown in figure 6-23.

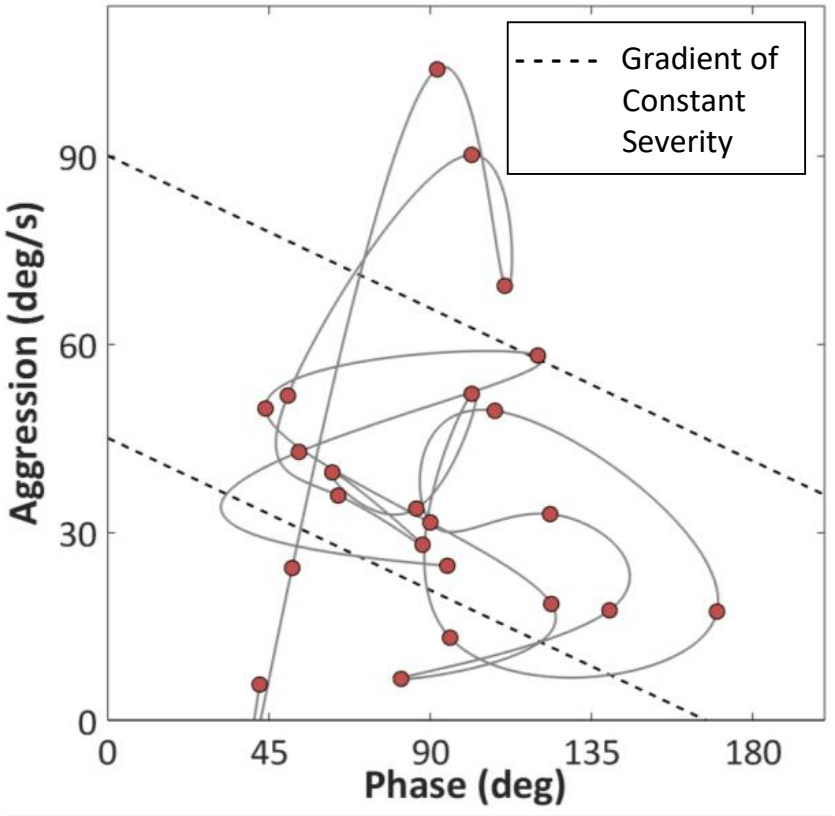

Figure 6-23: PAC Chart, Isometric MTE with Failure, Configuration 8, Attitude Command, Pilot J, Pitch axis

- The three most severe calculated PAC points on each chart were then selected using the following philosophy:
    - It was assumed that from earlier similar analysis in the rate command, a line of constant severity was represented in the pitch axis PAC charts by the gradient of the diagonal boundaries between the severity regions (-

0.188s^{-2} between the 'No PIO' and 'Moderate PIO' areas and -0.214s^{-2} between the 'Moderate PIO' and 'Severe PIO' areas).

- From table 6-5, in the pitch axis, $H_{sF\ RC}$ = 1.29°$s^{-1}N^{-1}$ and $H_{sF\ AC}$ = 1.74° N^{-1} for rate command and attitude command respectively (1N of force per second causes a response of 1.29°s^{-2} for rate command and 1.74°s^{-1} for attitude command).
- Therefore for the same inceptor input, the equivalent attitude response for an attitude command controller is calculated as 1.35s times that of the rate response for a rate command controller. It is assumed that within the limited inceptor and aircraft states there is a linear aircraft response to both the command types.
- If the 'rate to attitude' control response factor (1.35s) is applied to an average of the boundary gradients (-0.20s^{-2}), then an equivalent boundary gradient of -0.27s^{-1} approximately characterises the constant severity of the APC in the attitude command type.
- The three most severe PAC points were then selected as those at greatest perpendicular distance (in the positive direction) from a line of gradient -0.27s^{-1}. The dashed lines on figure 6-23 indicate lines of gradient -0.27s^{-1}.
- An average of the selected PAC points was calculated (subsequently referred to as 'Average PAC Point').

- The APCR of each test point was converted into a severity using the equivalence in table 6-7.

APCR	PAC Equivalent Severity
1	None
2	None
3	None
4	Moderate
5	Moderate
6	Severe
7	Severe
8	Severe
9	Severe

Table 6-7: APCR Equivalence of PAC Severity

- The Average PAC Point was plotted as shown in figure 6-24 with its APCR severity identified by colour (Severe – red; Moderate – blue; None – green).

Hence, the 98 points represented the maximum severity of APC identified by the PAC tool in each of the attitude command test points.

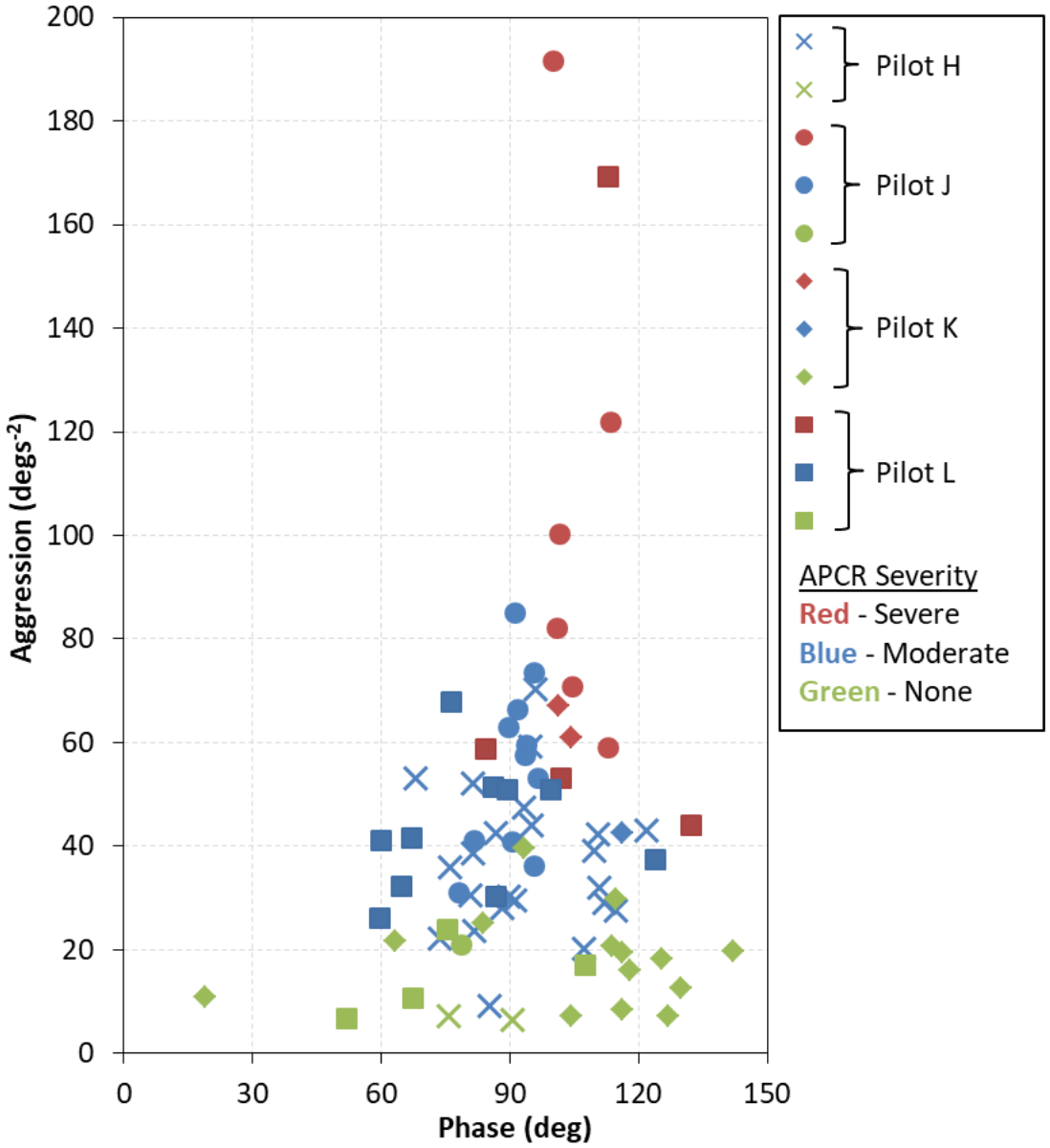

Figure 6-24: Averaged Maximum PAC severity for all Isometric MTE Test points in Attitude Command, All Configurations

Severity boundaries were determined from figure 6-24 by manual observation to create continuous lines that enclosed most of the Average PAC Points into appropriate severity regions. It was impracticable to create boundaries which separated the points with absolute success due to some scatter of the data, however boundaries were selected that maximised the correlation as best as was possible. Figure 6-25 shows the same example data as in figure 6-23 but with the boundaries included.

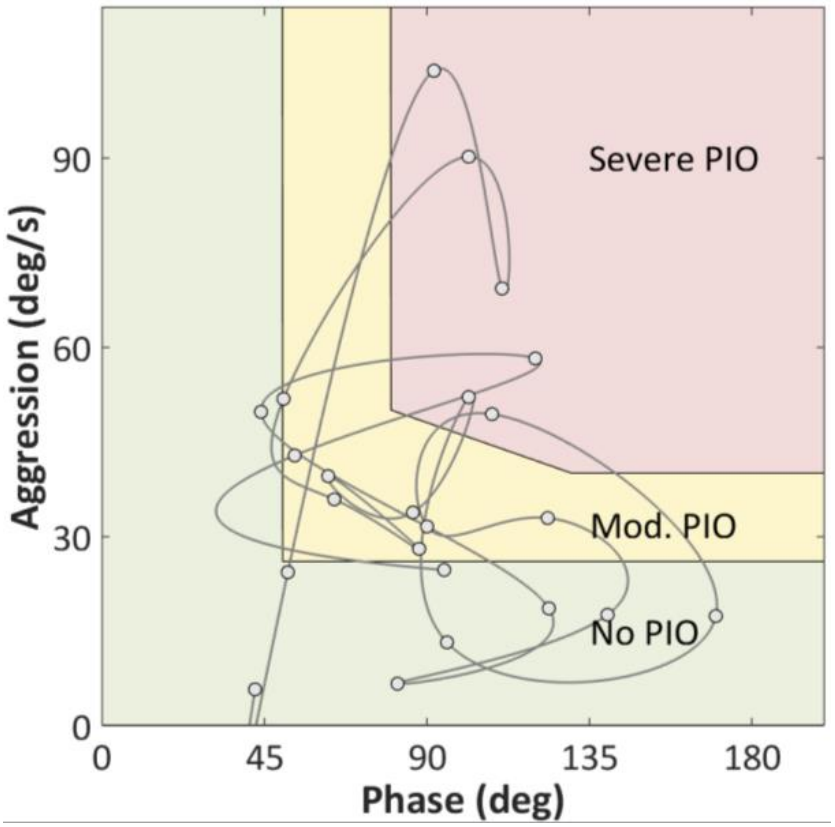

Figure 6-25: PAC Chart, Isometric MTE with Failure, Configuration 8, Pilot J, Attitude Command, Pitch axis

A subsequent analysis of the adequacy of the boundaries was conducted by comparing the severity region in which each average PAC point was located with the subjective APCR severity converted using table 6-7.

This correlation between the APCR and PAC results can be determined using the Global Success Rate (GSR) [121, 122] statistical indicator as defined in equation 6-15. The GSR describes the correlation of a data population with respect to one binary success criterion. The results of this analysis are presented in full in appendix F and have been summarised in table 6-8. For the 72 applicable PAC severity points shown in figure 6-24 the GSR was 80.6%. During the only flight validation of the PAC in rate command [96], the much smaller data population of 10 PAC severity points presented a GSR of 80.0% correlation between the APCR and rate command boundaries. Similar GSR values suggest that the selected severity boundaries for the attitude command are of similar conformity as the more validated boundaries for rate command.

$$GSR = \frac{Conformal\ results}{All\ results}$$

Equation 6-15

		Subjective APC Rating		
		None	Moderate	Severe
Objective PAC	None	18	6	0
	Moderate	2	31	1
	Severe	0	5	9

Table 6-8: Statistical Summary of PAC Boundary Correlation in Attitude Command

6.6 Frequency Response Analysis

In general terms, as the frequency of an input is increased, the aircraft's attitude response exhibits an increased phase lag. At the crossover input frequency (also referred to as ω_{180}) this phase lag reaches 180°, and in order to suppress the oscillation at this frequency, the pilot must apply corrective inputs in the same direction as the existing attitude displacement. Whilst this may be possible to achieve by the pilot applying a large lead to his inputs, the tendency to enter an oscillatory APC would increase the pilot's workload significantly [90]. Clearly, operating the aircraft at or near ω_{180} causes undesirable phase lag and so flight control system designers aim to ensure that ω_{180} is greater than the frequency required for all expected flying manoeuvres. However, if due to a degradation of the control system the ω_{180} is unintentionally reduced, it may breach the normal spectrum of input frequencies causing a proneness to oscillatory APCs in high gain tasks.

All of the frequency response characteristics presented in the Bode plots within this study were gathered using either Simulink models or a standard manual frequency sweep technique. This technique is essentially an open loop task of a single axis oscillatory input with a gradually increasing frequency. Hoh [123] noted that, as high gain tasks were by nature closed loop, the frequency sweep data was not directly comparable with the open loop data. He determined that within a high gain task, the neuro-muscular lag associated with a pilot operating at full attention but less than maximum effort was equivalent to 45°. This consequently led to the definition of phase limited bandwidth ($\omega_{BW\ PHASE}$) as the frequency of a control system at which the phase lag is 135°.

The tendency for a control system to suffer from oscillatory APCs is also related to the rate of phase change around ω_{180} [112]. ADS-33E [36] defines the phase delay using equation 6-16, where τ_P is the phase delay, ω_{180} is the crossover frequency (measured in rads^{-1}) and $\Delta\phi_{2\omega_{180}}$ is the difference between the phase (measured in degrees) at ω_{180} and at $2\omega_{180}$. A higher phase delay implies that a pilot trying to control the aircraft above the bandwidth will find a rapidly reducing phase margin which increases the risk of instability [65]. As the phase delay has units of seconds and so is also often referred to as time delay.

$$\tau_P = \frac{\Delta\phi_{2\omega_{180}}}{57.3\ (2\omega_{180})}$$

Equation 6-16

The relation between phase delay and phase limited bandwidth are used in combination with the charts presented in figure 6-26 and 6-27, to predict APC proneness and HQ levels [15, 65, 121]. The HQ level boundaries shown were from ADS-33E and were defined for all MTEs other than target acquisition and tracking, in fully attended operations.

Specifically for rate command controllers, the variation of the gain with input frequency also has a significant effect on the aircraft's HQ. Hoh [123] stated that the HQ deteriorated in aircraft that had near constant gain with increasing frequency in the vicinity of ω_{180}. This is supported by the subjective argument that within a high gain closed loop task a pilot sub-consciously reacts to an increasing phase lag by increasing the input aggression. Due to the combined stick and hand momentum as well as anatomical or muscular limitations, the size of the inputs also increases with the aggression and consequently with the frequency. Ideally, and in most cases, the gain attenuates with increasing frequency thereby compensating for this problem. However, if there is a low or negligible attenuation in the region of the phase limited bandwidth, oscillatory APCs become more likely [90]. ADS-33E defines the gain limited bandwidth as the frequency at which the gain is 6dB greater than the gain at ω_{180}.

For rate command controllers, ADS-33E further states that the overall bandwidth is the lower of the determined phase or gain limiting bandwidths. For attitude command controllers, the overall bandwidth is always the phase limited bandwidth (however, if the gain limited bandwidth is less than the phase limited, the aircraft will be PIO prone) [36].

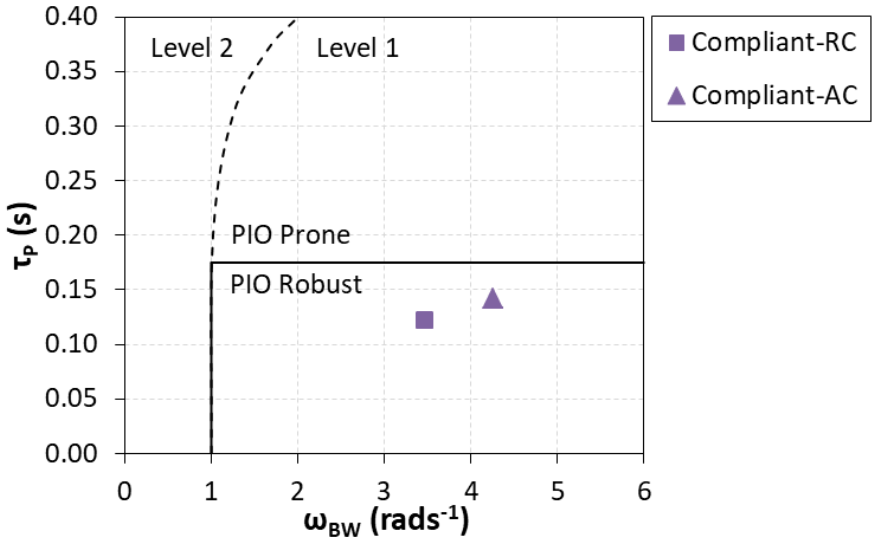

Figure 6-26: HQ and PIO Prediction for Small-Amplitude Pitch Attitude Changes in Fully Attended Non-Tracking Operations with Compliant AIS mode [15, 36, 65]

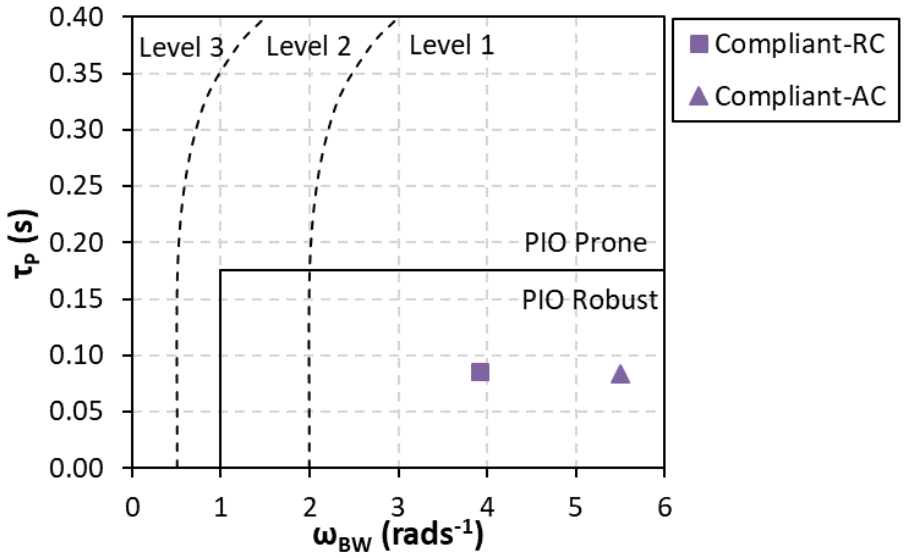

Figure 6-27: HQ and PIO Prediction for Small-Amplitude Roll Attitude Changes in Fully Attended Non-Tracking Operations with Compliant AIS mode [15, 36, 65]

In summary, there are two parameters that can be extracted from the Bode plots of an aircraft's frequency response that can predict poor HQ and proneness to oscillatory APCs:

- Bandwidth is *the measure of the range of frequencies over which a pilot can exert good closed loop control without having to compensate excessively* [64]
    - Phase limited bandwidth ($\omega_{BW\ PHASE}$) is the input frequency at 135° phase lag
    - Gain limited bandwidth ($\omega_{BW\ GAIN}$) is the input frequency at 6dB greater gain than at ω_{180}.
- Phase delay (τ_P) is the phase gradient at ω_{180}, and is *a measure of the steepness of the slope of the phase curve at frequencies above the bandwidth.*

Frequency response data of the combined aircraft model, stability augmentation and active sidestick was recorded in the AVES simulator for both cyclic axes, in both rate and attitude commands and in both the compliant and the isometric modes. The Bode plots were created by the FitlabGUI app within MatLab as detailed in [124, 91] using the Ockier method. In accordance with ADS-33E [36] and standard practices [95], the output signals presented in the plots were aircraft pitch / roll attitude. For the attitude command data, the output of attitude signal could be used directly, but for the rate command data, in order to improve the spread of energy across the frequency range the rate signal was used and then integrated in post processing [90].

The selected input signal for the frequency analysis was dependent on the purpose of the subsequent consideration. Comparing the resulting bandwidth and phase delay with ADS-33E HQ prediction methods could only be done with an input signal of inceptor position. This condition is implicit within ADS-33E as the primary criterion, and is also a recommendation by Lusardi et al based on the findings of an evaluation of HQ of active sidestick in the UH-60M RASCAL and EC135 ACT/FHS [79]. However for the comparative

analysis between the different isometric configurations, the position signal was not relevant and so it was only possible to use inceptor force signals.

Command	Sidestick Condition	Axis	$\omega_{BW\text{-}Phase}$		$\omega_{BW\text{-}Gain}$		τ_p	HQ Level
-	-	-	Hz	$rads^{-1}$	Hz	$rads^{-1}$	s	-
Rate	Compliant	Pitch	0,55	3,46	0,55	3,46	0,122	1
Rate	Compliant	Roll	0,62	3,92	0,82	5,16	0,086	1
Att.	Compliant	Pitch	0,68	4,26	0,62	3,92	0,142	1
Att.	Compliant	Roll	0,88	5,50	0,88	5,50	0,083	1
Rate	Isometric Config. 1	Pitch	0,43	2,67	0,39	2,47	0,238	1
Rate	Isometric Config. 1	Roll	0,57	3,56	0,50	3,15	0,151	1
Att.	Isometric Config. 1	Pitch	0,64	4,05	0,42	2,62	0,193	1
Att.	Isometric Config. 1	Roll	0,72	4,54	0,49	3,07	0,188	1
Rate	Isometric Config. 4	Pitch	0,43	2,67	0,38	2,39	0,249	1
Rate	Isometric Config. 4	Roll	0,57	3,56	0,58	3,64	0,169	1
Att.	Isometric Config. 4	Pitch	0,64	4,01	0,37	2,34	0,186	1
Att.	Isometric Config. 4	Roll	0,72	4,54	0,54	3,40	0,145	1
Rate	Isometric Config. 7	Pitch	0,43	2,67	0,35	2,18	0,268	1
Rate	Isometric Config. 7	Roll	0,55	3,48	0,59	3,72	0,159	1
Att.	Isometric Config. 7	Pitch	0,51	3,23	0,40	2,50	0,244	1
Att.	Isometric Config. 7	Roll	0,55	3,48	0,59	3,72	0,177	1

Table 6-9: Frequency Response Characteristics

The frequency response characteristics are detailed in table 6-9 for each axis, each control type and for the compliant mode and three isometric mode filter configurations.

Only the isometric filter configurations 1, 4 and 7 (as defined in table 6-4) were analysed. The configuration 1 represents the datum first order filter (Apparent Gain=1.0 and τ=0.1s); configuration 4 represents a decreased gain (Apparent Gain=0.6 and τ=0.1s) and configuration 7 represents an increased time constant (Apparent Gain=1.0 and τ=0.2s). For some configurations, the phase became non-linear between ω_{180} and $2\omega_{180}$ and so in accordance with ADS-33E, the phase delay was calculated from a linear least squares fit of the phase curve.

Figure 6-28 shows the Bode plot used to attain the frequency response data in table 6-9 for the compliant mode, attitude command, pitch axis for which the input was inceptor force and the output was aircraft attitude. All other Bode plots for each compliant and isometric configuration in each cyclic axis are shown in appendix D.

Figure 6-29 shows the equivalent Bode plot for the same compliant configuration as figure 6-28 but using an input of the inceptor force instead of inceptor position. Comparison of these two plots shows that the phase of the plot using force input lags the plot using position input by between 70 and 120°. This lag is due to the second order filter that in the compliant mode lies between the force signal source and the position signal source which would create a lag of between 0 and 180° as defined by the Bode plot in figure 6-4. Further details of the compliant mode second order filter and its function are described in chapter 3.

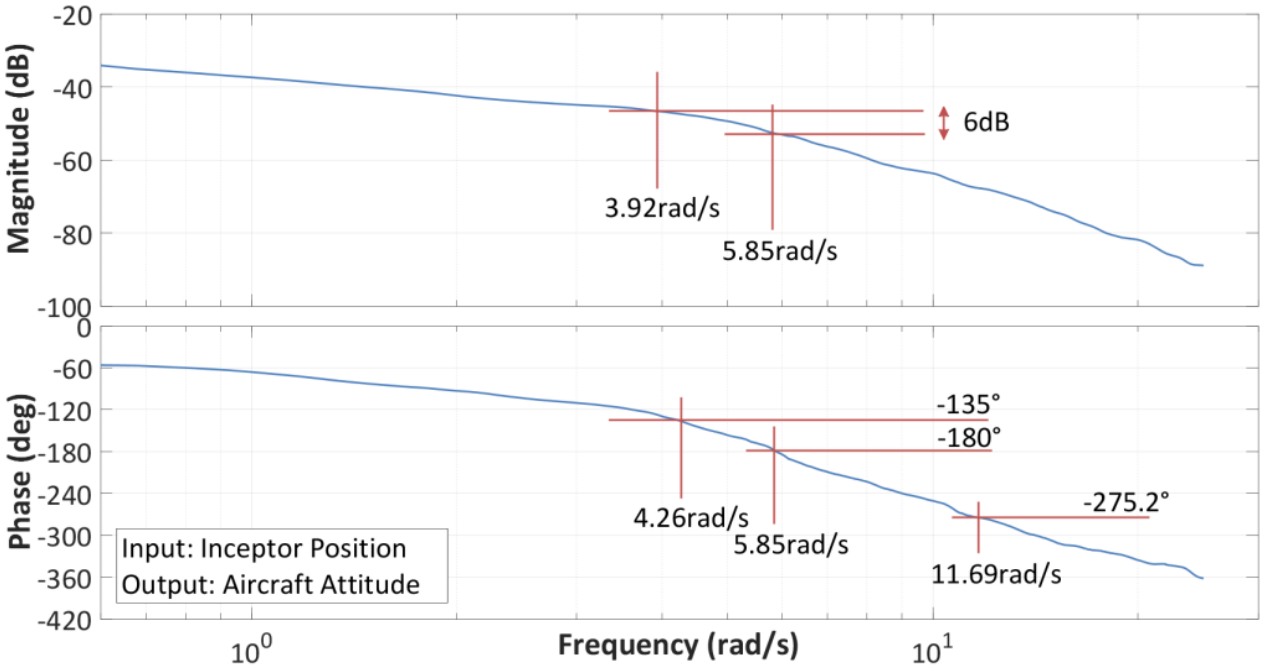

Figure 6-28: Bode Plot, Position-Attitude, Attitude Command, Pitch Axis, Compliant Mode

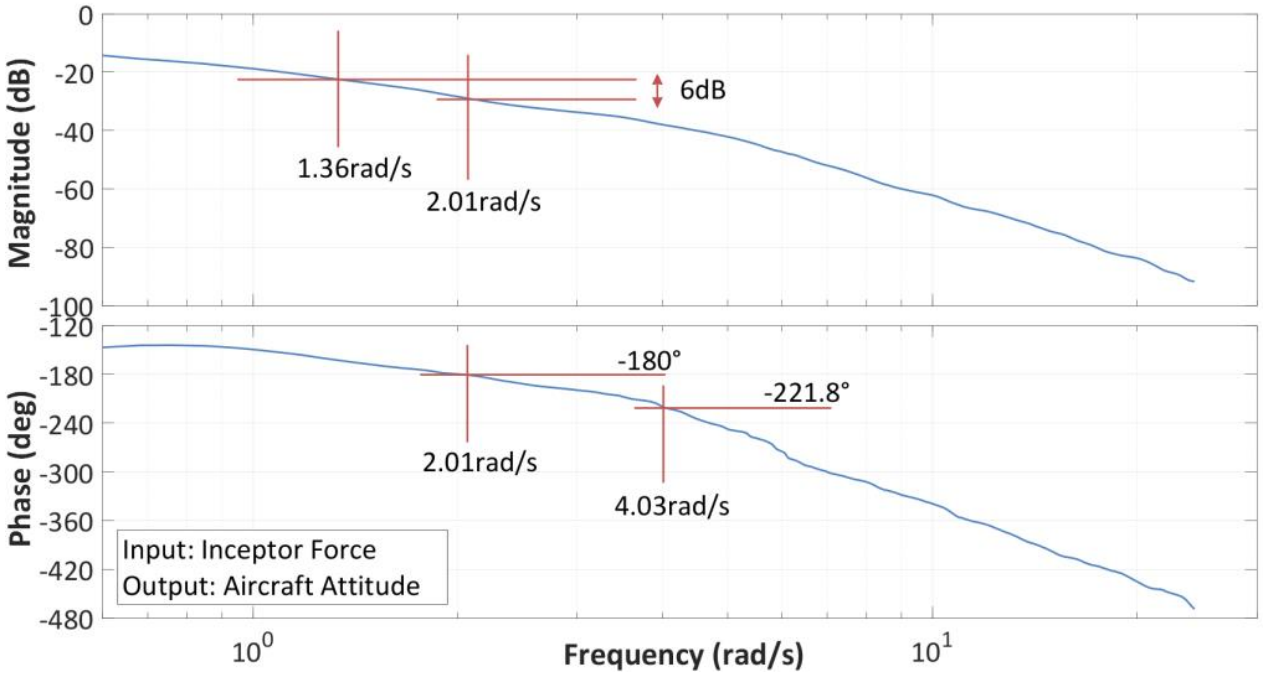

Figure 6-29: Bode Plot, Force-Attitude, Attitude Command, Pitch Axis, Compliant Mode

Comparison of the theoretically modelled frequency responses with those recorded during the pilot induced frequency sweep presented some variances which are considered to be the result of:

- Sidestick position motor delay and lag;
- Sidestick position motor maximum rate;
- Inherent damping and friction in sidestick system that are in addition to the artificially defined forces within the second order model of the compliant sidestick;
- Exceedance of the maximum sensed sidestick force;
- Maximum processing rate of sidestick CPU.

6.7 Baseline Aircraft

The HQs of the baseline simulated aircraft with the sidestick in the normal compliant mode were assessed using the Isometric Failure MTE described in chapter 5 and in accordance with the HQ rating within ADS-33E [36]. The overall averaged CHR across the 3 test pilots and for each track direction was 3.1 for the attitude command and 4.0 for the rate command. The full results are presented in appendix D. In accordance with Cooper and Harper [51], level 1 HQ are defined as less than 3.5, therefore the attitude command controller fulfilled level 1 and the rate command was marginal but just into the level 2 region. In section 5.3 it was stated that the IFES scale assumed that a rotorcraft without failure fulfilled level 1 HQ. Whilst the rate command controller model fell just outside of this requirement, all test pilots awarded a CHR 4 in all test conditions, thereby confirming that the desired tolerances were consistently achievable but with moderate pilot compensation. After further optimisation of the augmentation parameters, the HQ were

unable to be improved significantly and so the minor nonconformity from the IFES assumptions was accepted.

In order to establish the predicted HQ levels in the frequency domain, data of the time delay and bandwidth for the compliant sidestick for both the rate and attitude commands were taken from table 6-10. The data was plotted on figures 6-26 and 6-27 (with HQ level boundaries copied from ADS-33E) which showed regions of expected HQ levels during fully attended operations for small amplitude attitude changes in the hover and low speed environment for the pitch and roll axes respectively. The HQ level regions within which each test configuration was located was returned to table 6-10 and identify that for both command types and both cyclic axes the predictions were consistently level 1.

The relationship between bandwidth and phase delay has also been shown to be capable of predicting the susceptibility of an aircraft configuration to oscillatory APCs. The ARISTOTEL project [121] investigated this application with a Bo-105 helicopter simulator during a pitch and roll tracking task with increasing time delays. The results identified that as the bandwidth decreased and the phase delay increased the helicopter became more APC prone [65]. Boundaries of susceptibility to oscillatory APCs were defined within this project and these boundaries have been plotted on figures 6-26 and 6-27 [15, 65, 121]. The plotted positions for both command models indicated robustness to oscillatory APCs when using the sidestick in normal compliant mode.

Further details of the baseline simulated aircraft, EC135T2+, right sidestick, flight control mechanical characteristics, flight control system and simulator can be found in chapter 3.

6.8 Deselection of Roll Axis in PAC Analysis

Figure 6-30 shows the phase delay against bandwidth for the compliant mode and for the isometric mode (configuration 1) in two separate plots. The PIO proneness boundaries are indicated but the predicted HQ boundaries have been removed. The axis and command type are presented consistently for both plots in accordance with the legend.

In consideration of the compliant mode data points, both pitch data points have a higher phase delay than their corresponding roll data points and are consequently closer to the PIO proneness boundary. It is therefore anticipated that as the margin of phase delay to the PIO proneness boundary is less for the pitch axis, it would be more prone to APC than the roll axis. The isometric (configuration 1) data points show that the theoretically higher APC susceptibility in the pitch axis also remains consistent for the isometric mode.

This result concurs with ADS-33E, which states that for the attitude command response only, if the bandwidth defined by gain margin is less that the bandwidth defined by phase margin, the aircraft may be PIO prone. This criterion is fulfilled for the pitch axis but not the roll axis therefore predicting that the pitch axis would be PIO prone but the roll axis not.

Furthermore, it was also apparent that each pitch axis data point had a lower bandwidth than its corresponding roll axis data point thus indicating that the pitch axis was generally less stable than the roll axis at higher frequencies.

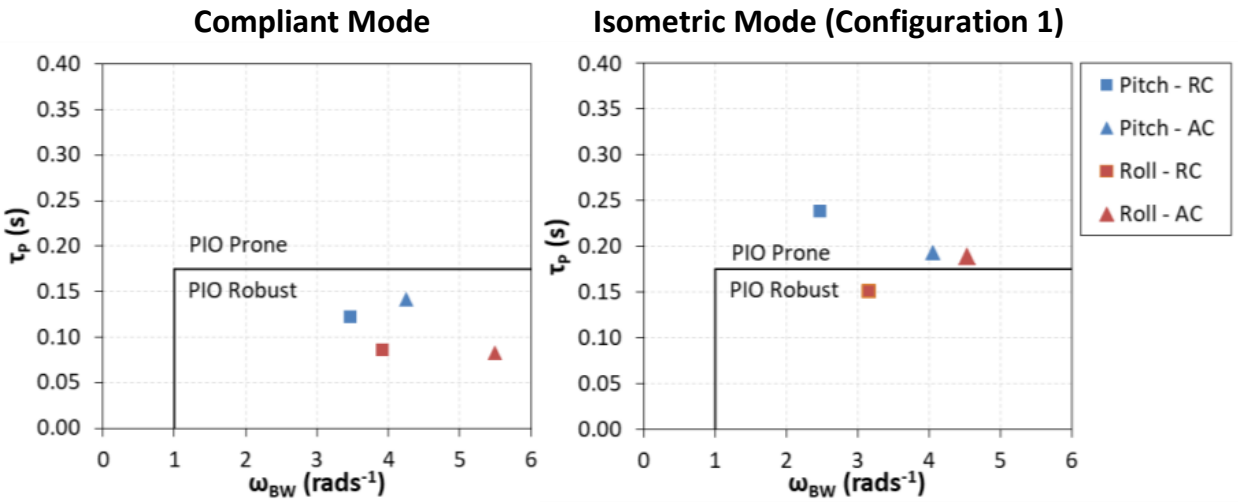

Figure 6-30: PIO Prediction for Small-Amplitude Pitch and Roll Attitude Changes for Fully Attended Non-Tracking Operations [15, 36, 65]

In order to confirm this theoretical assertion, the relative APC severity between the pitch and the roll axes for the configurations 1-8 were analysed with the PAC tool. The analysis was conducted using the data gathered from the test points described in 6.3.8 and presented in appendix F, in which the Isometric MTE was flown with a sudden isometric sidestick failure initiated during the deceleration to the hover. Data was recorded in each of the test configurations, (configurations 1 to 8, as detailed in table 6-4) and was repeated at least once for each configuration in the same test condition (test points A, B and C). Whilst for this investigation, the severity of the APCs in relation to the configuration was unimportant; a full analysis of the data considering a broader range of influences is discussed in chapter 7. For each test point a PAC analysis was conducted for both the pitch and roll axes and the detected severity presented in figures 6-31, 6-32, 6-33 and 6-34 for the pilots H, J, K and L respectively.

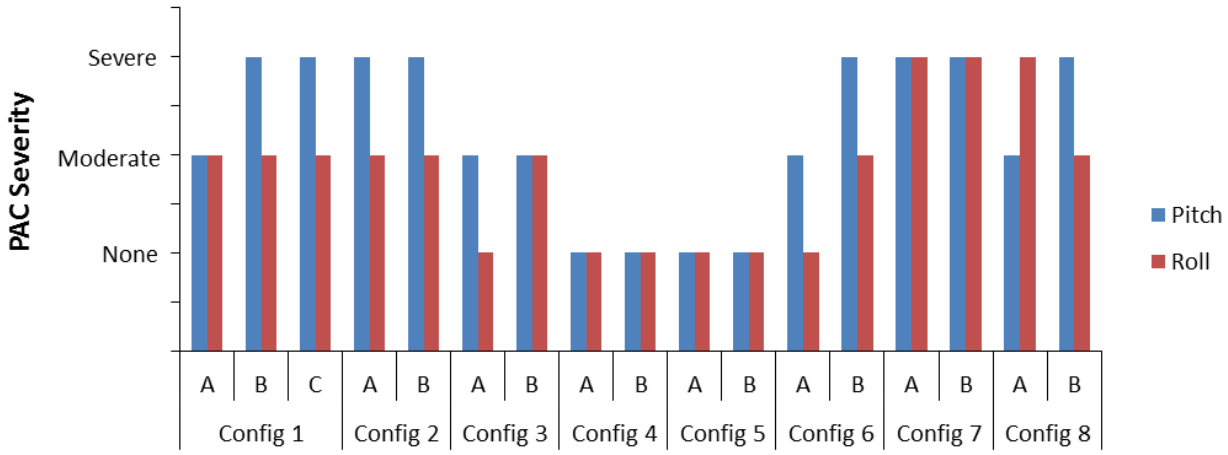

Figure 6-31: APC Severity, for all Isometric MTE Test Points with Failures in Rate Command, Pilot H, All Configurations

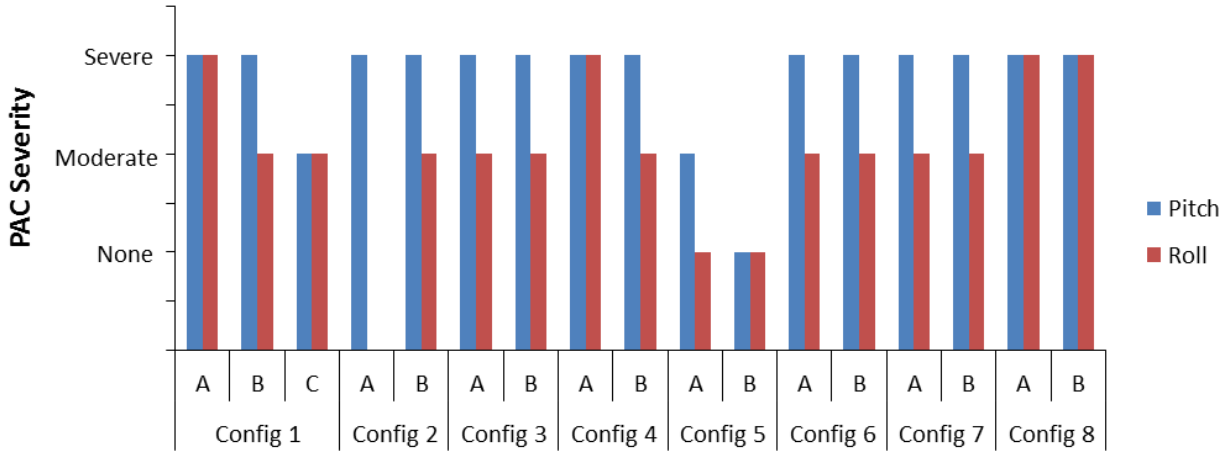

Figure 6-32: APC Severity, for all Isometric MTE Test Points with Failures in Rate Command, Pilot J, All Configurations

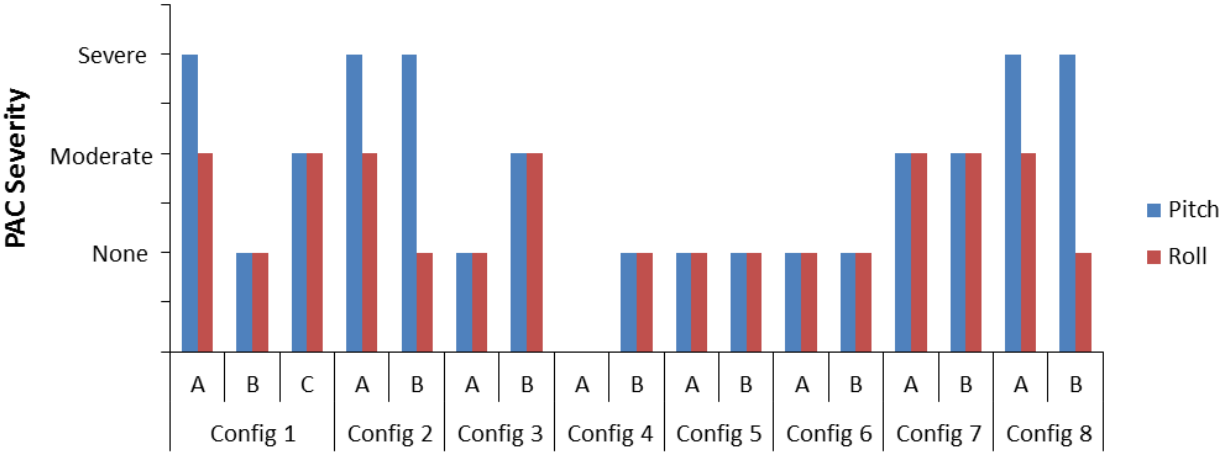

Figure 6-33: APC Severity, for all Isometric MTE Test Points with Failures in Rate Command, Pilot K, All Configurations

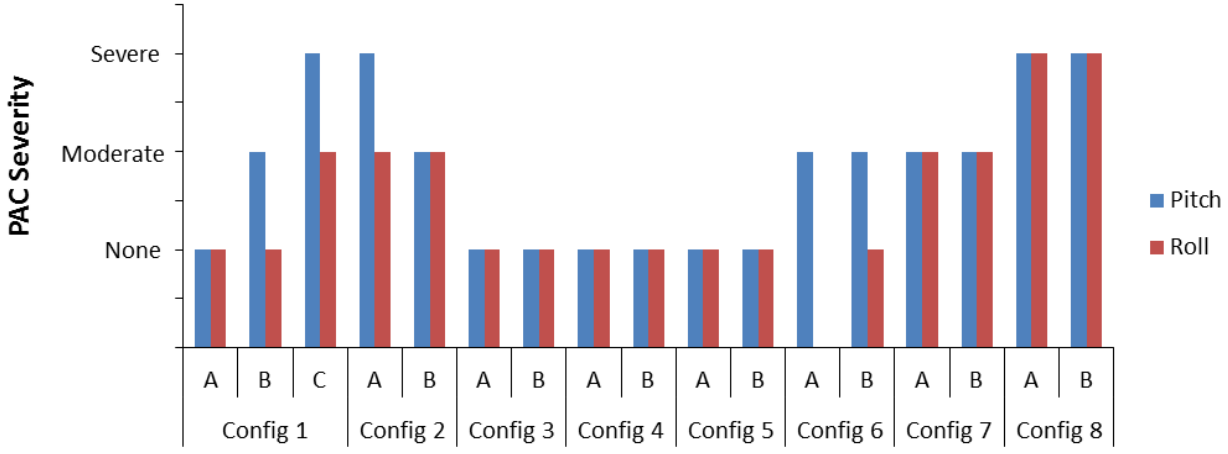

Figure 6-34: APC Severity, for all Isometric MTE Test Points with Failures in Rate Command, Pilot L, All Configurations

On three occasions the PAC tool failed to read the data, hence there are some blank spaces in the figures. The PAC analysis shows that for every test point considered, the severity of the pitch APCs was always equal or greater than the severity of the roll APCs.

This confirms the theoretical expectation that due to lower phase bandwidth and higher phase delay of a helicopter's pitch axis, an APC is generally more apparent and severe in the pitch axis than in the roll axis [64].

In order to avoid redundant data analysis and to prioritise the critical conditions for identifying APCs, all of the subsequent PAC analysis was conducted in the pitch axis only.

6.9 Test Pilot Selection with Respect to Previous Isometric Inceptor Experience

The minimum number of independent test pilot opinions for a subjective rating in each configuration is three [36]. However, during the assessment with pilot K, it became apparent that although he was a qualified helicopter test pilot, he had previously received isometric specific training and spent approximately 900 hours flying the F-16A which was equipped with a pseudo-isometric controller (moving a maximum of ¼ inch) [81]. During the training the risk of APC, particularly during high gain tasks such as air to air refuelling and carrier landings, was emphasised and mitigation solutions taught and practiced. These solutions involved methods of recognising and suppressing incipient APCs. Although the data gathered by pilot K was greatly influenced by his isometric experience, it was of value in comparing with other test pilot's performance and opinions. Therefore in order to meet the requirement for three test pilots whilst avoiding the influenced data from pilot K, an additional test pilot without isometric experience was introduced to the study. Hence, in total four test pilots were used in the first order filter assessment, one with previous isometric experience and three without.

6.10 General Assessment Conventions and Conduct

The priority of each test configuration is defined in table 6-4. Each of the high priority test configurations were flown by each test pilot twice. The medium and low priority test configurations were flown as time permitted.

As previously discussed in section 6.3, in order to maintain a consistent assignment of subjective ratings throughout each pilot's assessment, it was essential that the test pilot was able to refer back to a datum configuration regularly. The 'qualitative calibration' test points were conducted after every second configuration change and therefore after every fourth test point.

6.11 Data Quality Rating

In addition to the subjective ratings of the IFES transient, IFES recovery and APCR, the test pilot assigned a 'Data Quality' to each test point. The options of High; Medium or Low referred to the test pilot's perception of:

- The accuracy with which the MTE was flown in accordance with the course description (not the performance standards);
- The confidence he had in assigning the IFES and APCR ratings;

- The representation of the failure with regards to timing and inceptor mechanical definition;
- The presence of any anomalies that affected the credibility of the data.

All test points that were assigned a data quality of low (a total of 7.6% for pilots H, J, L and 3.7% for pilot K) were removed from the data set.

6.12 Test Conditions

During all test points there was no wind, the atmospheric environment was 10km visibility and no cloud or precipitation. The visual environment was therefore considered a GVE.

The Simulated Day Useable Cueing Environment (SIMDUCE / UCE) for this investigation was assessed by 3 test pilots in accordance with ADS-33E [36] and described fully in chapter 3. The overall SIMDUCE / UCE for the Isometric Failure MTE in the GVE conditions was 1.

6.13 Summary

This chapter covered the experimental provision, relevant analysis tools, theoretical predictions and test conditions of a HQ and APC investigation of the variation of first order filter parameters after an isometric failure. The following subjects were discussed and conclusions reached:

- A summary of first order filter theory and the conventions used in this dissertation were reviewed.
- The use of a first order filter was justified as the simplest form of signal processing that would fulfil the expected requirements of reducing gain, reducing signal noise and increasing the control force signal damping.
- A range of low, medium and high priority test configurations were selected that varied the apparent gain from 0.4 to 1.2; the time constant from 0.01s to 0.40s and the ramp attenuation period from 0s to 3.75s. The investigation would also be conducted with either a rate command or attitude command controller.
- The development of the APCR was reviewed and an updated validation was conducted with reference to similar flight and simulator research.
- The development of various objective analysis tools for the detection of APCs was reviewed and the PAC was selected as the most appropriate. Previous validation of the PAC with rate command controllers was examined and a new validation with an attitude command controller using experimental simulator data was presented.
- Frequency response analysis was conducted in the compliant pre-failure mode in accordance with the ADS-33E small amplitude attitude change criteria. It identified that the baseline aircraft was robust to APC and its predicted HQ level was 1.
- Further frequency response analysis was conducted in a limited number of isometric first order filter configurations to provide APC proneness and HQ level predictions.

- Through both analysis of PAC data and frequency response data the pitch axis was identified as more significant and consistently developed more severe APCs in equivalent test configurations than the roll axis. Subsequent data analysis was limited to the pitch axis only.
- CHRs were presented for the baseline aircraft in the compliant pre-failure mode. In the attitude command the awarded HQ level agreed with the frequency response prediction of level 1, but in the rate command the awarded HQ level was just in level 2, in comparison to the predicted level 1.
- The relevance of previous isometric experience was discussed and three test pilots were selected that had no significant isometric experience as well as one test pilot who had previously flown 900 hours in the isometric sidestick equipped F-16A.
- The assessment conventions, conduct and test conditions were described and a data quality rating was introduced that offered a confidence level of the ratings awarded by the test pilots for each test point.

Chapter 7: First Order Filter Results, Analysis and Discussion

7.0 Overview

This chapter presents the data that was collected in the main investigation of the first order filter and ramp attenuator during isometric sidestick failures as described in chapter 6.

The parameters of the filter and attenuator were varied in selected configurations and their effects analysed using the subjective IFES and APCR scales and the objective PAC. Frequency response analysis was conducted on some configurations to assess the accuracy of APC prediction methods. Other influencing factors including the aircraft's command type and the pilot's previous isometric experience were also investigated.

The data is presented, analysed and discussed in order to reach conclusions on the following objectives:

- Assess the relative strengths of the factors that influence the aggression and continuation of APCs after an isometric failure.
- Identify the influences of
  - A first order filter apparent gain,
  - A first order filter time constant,
  - A ramp attenuator of first order filter apparent gain,
  - Helicopter command type (attitude or rate),
  - Previous isometric specific training and experience

  on the following characteristics after an isometric AIS failure:
  - The HQ, urgency, effort and compensation required, as assessed by the IFES transient and recovery ratings.
  - The tendency and severity of oscillatory APCs, as assessed by the PAC and APC ratings.
- Assess the accuracy of the prediction of oscillatory APC proneness in both command types using a defined boundary criterion on a plot of phase delay against bandwidth.

7.1 Factors Influencing the Aggression and Continuation of APCs

After their final simulator session each test pilot was asked to assign a subjective rating of influence for the following seven factors that could affect the aggression and continuation of isometric mode oscillatory APCs:

- Attitude / attitude rate at moment of failure
- Cyclic control force / displacement magnitude at moment of failure
- Cyclic control force / displacement direction from trim at moment of failure
- Pre-failure required pilot gain
- Post-failure required pilot gain
- Timing of Failure

- Visual references

A rating from 1-5 was awarded with 1 corresponding to a perceived low influence and 5 corresponding to a perceived high influence. The pilots were also tasked with ranking the seven factors in their order of significance with the highest ranked factor as 7 and the lowest ranked as 1. The questionnaire that was used is presented in appendix B and the full data for pilots G, H, J, K and L is presented in appendix F. A graphical summary of the data is presented in figure 7-1.

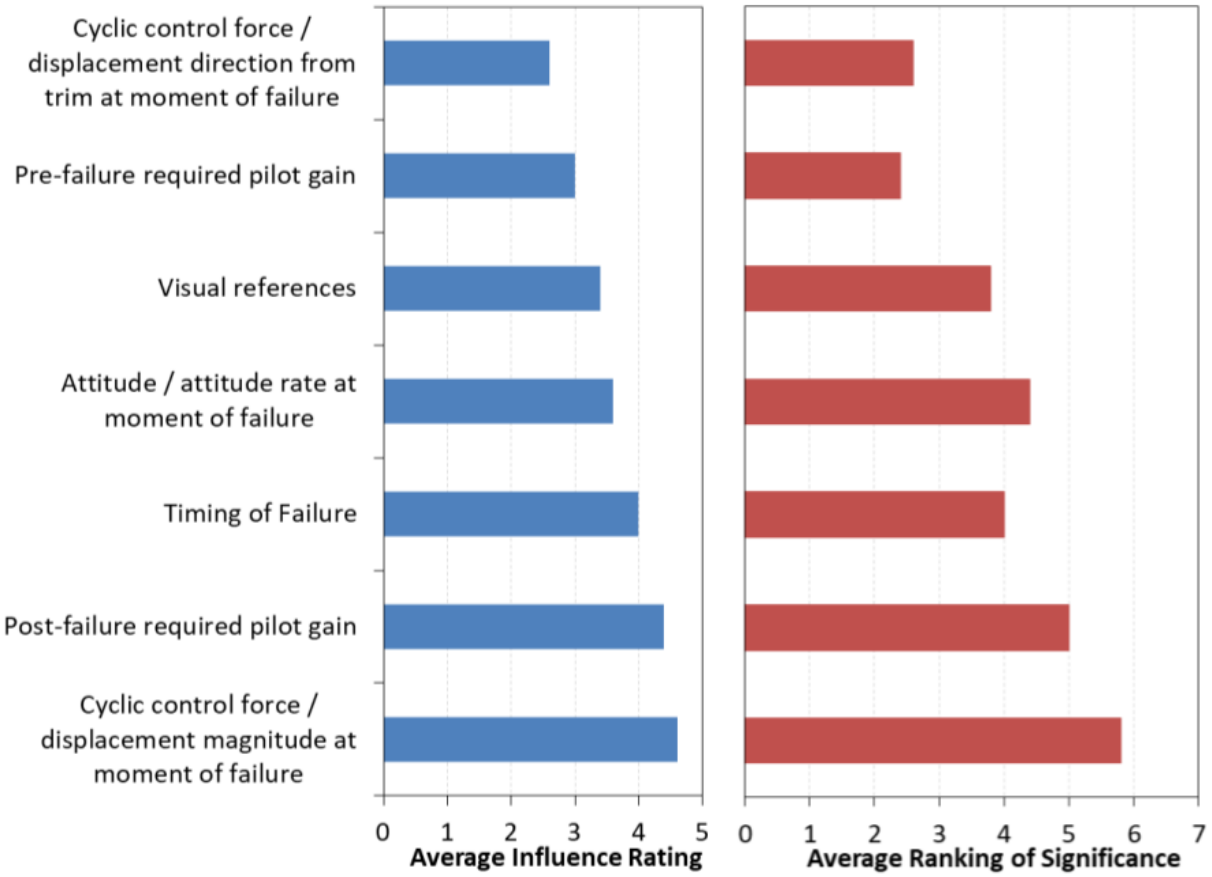

Figure 7-1: Averaged Influence Rating and Significance Ranking Across All Pilots of Factors in the Severity of Isometric Mode Oscillatory APCs

The average ratings across all pilots concurred with the average ranking with one exception, that the *timing of failure* had a higher influence rating than *the attitude / attitude rate at moment of failure,* whereas in the order of ranking it was reversed.

The *cyclic control force / displacement magnitude at moment of failure* was perceived as the most significant because of the potential for sustained out of trim forces after the failure. As discussed further in section 7.3.1, at the moment of failure the current position signal automatically becomes the new (zero force) trim value but the required inceptor force to achieve the subsequent hover attitude may be different from this trim value. As the force cannot be re-trimmed to zero once in the hover, the pilot must hold this constant larger force whilst superimposing smaller variable forces to maintain the hover

position and attitude. The greater the control displacement at failure, the greater the held constant force will be and the more difficult the hover sub-task will be for the pilot.

The second most significant factor was the *post-failure required gain*. The primary method of suppression of an oscillatory APC is to reduce the pilot gain (also recognised as partially retreating out of the control loop). The subjective extent to which a pilot may reduce his gain whilst retaining adequate control for task performance may be considered the suppression margin. If the task of the pilot was to maintain an approximate hover over a large field within a height band of 20 to 100ft, the required accuracy would be low and the pilot could afford to reduce his gain by a large margin to suppress an oscillatory APC. The suppression margin would therefore be considered large. Conversely, if the task had tighter tolerances such as for the isometric MTE of ±3ft position, ±5ft height and ±5°, the pilot could afford only to reduce the pilot gain by a lesser extent before the task tolerances would be exceeded. The lower the suppression margin available to the pilot, the more difficult it was to fulfil the task without entering an oscillatory APC which would lead to generally worse IFES ratings being awarded. Consequently, the *post-failure required pilot gain,* that has a direct influence on the suppression margin, had a high significance in the aggression and continuation of oscillatory APCs.

The effect of *attitudes and attitude rates at the moment of failure* had a lower perceived significance than the *post-failure pilot gain* and *control forces at failure;* however the pilots considered that their relevance was still influential. High attitudes or attitude rates at the failure meant that any additional transient attitude changes could cause an encroachment on the SFE boundaries. As the IFES transient scale refers to the proximity and exceedance of the SFE boundaries within the descriptors, it was probable that the transient ratings would be higher for instances with failures at higher attitudes and rates.

Additionally, when the failure occurred at a high attitude or rate, the recovery required a larger attitude correction. The pilot would apply a more aggressive or larger control input to recover the aircraft to the hover within the allocated time of 6 seconds which would increase the risk of triggering an oscillatory APC and therefore a higher recovery rating would be awarded.

The *timing of failure* influence was difficult to disengage from the influences of *attitude / rate at moment of failure* and *control force / displacement at moment of failure* because of their inter-dependencies. Optimal failure timing for lowest IFES and APCR occurred when the aircraft was in the hover and the cyclic was stable. Conversely, the most severe results occurred when the attitude / rate and cyclic displacement / force were all high. As the failure was initiated during the dynamic deceleration prior to the hover, any timing deviation from the desired most severe case was able to create large variations in the IFES and APC ratings. Furthermore, the cyclic displacement and attitude / rate were also broadly linked by the short term aircraft response to control inputs (the larger the displacement / force, the larger the attitude / rate). Therefore, of the top 4 ranked influences, 3 were strongly connected and could be combined to conclude that the pilots perceived that high forces at the time of failure were paramount in the influence and severity prediction of subsequent APCs.

The cyclic force / displacement direction, pre-failure gain and visual references were of less relevance to the influence of the oscillatory APCs.

7.2 General Presentation of Common Data Formats

A common presentation format has been used to illustrate the distribution of PAC, APCR, IFES Transient and IFES Recovery ratings with variation of the first order filter parameters (e.g. Figure 7-2). The shared x-axis defines the variation of the specific first order filter parameter under consideration (apparent gain, time constant or ramp attenuation period). The split y-axis defines each of the individual performance indicators: IFES Transient blue squares (left y-axis); IFES Recovery red diamonds (right y-axis); APCR green triangles (left y-axis); PAC Severity blue circles and red diagonal crosses (right y-axis).

Whilst it is acknowledged that subjective pilot rating scales cannot be truly linear, in accordance with the originators' intentions the ratings for each of the configurations was arithmetically averaged across all test pilots to create a single data point.

The error bars for the IFES and APCR points represent the range of all the relevant and admissible (not 'low' data quality) awarded ratings from all of the applicable test pilots. The numbers next to the PAC severity circles / crosses represent the number of data points that coincide with the plotted position.

The data from pilots H, J and L (those without significant previous isometric inceptor experience) were used within sections 7.3: variation of apparent gain; 7.4: variation of time constant; 7.5: variation of ramp attenuator period and 7.6: variation of command type. The data from pilot K who had benefitted from significant previous training and experience was only used within section 7.7: effects of isometric training and experience.

7.3 Analysis of Variation in Apparent Gain

7.3.1 Effect on IFES Ratings

With reference to figure 7-2, both the IFES recovery and IFES transient ratings for rate command improved with reducing apparent gain, reaching an optimum at 0.6 with corresponding ratings of between C and D. As the apparent gain was reduced further to 0.4 the IFES ratings deteriorated again to between D and E.

For the attitude command data depicted in figure 7-3 the trend was similar but the improvement of ratings with reducing apparent gain was weaker. The optimum IFES transient was between B and C at an apparent gain of 0.8 and the optimum IFES recovery was also between B and C but at an apparent gain of 0.6. Both ratings deteriorated again slightly as the apparent gain was further reduced to 0.4.

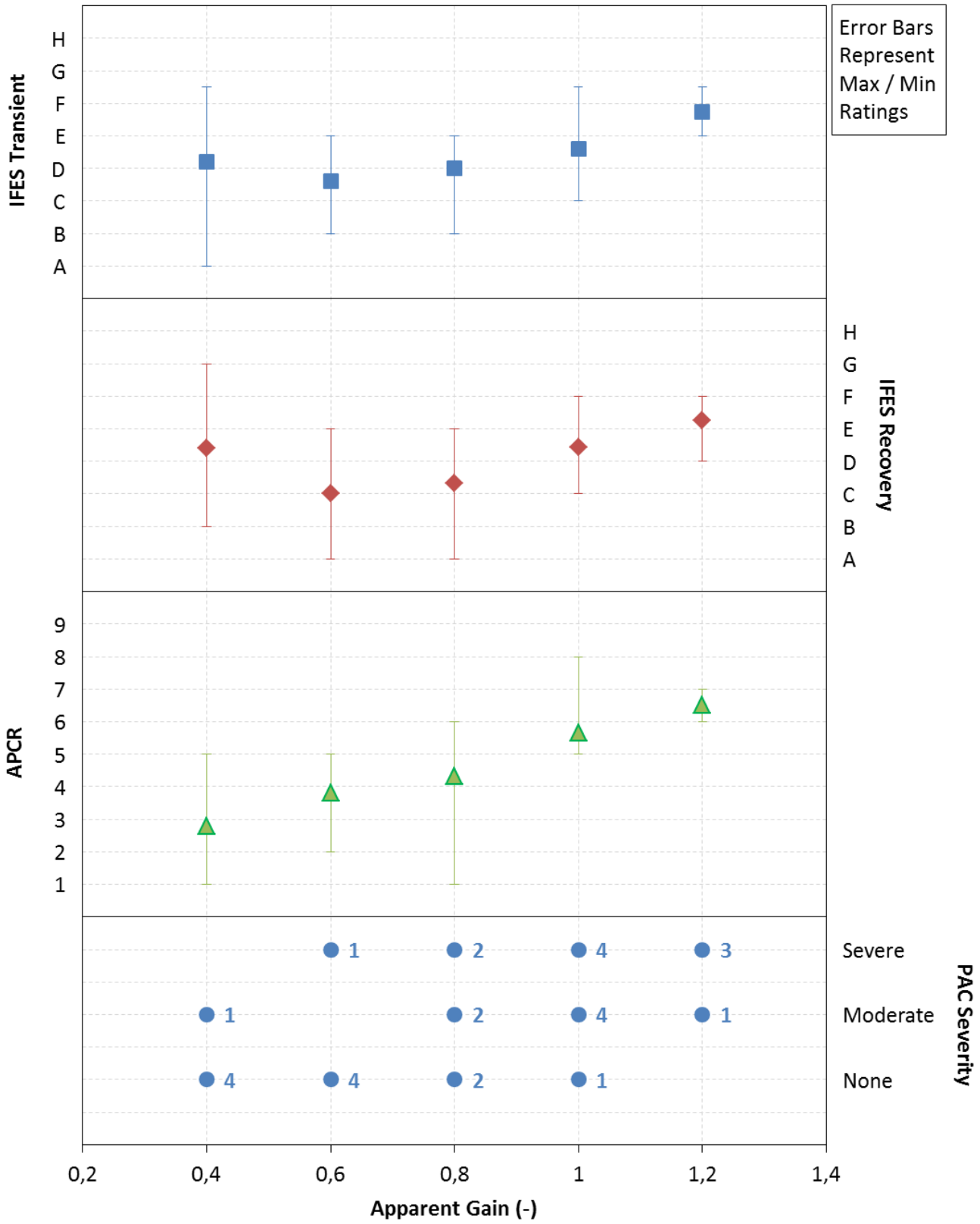

Figure 7-2: Effect of IFES Transient and Recovery Ratings, APCR and PAC Severity on the Variation of Apparent Gain in Rate Command from Pilots H, J, L

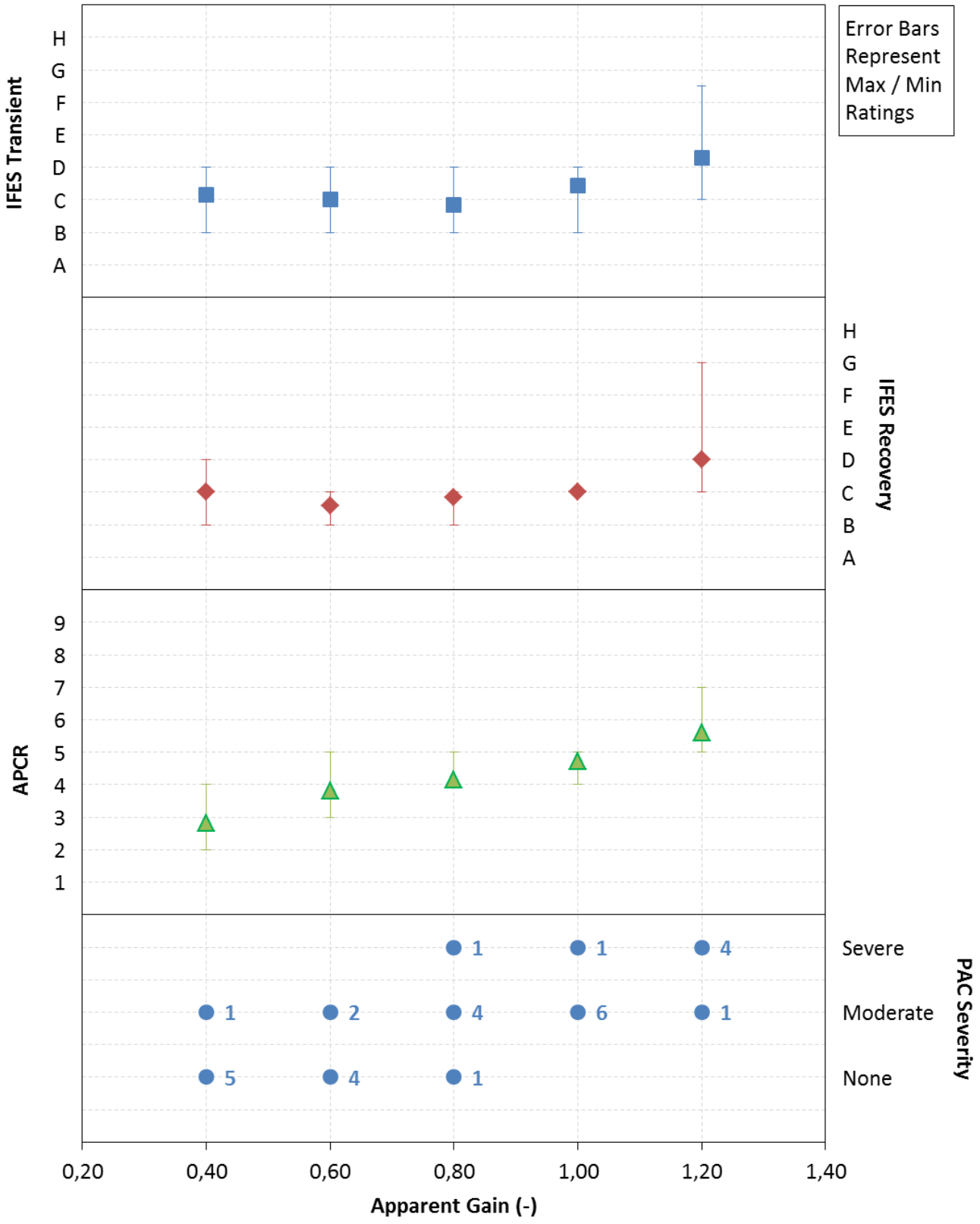

Figure 7-3: Effect of IFES Transient and Recovery Ratings, APCR and PAC Severity on the Variation of Apparent Gain in Attitude Command with Pilots H, J, L

This u-shaped unimodal variation of IFES ratings with apparent gain was a result of the balance between the following opposing factors:

Factors that caused deterioration in IFES ratings with decreasing apparent gain:

- As the apparent gain was reduced, the required inceptor force to create a given attitude or attitude rate was increased proportionally. As a demonstrative example, in configuration 1 a longitudinal step input of 10N created a step response of 12.9°/s in rate command or 17.4° in attitude command. As the apparent gain was reduced to 0.6 in configuration 4, the force required to create the same step responses was increased to 25N and hence constituted a reduced control power.

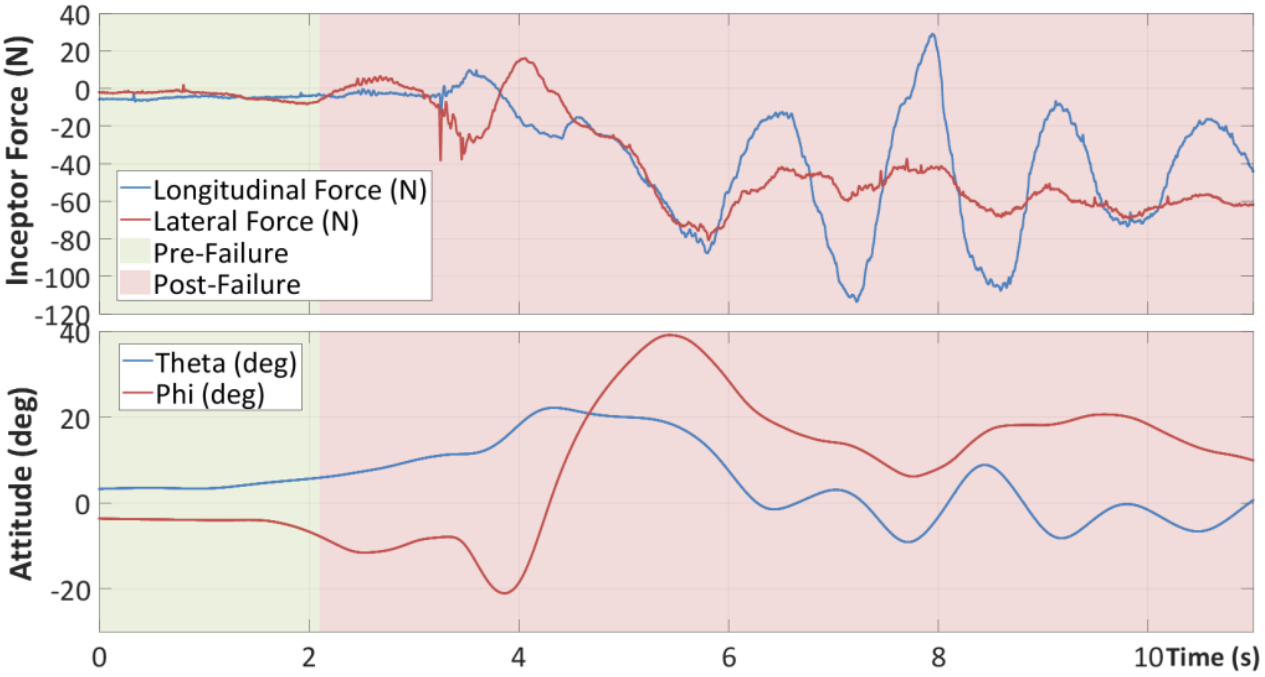

Figure 7-4: Isometric MTE with Isometric Failure in Rate Command, Direction Forward and Right, Configuration 5

During the post-failure transient and recovery with an apparent gain of 0.4 (configuration 5), the maximum longitudinal inceptor force observed was 113N in rate command with pilot J as shown in figure 7-4. However, across each pilot recorded in configuration 5 the average maximum recovery force was 61.5N in rate command and 24.9N in attitude command. These inceptor forces were subjectively considered by the test pilots to be unreasonably high and had a detrimental effect on the IFES recovery rating. Furthermore, ADS-33E [36] specifies that the maximum control forces required throughout any defined MTE shall not exceed those stated within the Limit of Cockpit Control Forces Table which details that in the hover and low speed environment, for level 1 HQ, the maximum specified force in the pitch axis is 66.7N. This supported some of the test pilots' opinions that the inceptor forces in rate command at low apparent gain were excessive but in attitude command were less significant.

- Not only did the constant, low control power cause a detrimental HQ within the recovery rating, the change in control power at the failure initiation also caused a deterioration of the transient rating. The sudden shift in control power created an unexpected change of aircraft response and the unpredictability to the pilot during the 2-3 seconds after the failure enhanced the transient effects.

  These results concur with the research conducted by Weir et al [68] in which they identified that a small change in control dynamics during a failure corresponded to a minimal effect on the pilot's transition response and performance. Conversely, the large change in control power between the pre-failure and post-failure state presented a significant degradation in HQ.

- Undesirable out of trim inceptor forces also increased in magnitude and relevance as the apparent gain was reduced. The trimmed zero force condition was fixed at the same time as the failure initiation which was targeted as the point of maximum decelerative attitude prior to the hover selection. The subsequent selection of the hover attitude from the deceleration required a large inceptor force input to induce both an attitude rate and a change of attitude. The average out of trim force identified for all configuration 4 test points in rate command was 23.9N and in attitude command was 7.9N. As the trim force could not subsequently be reset to zero, this large out of trim force was superimposed on the small high gain force inputs required in the hover maintenance sub-task.

  Section 4.4.1 details an investigation of the ability of pilots to maintain a constant inceptor force of 10.0N in each cyclic direction individually without any visual reference. The results showed that over a 60 second period the qualified pilots (including those both with and without previous isometric experience) varied the force on average by 52.2% of the initial force input across all cyclic directions.

  As the out of trim forces in successive test points were increased as a result of decreased apparent gain, the force errors introduced by the pilot (actual inceptor force relative to the required inceptor force for the hover attitude) also increased. When the aircraft's response to these errors was recognised by the pilot, corrective inputs were required to regain the hover attitude which therefore resulted in an increase in pilot workload. This evidence supports the premise that the higher out of trim forces observed as the apparent gain was reduced, were difficult to maintain accurately and would increase the workload of the pilot when a concurrent high gain task was conducted.

Factors that caused an improvement in IFES ratings with decreasing apparent gain:

- As the apparent gain was reduced the tendency for oscillatory APCs was reduced. Section 6.6 discusses how a desirable high gain bandwidth occurs when the gain reduces with increasing frequency in the vicinity of ω_{180}. During an active oscillatory APC in the isometric condition, the pilot is making aggressive, high frequency inputs which due to the anatomical limitation of the

hand and arm, tend to increase in amplitude with increasing frequency [123]. Figure 7-5 shows the theoretical Bode plot of the implemented first order filter only,[57] with variation of apparent gain (inceptor force signal input and equivalent inceptor position signal output). It demonstrates that a reduction in gain of the isometric first order filter may be generated through either an intentional configuration change of apparent gain or the conventional gain reduction with increasing frequency caused by the time constant. Regardless of its origin, it causes a reduction in the oscillatory signal input to the FCS, a consequent reduction in the aircraft response and therefore a tendency to reduce oscillatory APCs.

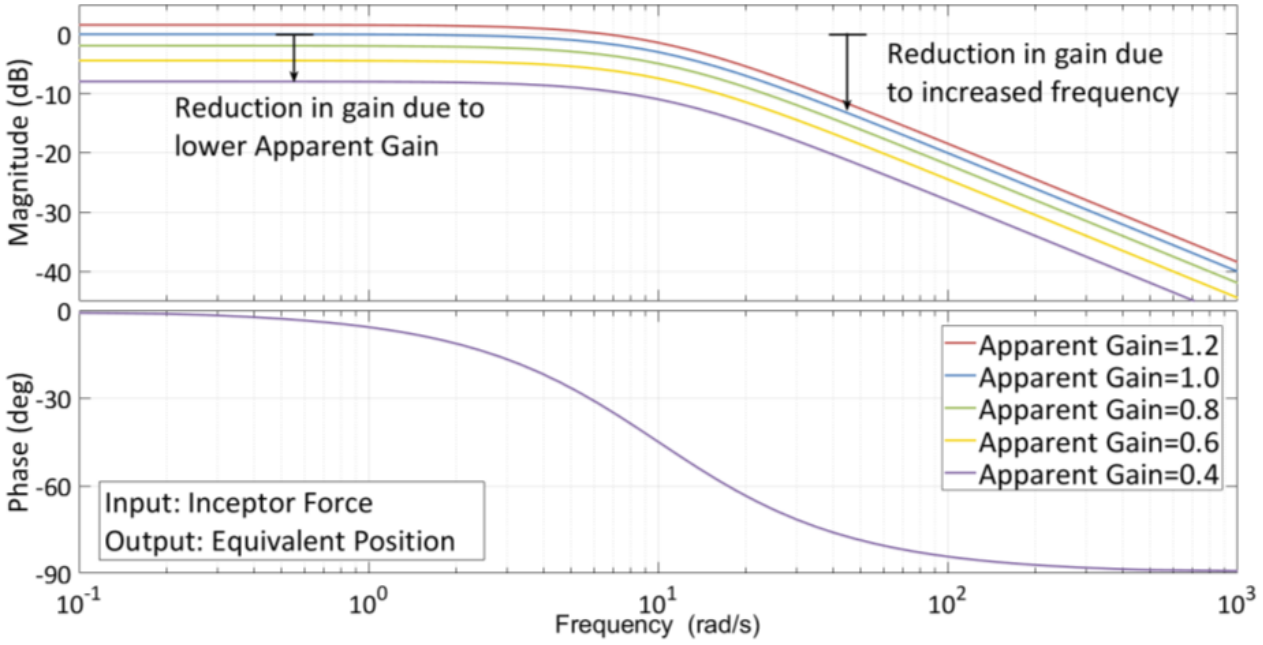

Figure 7-5: Theoretical Bode Plot of First Order Filter with Variation of Apparent Gain

- Immediately after the isometric failure the pilots tended to instinctively apply a higher force than was required to initiate the recovery to the hover attitude (also known as over-controlling). Section 4.4.2 details an investigation on the accuracy with which pilots can repeat an inceptor force input in the isometric mode having previously experienced the desired datum force in compliant mode. Visual inceptor force and position references were available to the pilots in the compliant datum but not in the subsequent assessment test points. The average inaccuracy for qualified pilots in the isometric mode was a force 49% more than the datum. These results showed that qualified pilots were very poor at selecting a specific inceptor force with which they could consistently expect a specific aircraft response when there was no inceptor position feedback.

[57] Excluding any frequency response of the helicopter control system, flight dynamics model and simulator model.

Figure 7-6 shows two test points of a standard isometric MTE, both flown by pilot L in the forwards-right direction with an attitude command controller. The first (7-6a) is flown without failure, and the second (7-6b) was flown immediately afterwards and with an isometric failure (indicated by the background colour change to red). The datum first order filter configuration was used for the failure test point so that the aircraft control power was consistent with the non-failure test point. Figure 7-6b shows that just prior to the point of failure the pilot had been applying a reasonably constant left input and had just started to apply an aft input to create the respective decelerative attitudes. As the failure was initiated he increased the aft input from 8.5N to 25.9N in order to continue the longitudinal deceleration. In comparison, the maximum aft force that was applied in the non-failure test point was only a consistent 8.7N.

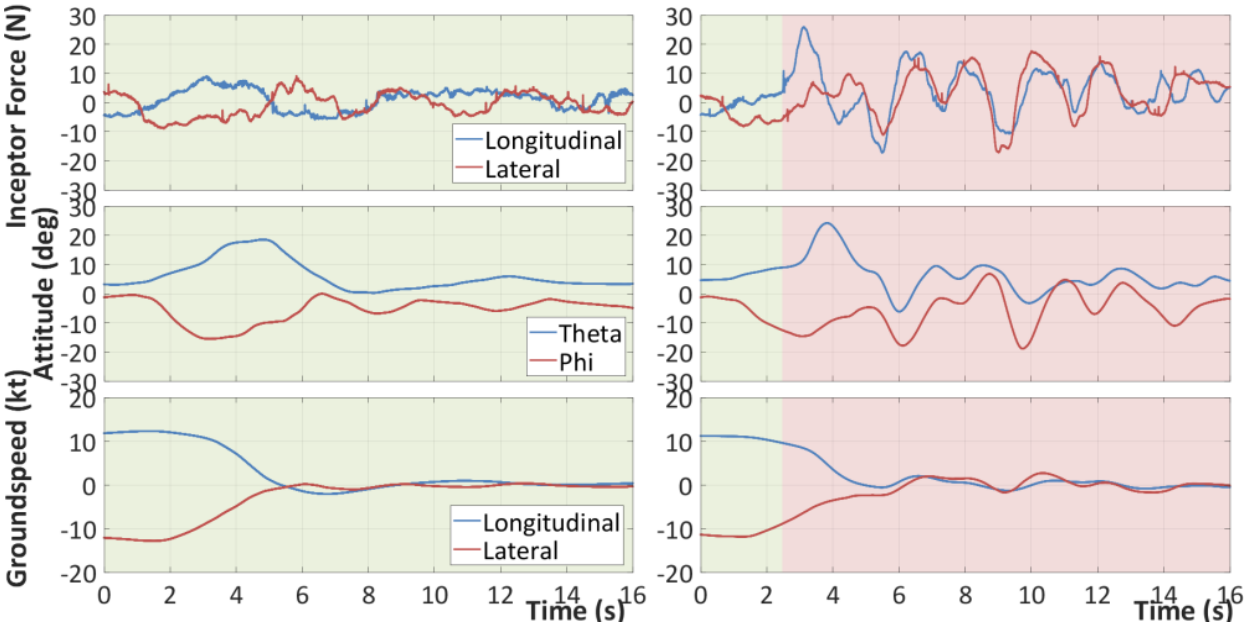

Figure 7-6: Isometric MTE in Attitude Command, Direction Forward and Right:
(left trace) Without Failure – Compliant; (right trace) With Failure – Isometric Config 1

As the deceleration sub-task and conditions were the same for both cases the difference in forces indicated that the pilot had unintentionally applied a larger force when he was unable to use the inceptor position as an input cue. In the lateral axis the deceleration was further advanced at the point of failure and so the pilot had already begun to reduce his input to achieve the hover attitude. A less clearly defined over-controlling can still be seen at 9-10 seconds in the lateral axis as the oscillatory APC was initiated during the hover selection sub-task. In both axes the initial unintentionally large force inputs created an undesired large aircraft response which, once recognised required a higher workload to correct.

As the apparent gains of the configurations were reduced the aircraft's response to the initial excessive force inputs were also reduced causing less over-reaction and a reduction in the tendency for oscillatory APCs.

7.3.2 Deviation of IFES Ratings

The error bars of the IFES ratings represent the range of the awarded ratings and followed different patterns in each command type. The rate command data range was fairly large and very similar for both the transient and recovery, being an average of 3.5 ratings, but increasing up to 5.5 and 5 ratings for transient and recovery respectively as the apparent gain decreased. The attitude command data range was comparatively smaller at an average of 2.1 ratings but included one anomalous test condition at an apparent gain of 1.2 which had a corresponding range of 3.5 and 4 ratings for transient and recovery respectively.

A significant source of data range was from the accuracy of the failure initiation timing. An optimum failure initiation was achieved at the point of maximum decelerative attitude and just as the pilot induced an inceptor input to select the hover. This would cause a large out of trim force after the failure and require a large attitude change in the subsequent recovery. Figure 7-7 shows a time trace of a near-optimal failure timing. If in this case the failure had been initiated a short time earlier the force applied to the sidestick would have been less and if it had been initiated a short time later the required attitude change to select the hover would have been less. Either of these two timing error elements would have the effect of reducing the severity of the failure with a consequent improvement in IFES ratings.

Whilst every effort was made to minimise the failure timing error, it was potentially present during all of the test points. The pilots rated it as the third most influential factor in the aggression and continuation of APCs, after cyclic control displacement at the time of failure and the post-failure required pilot gain (figure 7-1). However, as the apparent gain was reduced, the effect of a timing error on the inceptor force was enhanced. This was caused by the increase of the post-failure out of trim force for any given failure timing error relative to the datum apparent gain of 1.0. The effect of the timing error on the attitude change required to achieve the hover was not affected by the apparent gain. The larger variation of the out of trim force was reflected by a greater range of IFES ratings at lower apparent gains.

The large variation in the IFES ratings at an apparent gain of 1.2 in attitude command was due to pilot L entering a severe oscillatory APC. The pilot rated the data quality of this test point as high and stated that the cause of the APC was the unexpected need to adapt his control strategy to the higher gain. He awarded a transient rating of F/G (numerical equivalent 6.5) and a recovery rating of G (7), in contrast to the average ratings of D (4.3) and D (4.0) respectively. His second attempt at the same configuration was consistent with the other pilots.

Whilst there would inevitably be a small variation in the ratings awarded between pilots, each pilot was a trained test pilot and so should be able to maintain reasonably constant control and assessment strategies. The accurately defined course description,

performance tolerances and guidance notes on the novel rating scales were intended to reduce the pilot variation.

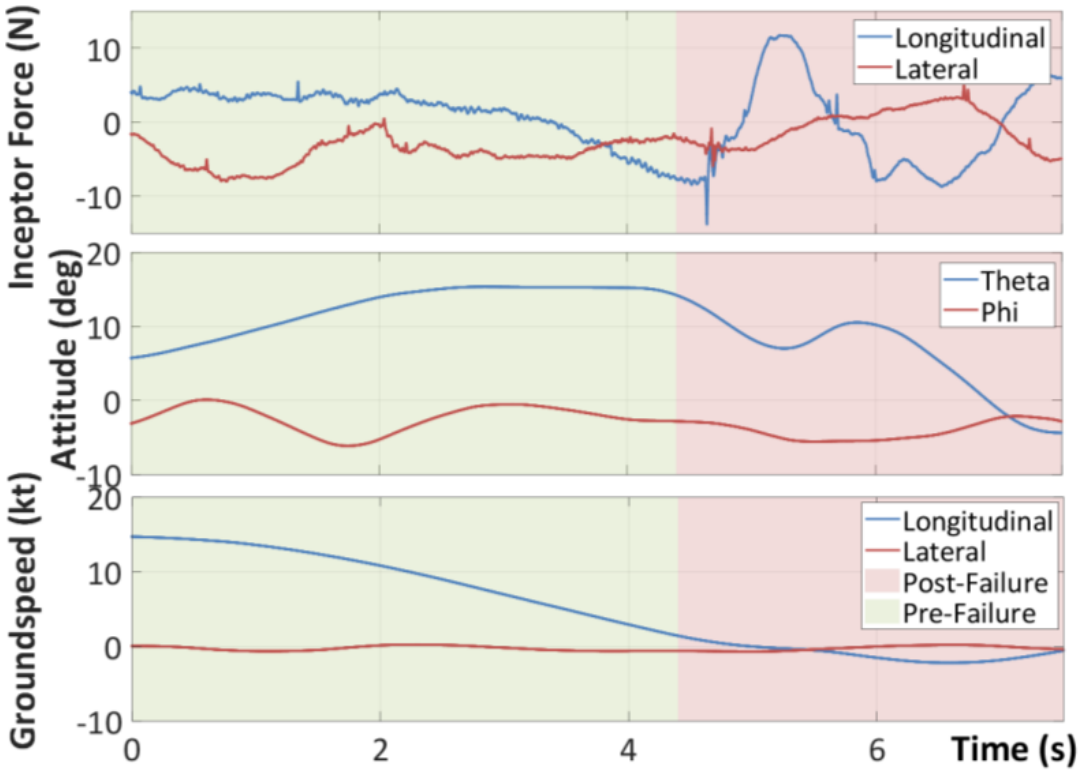

Figure 7-7: Isometric MTE with Isometric Failure in Rate Command, Direction Right, Configuration 1

7.3.3 Effect on APCR and PAC

Figure 7-8 shows frequency response data depicted as a plot of phase delay against bandwidth for specific test configurations (as defined by table 6-9). The source Bode plots for this data are shown in appendix D, and use an input of the inceptor force and an output of aircraft attitude, thus representing the complete control, aircraft and simulator model systems. In accordance with ADS-33E [36], for rate command the ω_{BW} is the lesser of $\omega_{BW\text{-}GAIN}$ and $\omega_{BW\text{-}PHASE}$; whereas for attitude command the ω_{BW} is the $\omega_{BW\text{-}PHASE}$, with a caveat that if $\omega_{BW\text{-}PHASE}$ is greater than $\omega_{BW\text{-}GAIN}$ then the aircraft may be PIO prone for 'super-precision' tasks or aggressive pilot technique.

Figure 7-5 shows that the first order filter apparent gain has no effect on its phase bode plot and therefore no effect on the $\omega_{BW\text{-}PHASE}$ or phase delay. Similarly, on the gain Bode plot, variation in the apparent gain results in a series of parallel lines which also cause no effect to the $\omega_{BW\text{-}GAIN}$. The data points taken from the frequency responses presented on figure 7-8 concurred with this theory and for both command types show that the respective configuration 1 and 4 data points are co-located.

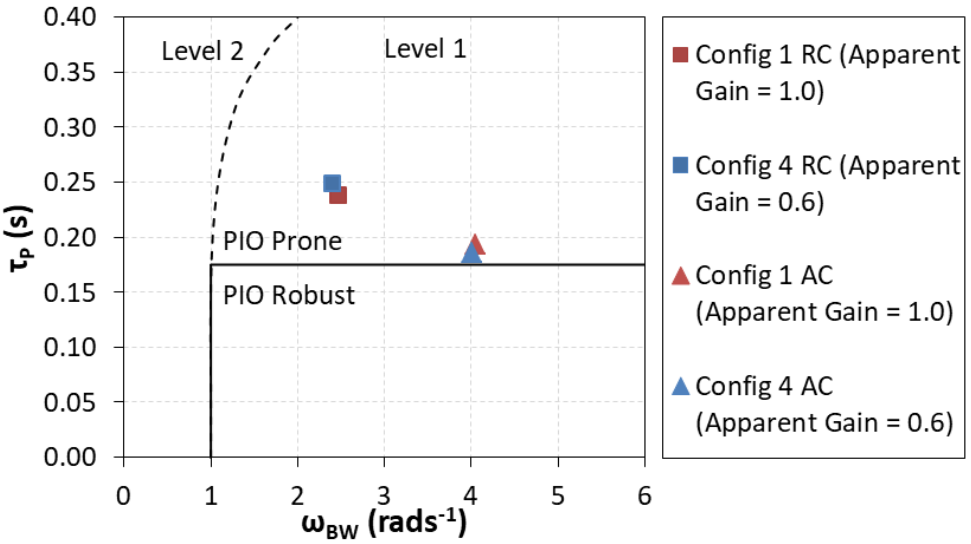

Figure 7-8: HQ and PIO Prediction for Small-Amplitude Pitch Attitude Changes in Fully Attended Non-Tracking Operations, Isometric Filter Variations of Apparent Gain [15, 36, 65]

The PIO proneness boundaries for small-amplitude pitch and roll attitude changes [65], that have been presented on figure 7-8 predict that for configuration 1 (apparent gain of 1.0), the combined control and aircraft system was PIO prone in both command types. Furthermore, for the attitude command, the $\omega_{BW\text{-}PHASE}$ was greater than $\omega_{BW\text{-}GAIN}$ which also predicted PIO proneness for 'super-precision' tasks. The pilots' subjective data for configuration 1 showed that in rate command the average APCR was 5.7 and in attitude command it was 4.7. From the definitions in figure 6-16, an APCR of 4 is 'mild predictable oscillations', 5 is 'moderate oscillations' and 6 is 'Severe oscillations'. Thus the PIO proneness prediction concurred with the subjective data in that for configuration 1, both command types displayed at least mild oscillations. Furthermore, the PAC detected moderate or severe APCs in 8 out of 9 test points in rate command and all 7 out of 7 in attitude command.

In configuration 4 (apparent gain of 0.6) the prediction also indicated PIO proneness in both command types. The corresponding pilots' subjective data showed that the average APCR in both command types was 3.8 which again established an agreement between the pilots' subjective opinion of the presence of APCs and the prediction. However, the PAC detected moderate and severe APCs only 1 out of 5 times in rate command and 2 out of 6 times in attitude command, therefore disagreeing with the prediction.

Consequently the PIO proneness prediction agreed with both the APCR and PAC in configuration 1, but for configuration 4 the prediction agreed with the APCR only, and not the PAC.

Many of the test configurations with higher apparent gain (≥0.8) developed oscillatory APCs that were initiated by the change of sidestick mode from compliant to isometric. The APCR improved consistently with reducing apparent gain, with the best average ratings for both command types of 2.8, occurring with an apparent gain of 0.4. The rate of

improvement with decreasing apparent gain was relatively stronger with the rate command as the average APCR varied by 3.7 across the full range of apparent gain tested (compared with a variation of 2.8 across the same apparent gain range for attitude command).

The PAC data reflected the APCR data in that for both command types the derived APC severity consistently reduced as the apparent gain reduced.

The generally linear distribution of decreasing APCR and PAC severity with decreasing apparent gain was not consistent with the U-shaped distribution of the IFES ratings. The IFES predominantly considered the aircraft and control excursions in the transient rating and the urgency and pilot effort within the recovery rating, whereas the APCR considered the APC severity and the pilots level of adaptation required to suppress it. Whilst all of the factors (7.3.1) that contributed to the IFES ratings improvement with decreasing apparent gain applied equally to the APCR and PAC, the factors that caused the opposing deterioration of the IFES ratings at low apparent gains were not applicable to the APCR scale and so had a negligible influence on its severity.

For the sake of clarity and comprehensiveness, the APC trigger should also be considered for its possible influence on the subsequent severity of an APC. The dominant trigger came from the sudden change of control force required to maintain the inceptor position and the consequential change in control strategy. Prior to the failure, the sidestick was in compliant mode and the inceptor force applied was relative to its displacement from trim in accordance with figures 3-13 and 3-14. After the failure the force became zero as the new trim position automatically became coincident with the failure position. With a greater difference in applied force immediately after the failure, the trigger effect was stronger and the corresponding control strategy adaptation was also greater. These effects increased the risk of inducing an oscillatory APC.

As most of the pre-failure force was a result of a spring force that increased with displacement from the trim position, the worst case condition for APCs would occur with a high spring gradient or large control input immediately prior to failure. However, as the pre-failure input force was independent of the post-failure isometric filter parameters, the trigger severity was not considered an influential factor in the specific analysis of these parameters.

7.3.4 Deviation of APCR

The range of the APCR data in rate command was an average of 3.2 ratings across all apparent gains with the largest range occurring at an apparent gain of 0.8. For this configuration of the 6 valid test points all except one was awarded an APCR of 4 to 6. The anomaly test point was flown by pilot L who awarded an APCR of 1. He commented that '*sometimes you are lucky*' as the failure timing occurred such that there was no out of trim force and he was able to hover accurately with a very low level of involvement (IFES transient B and recovery A).

The average range for attitude command was only 1.6 ratings with little variation across all apparent gains.

7.4 Analysis of Variation in Time Constant, τ

7.4.1 Effect on IFES Ratings

Figure 7-9 and 7-10 show a predominantly constant distribution of both average IFES ratings with respect to increasing time constant for the attitude and rate commands respectively. A very weak U-shaped trend could be identified, but the distribution of the data lacks robust definition and the large range of the data is insufficient to justify such a correlation argument.

The rate command average ratings varied between D/E (numerical equivalent of 4.6 transient; 4.4 recovery) at τ=0.1s to E/F (6.1 transient; 5.5 recovery) at τ=0.3s. The attitude command average ratings had a similar spread but generally one rating lower in severity, from C/D (3.4 transient; 3.0 recovery) at τ=0.1s and D/E (4.1 transient; 4.3 recovery) at τ=0.3s.

In both command types the weakly identified optimum time constant was at the datum configuration of 0.1s which, as discussed in sections 6.3.4 to 6.3.6, was the proposed balance of damping the noise from the force signals and avoidance of excessive phase lag which could lead to potential APCs. Figure 7-11 compares the different time constants on a Bode plot of the implemented first order filter only[58] (force signal input and equivalent position signal output). At the representative input frequency of 2.6rads^{-1} the additional phase lag caused by the filter increased from 1.43° at τ=0.01s to 37.25° at τ=0.3s (detailed further in table 6-3). The additional phase lag would reduce the bandwidth of the overall aircraft and would therefore increase the risk or severity of oscillatory APCs. Therefore, unlike a variation in the first order filter apparent gain, an increase in the time constant would have a detrimental effect on $\omega_{BW\text{-}GAIN}$, $\omega_{BW\text{-}PHASE}$ and the phase delay.

[58] Excluding any frequency response of the helicopter control system, flight dynamics model and simulator model.

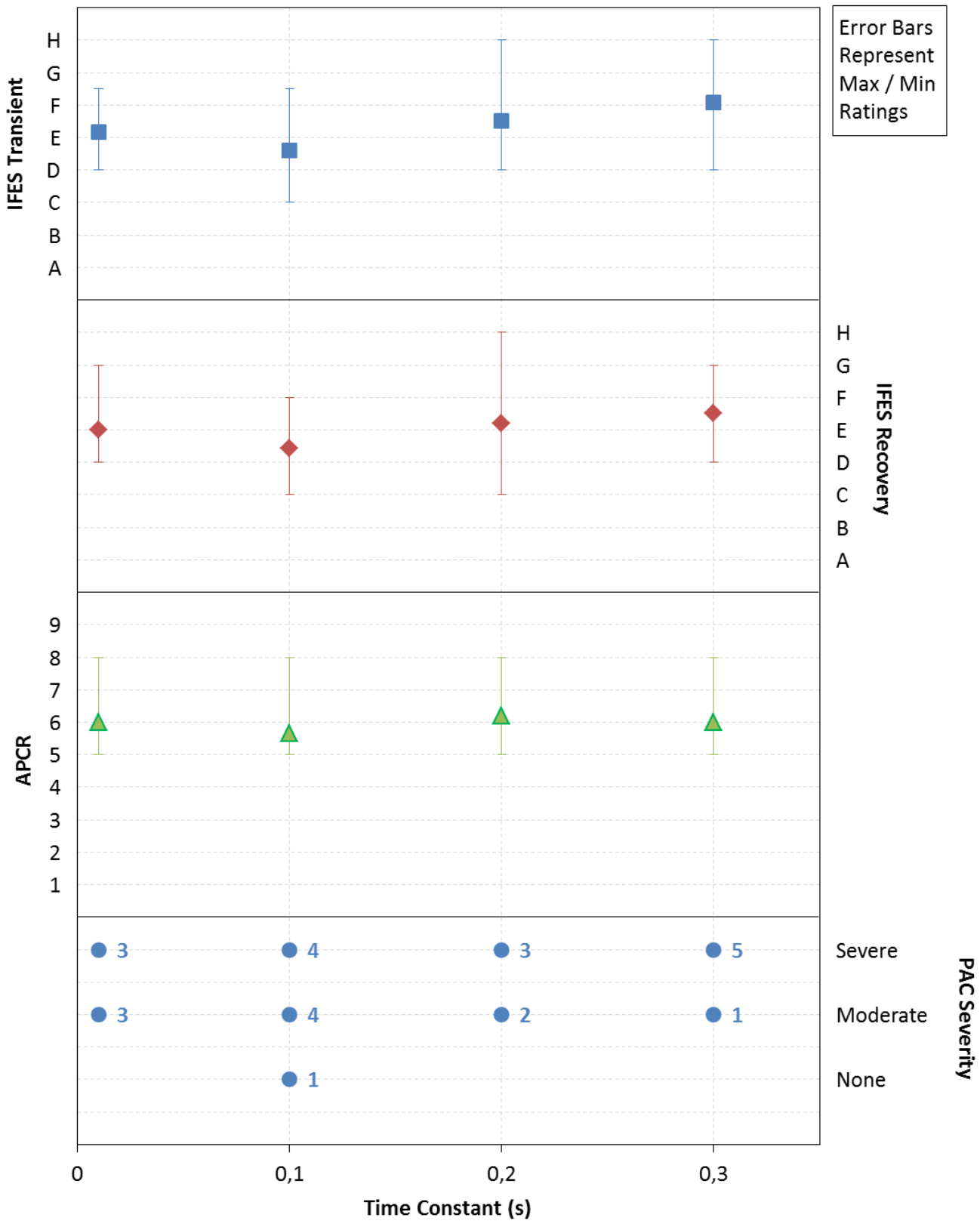

Figure 7-9: Effect of IFES Transient and Recovery Ratings, APCR and PAC Severity on the Variation of Time Constant in Rate Command with Pilots H, J, L

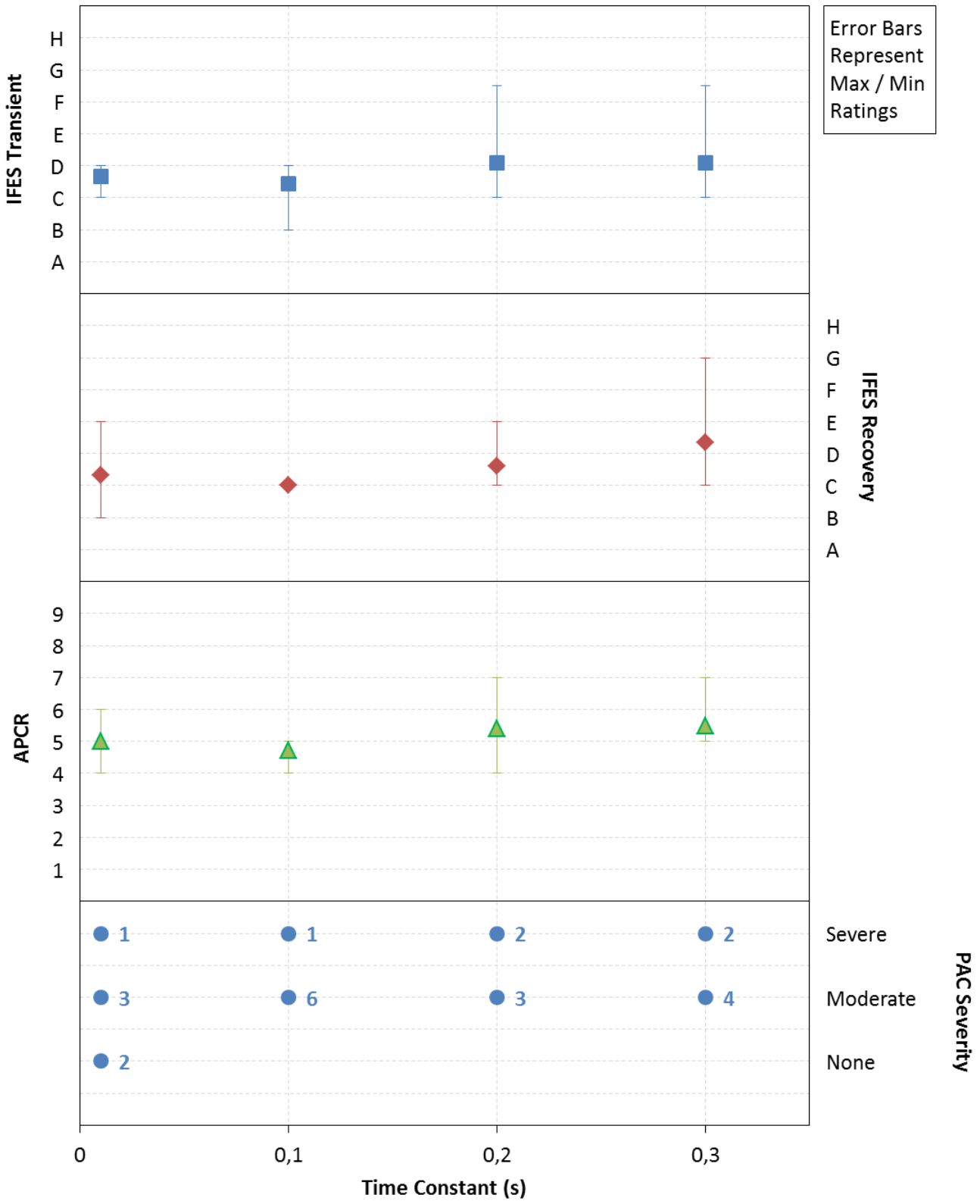

Figure 7-10: Effect of IFES Transient and Recovery Ratings, APCR and PAC Severity on the Variation of Time Constant in Attitude Command with Pilots H, J, L

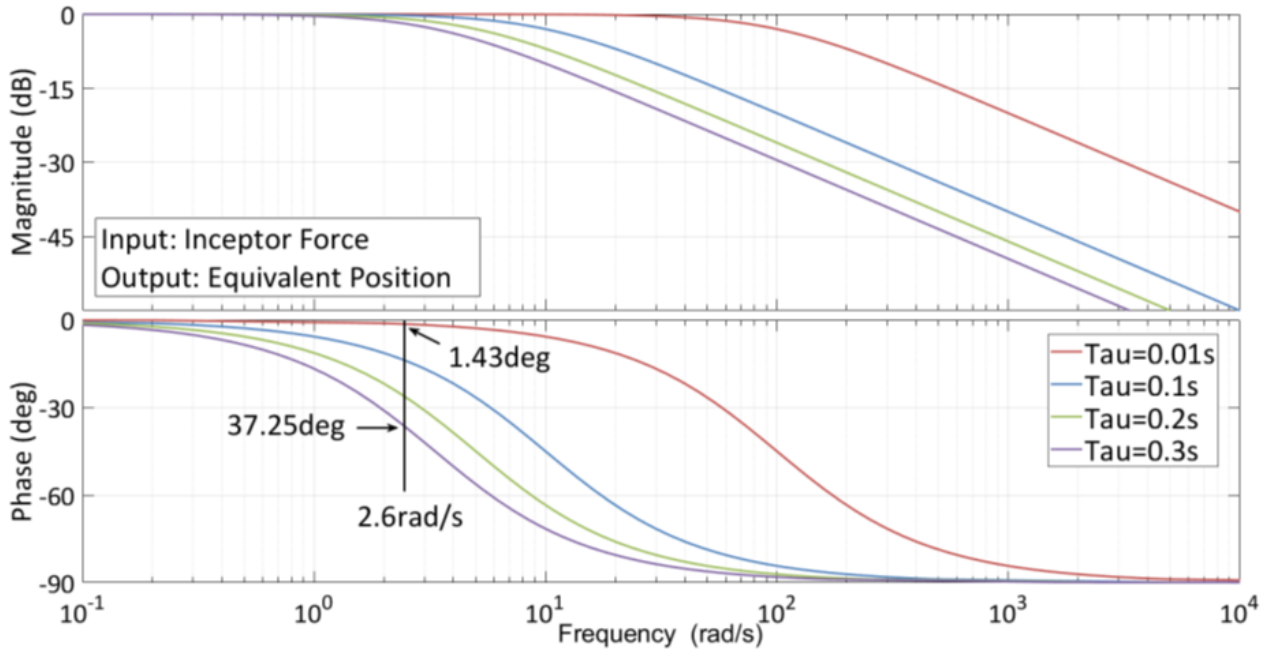

Figure 7-11: Theoretical Bode Plot of First Order Filter with Variation of Time Constant

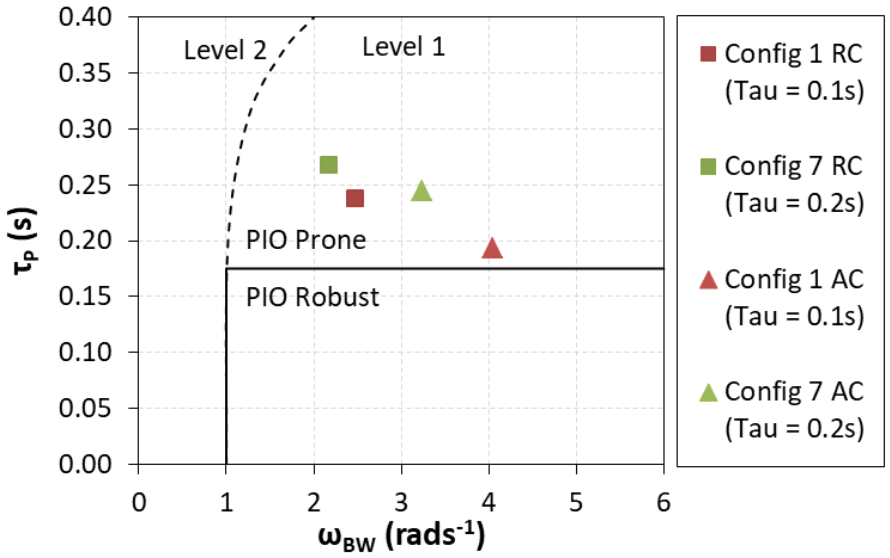

Figure 7-12: HQ and PIO Prediction for Small-Amplitude Pitch Attitude Changes in Fully Attended Non-Tracking Operations, Isometric Filter Variations of Time Constant [15, 36, 65]

Figure 7-12 concurs with this theory by showing that the bandwidth of the whole aircraft system[59] reduced in the rate command from 2.47rads^{-1} with τ=0.1s to 2.17rads^{-1} with τ=0.2s and in the attitude command from 4.05rads^{-1} to 3.24rads^{-1} respectively. Whilst the

[59] Frequency response analysis from inceptor force input to aircraft attitude output, thus representing the complete control, aircraft and simulator model systems. The source Bode plots for this data are shown in appendix D.

correlation with theory can be identified in the distribution of the deteriorating average IFES ratings with increasing time constant, the correlation is weaker than expected.

At a very low time constant, section 6.3.5 predicted that the low noise damping of the force signal may have an effect on the aircraft response. It was also considered that some damping in the first order filter may be able to reduce the equivalent position signal rates and provide some damping to the oscillatory PACs.

For both command types there was a small deterioration of averaged IFES ratings (0.55 of a rating for rate command and 0.28 of a rating for attitude command) with a corresponding reduction in time constant from the datum τ=0.1s to τ=0.01s. However, the deterioration of the IFES ratings was small and the averages of range of ratings were quite large (3.5 ratings for rate command and 2.4 ratings for attitude command) and so the correlation with the proposed expectations was weak.

Further analysis of the data using the Global Success Rate (GSR) provided greater legitimacy and reduced the errors associated with variation of ratings awarded by different pilots. The GSR is a measure of the ratio of conformal results to all results as defined in equation 6-17. If conformity was measured as positive when a test pilot awarded a worse rating at 0.01s than at 0.1s for the same conditions, the GSR could report any compliance with the proposed expectations. The GSR for the 12 pairs of comparative data points (6 rate command and 6 attitude command) are presented in table 7-1 and also show a consistently poor support of correlation with the expectation.

	IFES Transient	IFES Recovery
Rate Command	0.33	0.66
Attitude Command	0.33	0.33

Table 7-1: GSR of Deterioration of IFES with Time Constant Reduced from 0.1s to 0.01s

7.4.2 Deviation of IFES Ratings

The large range of the data in the rate command with variation of time constant was similar for both the transient and recovery ratings, showing average ranges of 3.5 ratings for both command types across all relevant test points. The expected source of the large ranges was the failure initiation timing as described in 7.3.2.

The range of the attitude command data was significantly lower than the corresponding rate command data, with an average range of 2.4 ratings for both transient and recovery across all time constant values.

The range of ratings for the time constant data was consistent with that observed in the apparent gain data.

7.4.3 Effect on APCR and PAC

Whilst the relationship of the APCR average ratings with variation of time constant had a very small but discernible shallow U-shaped distribution, the large range of data could have supported an alternative flat distribution. The lowest rating was at the datum configuration 1 (τ=0.1s) with ratings of 5.7 for rate and 4.7 for attitude command and with increasing time constant the maximum average ratings were 6.2 for rate command and 5.5 for attitude command.

As any inferences drawn from this data were only marginally conclusive, the GSR was again used for each test pilot in each command type between τ=0.3s and τ=0.1s. In this argument, conformity was measured as positive when a test pilot awarded a higher APCR with τ=0.3s than with 0.1s for the same conditions. The results for the 12 pairs of comparative data points (6 rate command and 6 attitude command) are shown in table 7-2 and show that the data is inconclusive.

The distribution of the PAC severity with variation of time constant also reflected the APCR distribution with an almost constant severity of APCs. The PAC detected moderate or severe PACs in all but one of the 26 test points in rate command and all but 2 of the 24 test points in attitude command.

	APCR
Rate Command	0.50
Attitude Command	0.33

Table 7-2: GSR of Deterioration of APCR with Time Constant Increased from 0.3s to 0.1s

As previously discussed in section 7.3.3, the configuration 1 was predicted to be PIO prone by analysis of the frequency response characteristics shown in figure 7-8 and was subsequently confirmed using test data. Figure 7-12 then predicted that both command types in configuration 7 (τ=0.2s) would also be PIO prone. In addition, their frequency responses showed a lower bandwidth and higher phase delay, predicting that they would not only be PIO prone, but be more PIO prone than the corresponding configuration 1. The recorded data for configuration 7 supported this prediction, where in the rate command the average APCR was 6.2 and in attitude command it was 5.4 which by using the definitions in figure 6-16 describe severe and moderate oscillations respectively. Furthermore for the configuration 7 data, the PAC detected moderate or severe APCs in all 5 test points in rate command and all 7 test points in attitude command. In all cases the APCR and PAC results showed higher severity of APCs in the configuration 7 data than in the configuration 1 data.

7.4.4 Deviation of APCR

The range of the APCR data in rate command was an average of 3.0 ratings across all time constants and in attitude command the average range was 2.0 ratings. In common with

the variation seen in the IFES ratings, the most significant source of variation of the APCR was from the failure timing.

7.5 Analysis of Variation in Ramp Attenuator Period

7.5.1 Implementation of Ramp Attenuator

In section 7.3.3 it was identified that for both command types a reduction in apparent gain caused a predominantly linear reduction in APCR and PAC severity. Furthermore, with a reduction in apparent gain not below 0.6, there was also an improvement in both the IFES transient and recovery ratings.

However, there was an expectation that after the recovery phase and through the continuation of flight phase (long term), a permanent reduction in agility caused by the reduced apparent gain would deteriorate the longer term HQ. It was therefore considered that a reduction in apparent gain would be desirable in the short and medium term but undesirable in the longer term.

Any step change in a control law or signal process of a rotorcraft would cause a non-predictable response to the pilot's inputs over the change period, resulting in additional undesirable HQ. As this unpredictability could potentially mask the short and medium term improvements, it was essential that the change in the apparent gain was introduced over a change period that would not adversely affect the overall HQ.

The chosen solution was to introduce a ramp attenuator into the first order filter datum configuration 1 which would multiply the apparent gain by a factor that increased linearly over a time period from zero to unity (detailed further in section 6.3.7). The ramp time periods selected were 1.25s, 2.5s and 3.75s which represented 0.5, 1.0 and 1.5 times the period of a 2.6rads^{-1} oscillation (previously identified in section 5.6 as the predominant pilot input frequency of oscillatory APCs for the given aircraft-pilot system). The ramp attenuator could also be removed from the system entirely (indicated by a ramp time of zero).

Figures 7-13 and 7-14 show the standard data format presentation for variation of ramp period for the rate command and attitude command respectively. There were a low number of data points for the 3.75s ramp period in rate command and all of the test configurations in attitude command due to one of the pilots feeling nauseous, therefore rating his data quality as 'low'.

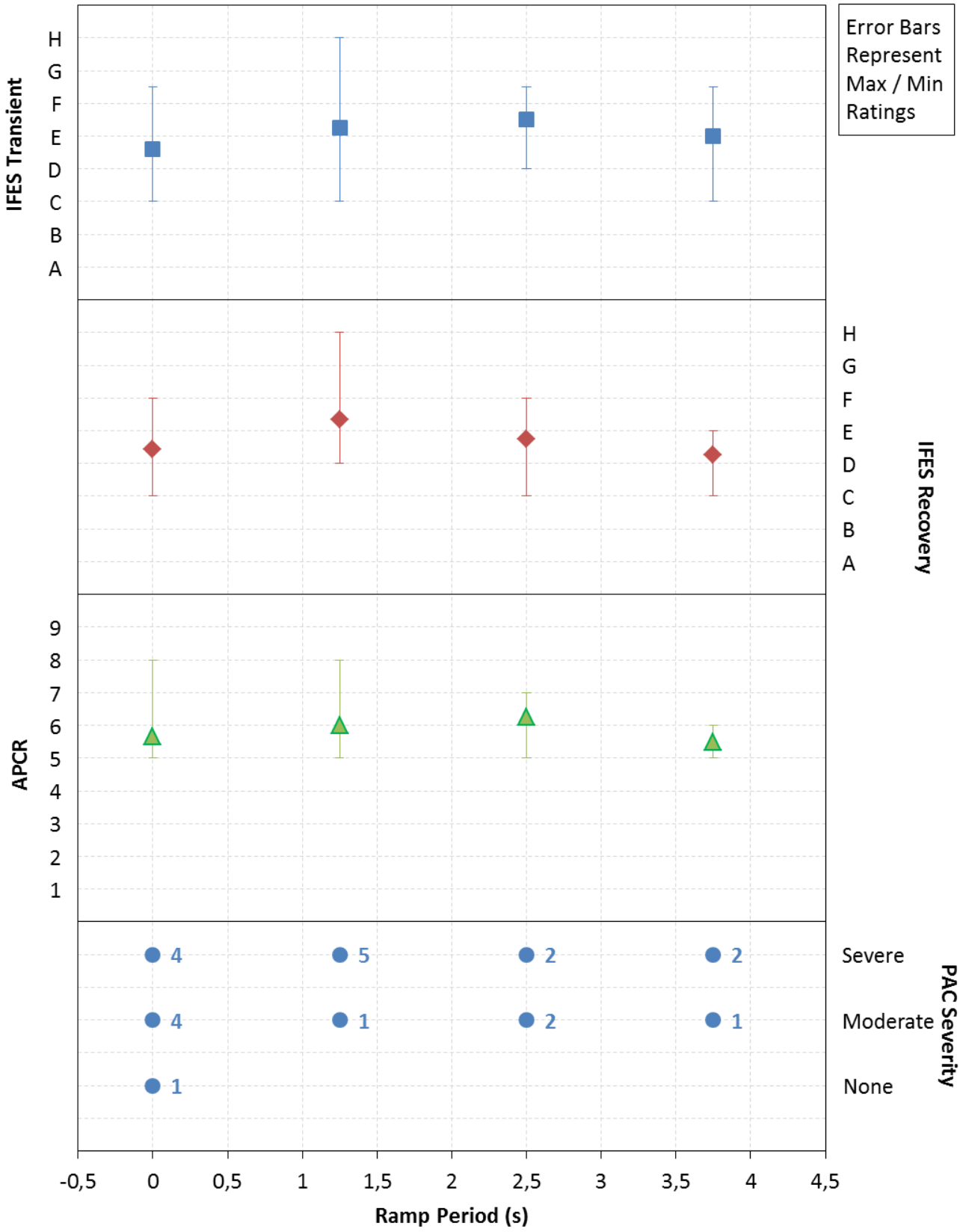

Figure 7-13: Effect of IFES Transient and Recovery Ratings, APCR and PAC Severity on the Variation of Ramp Attenuation Period in Rate Command with Pilots H, J, L

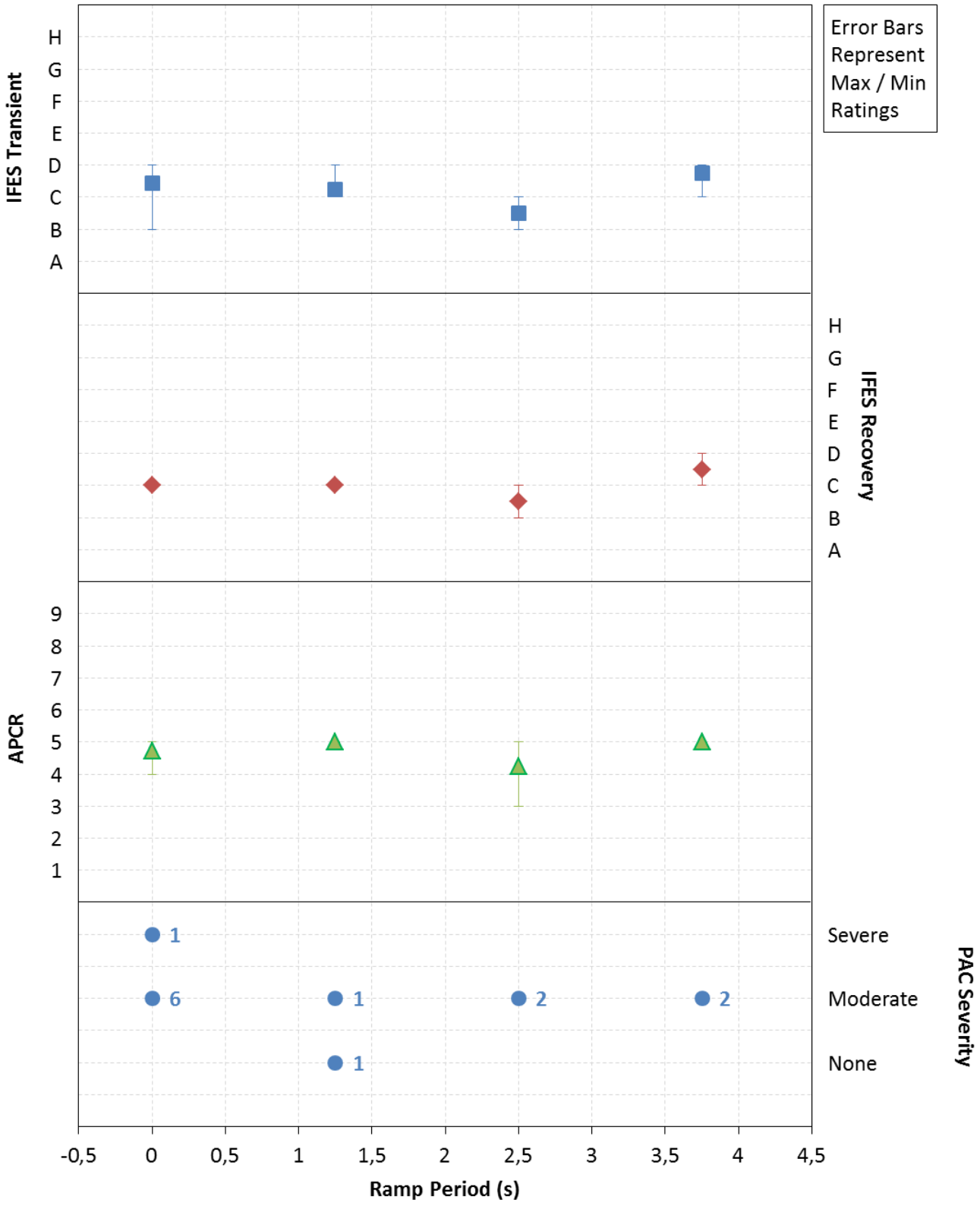

Figure 7-14: Effect of IFES Transient and Recovery Ratings, APCR and PAC Severity on the Variation of Ramp Attenuation Period in Attitude Command with Pilots H, J, L

7.5.2 Effect on IFES Ratings

The success of a configuration was considered positive if it could offer a beneficial solution in the short term (transient) and medium term (recovery) HQ of at least as good as those observed for the datum apparent gain *and* the ramped increase in apparent gain resulted in no adverse HQ. Identifying or analysing the comparative improvement or deterioration of these two criteria proved very difficult and inconclusive, and the pilots were only able to determine overall IFES ratings that considered the factors together.

The rate command data indicated that with increasing ramp period, the IFES transient rating slightly deteriorated and then slightly improved again at 3.75s at E (numerical equivalent 5) but still remained worse than with no ramp attenuator of D/E (4.6). The IFES recovery rating also deteriorated then improved with increasing ramp period but at 3.75s was awarded an average rating of D/E (4.3) that was only slightly better than with no ramp attenuator of D/E (4.5). The attitude command data showed similar data as for the rate command in that both transient and recovery ratings remained within the C/D band except for a slight improvement at 2.5s with a rating of B/C (2.5).

Subjective opinion from the test pilots supported the understanding that the fairly constant variation of transient, recovery and APC ratings were due to the balance of 3 factors:

- Inconsistent and unpredictable control response for low ramp periods created very different aircraft responses to control inputs depending upon how long after the failure an input was made. A cyclic input of 1cm at 500ms after the failure created double the aircraft response as for the same input at 250ms. Similarly, a constantly held input, for example due to a failure occurring with an out of trim inceptor force that needed to be offset with an applied input, created an increasing aircraft response over time. This negative effect was greatest for the configurations which presented the highest gradient of control response with respect to time after the failure. Therefore the effect was more significant for the 1.25s and 2.5s ramp periods which constituted the higher rates of change of control response with time. It was less noticeable at 3.75s ramp periods in which the rate of change of control response with time was lower and the effect was negligible if the ramp was not implemented.

- Long ramp periods caused the initial low control power to remain effective for a long period of time after the failure. As was identified in 7.3.1 an apparent gain of 0.4 caused a deterioration of the IFES and APC ratings due to the large forces required to create aircraft responses (in comparison to an apparent gain of 1.0). For the 3.75s ramp period, the apparent gain remained below 0.4 for the first 1.5s. For this period each pilot was required to make very large and uncharacteristic force inputs to recover the aircraft to a stable condition. This negative effect increased with increasing ramp period.

- An oscillatory APC was usually initiated by the pilot making an unnecessarily large (and often unintentional) control input after the failure. The initially low control response reduced the effect of these reactive, or surprise induced

inputs for the short period that the pilot required to subconsciously compose himself. This positive effect increased with increasing ramp period.

With consideration for the range of the awarded data, it could only be identified that there wasn't a significant or recognisable improvement in either the transient or recovery ratings through the use of the ramp attenuator above those of the datum configuration.

Whilst the assumption that the lower apparent gain would deteriorate the HQ in the longer term, for example during transit or landing, such testing was not conducted and so could not be verified.

7.5.3 Deviation of IFES Ratings

The large deviation of the data in the rate command was similar for both the transient and recovery ratings and fairly consistent with variation of ramp period, with a range of between 2.0 and 5.0 ratings and an average range of 3.3 ratings across all relevant test conditions. The expected source of the large ranges was the failure initiation timing as described in 7.3.2.

The deviation of the attitude command data was significantly smaller than the corresponding rate command data, with a range between zero and 2.0 ratings and an average range of 0.9 ratings across all ramp periods for both transient and recovery.

The range for the ramp attenuator data was consistent with that observed in the apparent gain and time constant data.

7.5.4 Effect on APCR and PAC

The average APCR for rate command remained fairly constant at between 6.25 and 5.5 with an absolute maximum rating of 8 and a minimum of 5 for all ramp periods. The data for the attitude command was similarly constant but approximately 1-2 ratings lower, varying between 4.25 and 5.0.

The distribution of PAC severity with variation of ramp period was consistent with the subjective APCR results. The PAC severity was fairly constant and an average PAC severity lay between 'severe' and 'moderate' for all tested ramp periods.

The factors influencing the IFES ratings, discussed in 7.5.2 apply also to the APCR and PAC results and offer an explanation for the constant distribution of APC severity with increasing ramp attenuation time periods.

7.5.5 Deviation of APCR

The average range of the APCR data across all ramp periods in rate command was 2.25 ratings and in attitude command was 0.8 ratings.

7.5.6 Configuration Review

Given the results of the investigation in 7.3 and in hindsight it may have been more appropriate to set the ramp's initial value of apparent gain at 0.6, the final value at unity and to start the ramp after a short period at the constant initial value. These values would

have represented the best values of apparent gain during the short / medium terms and that expected in the long term respectively. However, due to the time required to analyse the data from the apparent gain investigation and the limited availability of the test pilots, the information and proposal was not implemented within this study.

7.6 Analysis of Helicopter Control Command Types

The figures 7-15 to 7-17 compare the effect of the different command types with pilots H, J and L and so present both rate and attitude command helicopter models on the same figure. The presented data format has been changed from the standard format such that all rate command data points are blue and all attitude command data points are red.

7.6.1 Effect on IFES Ratings

The transient and recovery IFES ratings in rate command are worse than in attitude command for all first order filter configurations. Generally, the difference in the ratings for constant command type and filter configurations was 1-1.5 ratings. However, at an apparent gain of 0.6 the attitude command rating was only 0.6 (transient) and 0.4 (recovery) better than the rate command. The largest difference of 3 (transient) and 2.25 (recovery) ratings occurred in the datum configuration and a ramp attenuation of 2.5s, but as there were only 2 test points conducted in the corresponding attitude command the confidence of this comparison is accordingly reduced.

The CHR for the Isometric Failure MTE with the aircraft in compliant mode (without failure) was 4 in rate command and 3 in attitude command (section 6.7 and appendix D contains further details of the baseline HQ). For the test points in which the failure was initiated, only the inceptor mode was affected and the augmentation of the aircraft remained unchanged. It was therefore expected and subsequently observed that the comparison between rate and attitude command of the IFES ratings with failure would reflect the CHR of the same MTE without failure.

Figures 7-8 and 7-12 show that for all the configurations in which frequency sweeps were recorded, the bandwidth for the rate command was consistently lower than for attitude command. The lower bandwidth indicated that the pilot could exert good closed loop control only over a reduced range of frequencies and so would have a greater tendency to enter and maintain an oscillatory APC than for a higher bandwidth configuration. The higher IFES ratings in rate command concurred with the theory that the identified lower bandwidth would increase the pilot's compensation in controlling the aircraft in a high gain (high frequency) task and suppress any oscillatory APC.

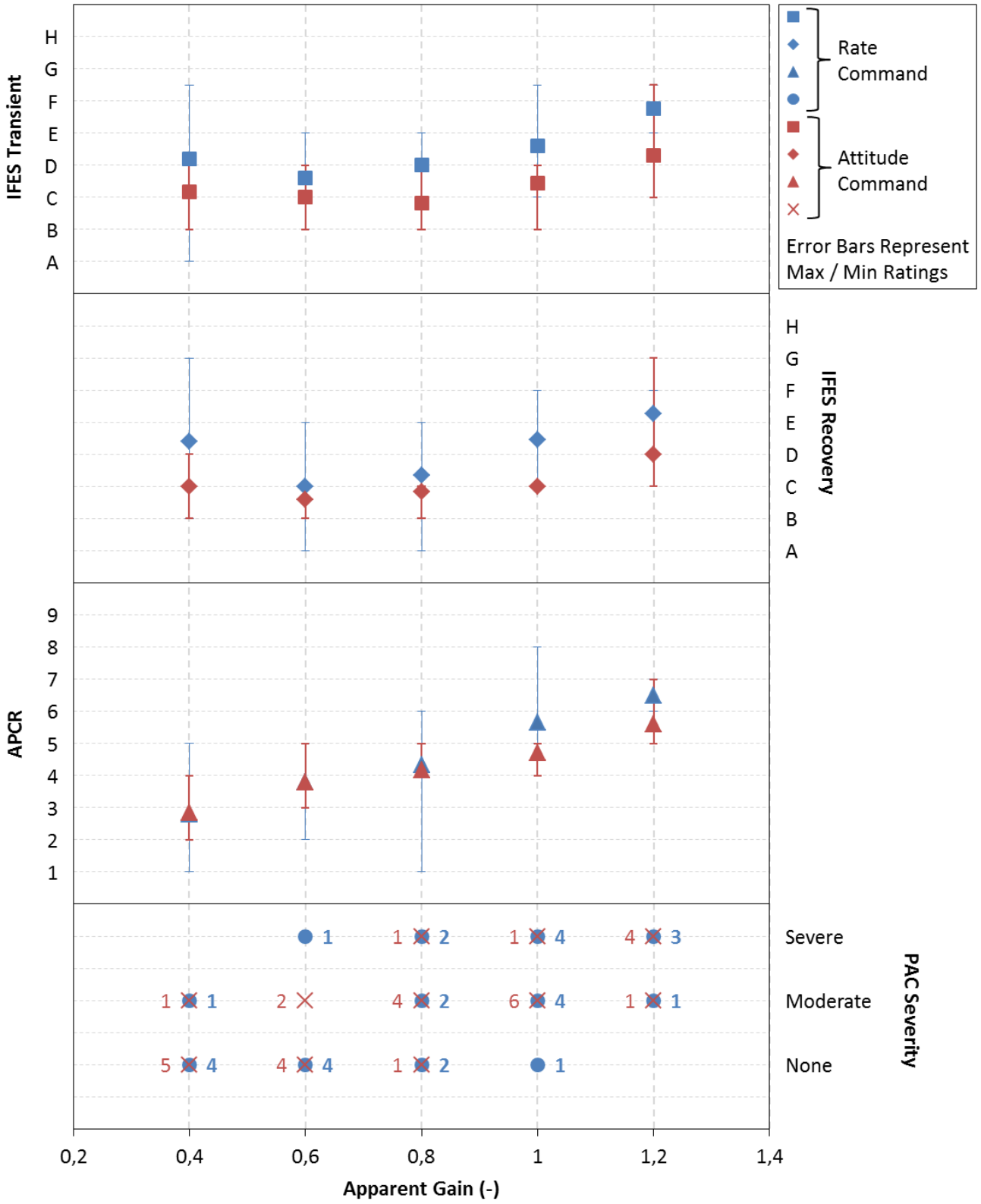

Figure 7-15: Effect of IFES Transient and Recovery Ratings, APCR and PAC Severity on the Variation of Apparent Gain in Rate and Attitude Command with Pilots H, J, L

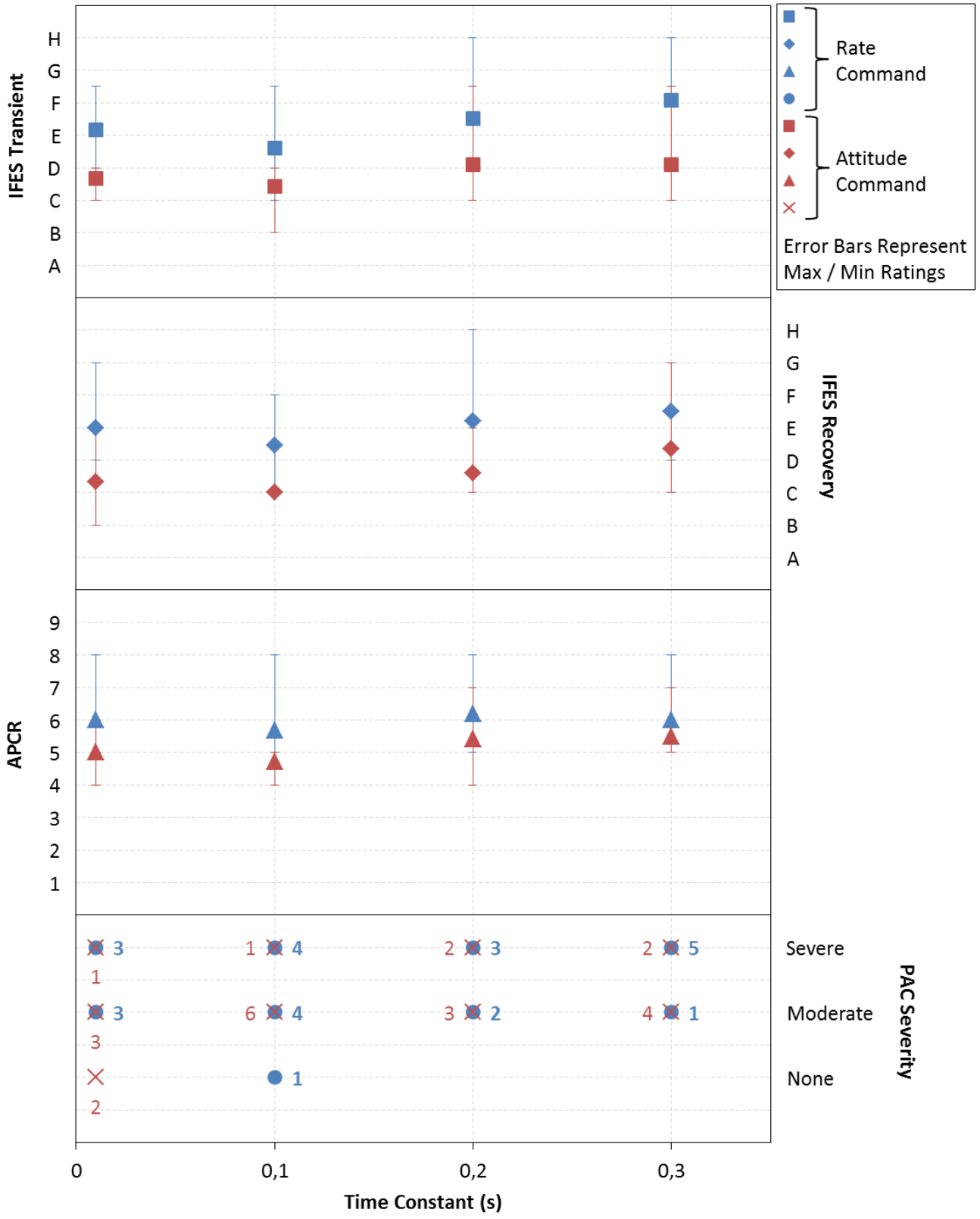

Figure 7-16: Effect of IFES Transient and Recovery Ratings, APCR and PAC Severity on the Variation of Time Constant in Rate and Attitude Command with Pilots H, J, L

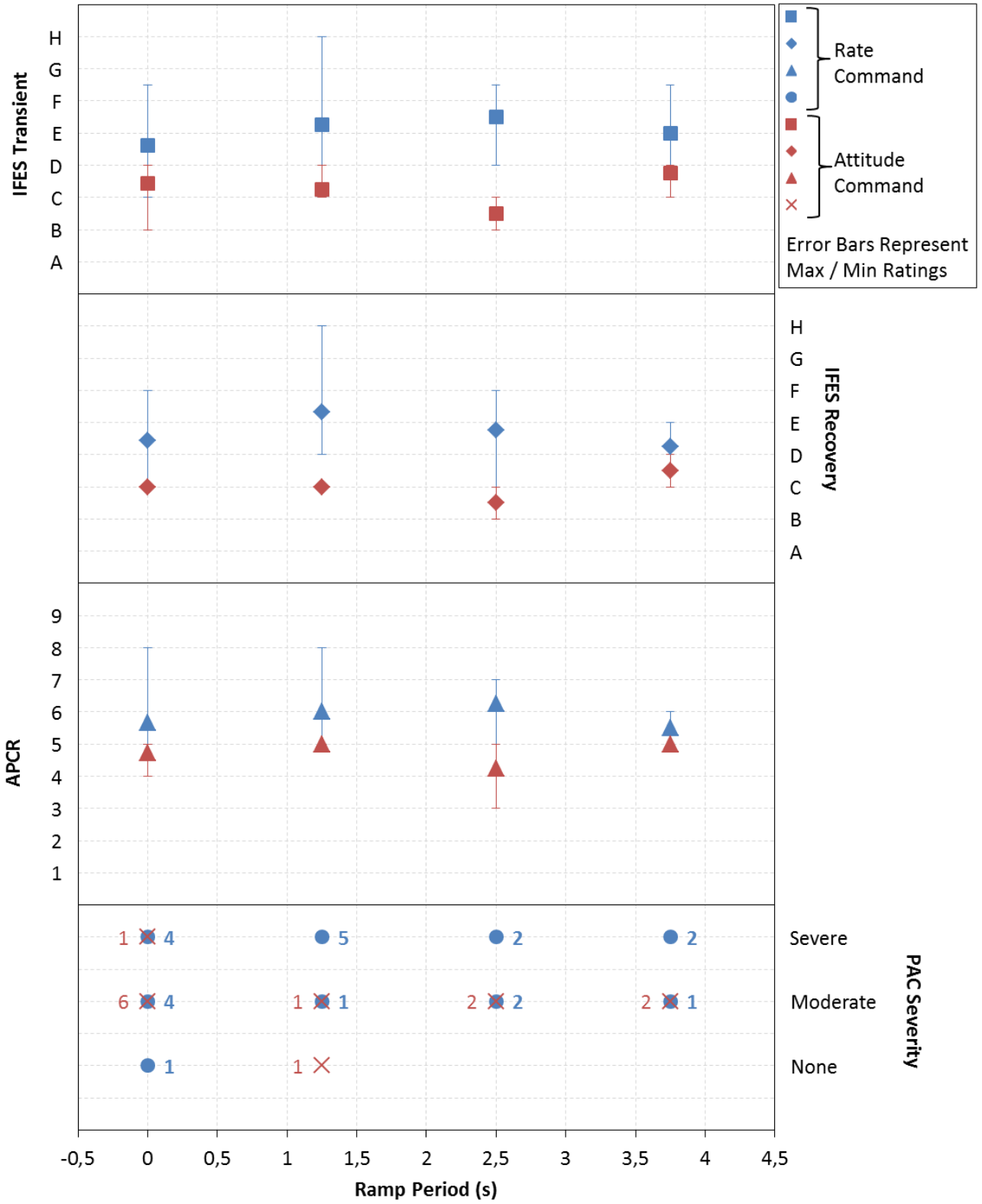

Figure 7-17: Effect of IFES Transient and Recovery Ratings, APCR and PAC Severity on the Variation of Attenuation Period in Rate and Attitude Command with Pilots H, J, L

7.6.2 Deviation of IFES Ratings

The range of the IFES ratings was consistently larger in rate command than in the attitude command despite a similar number of test points in each command type at each configuration. The average range of ratings for all configurations in rate command was 3.46 (transient) and 3.39 (recovery) whereas in attitude command it was 2.04 (transient) and 1.54 (recovery).

The much smaller range of ratings in attitude command was considered to be due to lower failure timing errors. As discussed in section 7.3.2 the optimum failure occurred at maximum decelerative attitude and maximum control input required for selecting the hover. An ideal or perfect lateral deceleration is presented in figure 7-18 with schematic indications of the lateral groundspeed (V_Y) and roll attitude (ϕ) of the aircraft and inceptor displacements in compliant mode for either attitude command ($\delta_{1S\text{-}AC}$) or rate command ($\delta_{1S\text{-}RC}$). The trim position of the inceptor is as required for a hover attitude. Real data from a flown lateral deceleration would superimpose additional control inputs for control quickening and control adjustments due to the pilot's visual feedback; however for the purposes of a theoretical explanation an idealised control input suffices.

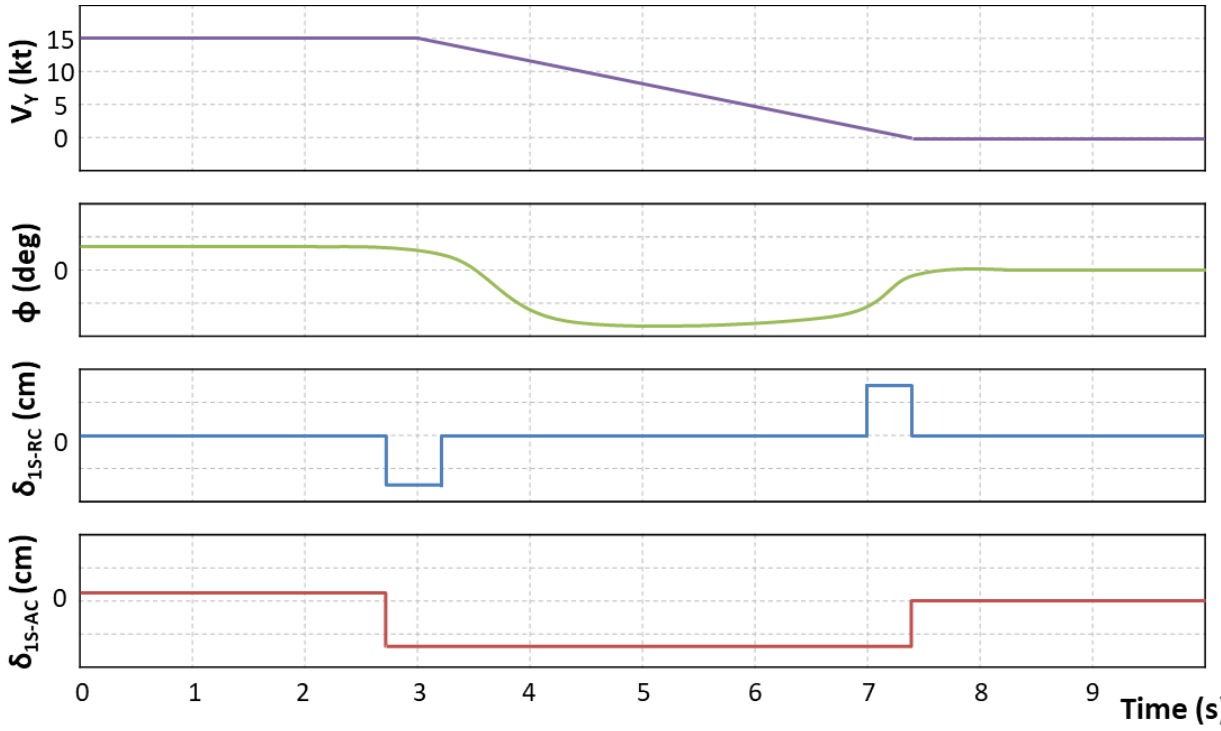

Figure 7-18: Modelled Time Trace of Lateral Deceleration; Direction Left to Right from 15kt Groundspeed to Hover

In order to achieve the constant deceleration in rate command, an input is first required to initiate a roll rate which once the aircraft is at the desired attitude is removed; as the aircraft approaches the hover groundspeed, an input is then made to initiate an opposing roll rate until the hover attitude is approached and the input is then removed.

In attitude command the inceptor input is held constant until the aircraft approaches the hover where the input is then reduced to the trim position whilst the aircraft adopts a hover attitude.

It is apparent that the number of discrete inputs in rate command is double those required in attitude command and their durations are shorter. Both of these control characteristics make it more difficult to initiate an accurate failure in rate command at the moment of a large control input. This therefore causes a larger variation in the severity of the failure in rate command.

7.6.3 Effect on APCR and PAC

The average APCR for rate command was generally 0.5 to 1.0 ratings higher than for attitude command at each of the configurations except for at low apparent gains of 0.4 to 0.8 where the average ratings were equal between the command types (figure 7-15). A further exception to this trend was the anomalous test point in attitude command with a ramp attenuation of 2.5s, as previously identified with the IFES ratings (section 7.5.2), that caused a difference of 2.0 ratings between the rate and attitude command in this configuration.

The trend in PAC severity reflected that identified with the APCR, in that in rate command there were more test points with greater severity than in attitude command for each configuration.

Consequently it can be surmised that an aircraft with a rate command controller exposes a higher tendency and severity of oscillatory APCs and worse IFES ratings after an isometric failure than an equivalent aircraft with an attitude command controller.

7.6.4 Deviation of APCR

Similar to the IFES ratings, the range of the APCR was also larger in the rate command than in the attitude command with an average range of 2.85 ratings in rate and 1.46 ratings in attitude. The causes for this difference are considered to be the same as described in 7.6.2 for the IFES ratings.

7.7 Effects of Significant Isometric Inceptor Training and Experience

As detailed in section 6.9, the pilots H, J and L had no significant (less than 2 hours) previous isometric experience. However, prior to completing his rotary test pilot training, pilot K had flown approximately 900 hours in the F-16A. This aircraft was fitted with a pseudo-isometric sidsetick controller that moved only ¼ inch [81] and therefore the control strategy was considered by pilot K to be very similar to the isometric controller used in this study. Furthermore, much of the pilot's F-16 experience was in formation flight which is of a similar pilot gain for fixed wing as hovering is for helicopters.

Regarding his F-16A experience, he described an effective control strategy that was taught during the type conversion. The right arm and shoulder must be relaxed and the forearm comfortably positioned on the arm rest such that the hand could naturally hold the controller grip with minimum arm muscle tension. The hand should grasp the

controller grip lightly whilst maintaining a full hand contact. The control inputs should be made with a conscious balance of pilot gain reduced as low as possible whilst maintaining the desired flight accuracy. The danger of over-controlling leading to PIOs was frequently emphasised during the type training.

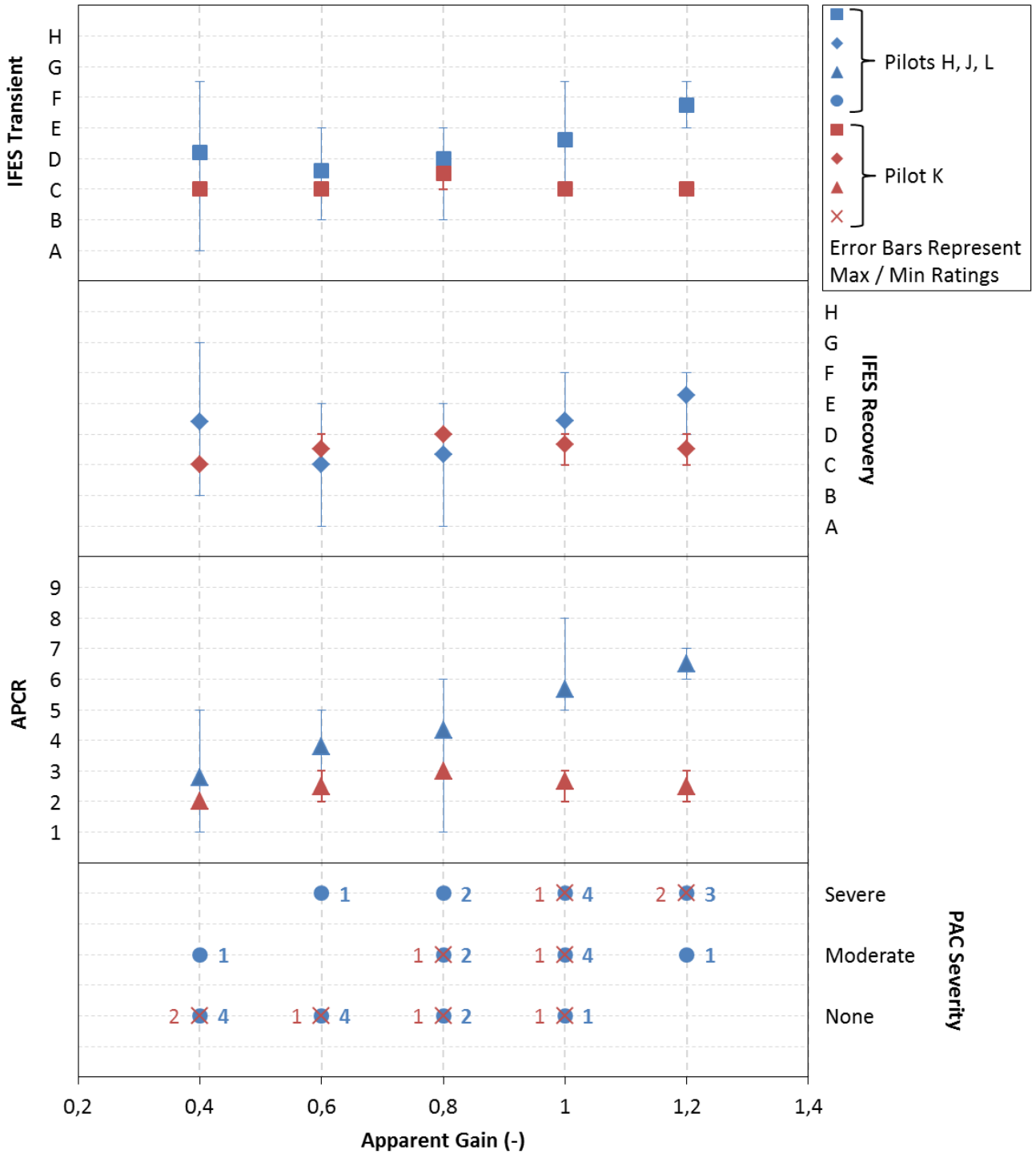

Figure 7-19: Effect of IFES Transient and Recovery Ratings, APCR and PAC Severity on the Variation of Apparent Gain in Rate Command with Pilots H, J, L and K

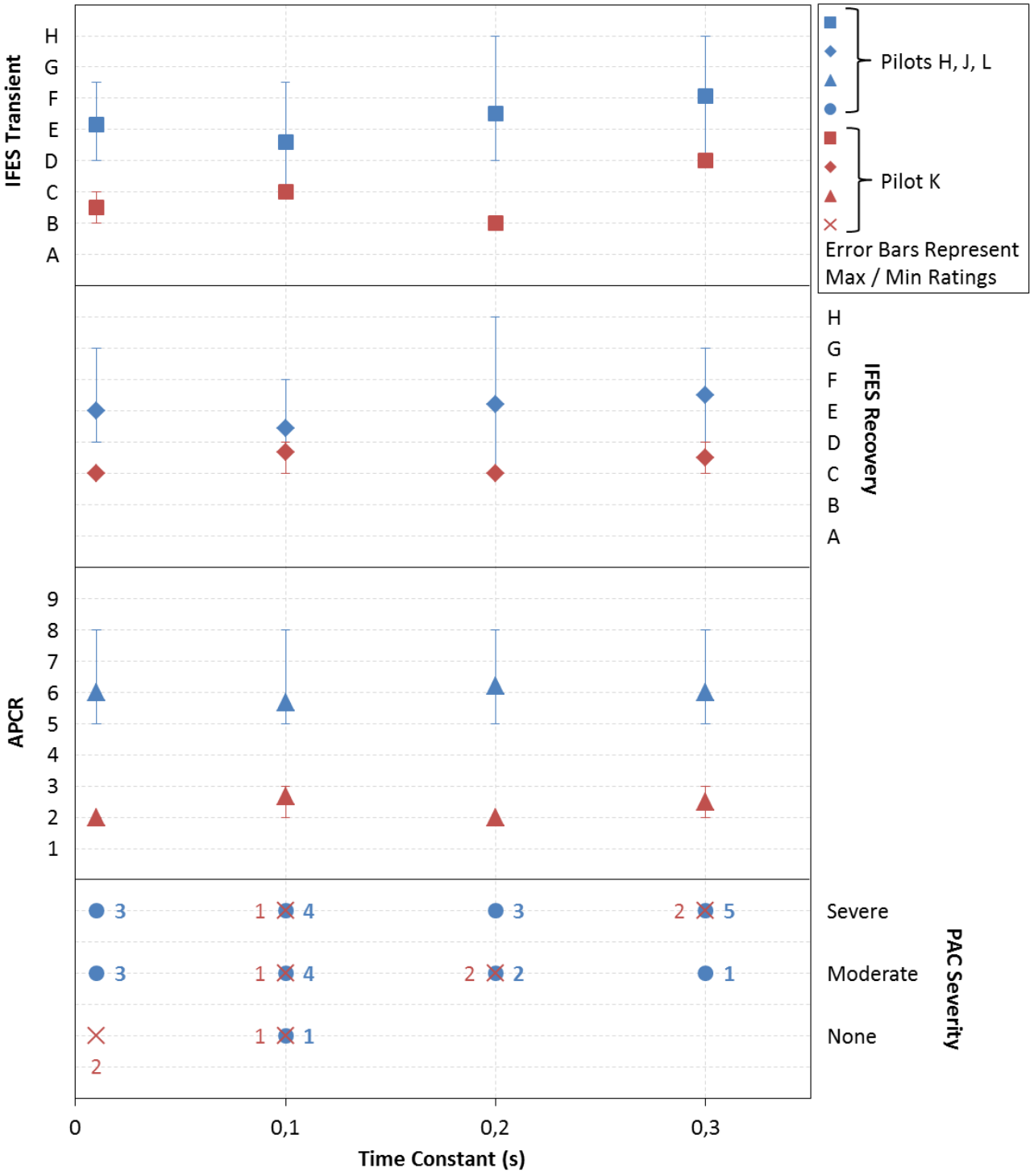

Figure 7-20: Effect of IFES Transient and Recovery Ratings, APCR and PAC Severity on the Variation of Time Constant in Rate Command with Pilots H, J, L and K

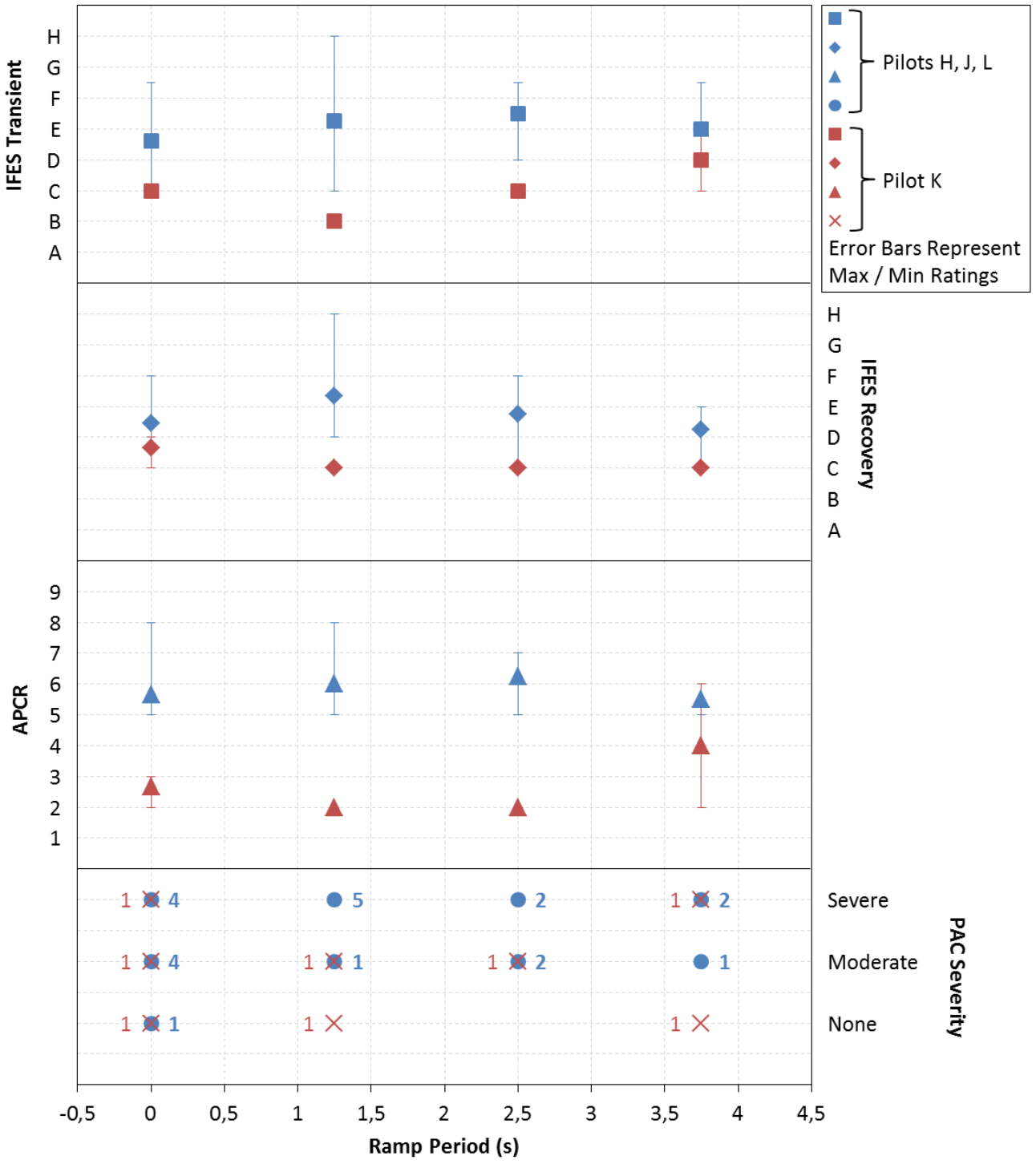

Figure 7-21: Effect of IFES Transient and Recovery Ratings, APCR and PAC Severity on the Variation of Ramp Attenuation Period in Rate Command with Pilots H, J, L and K

The analysis of the effect of isometric specific training and experience has been conducted using the rate command data only. Figures 7-19 to 7-21 present the results in the standard format. The blue data points represent the average ratings for pilots H, J and L, whereas the red data points represent the average ratings for pilot K. For further reference, the attitude command data is presented in appendix F (variation of apparent gain and time constant only as there was insufficient acceptable quality data for the variation of ramp attenuation period to be presented).

7.7.1 Effect on IFES Transient Rating

Figures 7-19 to 7-21 show that the transient rating for pilot K was consistently lower than for the other pilots across all filter and ramp attenuator configurations. The average difference across all configurations was 1.9 ratings lower for pilot K and the greatest difference in ratings was 3.5 for the 0.2s time constant configuration 7. Pilot K also awarded transient ratings only between B and D (numerical equivalent 2 and 4) across all configurations, demonstrating that the change in transient ratings of pilot K across the variation of apparent gain, time constant and attenuation ramp period was much flatter than the other 3 pilots.

Pilot K was more accustomed to the isometric controller and more aware of its tendency to cause the pilot to over- control in high gain tasks (application of a control force greater than required to create an intended aircraft response). He was also conscious that the over-controlling could easily develop into an oscillatory APC and he had the benefit of instruction and practice in using a control strategy to reduce these risks. His subconscious effort to make smaller inputs immediately after the failure meant that he did not worsen the failure by his own interaction and therefore observed a less severe post-failure transient.

Pilot K potentially also had a significant psychological advantage over the other pilots that he was confident that he had accurately controlled aircraft with an isometric controller in the past and so in this study reacted more calmly and steadily immediately after the failure.

7.7.2 Effect on IFES Recovery Rating

Similar to the transient ratings, pilot K generally awarded lower recovery ratings than the other three pilots; however it was not consistent across all configurations. Whilst the average difference across all configuration was 1.22 ratings lower for pilot K, there were two configurations (apparent gain 0.6 – configuration 4; and apparent gain 0.8 – configuration 3) for which pilot K awarded slightly worse ratings (0.5 and 0.66 ratings respectively). The difference in recovery ratings awarded by pilot K across the variation of configurations was even flatter than for the transient ratings and varied only between C and D.

In the recovery phase pilot K found it was easier than the other pilots to stabilise the aircraft without entering an oscillatory APC due to his previous experience. Specifically, during his type training he had developed a more effective self-moderation of pilot gain

such that it could be more accurately optimised for maximum accuracy just below the onset of an oscillatory APC.

An analogy can be drawn from motor racing where a novice driver might lose traction in a turn and try to control the skid which has already initiated (analogous to suppression of an APC); whereas the expert driver will be more aware of the conditions in which traction would be lost and stay just below them whilst maintaining the maximum speed through the turn (analogous to self-moderation). Pilots without isometric experience certainly have the ability to moderate their pilot gain, but they generally regulate it at a much more coarse level or with a greater margin. The development of this superior self-moderation is not specific to pilot K (although it is reasonable to expect that some humans are better than others) and according to pilot K was common amongst the F-16A cohort.

Consequently, when the sidestick failed to the isometric mode, he subconsciously reverted to the control strategy that had worked successfully in the F-16A and immediately reduced the size of force inputs and applied an appropriate pilot gain.

The smaller (and in some cases negative) difference between pilot K and the other pilots for the recovery rating compared to the transient rating was considered to be due to the relative strength of advantage for the two phases. Pilot K benefitted significantly from his experience and training during the transient phase through a reduction of over-controlling, which pilot K considered to be a habitual or trained instinct. However, whilst he still generally benefitted in the recovery phase, it was weaker because the time periods afforded a more conscious than instinctive effort which the other pilots could also apply (albeit generally with less refinement).

7.7.3 Effect on APCR and PAC

The APCR awarded by pilot K was consistently lower across all configurations than for the other pilots, with an average difference of 3.14. This indicated that he subjectively found a lesser tendency to enter an oscillatory APC than pilots H, J and L, which concurred with the results for the IFES ratings. Generally, the PAC also showed that he experienced less severe (and in very limited cases equivalent severity) APCs than the other pilots but with a weaker coherence.

Furthermore, his interpretation of the APC agreed inconsistently with the PAC detection for his corresponding test points. Of the 27 test points, 26 points were at or below an APCR of 3 which in accordance with table 6-7 would predict no PAC detection. This expectation did not concur with the PAC results which showed only 11 out of the 27 test points detected no APCs. The results may have been influenced by his confidence with the isometric controller in which he believed that there was no APC but in fact he was successfully suppressing it with a low effort or compensation level.

Despite the anomaly between the APCR and PAC results, both metrics showed that pilots who have undergone specific isometric training or have significant isometric experience are less prone to developing or maintaining oscillatory APCs in the isometric mode than

those pilots who have only conventional pilot training and experience with compliant inceptors.

7.8 Summary

This chapter covered the results and analysis for the investigation of the HQ and APC severity after an isometric failure with variations of the first order filter parameters. The following analyses and conclusions were reached that reflected the objectives of the investigation:

- The pilots perceived that the most significant factor that influenced the severity of the APC was the control force or displacement magnitude applied at the moment of failure. The required post-failure pilot gain; the precise timing of the failure; and the attitude or rate at the moment of failure were also considered to be highly significant.
- The best transient and recovery IFES ratings occurred with an apparent gain of 0.6 to 0.8. The deterioration of ratings at low apparent gain was due to a combination of excessively high control forces; sudden change in control power at failure; and the potential for large out of trim control forces. The deterioration at high apparent gain was due to large aircraft response during APC suppression at higher frequencies and a larger response to the instinctive over-controlling immediately after failure.
- Both APCR and PAC severity increased with increasing apparent gain due to the larger aircraft response during suppression and immediately after failure.
- The best transient and recovery IFES ratings occurred with a time constant of 0.1s with only mildly worse ratings with increasing time constant due to the increased phase lag and with decreasing time constant due to lower signal damping.
- Both APCR and PAC severity marginally increased with increasing time constant, however the large range of the awarded data offered only weak support for the correlation.
- The use of a ramp attenuator to linearly increase the apparent gain from zero to the datum value over a range of time periods presented limited success. The IFES, APCR and PAC severity results for all of the time period configurations presented little or no improvement over the configurations with no ramp attenuation.
- Across all first order filter configurations, the IFES and APC ratings as well as the PAC severity were worse in the rate command as in the attitude command due to the corresponding difference in pre-failure HQ and the greater post-failure bandwidth in attitude command.
- For the pilot with prior isometric inceptor training and experience, the IFES and APC ratings showed that he required less effort and compensation to control

the aircraft and avoid oscillatory APCs after the isometric failure than the other three pilots. Whilst the PAC severity did not fully concur with the APCR results, it did confirm that there was generally lower severity of APCs for the pilot with prior isometric experience than for the other pilots.

- The prediction of PIO proneness by using the phase delay-bandwidth criteria of ADS-33E showed a general correlation with the test results for different time constants and higher apparent gains but was inconclusive with lower apparent gains.

Chapter 8: Conclusions and Future Research Opportunities

8.1 Research Contributions

The findings of this study were all associated with one of the five research contributions identified in the introduction.

8.1.1 Identify the factors that influence the HQ of rotorcraft during and immediately after isometric AIS failures.

As the first phase in the conception of the MTE an initial investigation was conducted on the factors that created the most influential conditions during isometric failures. Subsequent conclusions based on subjective and objective results were formed by the further development of the MTE and the results of the first order filter and ramp attenuator configuration study. Using a combination of the test pilot's subjective ratings and rankings of the influential factors from figure 7-1; the MTE development information discussed in chapter 5 and the analysis of data in chapter 7, the factors were arranged into the following categories of significance:

High significance

- Inceptor force at the moment of failure. A large difference between the force at the failure and that required for the subsequent trim in the stabilised flight condition resulted in worse HQ;
- Required gain of the post-failure task. The higher the gain of the post-failure task, the greater the tendency for APCs and the higher the HQ ratings;
- Command type. The rate command controller caused worse HQ than the attitude command controller;
- Pilot's previous training and experience in the isometric mode;
- Element of surprise.

Medium significance

- Axis of aircraft motion and inceptor displacement at the moment of failure. More severe oscillatory APC were observed in the pitch axis than the roll axis;
- Visual environment. Specifically with the rate command controller, the DVE was more prone to oscillatory APCs than the GVE;
- Attitudes and rates at moment of failure.

Low significance

- Pre-failure pilot gain;
- Control direction at moment of failure.

The precise timing of the failure during the hover selection sub-task was a prominent cause for the large range in some data but as discussed in section 7.3.2, it was a combined function of the attitude / rate and the inceptor force at the moment of failure. Therefore, despite its importance in the development of the assessment method, its independent significance as an influence of the HQ during isometric failures is minimal.

8.1.2 Develop and validate methods for assessing the HQ and tendency of APCs during isometric failures of AIS.

A MTE was developed in conjunction with the IFES and APCR rating scales to assess the HQ and APC tendencies during isometric failures. The MTE comprised 4 sub-tasks and was conducted on a flat area with ground markings of a large square and an array of positioning cones at each corner. The first 2 sub-tasks involved the non-assessed set-up: from the hover at one corner, a translational groundspeed of 15kt was selected in the direction of another corner whilst retaining the original aircraft heading; the groundspeed, height and aircraft heading was then maintained until approaching the target corner. The third sub-task consisted of an aggressive deceleration to a hover at the corner and then finally the fourth sub-task was to maintain the hover within tight tolerances of position, height and heading until re-directed to the next corner by the FTE. The task parameters and performance tolerances were precisely defined for accurate repeatability and compatibility with the subjective rating scales. The pattern was continued until a failure was initiated during the deceleration sub-task at maximum aircraft attitude and inceptor displacement.

The MTE fulfilled the following general requirements:

- **Safety:** Whilst the course was designed within the higher risk low speed environment inside the ground effect, it was located in a clear area and free of all obstructions or structures. The defined height of 15ft would preclude the possibility of entering vortex ring and provide sufficient space to recover from transient attitudes generated by the failure.
- **Repeatability:** The course description was precisely defined and easy to remember (15kt groundspeed, 15ft height and tolerances identical to the hover MTE that all test pilots are familiar with). The ground markings provided adequate visual cues for accurate flying and the accompanying instructions were clear and unambiguous.
- **Universality:** Most of the course definition and tolerances would be suitable for all types and sizes of helicopter. However the time to stabilise the hover may require reassessment for larger helicopters.
- **Utility:** The MTE encompassed the most critical conditions of groundspeed, height, aggression, stabilisation time and position tolerances that had been identified in chapter 4. Furthermore the course definition and performance tolerances were applicable in both GVE and DVE and with either rate or attitude command controllers. The sub-tasks were sufficiently demanding to reduce the pilot's capacity to predict when the failure would occur providing a limited element of surprise.
- **Ubiquity:** The isometric MTE requires only ground markings and traffic cones and no bespoke ground structure or aircraft instrumentation was required.

The MTE was confirmed by the test pilots during the first order filter investigation in chapter 7 as a suitable method to expose an aircraft and AIS to conditions that could indicate a broad spectrum of HQ degradation and APC tendency. However, it was noted that the spread of subjective IFES ratings and APC severity for each test condition could be reduced by improving the failure timing initiation. An automatic trigger system is recommended for future studies that could initiate the failure at maximum attitude and inceptor displacement during the deceleration sub-task.

8.1.3 Identify, adapt and validate appropriate rating scales and analysis tools for the investigation of HQ during isometric failures.

The IFES rating scale [47] had been previously identified and validated for the transient and recovery investigation of the isotonic failure mode by Barnett and Müllhäuser [35]. Similarly, the subjective APCR and objective PAC had already been used by Jones and Barnett [15] for APC detection in the long term isometric mode. In both cases the rating scales and analysis tool functioned well and were consequently selected for use in this study. During the preliminary MTE development an adaptation recommended by test pilot feedback of the IFES scale was implemented.

The upper-range of ratings (B-C) were adapted to give the test pilots a more defined effort description that supported stronger linearity of pilot compensation through the scale and corresponded better to the level of urgency required. Additionally, as the relative significance of urgency and effort was not always equal in the isometric failures, the mid-range of ratings (B-E) was adapted to specify that the awarded rating would be the highest level of either urgency or effort.

The APCR was validated against the legacy PIOR, both in the simulator and in flight. It received general confirmation amongst test pilots as an improvement over previous APC and PIO rating scales.

The combined assessment methods of IFES, APCR and PAC were validated during the subsequent investigation of first order filter and ramp attenuator parameter variation. Throughout this investigation the test pilots confirmed that the subjective rating scales, including the modifications to the IFES scale, were applicable to the isometric failure and that they contained appropriate decision processes and descriptions for the HQ and APCs that were encountered. Furthermore, the objective PAC which had previously been limited to rate command controllers was successfully validated in the simulator for attitude command controllers against the subjective APCR scale.

8.1.4 Identify an effective mitigation principle to improve the isometric post-failure HQ.

A broad range of potentially viable mitigation solutions that could improve the HQ after an isometric failure were identified in chapter 1:

- Redundancy of subsystem components
- Redundancy of entire AIS for multi-pilot operations
- Automatic change of stability augmentation

- Automatic outer loop flight control system
- Shear pin for the isometric failure mode
- Inherent spring gradient for isotonic failure mode
- Flight envelope limitations
- Pilot training and experience
- Automatic change of Signal Filter

Of these, the automatic change of a signal filter was selected as it represented an attractive proposal in terms of cost, weight and complexity. A further advantage was that it could be applied equally to AIS installations which have been fully integrated into a helicopter design as well as AIS modifications to previously certified helicopters.

By using the developed assessment method it was possible to optimise the first order signal parameters for best post-failure HQ. For the aircraft and AIS combination used in this study, the results are summarised in table 8-1 in which the IFES and APCR have been averaged for the specified configuration across the applicable test pilots[60]. These results confirm that a significant improvement was achieved from the datum configuration to the optimised configuration 4 and further improvements were achieved with the attitude command controller and prior isometric training of the pilot. It could be expected that similar improvements would be observed with other aircraft and AIS combinations.

	IFES Transient	IFES Recovery	APCR
	Numerical Equivalent		
Rate Command Datum Configuration[61]	4.6 (D/E)	4.4 (D/E)	5.7
Rate Command Configuration 4[62]	3.6 (C/D)	3.0 (C)	3.8
Attitude Command Configuration 4[62]	3.0 (C)	2.6 (B/C)	3.8
Attitude Command Configuration 4[62] Isometric Trained Pilot[63]	3.0 (C)	2.5 (B/C)	2.5

Table 8-1: Summary of HQ Improvements

[60] In accordance with the rating scales originators' instructions

[61] Apparent gain 1.0; Time constant 0.1s; Ramp attenuator 0s

[62] Apparent gain 0.6; Time constant 0.1s; Ramp attenuator 0s

[63] Pilot K had completed USAF training on the isometric inceptor controlled F-16A and possessed over 900 hours of flight time on the type.

8.1.5 Identify and discuss the causes of variations in HQ and APC tendency with modification of the first order filter and ramp attenuator parameters.

Within the investigation discussed in chapters 6 and 7 the apparent gain and the time constant of a first order filter as well as the time period of a ramp attenuator were varied. The trends and causes of the HQ and APC tendency with each parameter for the aircraft and AIS used in this study are summarised below. Whilst the values of the configurations and results may differ with alternative aircraft and AIS, the trends are expected to be generally consistent.

With reducing apparent gain the APCR showed a consistent improvement due to two factors. Firstly, as the pilots naturally increased their control amplitude at higher frequencies an aircraft response that was reduced by the lower gain caused lower tendency to sustain oscillatory APCs. Secondly, the lower apparent gain caused a reduction in the pilot's over-controlling immediately after the failure that often caused large transient responses and initiated APCs. In support of the second argument, it was demonstrated that pilots made force inputs in the isometric condition an average of 47% greater than the force they intended to make and had immediately prior made in the compliant mode.

Both the transient and recovery IFES ratings presented a u-shaped curve with reducing apparent gain which was a result of the previously identified reduction of APC tendency, counteracted by three detrimental factors. These were the reduced control response during the recovery period; the sudden change in control response at the moment of failure that amplified the pilot's unpredictability during the transient period and the presence of undesirable large off-trim forces during the recovery period. The last of these factors was demonstrated by a separate investigation which showed that pilots who were seeking to maintain a constant off-trim force actually varied it by an average of 53% over the course of a minute which led to inadvertent control inconsistencies and hence worse HQ.

For the time constant, there was a weak correlation of a shallow u-shaped trend in both IFES or APCR but the large deviations of the data points reduced its confidence. Both HQ and PAC tendency were the balance between damping of the inceptor force signal noise and the avoidance of excessive phase lag which could lead to APCs.

The ramp attenuator model that was used in this study had a linear increase of gain from 0 to unity over a variable time period. The results showed little change in the HQ and APC ratings as the time period was iteratively increased from 1.25 to 3.75s (representing 0.5 to 1.5 time cycles of a typical APC oscillation). The flat trend was considered a balance of two main factors. Firstly, the rapidly changing control response for short ramp periods that brought detrimental unpredictability for the pilot. Secondly, the sustained very low control power observed initially for long ramp periods, that was beneficial through the transient phase in which it reduced the onset of oscillatory APCs; but was detrimental in the recovery phase in requiring large control forces to effect a stabilised flight condition.

An alternative ramp attenuator was recommended entailing a ramp which started after a short constant period of 0.6 apparent gain and increasing to unity over a further time

period. However, due to limited availability of test pilots after conclusion of the main data analysis, this solution had not been tested.

8.2 Scientific Question

Using the research conducted and the results analysed within this dissertation, it is now possible to answer the scientific question that was posed at the start of the study.

How can the degradation of handling qualities caused by an isometric failure of an active inceptor system in helicopters be quantified and mitigated?

Using the MTE developed in this study in combination with the subjective IFES and APCR rating scales and the PAC analysis tool it was possible to quantify the HQ and APC tendency during an isometric AIS failure. In its broadest function, the application of this integrated assessment method could be used as a certification specification to establish the success of a failure mitigation solution. However the structure of the MTE was also able to expose a wide range of HQ and APC severities and the fidelity of the ratings was able to distinguish between the corresponding small variations. These characteristics facilitated the use of the assessment methods in the optimisation of flight control parameters to improve the post-failure HQ.

A number of viable mitigation solutions were identified of which four were investigated further: a first order filter applied to the inceptor force signal; a ramp attenuator of apparent gain also applied to the inceptor force signal; two alternative command types and substantial previous isometric training and experience. An optimised configuration of the first order filter was identified that offered significant HQ benefits, however the tested configurations of ramp attenuator showed neither benefit nor detriment. The employment of both the attitude command and the previous isometric training and experience presented substantial mitigation to the post-failure flight accuracy and suppression of APC tendencies. Whilst these solutions have shown some success, the search for the optimum answer has neither been exhaustive nor would it be applicable to all helicopter and AIS permutations. However, the assessment method and optimisation process have both been proven to be functional and could be directly used in future more specific applications.

8.3 Future Research Opportunities

The following list details the recommendations and opportunities for further development of this research.

8.3.1 In-Flight Validation of Assessment Method

The main recommendation of this study is to validate the assessment method and analysis of the isometric failure in flight trials. One restriction of the research conducted thus far is that it has used only a ground based simulator with the inherent fidelity limitations of its aircraft and simulator models. An airborne campaign in an aircraft comparable to the simulator testing (i.e. the DLR EC135 ACT/FHS) would confirm the assessment methods, course dimensions and performance standards of the isometric MTE as suitable. Additionally, the PAC tool could be validated in flight for attitude

command type helicopters. In order for the failure assessment method to achieve acceptance in the airworthiness and flight test community its confirmation in flight with a focus on safety and practical considerations would be essential.

8.3.2 Validation Expansion of Assessment Method to Helicopters with Alternative Flight Characteristics

Whilst the isometric MTE and specifically its course description and flight parameter tolerances were designed to be applicable to all types and sizes of rotorcraft, in this study it was only tested on one aircraft model with two different control command types. A further investigation using an alternative aircraft (for example the CH-53K) could confirm the MTEs broader applicability. However gaining access to a suitably equipped aircraft and an operator with an appetite to conduct such a high risk test campaign may present significant hurdles. An interim study may therefore initially be proposed using the applicable type simulator model to mitigate the risks prior to a full flight campaign.

8.3.3 Expansion of Isometric Failure Investigation into Long Term HQ

As research had already been conducted for helicopters operating in a continuous, long term isometric mode [14, 96], the scope of this study was intentionally limited to the transient effects and recovery from the isometric failure. There would therefore now be an opportunity to research the three post-failure phases together (short – transient; medium – recovery; long – continuation of flight / landing). Such a study could investigate a proposed hypothesis that whilst the lower apparent gain was beneficial for the short and medium term it would be detrimental for the HQ in the longer term. It could also be expanded to research the potential for a 2-phase filter that automatically changes its configuration after a period of pilot adaptation during the short and medium terms.

8.3.4 Investigation of Alternative Ramp Attenuator Solutions

In section 7.5.6 it was identified that the tested ramp attenuator configuration that rose from zero to unity over a defined time period could be improved to achieve a better HQ. The suggestion was to commence the ramp at the previously identified optimum apparent gain for the short and medium term and for it to rise to unity as the optimum apparent gain for the long term. Further research of this solution could be conducted with a range of time periods and with an optional initial transient period of constant gain.

8.3.5 Implementation of Semi-Automatic Failure Initiation System

In chapter 7 the large deviation of some data sets was considered to be a result of the inaccuracies of the failure timing. Within this study a system was designed and implemented to initiate the failure once the inceptor force exceeded a specified value, however it functioned inconsistently and as it proved less reliable than the manual initiation, it was not used. A semi-automatic system could potentially be developed that could be ‘armed’ by the FTE when approaching the deceleration sub-task and then use a combined logic of both the inceptor force and aircraft attitude signals to trigger the failure. A successful solution would prove beneficial in achieving a more clinical test and therefore greater confidence in the results.

8.3.6 Development of PAC Tool with Variable H_S and H_{SF} Parameters

In section 6.5.2, using the PAC theory from [66] a constant value of the ratio of aircraft response to control input[64], H_S was calculated from the steady state response to a step input. However in the short term until it reaches its steady state value, H_S is a function of time (or frequency for an oscillatory control input). As much of the control input of an oscillatory APC occurs with an aggression and frequency such that the steady state response is not reached, there is an argument to adopt a variable value of H_S that is a function of frequency. Further development of this proposal may improve the accuracy and reliability with which the PAC identifies oscillatory APCs.

8.3.7 Investigation of Replacing First Order Filter with a Constant Gain Function

Chapter 7 identifies that the variation in time constant between 0.01 and 0.3s had little effect on the HQ and tendency to oscillatory APCs. Given the result that very low time constants seem not to deteriorate the HQ or APCR, then a simple gain could be tried in lieu of the complexity of a first order filter.

8.3.8 Investigation of Using the Isometric MTE for Isotonic Failure Assessments

Section 5.5 discussed why the already developed isotonic MTE was not suitable for the isometric failure mode. However, the reverse of attempting to use the isometric MTE for isotonic failures has not been pursued as an assessment method. With reference to table 5-4 all of the high and medium worst case conditions for the isotonic mode could be exposed by the isometric MTE, (with the exception that the isotonic failures were observed to be marginally worse in forward flight than the hover). The benefits of using the same MTE for both isometric and isotonic would be the savings in test pilot and test campaign preparation and a simpler single solution for certification specifications. The element of surprise for the test pilots would also be enhanced due to the uncertainty of not only the failure timing and direction but also the failure type.

[64] Aircraft response of attitude or attitude rate, dependent on command type; control input of displacement or force, dependent on AIS mode

References

1 Abildgaard, M., and von Grünhagen, W., “Demonstration of an Active Sidestick in the DLR Flying Helicopter Simulator (FHS),” 34th European Rotorcraft Forum, Liverpool, UK, 2008.

2 Müllhäuser, M., “Tactile cueing with active cyclic stick for helicopter obstacle avoidance: development and pilot acceptance,” CEAS Aeronautical Journal (2018) 9:27-37 31 October 2017

3 Rakotomamonjy, T., Binet, L., Müllhäuser, M., “ONERA-DLR Joint Research on Tactile Cueing for Reactive Obstacle Avoidance Dedicated to Low Speed Helicopter Manoeuvres,” ONERA, DLR, June 2016

4 Müllhäuser, M., Leißling, D., “Development and Inflight-Evaluation of a Haptic Torque Protection Corresponding with the First Limit Indicator Gauge”, American Helicopter Society 69th Annual Forum Proceedings, Phoenix, AZ, May 2013

5 Grünhagen, W., Müllhäuser, M., Höfinger, M., Lusardi, J., “In-flight evaluation of active sidestick parameters with respect to handling qualities for rate command and attitude command response types,” American Helicopter Society, Jan 2014

6 Sung K., Bothwell, M., Fortenbaugh, R., “The Bell 525 Relentless, The World’s First “Next Generation” Fly-by-Wire Commercial Helicopter”, American Helicopter Society 70th Annual Forum Proceedings, Montréal, CA, May 2014

7 Greenfield, A., Kubik, S., Faynberg, A., Litwin, J., Marzella, S., Sahasrabudhe, V., Rucci, J., Corry, C., McCulley, S., Pavelka, E., Rhinehart, M., Roark, S., Fletcher, J., Ott, C., “CH-53K Control Law Risk Reduction Flight Testing on the Rascal UH-60A In-Flight Simulator”, American Helicopter Society 68th Annual Forum Proceedings, Fort Worth, TX, May 2012

8 Irwin, J., Schwerke, M., Kocher, E., Brown, B., Rich, A., “AVMS H-47 Chinook with APAS Tactile Cueing Demonstration Results,” American Helicopter Society 72nd Annual Forum, 17-19 May 2016

9 Taylor, A., Greenfield A., Sahasrabudhe, V., “The Development of Active Inceptor Systems and the Scope and Design Issues of Tactile Cueing Systems”, American Helicopter Society 64th Annual Forum Proceedings, Montréal, CA, April 2008

10 Whalley, M. S., Hindson, W. S., and Thiers, G. G., “A Comparison of Active Sidestick and Conventional Inceptors for Helicopter Flight Envelope Tactile Cueing,” American Helicopter Society 56th Annual Forum, Virginia, US, 2000

11 Stevenson, B., "US Military to test BAe’s Fly-By-Wire Alternative on Chinook," Flight International, 26 June 2014,

https://www.flightglobal.com/us-military-to-test-baes-fly-by-wire-alternative-on-chinook/113610.article

12 Modesto, M., “Future Battlefield Rotorcraft Capability, Anno 2035 and Beyond,” Joint Air Power Competence Centre, Para 6.3.2

13 Luft, J., Ingham, H. (1955), "The Johari window, a graphic model of interpersonal awareness," Proceedings of the Western Training Laboratory in Group Development, Los Angeles: University of California

14 Müllhäuser, M., Schranz, G., “Acceptability Assessment Preparation for Isometric Backup-Mode of Active Inceptors”, 38th European Rotorcraft Forum Proceedings, Amsterdam, the Netherlands, September 2012

15 Jones, M., Barnett, M. P. C., “Analysis Of Rotorcraft Pilot Couplings During Active Inceptor Failures,” American Helicopter Society 74th Annual Forum and Technology Display, Phoenix, AZ, May 14-17 2018

16 Anon., “Flight Manual Appendix 11-9, EC135 T2+ ACT/FHS S/N 028,” Airbus Helicopters GmbH, July 2009

17 Wickramasinghe, V. K., “Dynamics Control Approaches to Improve Vibratory Environment of the Helicopter Aircrew,” Ph.D. Dissertation. Faculty of Graduate Studies and Research. Ottawa-Carleton Institute for Mechanical and Aerospace Engineering. Carleton University, Ottawa, Canada, 2012

18 Fletcher, J. W., Lusardi, J. A., Mansur, M. H., Moralez III, E., Robinson, D. E., Arterburn, D. R., Cherepinsky, I., Driscoll, J., Morse, C. S., and Kalinowski, K. F., “UH-60M Upgrade Fly-By-Wire Flight Control Risk Reduction using the RASCAL JUH-60A In-Flight Simulator,” American Helicopter Society 64th Annual Forum, Montréal, Canada, 2008

19 Dos Santos Sampaio, R., “Influence of Variable Inceptor Coupling on Dual Pilot Helicopters using Active Sidesticks,” PhD Thesis, Technical University Braunschweig, 2018

20 Kanbayashi, H., Tobari, S., Moriyama, M., and Nakamura, S., “Helicopter Side Stick Controller,” American Helicopter Society 55th Annual Forum, Montréal, Canada, 1999

21 Kubo, Y., Kuraya, N., Ikarashi, R., Amano, T., Ikeuchi, K., and Tobari, S., “The Development of FBW Flight Control System and Flight Management System for ATIC BK117 Experimental Helicopter,” American Helicopter Society 57th Annual Forum, Washington DC, US, 2001

22 Rumsfeld, D. H., Myers, R., “US DoD News Briefing Transcript”, 12 Feb 2002, https://archive.defense.gov/Transcripts/Transcript.aspx?TranscriptID=2636

23 Anon., “National Transport Safety Board Aviation Accident Data Summary, Bell 525, N525TA,” DCA16FA199, 6 Jul 2016

24 Masson, M., Morier, Y., “Methodology to Assess Future Risks, European Aviation Safety Plan (EASp),” Action EME 1.1 of the European Aviation Safety Plan (EASp), Presented to ECAST 4-12, 11 Dec 2012

25 Maragakis, I., Clark, S., Piers, M., Prior, D., Tripaldi, C., Masson, M., Audard, C., “Guidance of Hazards Identification,” Safety Management System and Safety Culture Working Group, March 2009

26 Anon., “Certification Specifications and Acceptable Means of Compliance for Small Rotorcraft, CS-27,” EASA, Amendment 6, 17 December 2018

27 Anon., “Certification Specifications and Acceptable Means of Compliance for Large Rotorcraft, CS-29,” EASA, Amendment 7, 15 July 2019

28 Anon., “ASN Aviation Safety Database – Bell-Boeing V-22,” Aviation Safety Network, https://aviation-safety.net/wikibase/dblist.php?AcType=V22

29 Anon., “Aviation Investigation Report – Main Gearbox Malfunction/Collision with water,” Transportation Safety Board of Canada, A09A0016, 12 March 2009

30 Anon., “Preliminary Report – Accident Sikorsky S-92A, EI-ICR,” Air Accident Investigation Unit Ireland, 2017-06, 13 April 2017

31 Traverse, P., Lacaze, I., Souyris, J., “Airbus fly-by-wire: A Process towards Total Dependability,” 25th International Congress of the Aeronautical Sciences, Hamburg, 3-8 September 2006

32 Faillot, J-L., “Electrical Flight Control Technologies for Rotorcraft,” 30th European Rotorcraft Forum, 2004

33 Von Grünhagen, W., Müllhäuser, M., Abildgaard, M., Lantzsch, R., “Active Inceptors in FHS for Pilot Assistance Systems,” 36th European Rotorcraft Forum, Paris, France, 7-9 September 2010

34 Anon., “Rotary Wing Flight Test Manual, Assessment of Helicopter Flight Controls,” ETPS, QinetiQ/SES/ETPS/RWFTM/3.0/9.0, 2014

35 Müllhäuser, M., Barnett, M., “Development Of A Generic Test For Transient Recovery Handling From Helicopter Active Inceptor System Failures To A Near-Zero Control Force Condition,” American Helicopter Society 71st Annual Forum, Virginia Beach, VA, May 5-7 2015

36 Anon., “Aeronautical Design Standard Performance Specification Handling Qualities Requirements For Military Rotorcraft,” ADS-33E-PRF, United States Army Aviation and Missile Command, Redstone Arsenal, AL, 2000

37 Zammali, A., deBonnerval, A., Crouzet, Y., Iyyo, P., Massimi, J-M., "Communication Integrity for Future Helicopters Flight Control Systems," 34th Digital Avionics Systems Conference (DASC), Prague, Czech Republic, Sep 2015, HAL ID: 01275304

38 Cherepinsky, I., Magonigal, S., Driscoll, J., Silder, S., "Development of a Fly-by-Wire Flight Control System to Achieve Level 1 Handling Qualities on a Black Hawk Helicopter," American Helicopter Society 68th Annual Forum, Fort Worth, TX, 1-3 May 2012

39 Anon., "SAE International, Aerospace Active Inceptor Systems for Aircraft Flight and Engine Controls," ARP5764, 2013

40 Anon., "Certification Specification – Operational Suitability Data (Flight Crew Data)," EASA, ED Decision 2014/008/R, Initial Issue, Feb 2018

41 Anon., "Rules for Air Operations," EASA, Regulation (EU) No 965/2012, Oct 2019

42 Anon., "Merlin HM Mk2, Aircrew Manual, Part 1, Chapter 7 / Hydraulics Systems" AP 101C-1702-15A, First Edition, March 2015

43 Anon., "EC135 T2+ Approved Rotorcraft Flight Manual," Latest Edition, Eurocopter Deutschland GmbH, Original Issue Feb 2006

44 Anon., "Eurofighter Typhoon Technical Guide," Eurofighter Jagdflugzeug GmbH, Issue 01-2013

45 Anon., "Sea King HAR Mk3, Aircrew Manual," AP 101C-0403-15, Second Edition, August 2001 (AL1 August 2004)

46 Anon., "Defence Standards, DEF STAN 00-970 Part 7, Leaflet 604," Ministry of Defence, Issue 2, 31 January 2007

47 Hindson, W. S., Eshow, M. M., Schroeder, J. A., "A Pilot Rating Scale For Evaluating Failure Transients In Electronic Flight Control Systems," AIAA-90-2827, AIAA Atmospheric Flight Mechanics Conference, Portland, OR, August 1990

48 Jones, M., Jump, M., "New Methods To Subjectively and Objectively Evaluate Adverse Pilot Couplings," Journal of the American Helicopter Society, Vol 60, (1), pp1-13, January 2015, DOI:10.4050/JAHS.60.011003

49 Jones, M., "Prediction, Detection and Observation of Rotorcraft Pilot Couplings," PhD Thesis, University of Liverpool, Liverpool, 2014

50 DiFranco, D. A., "Flight Investigation of Longitudinal Short Period Frequency Requirements and PIO Tendencies," AFFDL-TR-66-163, pp18, 1967

51 Cooper, G. E., Harper, R. P., "The Use Of Pilot Rating In The Evaluation Of Aircraft Handling Qualities," NASA TN D-5153, April 1969

52 Carboni, W., Donley, S., and Engel, D., "CH-53K Fly By Wire Flight Control System with Improved Handling Qualities," Aerospace Control

& Guidance Systems Committee, Charlottesville, US, 2009

53 Fenton, T., Barnett, M., “Email: Request for Information: CH-53K FBW and AIS Capabilities,” 15 Mar 2020

54 Huber, H., Hamel, P., “Helicopter Flight Control State of the Art and Future Directions,” 19th European Rotorcraft Forum, Cernobbio, Italy, 14-16 Sept 1993

55 Stiles, R., Mayo, J., Freisner, A., Landis, K., Kothmann, B., “Impossible to Resist – The development of Rotorcraft Fly-by-Eire Technology,” American Helicopter Society 60th Annual Forum, Baltimore, MD, 8-10 June 2004

56 Bellera, J., Lafisse, J., Mezan, S., “NH90 Control Laws Simulation and Flight Validation on the Dauphin 6001FBW Demonstrator,” European Rotorcraft Forum, 1997

57 Comeau, P., Barnett, M., “Email: Clarification Regarding NRC Helicopter Capabilities,” 20 Mar 2020

58 Morgan, J., “Some Piloting Experiences with Multi-Function Isometric Side-Arm Controller in a Helicopter,” Flight Research Laboratory, National Research Council Canada, 1982

59 Stiles, L., Knaust, G., Wittmer, K., “The S-92 goes Fly by Wire…,” American Helicopter Society 64th Annual Forum, Montreal, Canada, 2008

60 Venanzi, P., Frollo, G., “Exploiting a Flight Test Manoeuver for the NH-90 Helicopter. Definition of a Test Course within the Requirements of the ADS-33,” Associazione Italiana di Aeronautica ed Astronautica, Rome, 14-16 September 1999

61 Burgmair, R., Alford, A., Mouritson, S., “Definition and Verification of Active Inceptor Requirements for a Future Tiltrotor,” 31st European Rotorcraft Forum, Florence, Italy, 13-15 September 2015

62 Gray, W. R. III, “Handling Qualities Evaluation at the USAF Test Pilot School,” AIAA Atmospheric Flight Mechanics Conference, Chicago, AIAA Paper 2009-6317, 2009

63 Anon., “Final Report – Accident Agusta Westland AW609, N609AG,” Agenzia Nazionale per la Sicurezza del Volo, 30 October 2015

64 McRuer, D. T., et al, “Aviation Safety And Pilot Control: Understanding And Preventing Unfavourable Pilot-vehicle Interactions”, National Academy Of Sciences, Washington, DC, 1997

65 Pavel, D., Jump, M., Dang-Vu, B., Masarati, P et al., “Adverse Rotorcraft Pilot Couplings – Past, Present and Future Challenges,” Progress in Aerospace Sciences, 2013, paerosci.2013.04.003

66 Jones, M., Jump, M., Lu, L., “Development of the Phase-Aggression Criterion for Rotorcraft –Pilot Coupling Detection,” American Institute

of Aeronautics and Astronautics, Journal of Guidance, Control and Dynamics, Vol 36, No1, January - February 2013

67 Anon., “Federal Aviation Administration, System Safety Handbook – chapter 3: Principles of System Safety,” Dec 2000,

68 Weir, D. H., et al., “Pilot Dynamic Response To Sudden Flight Control System Failures and Implications For Design,” NASA CR-1087, 1968

69 Gregory, J. D. L., “The Principles of Flight Test Assessment of Flight-Safety-Critical Systems in Helicopters,” Advisory Group for Aerospace Research and Development, Flight Test Technique Series, AGARD-AG-300, Vol 12, August 1994

70 Kalinowski, K. F., Tucker, G. E., Moralez III, E., “In-Flight Validation Of A Pilot Rating Scale For Evaluating Failure Transients In Electronic Flight Control Systems,” American Helicopter Society 62nd Annual Forum, Phoenix, AZ, May 9-11, 2006

71 Weakley, J., Kleinhesselink, K., Mason, D., Mitchell, D., “Simulation Evaluation of V-22 Degraded-Mode Flying Qualities,” AHS Annual Forum, 6-8 May 2003

72 Bethwaite, C., Langley, R., “Notes on research into some aspects of Stall-Warning Devices,” Report No 72, The College of Aeronautics, Cranfield, April 1953

73 Alvermann, K., Bodenstein, M., Graeber, S., Oertel, H., “Experimental System Review,“ Doc No SWE L 220R0424 D01, Version 003, DLR, Oct 2015

74 Duda, H., Gerlach, T., Advani, S., Potter, M., “Design of the DLR AVES Research Flight Simulator,” AIAA-2013-4737, American Institute of Aeronautics and Astronautics Modelling and Simulation Conference, Boston, MA, 19-22 August 2013

75 Abildgaard, M., Binet, L., “Active sidesticks used for vortex ring state avoidance,” 35th European Rotorcraft Forum, Hamburg, September 2009

76 Abildgaard, M., L. Binet, L., Taghizad, A., Von Grünhagen, W., “VRS avoidance as active function on side-sticks,”65rd Annual Forum of the American Helicopter Society, Grapevine, May 2009

77 Einthoven, P., “Active Controller Performance Requirements,” American Helicopter Society 60th Annual Forum, Baltimore, MD, USA, June 2004

78 Von Grünhagen, W., Schönenberg, T., Lantzsch, R., Lusardi, J., Lee, D., Fischer, H., “Handling Qualities Studies into the Interaction Between Sidestick Parameters and Helicopter Response Types,” AMRDEC, June 2012

79 Lusardi, J. A., Blankern, C. L., Ott, C. R., Malpica, C. A., Von Grünhagen,

W., “In Flight Evaluation of Active Inceptor Force Feel Characteristics and Handling Qualities,” American Helicopter Society 68th Annual Forum, Fort Worth, TX, May 2012

80 Barnett, M., PFR Flight 2, “Flight Test Manoeuvres and Data Gathering,” 2 May 14, v1.0

81 Anon., “Flight Manual, F-16 A/B, Blocks 10 and 15,” T.O.1F-16A-1, Lockheed Martin Corporation, 15 August 2003, pp1-127

82 Barnett, M., PFR Flight 1, “Qualitative Sidestick Failures,” 16 Oct 13, v1.0

84 Jones, M., White, M., Fell, T., Barnett, M., “Analysis of Motion Parameter Variations for Rotorcraft Flight Simulators,” American Helicopter Society, 73rd Annual Forum, Fort Worth, TX, 9-11 May 2017

85 Anon., “Type Certificate Data Sheet EC135,” EASA.R.009, Latest Edition, Airbus Helicopters GmbH, July 2019

86 West, I., Higgins, O., “EC135 AFCS Evaluation, ETPS Presentation,” 31 Oct 2013

87 Evans, L., Barnett, M., “ETPS Post Flight Report: Comparison of unaugmented, augmented and augmented isometric FCS settings using MTEs for CSAR role,” 2 Oct 2014

88 Dutton, K., Thompson, S., Barraclough, B., “The Art of Control Engineering,” Pearson Education Ltd, ISBN 978-0-201-17545-5, 1997

89 Nonnenmacher, D., Müllhäuser, M., "Optimization of the equivalent mechanical characteristics of active side sticks for piloting a controlled helicopter,” CEAS Aeronaut Journal, DOI 10.1007/s13272-011-0022-8, August 2011

90 Cooke, A., Fitzpatrick, E., “Helicopter Test and Evaluation,” 1st Edn., Blackwell Publishing Ltd. Oxford, GB, 2002

91 Seher-Weiss, S., “FitlabGUI – A Versatile Tool for Data Analysis, System Identification and Helicopter Handling Qualities Analysis,” 42nd European Rotorcraft Forum, Lille, France, 5-8 Sep 2016

92 Anon., “Certification Specifications and Guidance Material for Master Minimum Equipment List, CS-MMEL,” EASA, Initial, 31 January 2014

93 Anon., “Airworthiness and Environmental Certification (Regulation (EU) No 748/2012),” EASA, December 2019

94 Anon., “Rotary Wing Flight Test Manual, Failure Testing,” ETPS, QinetiQ/SES/ETPS/RWFTM/4.4/2.0, 2006

95 Padfield, G. D., “Helicopter Flight Dynamics. The Theory And Application Of Flying Qualities And Simulation Modelling,” 2nd Edn., Blackwell Publishing Ltd. Oxford, GB, AIAA Inc., Reston, VA, 2007, p573

96 Jones, M., Alexander, M., Höffinger, M., Barnett, M. P. C., Comeau, P., Gubbels, A., “In-Flight Test Campaign To Validate PIO Detection And

Assessment Tools," 8th Asian Rotorcraft Forum, Ankara, Turkey, 2019

97 Barnett, M., PFR Sim 5, "Isometric Sidestick Failures," 10-13 Nov 15, v1.0

98 Barnett, M., PFR Sim 7, "Isometric Sidestick Failures," 28 Jan-4 Feb 16, v1.0

99 Barnett, M., PFR Sim 6, "Isometric Sidestick Failures," 21 Jan 16, v1.0

100 Barnett, M., PFR Sim 8, "Isometric Sidestick Failures," 12 Feb 16, v1.0

101 Barnett, M., PFR Sim 14, "Isometric Task Definition," 11 Nov 16, v1.0

102 Barnett, M., PFR Sim 16,"Isometric Task Definition," 9 Dec 16, v1.0

103 Barnett, M., PFR Sim 13, "Isometric Task Definition," 4 Nov 16, v1.0

104 Barnett, M., PFR Sim 12, "Isometric Task Definition," 27 Oct 16, v1.0

105 Anon., "AP3456 The Central Flying School (CFS) Manual of Flying," Royal Air Force, Version 10, Issued 2018

106 Barnett, M., PFR Sim 15, "Isometric Task Definition," 5 Dec 16, v1.0

107 Barnett, M., PFR Sim 17, "Isometric Task Definition," 16 Dec 16, v1.0

108 Redante, A., "Statische Kalibrierung und Bandbreitenermittlung fur aktive Sidesticks," IB 111-2013, DLR Institut für Flugsystemtechnik, November 2014

109 McPherson, T. M., Hogan Jr., E. J. H., "Low Altitude High Speed Flight Evaluation of the F-4A/B (F4H-1F/-1) Airplane," Tech. Rep. ANTC-RAD32-103, 1963

110 Weingarten, N.,Chalk, C. R., "In-flight Investigation of Large Airplane Flying Qualities for Approach and Landing," Tech. Rep. AFWAL-TR-81-3118, Calspan, 1981

111 Anon., "Flying Qualities Of Piloted Aircraft," Mil-HDBK-1797 A, 19 December 1997

112 Blanken, C. L., Hoh, R., Mitchell, D. G., Key, D. L., "Test Guide for ADS-33E-PRF," AMR-AF-08-07, pp26, 2008

113 Mitchell, D. G., and Hoh, R. H., "Development of Methods and Devices to Predict and Prevent Pilot-Induced Oscillations," U.S. Air Force Research Lab. VA-WP-TR-2000-3046, Jan. 2000

114 Mitchell, D. G., Arencibia, A. J., and Muñoz, S., "Real-Time Detection of Pilot-Induced Oscillations," Atmospheric Flight Mechanics Conf., AIAA Paper 2004-4700, 2004

115 Tischler, M., Ivler, C., Mansur, M., Cheung, K., Berger, T., Berrios, M., "Handling Qualities Optimization and Trade-offs in Rotorcraft Flight Control Design," RAeS Rotorcraft Handling Qualities Conference, University of Liverpool, UK, 4-6 Nov 2008

116 Duda, H., "Prediction of Pilot in the loop Oscillations due to Rate

Saturation," Journal of Guidance, Control and Dynamics, Vol 20, No 3, May - June 1997

117 Gray, W. R. III, "Boundary Avoidance Tracking: A new Pilot Tracking Model," AIAA Atmospheric Flight Mechanics Conference, San Francisco, AIAA Paper 2005-5810, 15-18 August 2005

118 Weltz, G. L., Shweyk , K. M., Murray, D. M., "Application of New and Standard Pilot-Induced Oscillation (PIO) Analysis Methods to Flight Test Data of the C-17 Transport Aircraft," AIAA Atmospheric Flight Mechanics Conference and Exhibit, Hilton Head, South Carolina, AIAA Paper 2007-6387, 20 - 23 August 2007

119 Mitchell, D. G., Klyde, D. H., "Identifying a PIO Signature – New Techniques Applied to an Old Problem," 2006 Atmospheric Flight Mechanics Conference, Keystone, CO, AIAA Paper 2006-6495, 21-24 August 2006

120 Johnson, D. A., "Suppression of Pilot Induced Oscillation (PIO)," Air Force Institute of Technology, AFIT/GAE/ENY/02-1, Wright-Patterson Air Force Base, OH, 2002

121 Dang-Vu, B., Pavel, M. D., Yilmaz, D., Lu, L., Jones, M., Jump, M., "Report Demonstrating the Results of the Helicopter Rigid Body Model Validation Exercise," ARISTOTEL, ACPO-GA-2010-266073, Deliverable 4.9, December 2012

122 Mitchell, D. G., Klyde, D. H., "A critical Examination of PIO Prediction Criteria," Proceedings of the AIAA atmospheric flight mechanics conference, Boston, MA, August 1998

123 Hoh, R. H., "Advances in Flying Qualities – Concepts and Criteria for a Mission Orientated Flying Qualities Specification," AGARD LS 157, 1988

124 Seher-Weiß, S., "FilabGui: A MatLab Tool for Flight Data Analysis and Parameter Estimation," Version 2.6, Institut für Flugsystemtechnik, Deutsches Zentrum für Luft- und Raumfahrt, Braunschweig, January 2018

125 Ebbatson, M., "The Loss of Manual Flying Skills in Pilots of Highly Automated Airliners," Cranfield University School of Engineering, PhD Thesis, 2009

126 Anon., "Manual of Criteria for the Qualification of Flight Simulation Training Devices - Helicopters," ICAO 9625 AN938 Vol II, International Civil Aviation Organisation, First Edition, 2012,

Appendix A: Test Participants' Experience and Qualifications

Qualified Pilot	No
Qualified Helicopter Pilot	No
Qualified Test Pilot (RW/FW and category)	No
Qualified Instructor / Examiner (type)	No
Current types	Nil
Total flying hours	Nil
Total helicopter flying hours	Nil
Pilot experience of helicopter sidesticks (> 2hours)	No
Pilot experience of active sidesticks (> 2hours)	No
Pilot experience of isometric controllers (> 2hours)	No
Pilot experience of optimisation trials (> 2hours)	No
Pilot experience of simulator fidelity trials (> 2hours)	No

Table A-1: Test Participant A Experience and Qualifications

Qualified Pilot	No
Qualified Helicopter Pilot	No
Qualified Test Pilot (RW/FW and category)	No
Qualified Instructor / Examiner (type)	No
Current types	Nil
Total flying hours	Nil
Total helicopter flying hours	Nil
Pilot experience of helicopter sidesticks (> 2hours)	No
Pilot experience of active sidesticks (> 2hours)	No
Pilot experience of isometric controllers (> 2hours)	No
Pilot experience of optimisation trials (> 2hours)	No
Pilot experience of simulator fidelity trials (> 2hours)	No

Table A-2: Test Participant B Experience and Qualifications

Qualified Pilot	Glider
Qualified Helicopter Pilot	No
Qualified Test Pilot (RW/FW and category)	No
Qualified Instructor / Examiner (type)	No
Current types	Nil
Total flying hours	<100 (Gliders)
Total helicopter flying hours	Nil
Pilot experience of helicopter sidesticks (> 2hours)	No
Pilot experience of active sidesticks (> 2hours)	No
Pilot experience of isometric controllers (> 2hours)	No
Pilot experience of optimisation trials (> 2hours)	No
Pilot experience of simulator fidelity trials (> 2hours)	No

Table A-3: Test Participant C Experience and Qualifications

Qualified Pilot	Glider, Powered Glider
Qualified Helicopter Pilot	No
Qualified Test Pilot (RW/FW and category)	No
Qualified Instructor / Examiner (type)	No
Current types	Glider, Powered Glider
Total flying hours	700
Total helicopter flying hours	Nil
Pilot experience of helicopter sidesticks (> 2hours)	No
Pilot experience of active sidesticks (> 2hours)	No
Pilot experience of isometric controllers (> 2hours)	No
Pilot experience of optimisation trials (> 2hours)	No
Pilot experience of simulator fidelity trials (> 2hours)	No

Table A-4: Test Participant D Experience and Qualifications

Qualified Pilot	Yes
Qualified Helicopter Pilot	No
Qualified Test Pilot (RW/FW and category)	FW Cat 2
Qualified Instructor / Examiner (type)	No
Current types	Learjet 35/55, Do228, A320
Total flying hours	6200
Total helicopter flying hours	Nil
Pilot experience of helicopter sidesticks (> 2hours)	No
Pilot experience of active sidesticks (> 2hours)	No
Pilot experience of isometric controllers (> 2hours)	No
Pilot experience of optimisation trials (> 2hours)	No
Pilot experience of simulator fidelity trials (> 2hours)	No

Table A-5: Test Participant E Experience and Qualifications

Qualified Pilot	Yes (FW)
Qualified Helicopter Pilot	No
Qualified Test Pilot (RW/FW and category)	FW Cat 2
Qualified Instructor / Examiner (type)	CRI SE/SP
Current types	Do228, A320
Total flying hours	2000 (all FW)
Total helicopter flying hours	Nil
Pilot experience of helicopter sidesticks (> 2hours)	No
Pilot experience of active sidesticks (> 2hours)	No
Pilot experience of isometric controllers (> 2hours)	No
Pilot experience of optimisation trials (> 2hours)	No
Pilot experience of simulator fidelity trials (> 2hours)	No

Table A-6: Test Participant F Experience and Qualifications

Qualified Pilot	Yes
Qualified Helicopter Pilot	Yes
Qualified Test Pilot (RW/FW and category)	RW Cat 1
Qualified Instructor / Examiner (type)	FTI, TRI (EC135, AB412)
Current types	EC135, Bo105, B412
Total flying hours	4500
Total helicopter flying hours	4000
Pilot experience of helicopter sidesticks (> 2hours)	Yes
Pilot experience of active sidesticks (> 2hours)	Yes
Pilot experience of isometric controllers (> 2hours)	Yes
Pilot experience of optimisation trials (> 2hours)	Yes
Pilot experience of simulator fidelity trials (> 2hours)	Yes

Table A-7: Test Participant G Experience and Qualifications

Qualified Pilot	Yes
Qualified Helicopter Pilot	Yes
Qualified Test Pilot (RW/FW and category)	RW Cat 1
Qualified Instructor / Examiner (type)	TRI (AS350, AS355, UH60)
Current types	Expired AS350, AS355, UH60
Total flying hours	1800
Total helicopter flying hours	1600
Pilot experience of helicopter sidesticks (> 2hours)	Yes
Pilot experience of active sidesticks (> 2hours)	Yes
Pilot experience of isometric controllers (> 2hours)	No
Pilot experience of optimisation trials (> 2hours)	No
Pilot experience of simulator fidelity trials (> 2hours)	Yes

Table A-8: Test Participant H Experience and Qualifications

Qualified Pilot	Yes
Qualified Helicopter Pilot	Yes
Qualified Test Pilot (RW/FW and category)	RW Cat 2
Qualified Instructor / Examiner (type)	TRI EC135, TRI/TRE Bo105
Current types	EC135, Bo105
Total flying hours	6400
Total helicopter flying hours	6000
Pilot experience of helicopter sidesticks (> 2hours)	Yes
Pilot experience of active sidesticks (> 2hours)	Yes
Pilot experience of isometric controllers (> 2hours)	Yes
Pilot experience of optimisation trials (> 2hours)	Yes
Pilot experience of simulator fidelity trials (> 2hours)	Yes

Table A-9: Test Participant I Experience and Qualifications

Qualified Pilot	Yes
Qualified Helicopter Pilot	Yes
Qualified Test Pilot (RW/FW and category)	RW Cat 1
Qualified Instructor / Examiner (type)	TRI EC135
Current types	NH90, EC135/145, AS350, PA28
Total flying hours	4100
Total helicopter flying hours	3700
Pilot experience of helicopter sidesticks (> 2hours)	Yes
Pilot experience of active sidesticks (> 2hours)	No
Pilot experience of isometric controllers (> 2hours)	No
Pilot experience of optimisation trials (> 2hours)	Yes
Pilot experience of simulator fidelity trials (> 2hours)	Yes

Table A-10: Test Participant J Experience and Qualifications

Qualified Pilot	Yes
Qualified Helicopter Pilot	Yes
Qualified Test Pilot (RW/FW and category)	RW Cat 1
Qualified Instructor / Examiner (type)	TRE MD500, TRI/TRE AW139
Current types	AW109, AW139, AW189, BK117
Total flying hours	3600
Total helicopter flying hours	1600
Pilot experience of helicopter sidesticks (> 2hours)	No
Pilot experience of active sidesticks (> 2hours)	No
Pilot experience of isometric controllers (> 2hours)	Yes
Pilot experience of optimisation trials (> 2hours)	Yes
Pilot experience of simulator fidelity trials (> 2hours)	Yes
Comments	900 hours F-16 (isometric stick)

Table A-11: Test Participant K Experience and Qualifications

Qualified Pilot	Yes
Qualified Helicopter Pilot	Yes
Qualified Test Pilot (RW/FW and category)	RW Cat 1
Qualified Instructor / Examiner (type)	Mil QHI(A2) Puma, HH60G, Gazelle, B412
Current types	Puma HC2, EC135, Merlin HC 3, HC4, H125
Total flying hours	4300
Total helicopter flying hours	4250
Pilot experience of helicopter sidesticks (> 2hours)	Yes
Pilot experience of active sidesticks (> 2hours)	No
Pilot experience of isometric controllers (> 2hours)	No
Pilot experience of optimisation trials (> 2hours)	No
Pilot experience of simulator fidelity trials (> 2hours)	Yes

Table A-12: Test Participant L Experience and Qualifications

Notes

- Test Pilot qualification refers to fixed wing (FW) or rotary wing (RW) equivalent EASA Flight Crew Licencing (Part-FCL) Flight Test (FT) category (1 or 2).
- Flying hours are approximated to nearest 100.
- QHI is the UK military term for Qualified Helicopter Instructor. A2 is the standard attained (from B2, B1, A2, A1).

Appendix B: Questionnaires and Scales

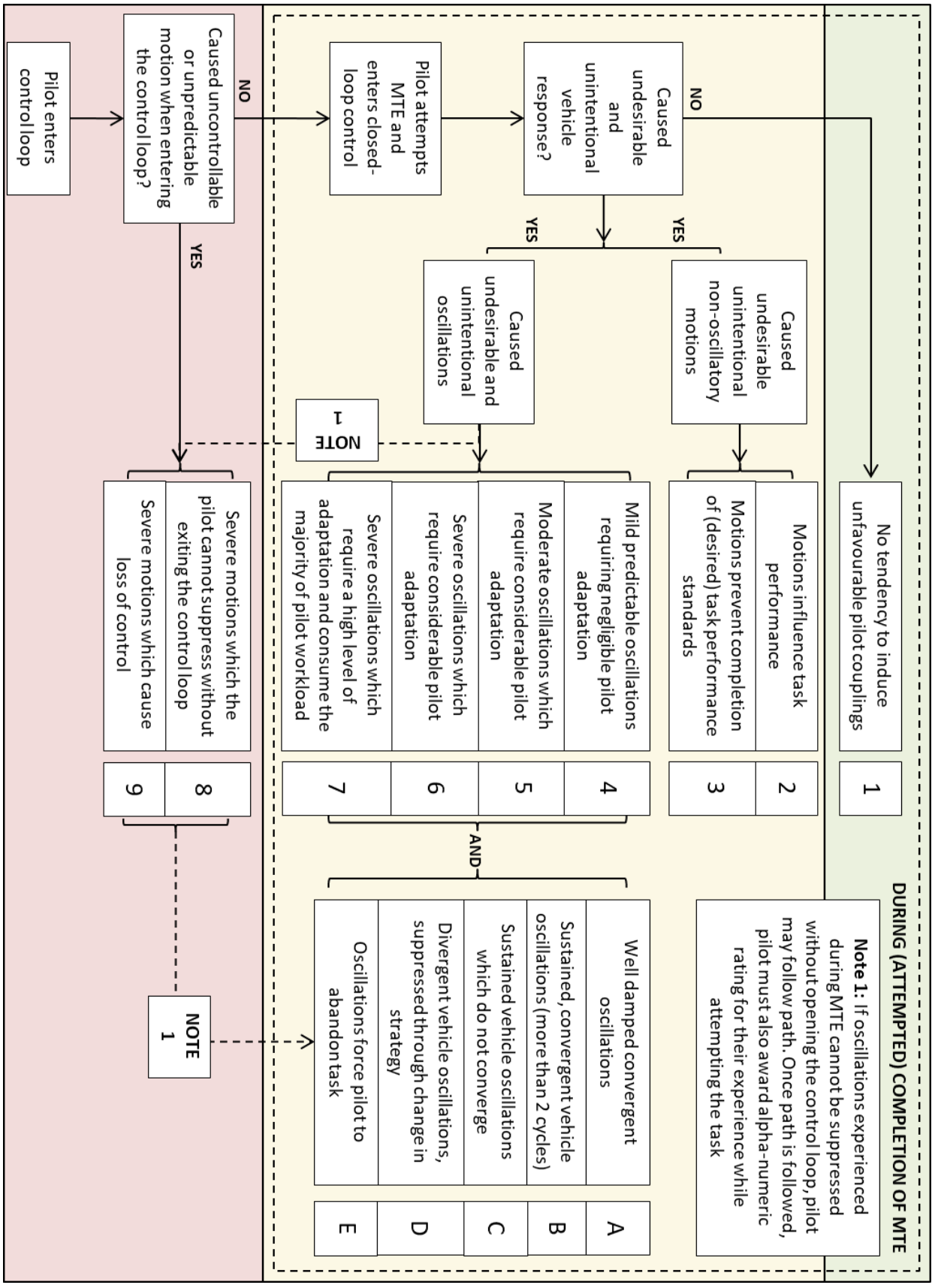

Figure B-1: Adverse Pilot Coupling Rating

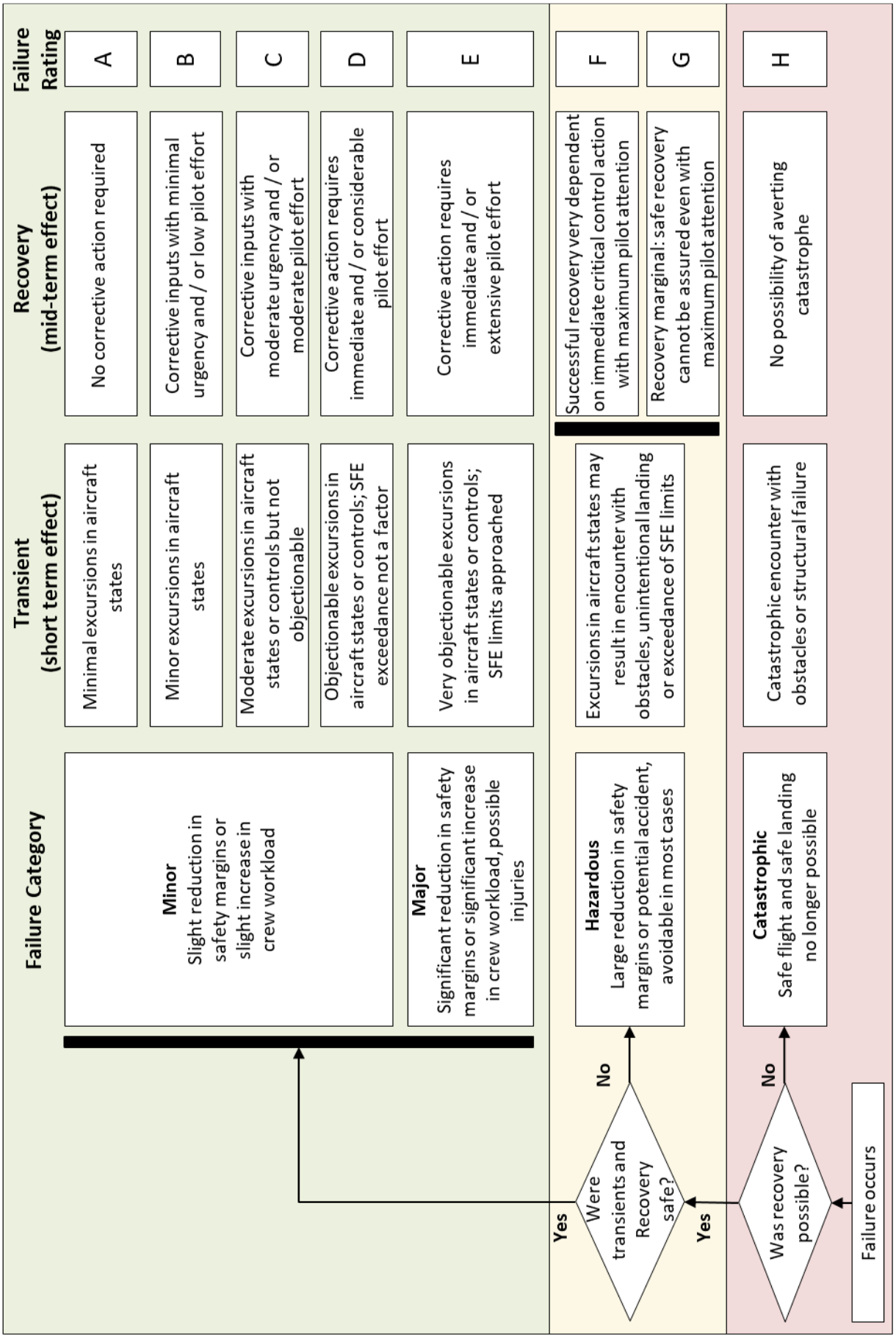

Figure B-2: Modified Integrated Failure Evaluation Scale

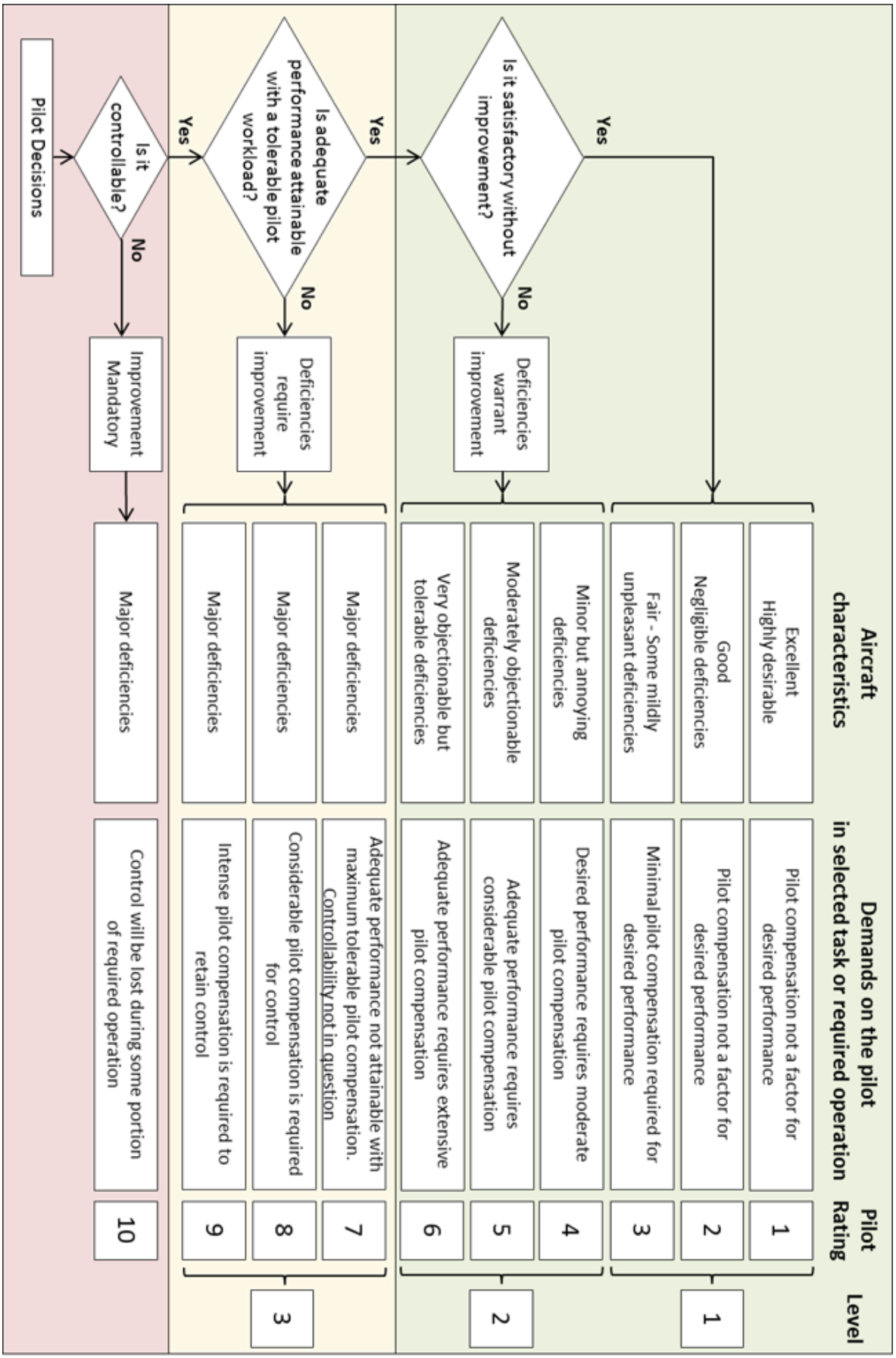

Figure B-3: Cooper Harper Rating Scale

Factors Influencing the Aggression and Continuation of PIOs

The test participant is asked to answer these questions after Session 1 with an option to confirm the results after session 2. For each of the following factors, provide a rating of influential significance (1-5) and a ranking order of the factor compared to the other defined factors (1-7). Comments and additional factors are also welcome:

Attitude / attitude rate at moment of failure					
Influence Rating	1 – Low	2	3 – Medium	4	5 – High
Ranking compared to other defined factors					

Cyclic control force / displacement magnitude at moment of failure					
Influence Rating	1 – Low	2	3 – Medium	4	5 – High
Ranking compared to other defined factors					

Cyclic control force / displacement direction from trim at moment of failure					
Influence Rating	1 – Low	2	3 – Medium	4	5 – High
Ranking compared to other defined factors					

Pre-failure required pilot gain					
Influence Rating	1 – Low	2	3 – Medium	4	5 – High
Ranking compared to other defined factors					

Post-failure required pilot gain					
Influence Rating	1 – Low	2	3 – Medium	4	5 – High
Ranking compared to other defined factors					

Timing of Failure					
Influence Rating	1 – Low	2	3 – Medium	4	5 – High
Ranking compared to other defined factors					

Motion cues					
Influence Rating	1 – Low	2	3 – Medium	4	5 – High
Ranking compared to other defined factors					

Visual references					
Influence Rating	1 – Low	2	3 – Medium	4	5 – High
Ranking compared to other defined factors					

Figure B-4: Factors Influencing the Aggression and Continuation of PIOs

Appendix C: Mission Task Elements

C.1 Cyclic Sidestick Isometric Failure MTE

Objectives

- Check that a rotorcraft is controllable after a sidestick failure to an isometric mode.
- Check that the rotorcraft has no APC tendency during a high gain task in an isometric sidestick mode.

Description of manoeuvre. Initiate the manoeuvre from a ground referenced hover at a Radar Altimeter height of 15ft agl at one of the corners of the course. Accelerate to 13-17kt ground speed towards another corner as directed by the FTE. The ground track should be along one of the lines as illustrated in figure C-1 and be such that the rotorcraft will arrive over the target hover point. The transition to the hover must be achieved in one smooth manoeuvre with the maximum decelerative attitude achieved immediately prior to the hover. It is not acceptable to accomplish most of the deceleration well before the target hover point and then to creep up to the final position. The trim release button shall not be used during the manoeuvre. After 10 seconds the FTE will select the next target hover point which the pilot must then manoeuvre to. The process is repeated until the FTE initiates the isometric failure during the deceleration to a hover point. After identifying the failure, the pilot must recover the aircraft and achieve the hover at the nominated target hover point. The manoeuvre shall be accomplished in calm winds. The recovery of the aircraft within ‘safe parameters’ as defined must be of greater importance than suppressing the APC. Loss of control means that a safe landing is not possible even outside of the safe area (ie on any flat ground)

Description of test course. The suggested course for this manoeuvre is presented in figures C-1 and C-2. Note that the altitude is maintained by reference to the radar altimeter on the cockpit displays.

Performance standards. The CHR performance standards are presented in tables C-1 and C-2. It is acceptable for the pilot to overshoot the target hover point slightly providing that he is still able to achieve the stabilised hover time.

Desired Performance	Cargo/Utility GVE
Attain a stabilised hover within X seconds of initiation of deceleration or sidestick failure, whichever comes latest	6 sec
Maintain a stabilised hover for at least	20 sec
Maintain the longitudinal and lateral position within ±Xft of a point on the ground	3ft
Maintain altitude within ±Xft	5ft
Maintain heading within ±X°	5°
There shall be no objectionable oscillations in any axis either during the transition to hover or the stabilised hover	**√**

Table C-1: CHR Desired Performance Standards, Isometric Failure MTE

Adequate Performance	Cargo/Utility GVE
Attain a stabilised hover within X seconds of initiation of deceleration or sidestick failure, whichever comes latest	10 sec
Maintain a stabilised hover for at least	20 sec
Maintain the longitudinal and lateral position within ±Xft of a point on the ground	6ft
Maintain altitude within ±Xft	10ft
Maintain heading within ±X°	10°

Table C-2: CHR Adequate Performance Standards, Isometric Failure MTE

The IFES safe recovery performance standards and SFE definitions are presented in Table C-3.

Safe Recovery Performance / SFE	Cargo/Utility GVE
Attain a stabilised hover within X seconds of initiation of deceleration or sidestick failure, whichever comes latest	10 sec
Maintain a stabilised hover for at least	20 sec
Maintain the longitudinal and lateral position within ±Xft of a point on the ground	6ft
Maintain altitude within ±Xft	10ft
Maintain heading within ±X°	10°

Table C-3: IFES Safe Recovery Performance and SFE Standards, Isometric Failure MTE

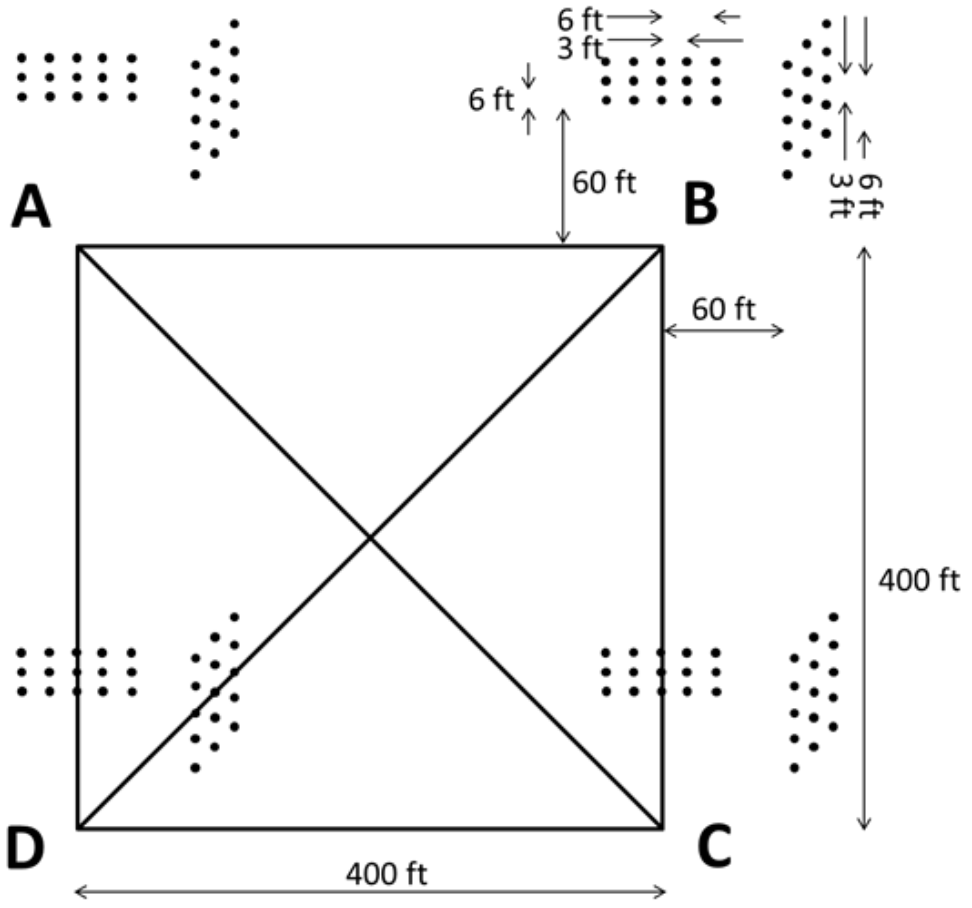

Figure C-1: Course Dimensions, Cyclic Sidestick Isometric Failure MTE

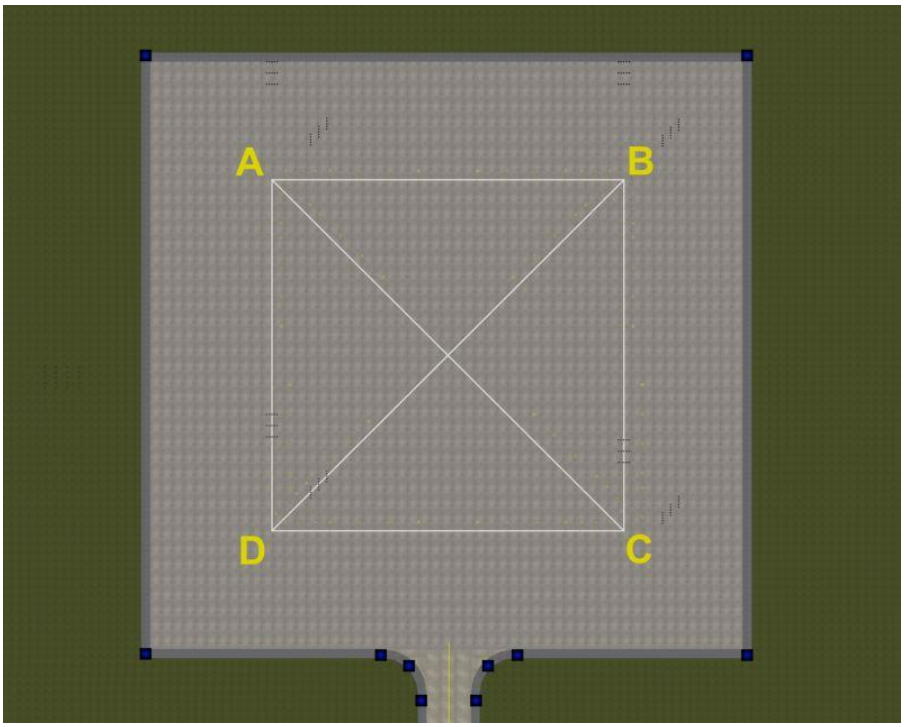

Figure C-2: Cyclic Sidestick Isometric Failure MTE Simulator Course (source: DLR)

C.2 Hover MTE

Objectives

- Check ability to transition from translating flight to a stabilized hover with precision and a reasonable amount of aggressiveness.
- Check ability to maintain precise position, heading, and altitude in the presence of a moderate wind from the most critical direction in the GVE; and with calm winds allowed in the DVE.

Description of manoeuver. Initiate the manoeuver at a ground speed of between 6 and 10 knots, at an altitude less than 20 ft. For rotorcraft carrying external loads, the altitude will have to be adjusted to provide a 10 ft load clearance. The target hover point shall be oriented approximately 45 degrees relative to the heading of the rotorcraft. The target hover point is a repeatable, ground-referenced point from which rotorcraft deviations are measured. The ground track should be such that the rotorcraft will arrive over the target hover point (see illustration in Figure C-2). In the GVE, the manoeuver shall be accomplished in calm winds and in moderate winds from the most critical direction. If a critical direction has not been defined, the hover shall be accomplished with the wind blowing directly from the rear of the rotorcraft.

Description of test course. The suggested test course for this manoeuver is shown in Figures C-4 and C-5. Note that the hover altitude depends on the height of the hover sight and the distance between the sight, the hover target, and the rotorcraft. These dimensions may be adjusted to achieve a desired hover altitude.

Performance standards. Accomplish the transition to hover in one smooth manoeuver. It is not acceptable to accomplish most of the deceleration well before the hover point and then to creep up to the final position.

Desired Performance	Cargo/Utility GVE
Attain a stabilised hover within X seconds of initiation of deceleration	5 sec
Maintain a stabilised hover for at least	30 sec
Maintain the longitudinal and lateral position within ±Xft of a point on the ground	3ft
Maintain altitude within ±Xft	2ft
Maintain heading within ±X°	5°
There shall be no objectionable oscillations in any axis either during the transition to hover or the stabilised hover	**√**

Table C-4: CHR Desired Performance Standards, Hover MTE

Adequate Performance	Cargo/Utility GVE
Attain a stabilised hover within X seconds of initiation of deceleration or sidestick failure, whichever comes latest	8 sec
Maintain a stabilised hover for at least	30 sec
Maintain the longitudinal and lateral position within ±Xft of a point on the ground	6ft
Maintain altitude within ±Xft	4ft
Maintain heading within ±X°	10°

Table C-5: CHR Adequate Performance Standards, Hover MTE

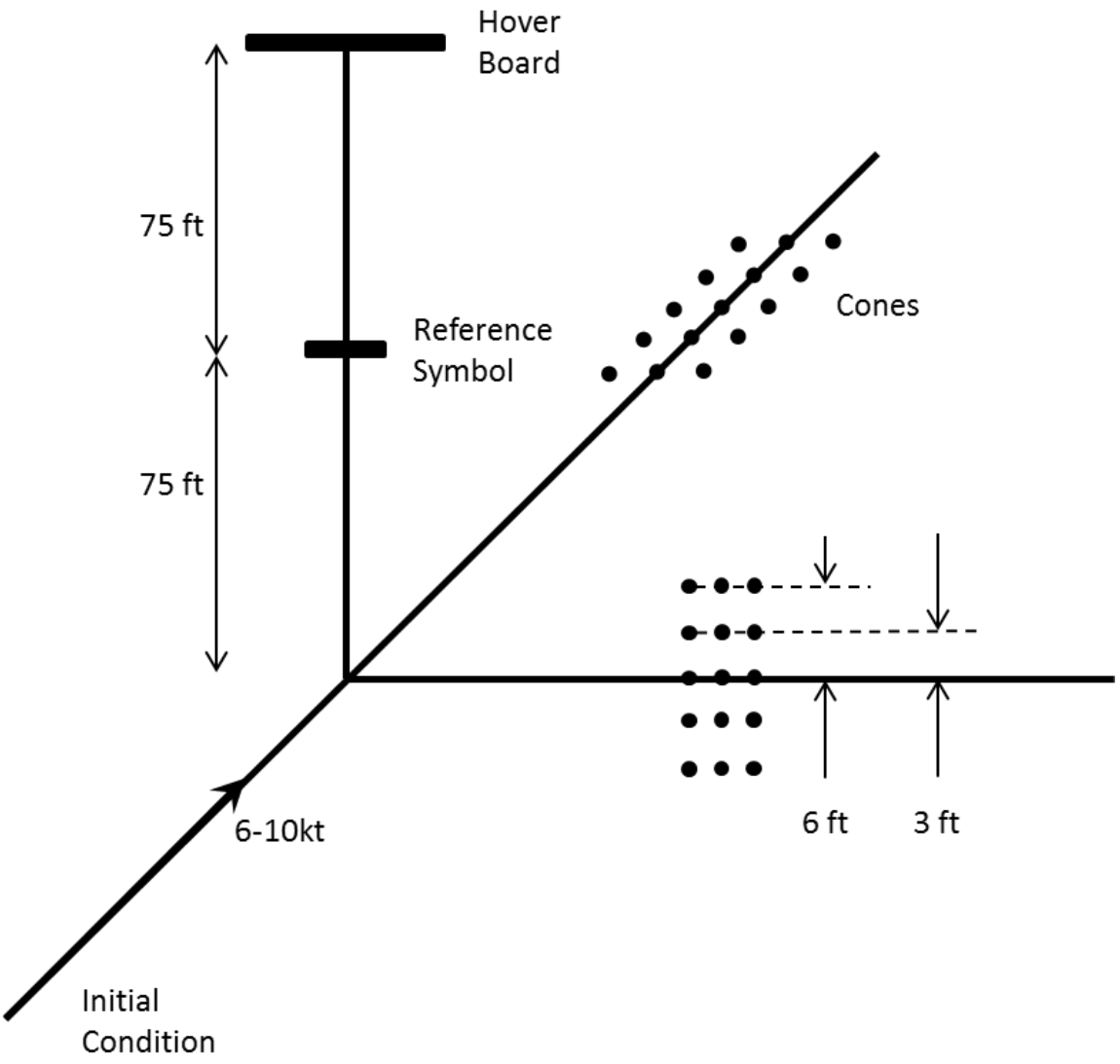

Figure C-3: Course Dimensions, Hover MTE, Top View

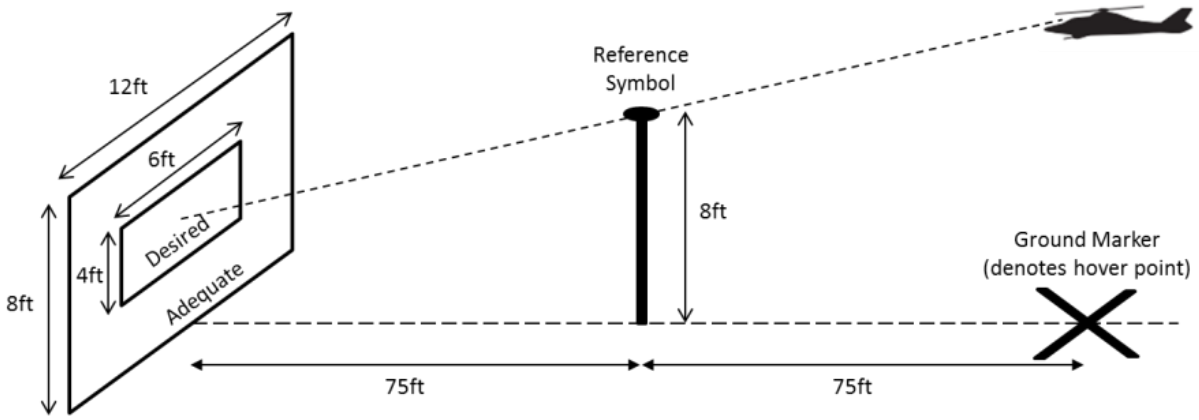

Figure C-4: Course Dimensions, Hover MTE, Side View

Appendix D: Baseline Handling Qualities

The HQ of the baseline simulator aircraft was assessed by 3 test pilots using the isometric MTE as described in appendix C. Each pilot flew the MTE to the right, forward and compound right-forward directions and awarded a rating from the Cooper-Harper Rating Scale in accordance with ADS-33E [36]. During all test points the wind was zero, the atmospheric environment was 10km visibility and no cloud or precipitation. The visual environment was considered a GVE and the UCE was level 1. The full results of are shown in tables D-1 and D-2 for rate command and attitude command respectively. The arithmetic average CHR across all pilots and directions was 4.0 for rate command and 3.1 for attitude command.

Pilot	Track	CHR
G	Forward	4
G	Right	4
G	Forward and Right	4
H	Forward	4
H	Right	4
H	Forward and Right	4
O	Forward	4
O	Right	4
O	Forward and Right	4

Table D-1: Baseline HQ, Isometric Failure MTE; Without Failure; Rate Command; Pilots: G, H, L

Pilot	Track	CHR
G	Forward	3
G	Right	3
G	Forward and Right	3
H	Forward	3
H	Right	3
H	Forward and Right	3
O	Forward	3
O	Right	3
O	Forward and Right	4

Table D-2: Baseline HQ, Isometric Failure MTE; Without Failure; Attitude Command; Pilots: G, H, L

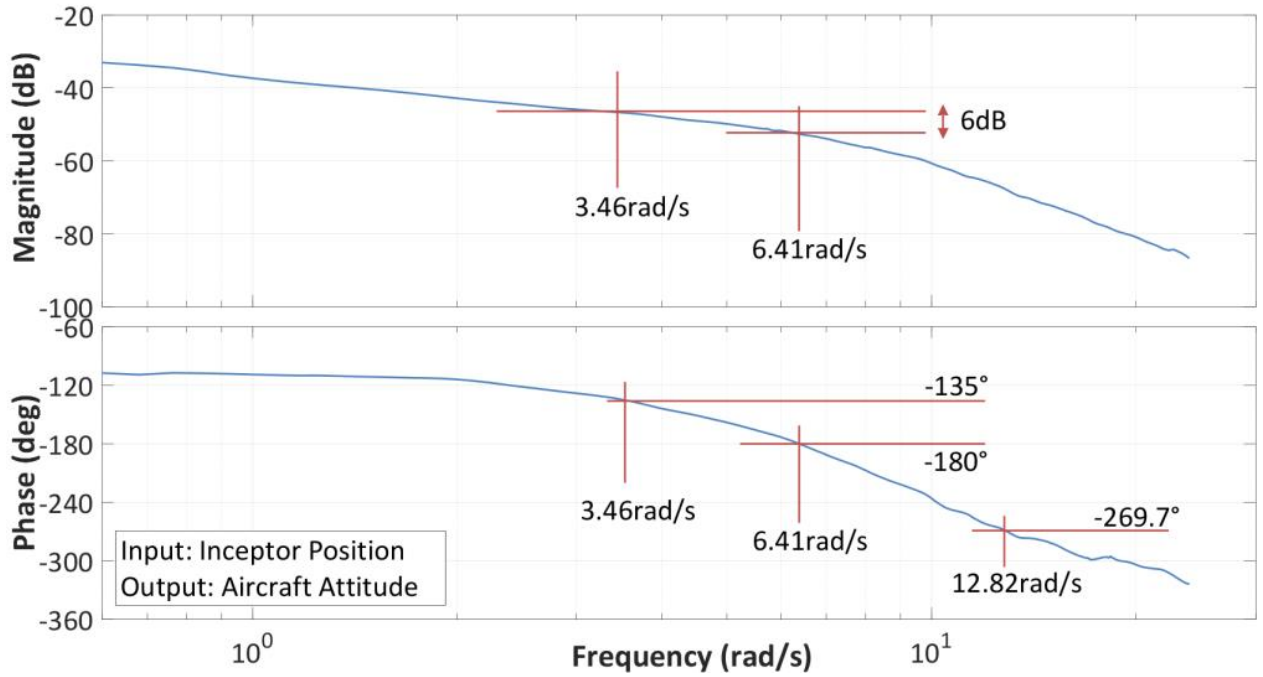

Figure D-1: Bode Plot, Position-Attitude, Rate Command, Pitch Axis, Compliant

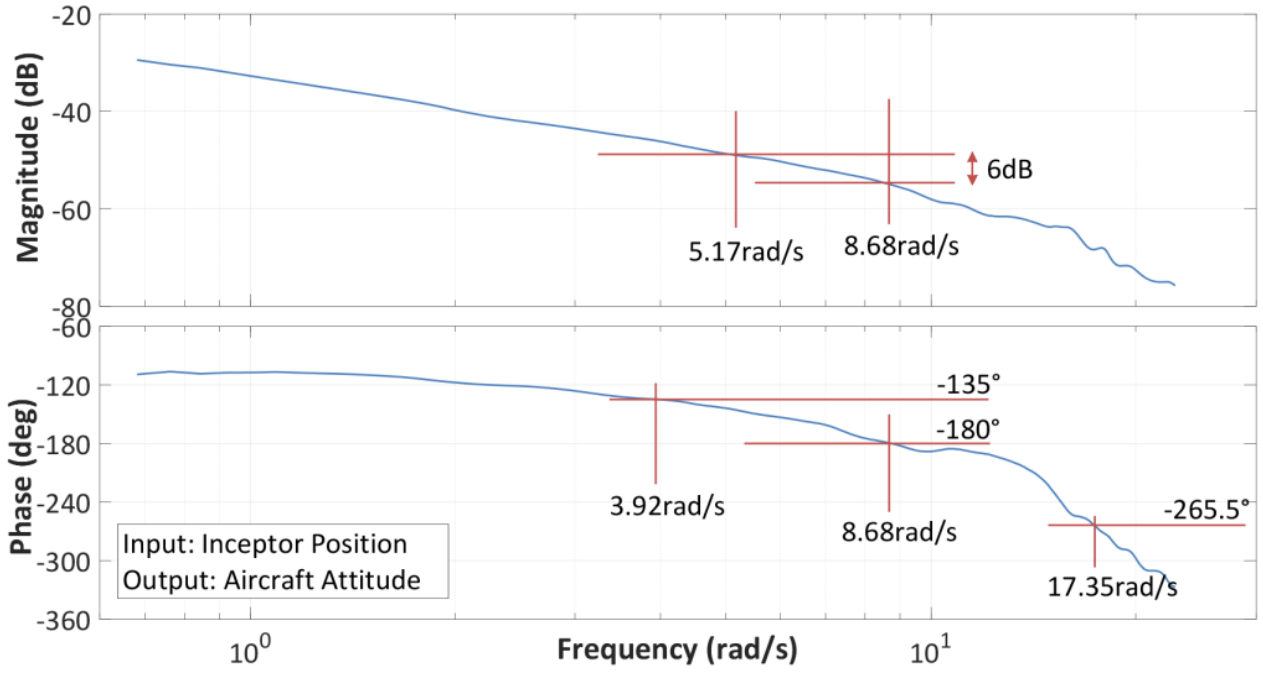

Figure D-2: Bode Plot, Position-Attitude, Rate Command, Roll Axis, Compliant

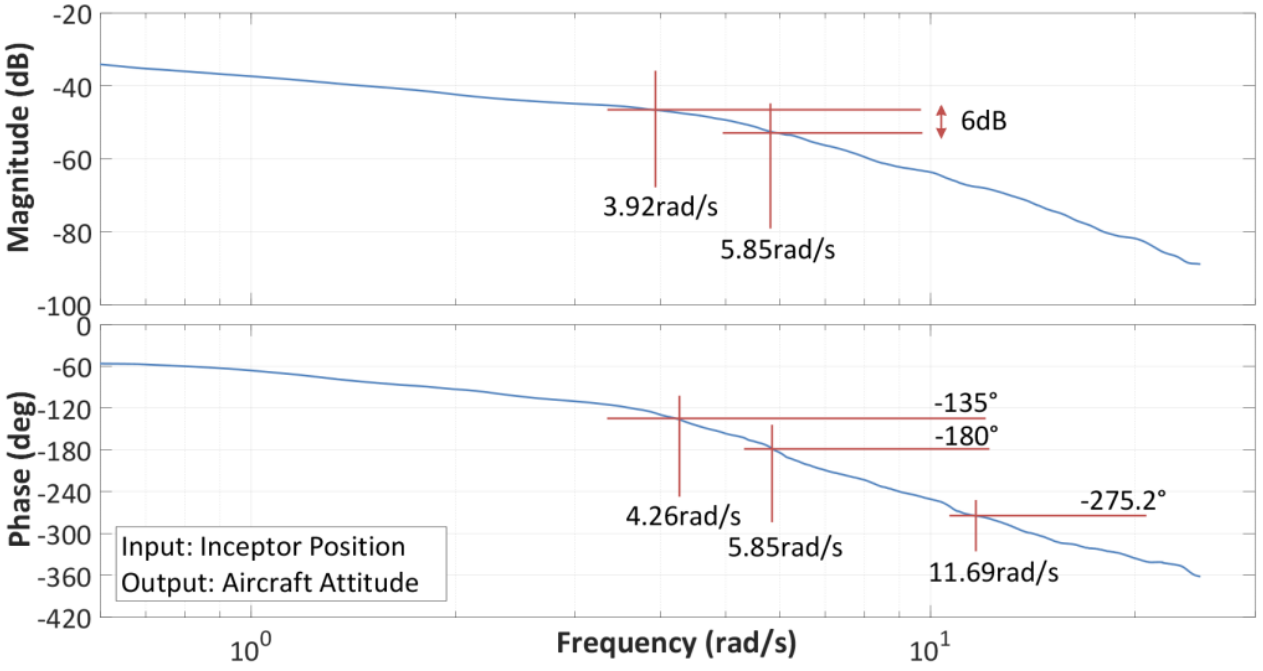

Figure D-3: Bode Plot, Position-Attitude, Attitude Command, Pitch Axis, Compliant

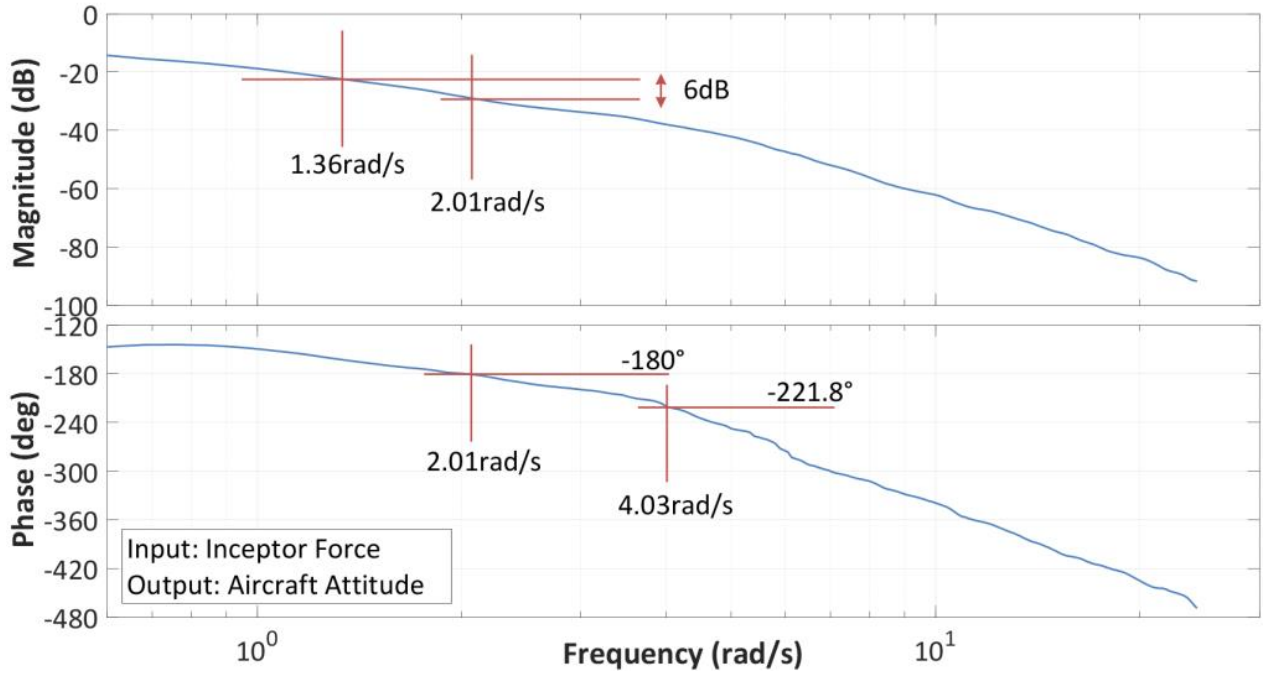

Figure D-4: Bode Plot, Force-Attitude, Attitude Command, Pitch Axis, Compliant

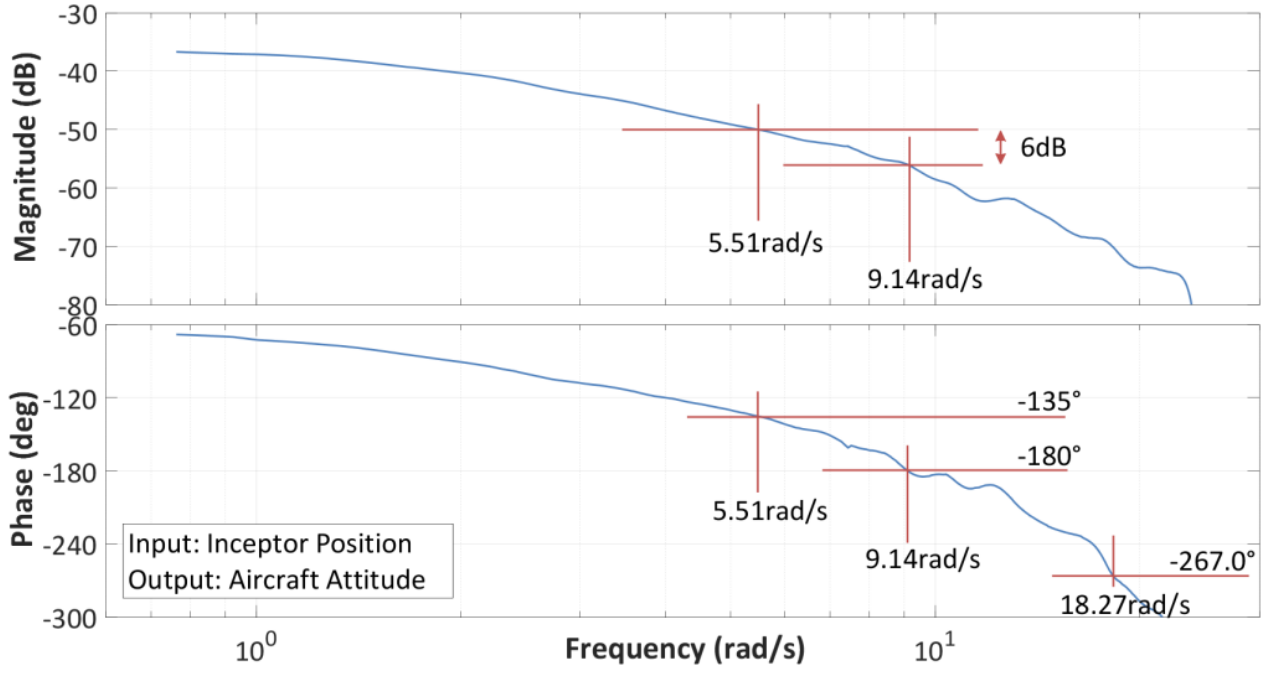

Figure D-5: Bode Plot, Position-Attitude, Attitude Command, Roll Axis, Compliant

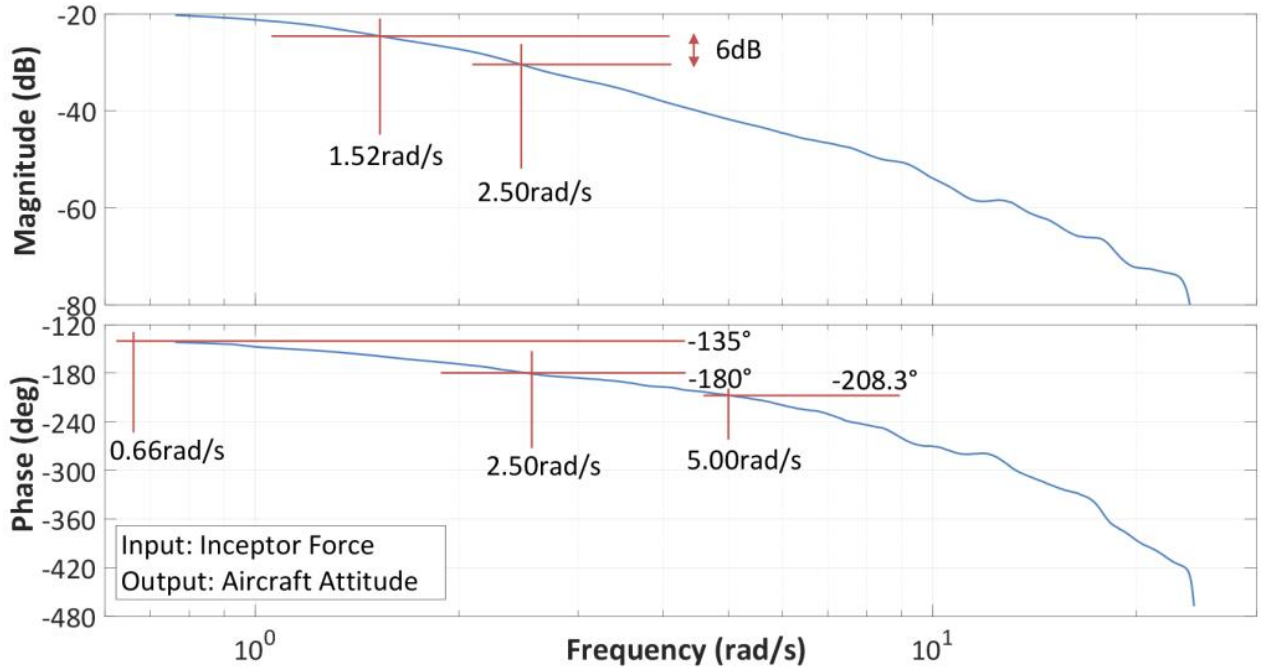

Figure D-6: Bode Plot, Force-Attitude, Attitude Command, Roll Axis, Compliant

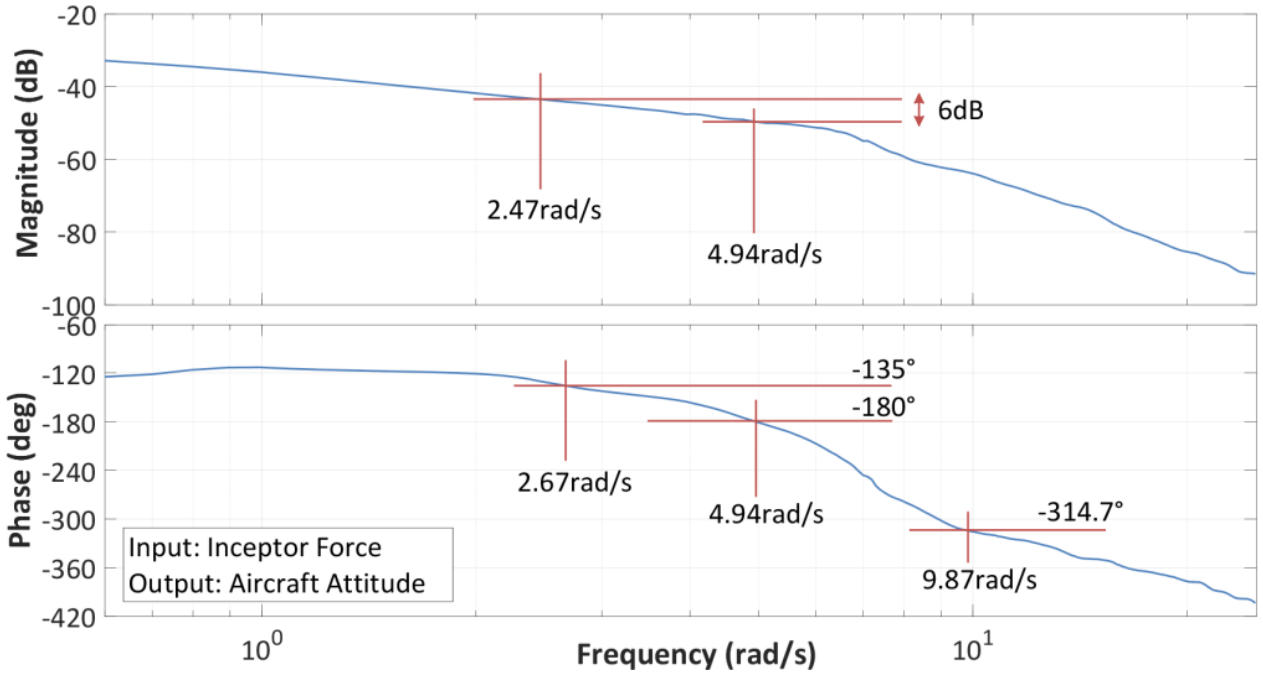

Figure D-7: Bode Plot, Force-Attitude, Rate Command, Pitch Axis, Isometric, Config 1

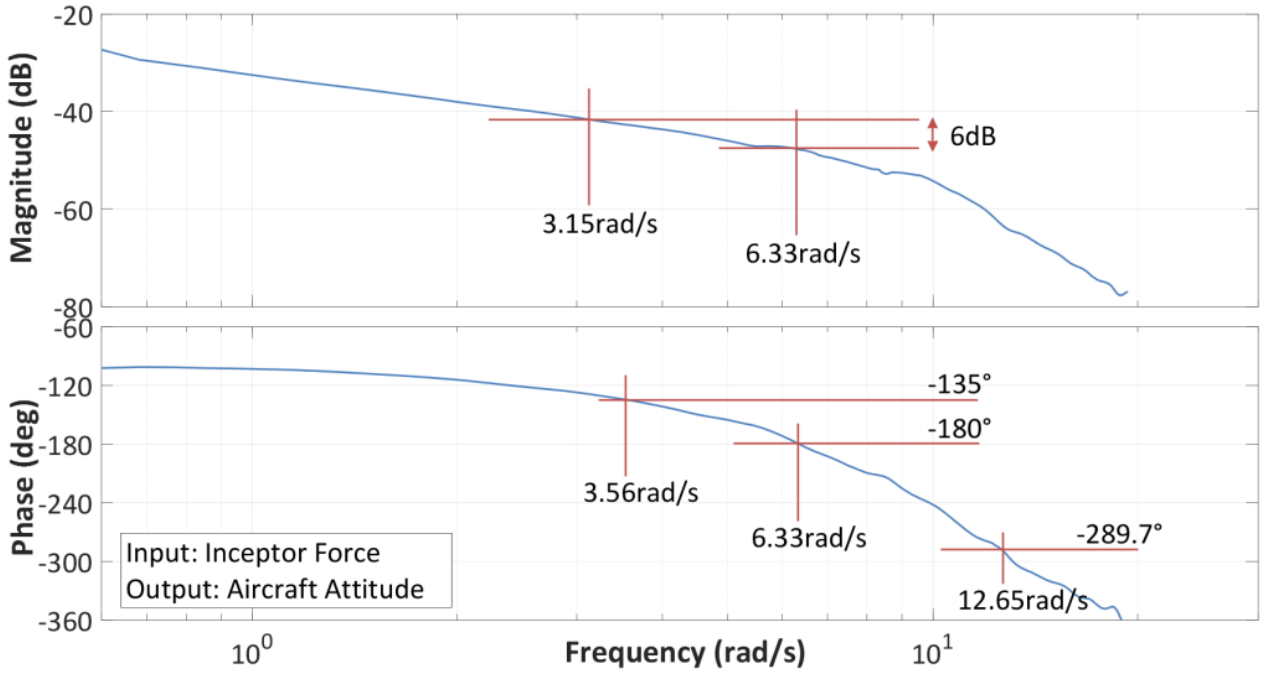

Figure D-8: Bode Plot, Force-Attitude, Rate Command, Roll Axis, Isometric, Config 1

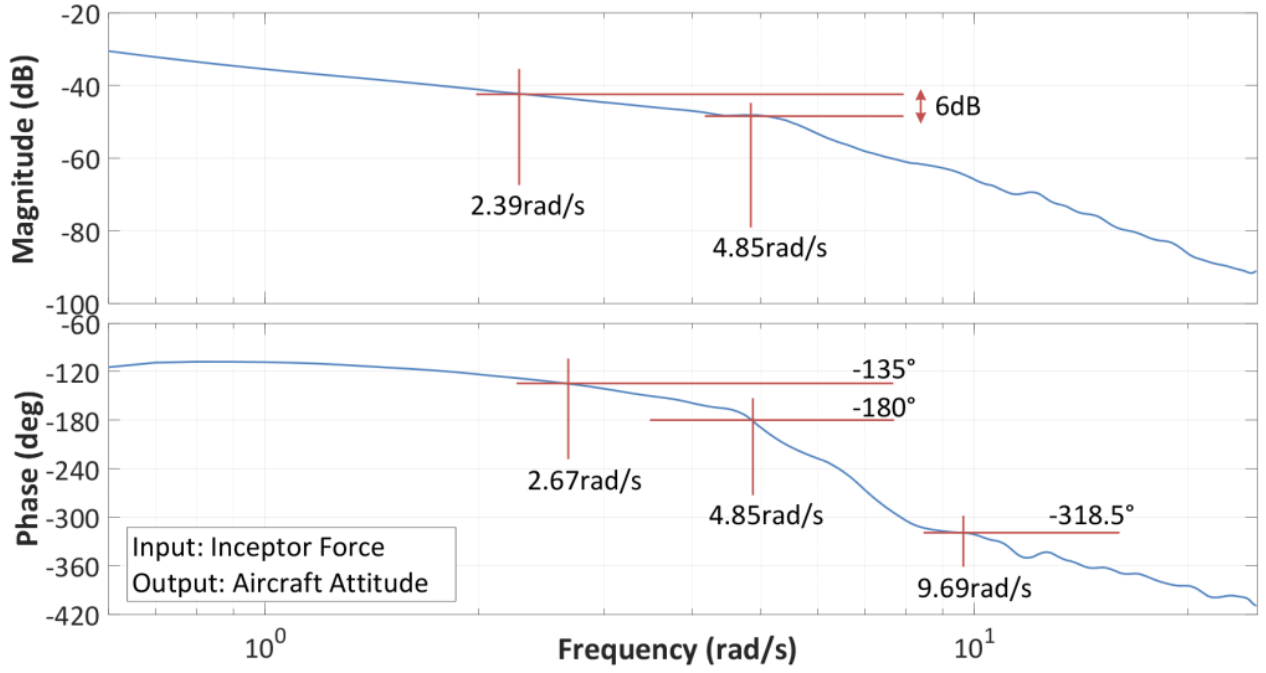

Figure D-9: Bode Plot, Force-Attitude, Rate Command, Pitch Axis, Isometric, Config 4

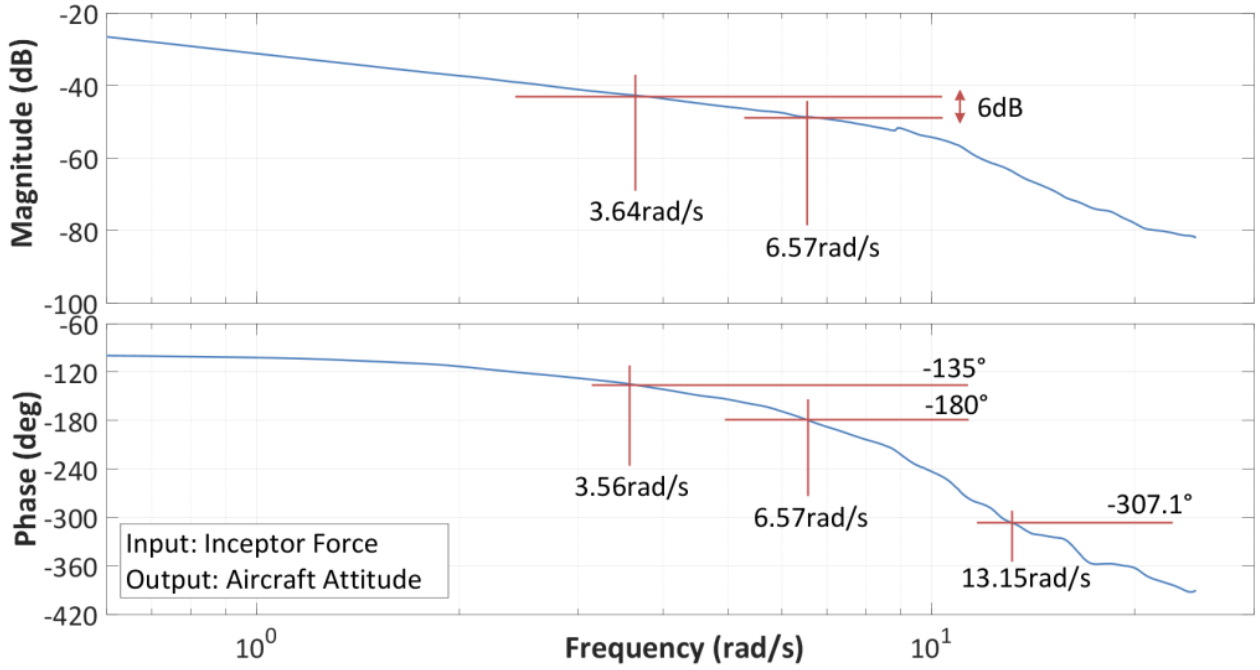

Figure D-10: Bode Plot, Force-Attitude, Rate Command, Roll Axis, Isometric, Config 4

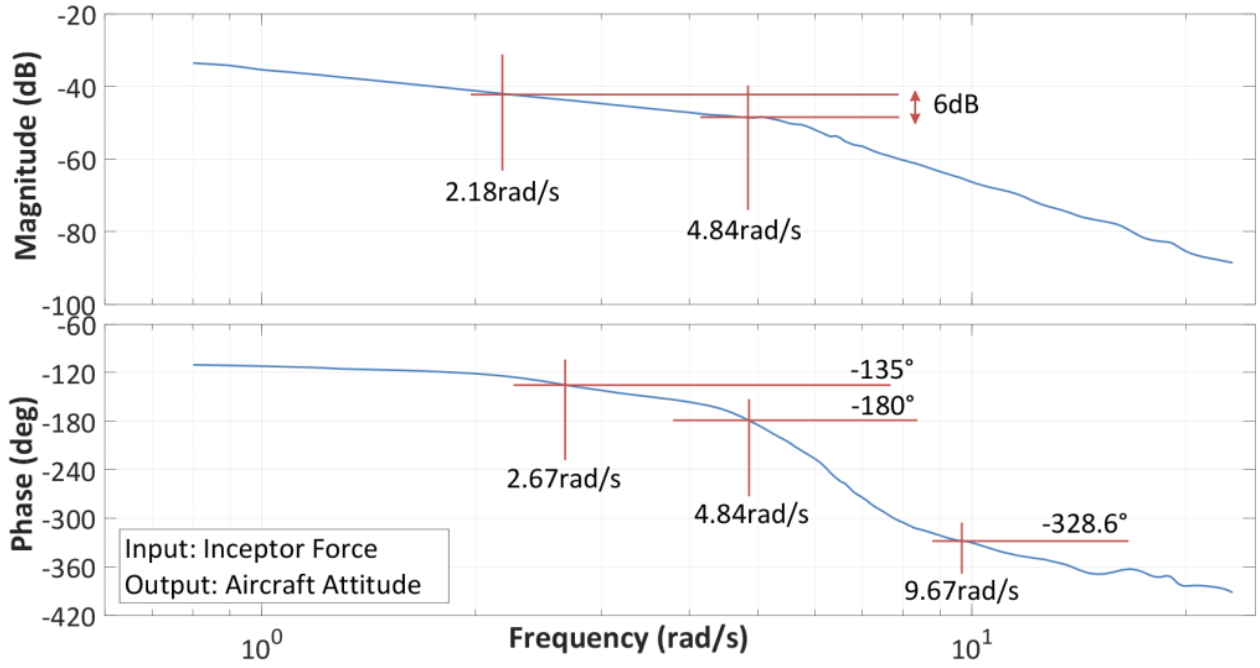

Figure D-11: Bode Plot, Force-Attitude, Rate Command, Pitch Axis, Isometric, Config 7

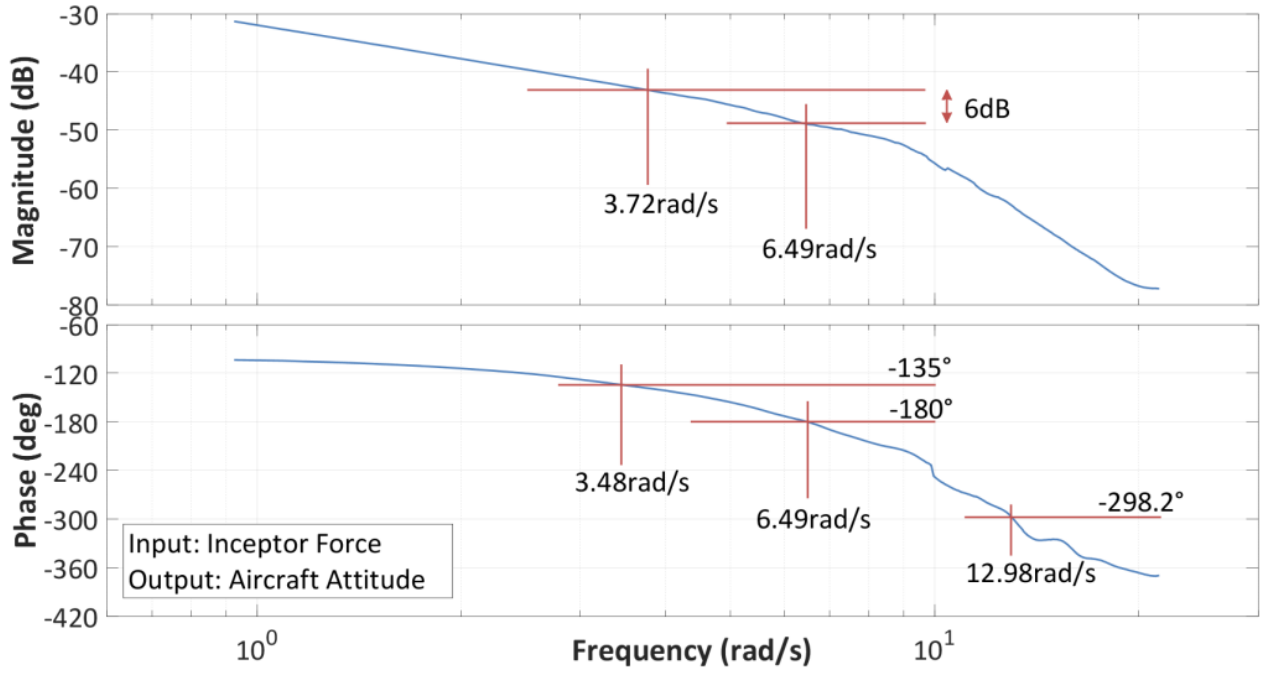

Figure D-12: Bode Plot, Force-Attitude, Rate Command, Roll Axis, Isometric, Config 7

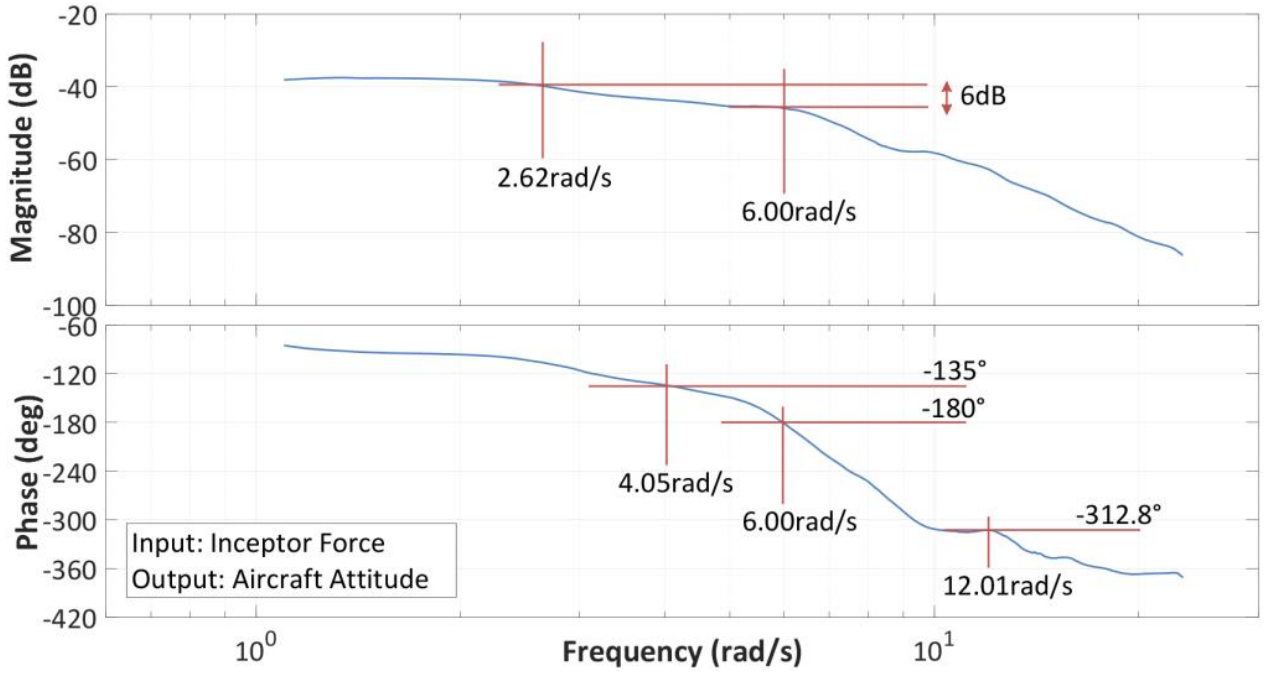

Figure D-13: Bode Plot, Force-Attitude, Attitude Command, Pitch Axis, Isometric, Config 1

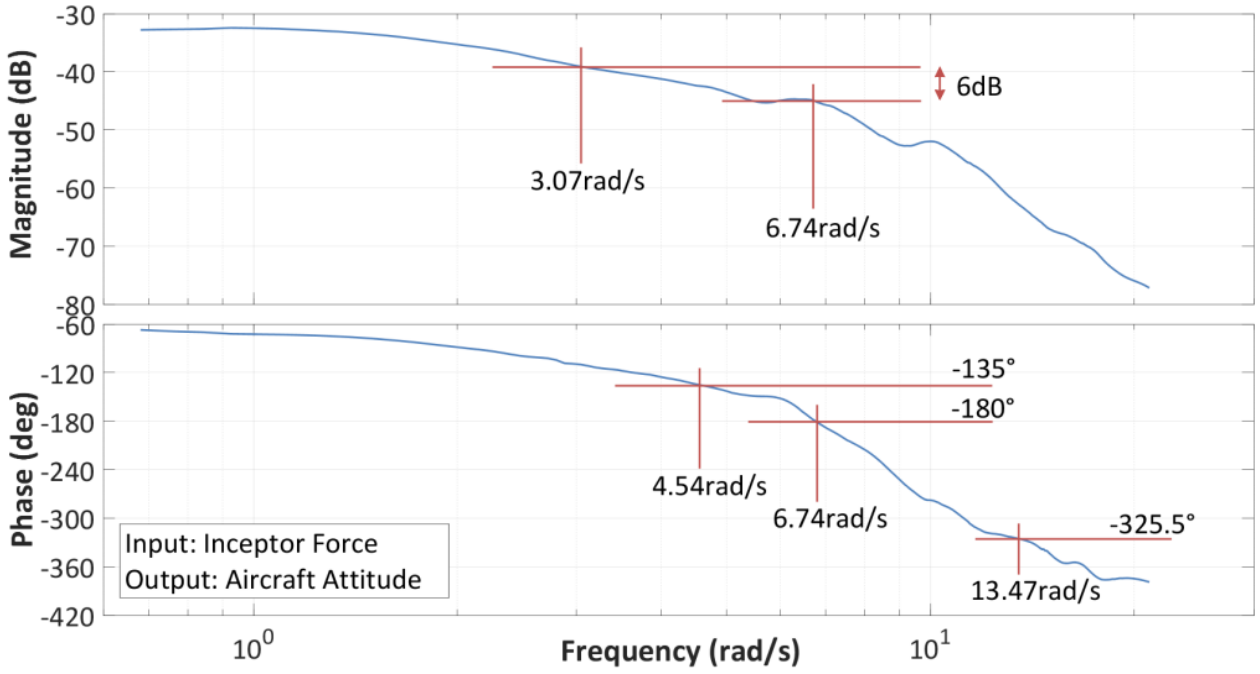

Figure D-14: Bode Plot, Force-Attitude, Attitude Command, Roll Axis, Isometric, Config 1

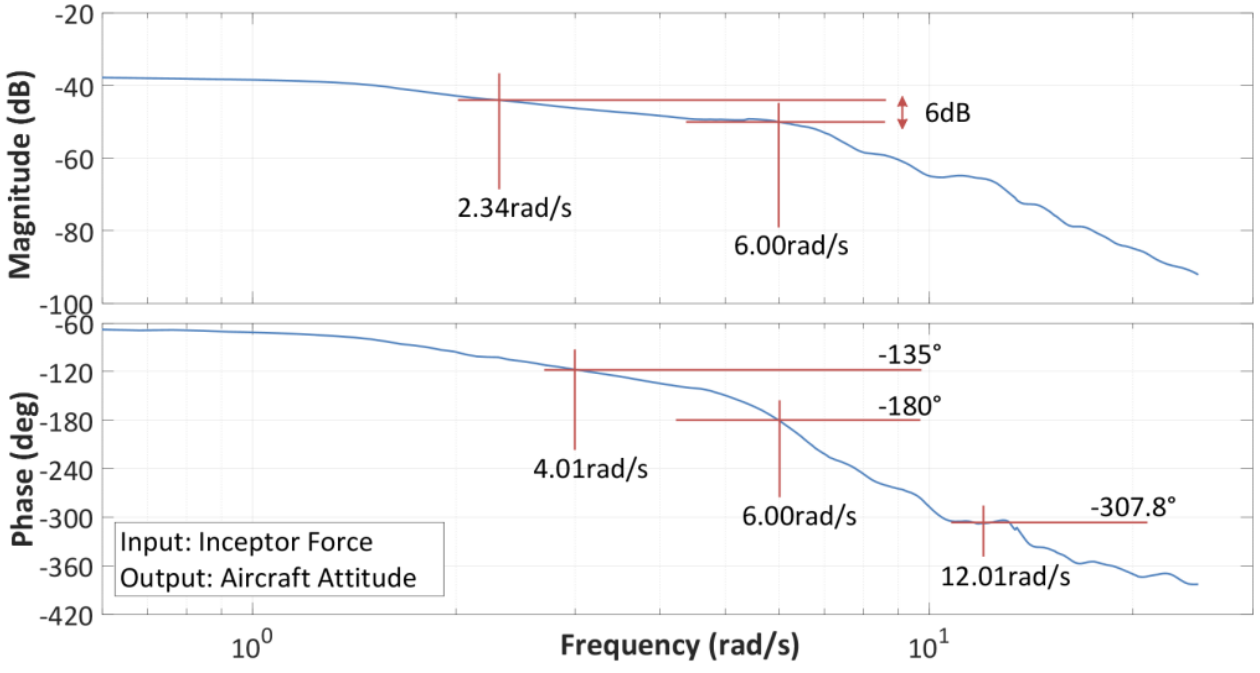

Figure D-15: Bode Plot, Force-Attitude, Attitude Command, Pitch Axis, Isometric, Config 4

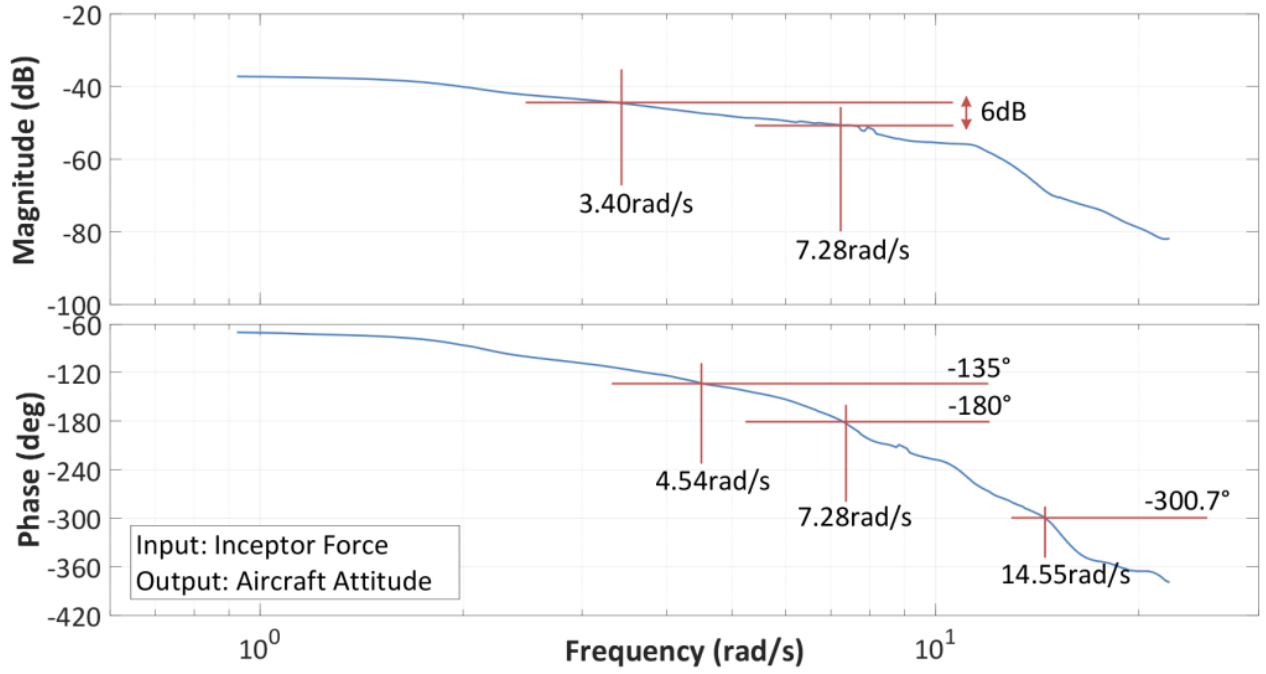

Figure D-16: Bode Plot, Force-Attitude, Attitude Command, Roll Axis, Isometric, Config 4

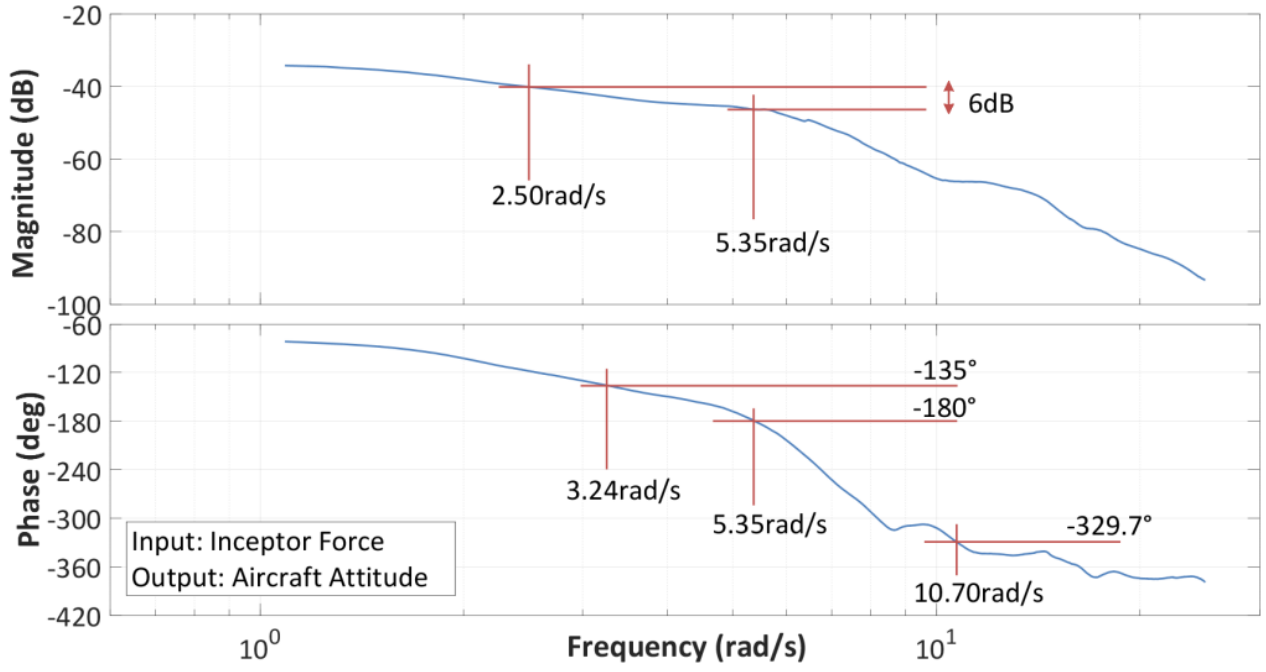

Figure D-17: Bode Plot, Force-Attitude, Attitude Command, Pitch Axis, Isometric, Config 7

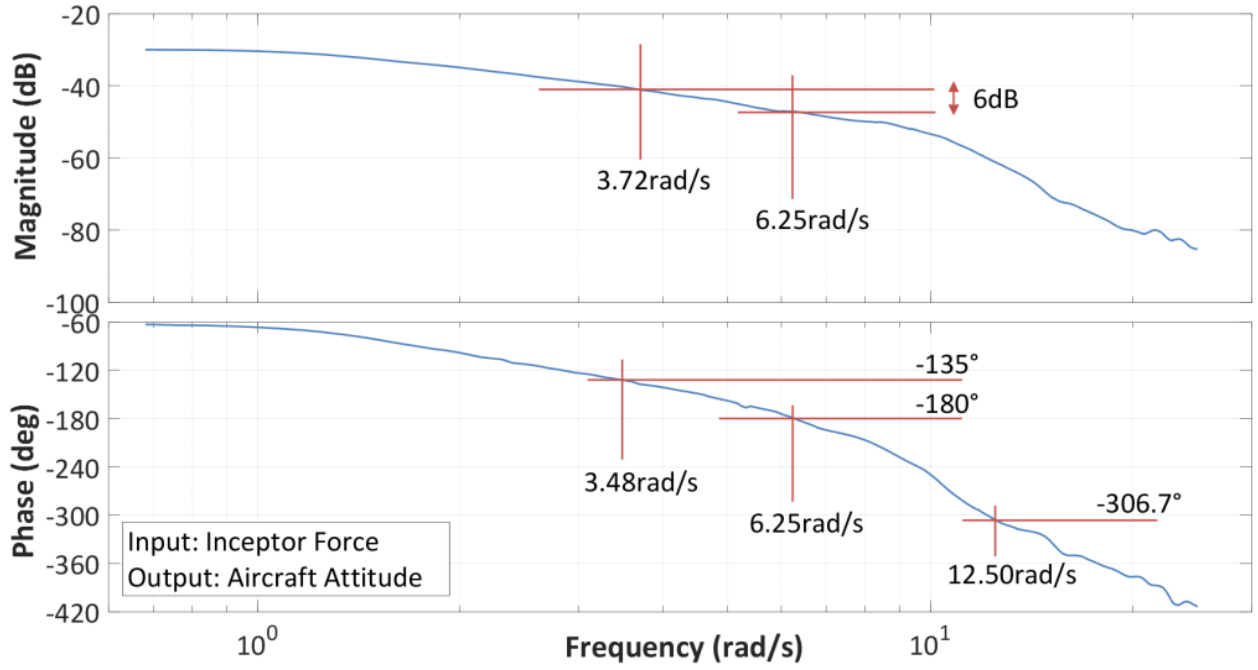

Figure D-18: Bode Plot, Force-Attitude, Attitude Command, Roll Axis, Isometric, Config 7

Appendix E: Phase Aggression Criteria

Direction	Δ Rate	Δδ	H_s	Average H_s		$\Delta F_{\theta 1}$	H_{sF}	Average H_{sF}	
				Pitch	Roll			Pitch	Roll
-	$rads^{-1}$	%	$rads^{-1}\%^{-1}$	$degs^{-1}\%^{-1}$	$degs^{-1}\%^{-1}$	N	$rads^{-1}N^{-1}$	$degs^{-1}N^{-1}$	$degs^{-1}N^{-1}$
Left	0,2760	13,86	0,020			5,744	0,048		
Right	0,2638	8,830	0,030			7,022	0,038		
Left	0,3944	17,27	0,023			7,464	0,053		
Forward	0,1533	8,470	0,018	1,000	1,267	7,049	0,022	1,633	2,451
Aft	0,2466	14,67	0,017			6,992	0,035		
Right	0,1832	10,13	0,018			6,251	0,029		
Left	0,2794	12,69	0,022			6,831	0,041		

Table E-1: H_s and H_{sF} Calculation, Compliant Mode, Rate Command

Direction	Δ Attitude	Δδ	H_s	Average H_s		$\Delta F_{\theta 1}$	H_{sF}	Average H_{sF}	
				Pitch	Roll			Pitch	Roll
-	rad	%	$rad\%^{-1}$	$deg\%^{-1}$	$deg\%^{-1}$	N	$radN^{-1}$	$degN^{-1}$	$degN^{-1}$
Forward	0,1585	6,620	0,024			6,853	0,023		
Aft	0,3471	14,21	0,024			6,880	0,050		
Right	0,2216	10,53	0,021			6,830	0,032		
Left	0,3739	13,77	0,027			6,302	0,059		
Forward	0,3107	14,27	0,022	1,332	1,454	9,494	0,033	2,209	3,069
Aft	0,2276	9,960	0,023			4,750	0,048		
Right	0,2324	8,680	0,027			3,522	0,066		
Left	0,2959	11,15	0,027			5,236	0,057		

Table E-2: H_s and H_{sF} Calculation, Compliant Mode, Attitude Command

Direction	Apparent Gain	Δ Rate	$\Delta F_{\theta 1}$	H_{sF}	H_{sF} / Gain Ratio	Average $H_{sF\ Datum}$	
						Pitch	Roll
-	-	$rads^{-1}$	N	$rads^{-1}N^{-1}$	$rads^{-1}N^{-1}$	$degs^{-1}N^{-1}$	$degs^{-1}N^{-1}$
Forward	1,00	0,211	9,965	0,021	0,021		
Aft	1,00	0,204	11,358	0,018	0,018		
Right	1,00	0,238	5,610	0,042	0,042		
Left	1,00	0,279	9,402	0,030	0,030		
Forward	1,00	0,157	6,514	0,024	0,024		
Aft	1,00	0,220	10,313	0,021	0,021		
Right	1,00	0,137	5,213	0,026	0,026		
Left	1,00	0,286	6,840	0,042	0,042		
Forward	1,20	0,278	9,494	0,029	0,024		
Aft	1,20	0,206	9,427	0,022	0,018		
Right	1,20	0,238	6,481	0,037	0,031		
Left	1,20	0,505	12,374	0,041	0,034		
Forward	1,20	0,341	11,782	0,029	0,024	1,2875	2,0539
Aft	1,20	0,213	9,429	0,023	0,019		
Right	1,20	0,267	6,139	0,043	0,036		
Left	1,20	0,630	12,581	0,050	0,042		
Forward	0,80	0,175	8,961	0,019	0,024		
Aft	0,80	0,199	13,449	0,015	0,018		
Right	0,80	0,209	7,122	0,029	0,037		
Left	0,80	0,222	10,107	0,022	0,027		
Forward	0,80	0,245	11,937	0,020	0,026		
Aft	0,80	0,211	13,409	0,016	0,020		
Right	0,80	0,315	9,4757	0,033	0,042		
Left	0,80	0,394	15,271	0,026	0,032		

Direction	Apparent Gain	Δ Rate	$\Delta F_{\theta 1}$	H_{SF}	H_{SF} / Gain Ratio	Average $H_{SF\ Datum}$	
						Pitch	Roll
-	-	$rads^{-1}$	N	$rads^{-1}N^{-1}$	$rads^{-1}N^{-1}$	$degs^{-1}N^{-1}$	$degs^{-1}N^{-1}$
Forward	0,60	0,281	19,946	0,014	0,023		
Aft	0,60	0,191	17,440	0,011	0,018		
Right	0,60	0,172	10,584	0,016	0,027		
Left	0,60	0,491	19,500	0,025	0,042		
Forward	0,60	0,423	28,975	0,015	0,024		
Aft	0,60	0,251	21,965	0,011	0,019		
Right	0,60	0,283	14,392	0,020	0,033		
Left	0,60	0,452	17,729	0,025	0,042		
Forward	0,40	0,245	24,049	0,010	0,025		
Aft	0,40	0,182	24,015	0,008	0,019		
Right	0,40	0,241	20,701	0,012	0,029		
Left	0,40	0,458	25,972	0,018	0,044		
Forward	0,40	0,322	31,188	0,010	0,026	1,2875	2,0539
Aft	0,40	0,263	29,426	0,009	0,022		
Right	0,40	0,360	26,320	0,014	0,034		
Left	0,40	0,502	35,801	0,014	0,035		
Forward	1,00	0,604	23,393	0,026	0,026		
Aft	1,00	0,345	13,827	0,025	0,025		
Right	1,00	0,286	8,220	0,035	0,035		
Left	1,00	0,450	11,762	0,038	0,038		
Forward	1,00	0,366	14,126	0,026	0,026		
Aft	1,00	0,326	12,210	0,027	0,027		
Right	1,00	0,414	10,935	0,038	0,038		
Left	1,00	0,438	10,336	0,042	0,042		

Table E-3: H_{SF} Calculation, Isometric Mode, Rate Command

Direction	Apparent Gain	Δ Attitude	$\Delta F_{\theta 1}$	H_{sF}	H_{sF} / Gain Ratio	Average $H_{sF\ Datum}$	
						Pitch	Roll
-	-	rad	N	$radN^{-1}$	$radN^{-1}$	$degN^{-1}$	$degN^{-1}$
Forward	1,00	0,357	11,006	0,032	0,032		
Aft	1,00	0,316	11,875	0,027	0,027		
Right	1,00	0,333	8,345	0,040	0,040		
Left	1,00	0,257	7,972	0,032	0,032		
Forward	1,00	0,390	13,051	0,030	0,030		
Aft	1,00	0,291	11,219	0,026	0,026		
Right	1,00	0,338	8,416	0,040	0,040		
Left	1,00	0,461	13,662	0,034	0,034		
Forward	1,20	0,572	15,440	0,037	0,031		
Aft	1,20	0,362	9,078	0,040	0,033		
Right	1,20	0,210	6,379	0,033	0,027		
Left	1,20	0,352	8,738	0,040	0,034		
Forward	1,20	0,273	6,715	0,041	0,034	1,7375	2,0964
Aft	1,20	0,285	7,428	0,038	0,032		
Right	1,20	0,295	5,547	0,053	0,044		
Left	1,20	0,497	10,528	0,047	0,039		
Forward	0,80	0,335	12,175	0,028	0,034		
Aft	0,80	0,205	8,494	0,024	0,030		
Right	0,80	0,267	8,832	0,030	0,038		
Left	0,80	0,312	10,045	0,031	0,039		
Forward	0,80	0,352	15,805	0,022	0,028		
Aft	0,80	0,214	10,677	0,020	0,025		
Right	0,80	0,207	7,002	0,030	0,037		
Left	0,80	0,278	9,261	0,030	0,038		

Direction	Apparent Gain	Δ Attitude	$\Delta F_{\theta 1}$	H_{SF}	H_{SF} / Gain Ratio	Average $H_{SF\ Datum}$	
						Pitch	Roll
-	-	rad	N	$radN^{-1}$	$radN^{-1}$	$degN^{-1}$	$degN^{-1}$
Forward	1,00	0,252	12,633	0,020	0,033		
Aft	1,00	0,183	10,661	0,017	0,029		
Right	1,00	0,186	9,979	0,019	0,031		
Left	1,00	0,327	13,897	0,024	0,039		
Forward	1,00	0,278	14,171	0,020	0,033		
Aft	1,00	0,288	14,728	0,020	0,033		
Right	1,00	0,205	8,798	0,023	0,039		
Left	1,00	0,283	11,542	0,025	0,041		
Forward	1,20	0,203	16,024	0,013	0,032		
Aft	1,20	0,134	14,359	0,009	0,023		
Right	1,20	0,171	11,521	0,015	0,037		
Left	1,20	0,217	18,569	0,012	0,029		
Forward	1,20	0,228	20,061	0,011	0,028	1,7375	2,0964
Aft	1,20	0,232	21,467	0,011	0,027		
Right	1,20	0,238	15,068	0,016	0,039		
Left	1,20	0,256	21,159	0,012	0,030		
Forward	0,80	0,358	10,063	0,036	0,036		
Aft	0,80	0,404	11,572	0,035	0,035		
Right	0,80	0,267	7,444	0,036	0,036		
Left	0,80	0,413	9,982	0,041	0,041		
Forward	0,80	0,304	9,808	0,031	0,031		
Aft	0,80	0,219	8,281	0,026	0,026		
Right	0,80	0,299	7,250	0,041	0,041		
Left	0,80	0,173	5,447	0,032	0,032		

Table E-4: H_{SF} Calculation, Isometric Mode, Attitude Command

Appendix F: Supplementary Data

The raw data of all recorded test points analysed within this thesis are detailed below:

- Validation of PAC Boundaries for Attitude Command
- Isometric Failure Mission Task Element
  - Rate Command (Pilots H, J, K, L)
  - Attitude Command (Pilots H, J, K, L)
  - Influencing factors of APC severity (Pilots H, J, K, L)
- Force Displacement Assessment (Pilots A, B, C, D, E, F, G, H, I)
- Isometric Control Strategy Adaptation (Pilots H, L, M)

Legend / Abbreviations:

- Track: F-Forward; B-Back; L-Left; R-Right; F/R-Forward/Right etc.
- Data Quality: H-High; M-Medium; L-Low
- PAC Severity Detected: N-None; M-Moderate; S-Severe

Serial	Groundspeed (kt)	Subjective Aggression
1	6-10	Standard
2	6-10	High
3	10-14	Low
4	10-14	Standard
5	10-14	High
6	14-18	Low
7	14-18	Standard
8	14-18	High
9	15-20	Low
10	15-20	Standard
11	15-20	High

Table F-1: Test Conditions Investigated, Varying Groundspeed and Aggression, Pilot G

Serial	Failure	Groundspeed (kt)	Stabilisation Time (s)
1	No	15	4
2	No	15	5
3	No	15	8
4	No	15	10
5	No	8	4
6	No	8	5
7	Yes	15	5
8	Yes	15	8
9	Yes	15	10

Table F-2: Conditions Investigated, Varying Groundspeed and Stabilisation Time, Pilot G

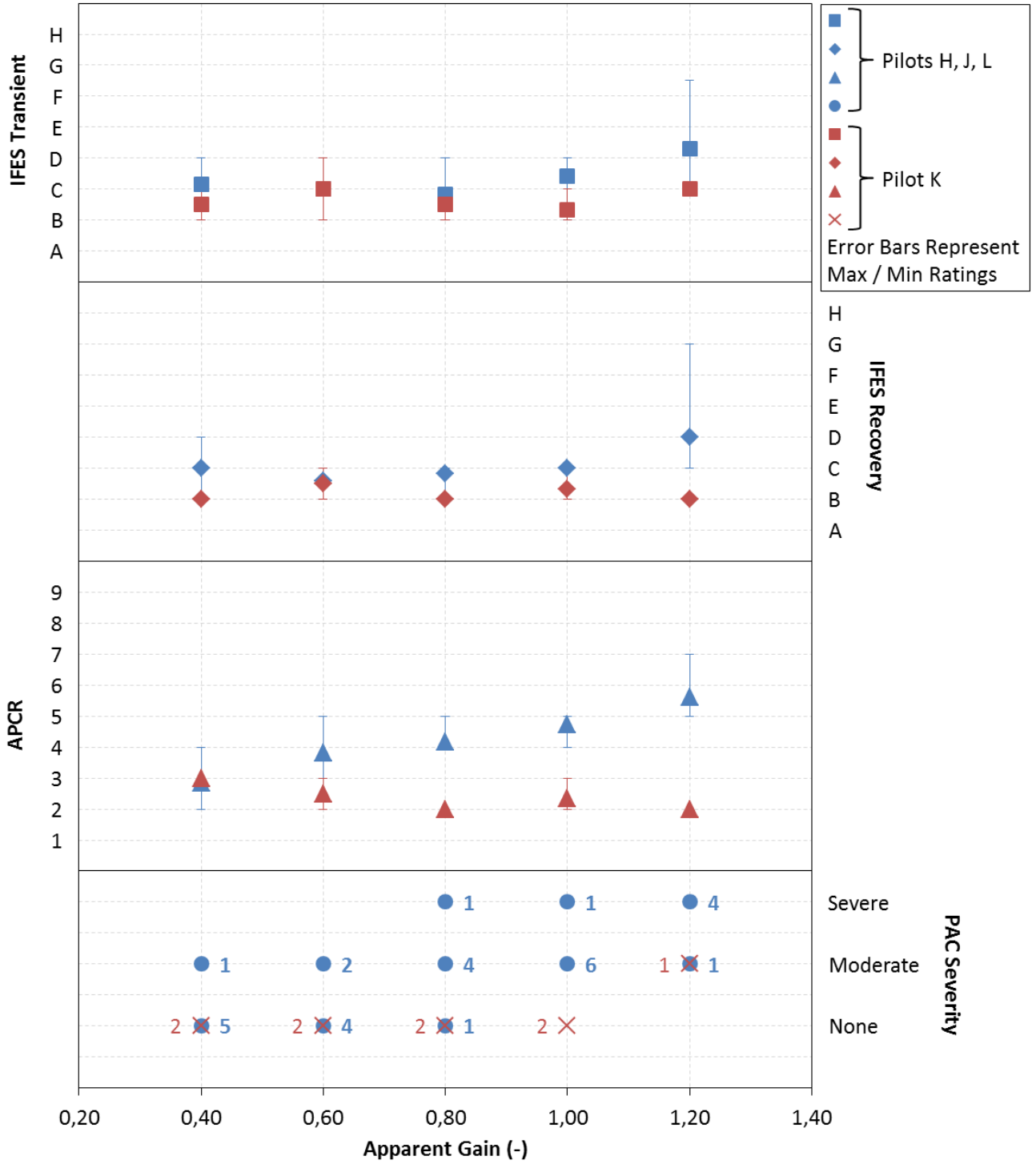

Figure F-1: Effect of IFES Transient and Recovery Ratings, APCR and PAC Severity on the Variation of Apparent Gain in Attitude Command with Pilots H, J, L and K

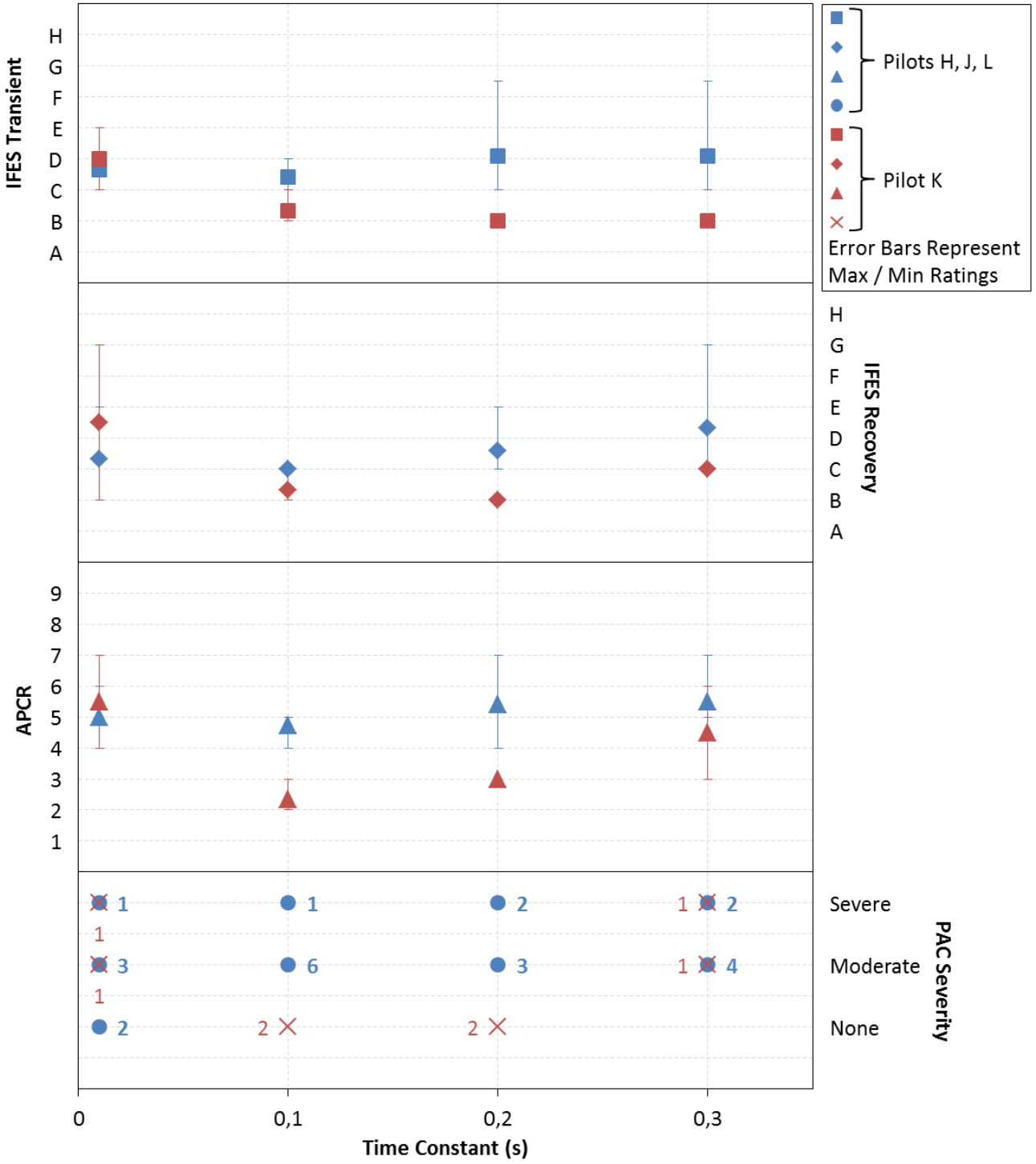

Figure F-2: Effect of IFES Transient and Recovery Ratings, APCR and PAC Severity on the Variation of Time Constant in Attitude Command with Pilots H, J, L and K

Test Point	Test Pilot	APCR	APCR Equivalent Severity	PAC Observed Severity	Conformal Result
51	Pilot L	5	Moderate	Moderate	√
52	Pilot J	6	Severe	Severe	√
	Pilot L	7	Severe	Severe	√
	Pilot H	5	Moderate	Severe	**X**
53	Pilot L	5	Moderate	Moderate	√
	Pilot H	5	Moderate	Severe	**X**
	Pilot K	2	None	Moderate	**X**
54	Pilot J	4	Moderate	Moderate	√
	Pilot L	4	Moderate	Moderate	√
	Pilot H	4	Moderate	Moderate	√
	Pilot K	2	None	None	√
55	Pilot J	4	Moderate	Severe	**X**
	Pilot L	4	Moderate	None	**X**
	Pilot H	5	Moderate	Moderate	√
	Pilot K	2	None	None	√
56	Pilot J	4	Moderate	Moderate	√
	Pilot L	5	Moderate	Moderate	√
	Pilot H	5	Moderate	Moderate	√
	Pilot K	2	None	None	√
57	Pilot J	4	Moderate	Moderate	√
	Pilot L	3	None	None	√
	Pilot K	3	None	None	√
58	Pilot J	4	Moderate	Moderate	√
	Pilot L	3	None	None	√
	Pilot H	5	Moderate	None	**X**
	Pilot K	2	None	None	√
59	Pilot J	4	Moderate	Moderate	√
	Pilot L	3	None	None	√
	Pilot H	2	None	None	√
	Pilot K	3	None	None	√
60	Pilot J	3	None	None	√
	Pilot L	3	None	None	√
	Pilot H	2	None	None	√
	Pilot K	3	None	None	√
61	Pilot J	4	Moderate	Severe	**X**
	Pilot L	5	Moderate	Moderate	√
	Pilot H	5	Moderate	Moderate	√
	Pilot K	3	None	None	√
62	Pilot J	5	Moderate	Moderate	√

	Pilot L	5	Moderate	None	**X**
	Pilot H	5	Moderate	Moderate	√
	Pilot K	7	Severe	Severe	√
63	Pilot J	4	Moderate	Severe	**X**
	Pilot L	6	Severe	Moderate	**X**
	Pilot H	5	Moderate	None	**X**
	Pilot K	4	Moderate	Moderate	√
64	Pilot J	6	Severe	Severe	√
	Pilot L	7	Severe	Severe	√
	Pilot H	5	Moderate	Moderate	√
	Pilot K	3	None	None	√
65	Pilot J	4	Moderate	Moderate	√
	Pilot H	5	Moderate	Moderate	√
	Pilot K	3	None	None	√
66	Pilot J	6	Severe	Severe	√
	Pilot L	5	Moderate	Moderate	√
	Pilot H	5	Moderate	Moderate	√
	Pilot K	3	None	None	√
67	Pilot J	7	Severe	Severe	√
	Pilot L	5	Moderate	Moderate	√
	Pilot H	5	Moderate	Moderate	√
	Pilot K	3	None	Moderate	**X**
68	Pilot J	6	Severe	Severe	√
	Pilot L	5	Moderate	Moderate	√
	Pilot H	5	Moderate	Moderate	√
	Pilot K	6	Severe	Severe	√
69	Pilot H	5	Moderate	None	**X**
70	Pilot H	5	Moderate	Moderate	√
71	Pilot H	5	Moderate	None	**X**
72	Pilot H	5	Moderate	Moderate	√
73	Pilot H	5	Moderate	Moderate	√
74	Pilot H	5	Moderate	Moderate	√
75	Pilot H	5	Moderate	Moderate	√

Total	72	N	M	S	N	M	S	80.6%
		20	42	10	24	34	14	

Table F-3: Validation of PAC Boundaries for Attitude Command

Test Point	Ramp Atten.	Apparent Gain	Time Constant	Track	Data Quality	IFES		APCR		Longitudinal PAC		
						Trans.	Rec.	Rating	Descriptor	Mean Phase	Mean Aggression	Severity Detected
-	/s	-	s	-	-	-	-	-	-	°	°/s²	-
1	Nil	1,00	0,1	F	M	D	D	5	B	137,83	14,40	M
2	Nil	1,20	0,1	F	H	F	F	7	C	69,43	24,91	S
3	Nil	1,20	0,1	F/R	H	F	F	7	D	67,41	34,48	S
4	Nil	0,80	0,1	R	M	D	D	6	B	94,03	21,87	M
5	Nil	0,80	0,1	F/R	H	E	D	6	C	162,46	13,88	M
6	Nil	1,00	0,1	F/R	H	D	E	6	B	88,09	19,75	M
7	Nil	0,60	0,1	R	H	C	C	5	A	85,85	12,27	N
8	Nil	0,60	0,1	F/R	M	E	E	5	B	128,04	7,73	N
9	Nil	0,40	0,1	F/R	M	E	D	5	A	52,49	4,56	N
10	Nil	0,40	0,1	R	M	F	G	3	-	71,33	12,30	N
11	Nil	1,00	0,1	F/R	M	D	C	5	B	85,33	22,36	S
12	Nil	0,97	0,01	F	H	D	D	5	B	91,27	21,45	M
13	Nil	0,97	0,01	F/R	M	D	D	5	B	56,85	30,80	S
14	Nil	1,08	0,2	R	M	F	F	7	C	89,92	24,32	S
15	Nil	1,08	0,2	F/R	M	E	E	6	B	86,77	23,74	S
16	Nil	1,00	0,1	F/R	M	D	C	5	B	74,96	21,95	S
17	Nil	1,21	0,3	F/R	M	F	F	7	D	253,87	17,54	M
18	Nil	1,21	0,3	F	H	H	G	8	D	96,73	35,32	S
19	0,8	1,00	0,1	R	M	E	E	6	B	80,19	31,84	S
20	0,8	1,00	0,1	F/R	M	E	E	6	B	228,88	33,41	S
21	Nil	1,00	0,1	-	-	-	-	-	-	-	-	-
22	0,4	1,00	0,1	R	M	F	F	7	D	57,74	19,23	M
23	0,4	1,00	0,1	F/R	H	F	E	6	B	116,01	24,79	M
24	0,27	1,00	0,1	F/R	M	F	E	6	B	94,06	25,26	S
25	0,27	1,00	0,1	F	M	F	E	6	B	-	-	-

Table F-4: Isometric Failure MTE; With Failure; Rate Command; Pilot H

Test Point	Ramp Atten.	Apparent Gain	Time Constant	Track	Data Quality	IFES		APCR		Longitudinal PAC		
						Trans.	Rec.	Rating	Descriptor	Mean Phase	Mean Aggression	Severity Detected
-	/s	-	s	-	-	-	-	-	-	°	°/s²	-
1	Nil	1,00	0,1	F/R	M	G	F	6	C	79,91	33,63	S
2	Nil	1,20	0,1	F/R	L	G	H	7	E	91,59	80,30	S
3	Nil	1,20	0,1	F	L	H	H	8	E	93,34	85,89	S
4	Nil	0,80	0,1	L	M	E	E	5	B	95,51	24,38	S
5	Nil	0,80	0,1	F/R	M	E	D	4	B	87,95	37,33	S
6	Nil	1,00	0,1	F/R	M	G	F	8	E	359,66	56,82	S
7	Nil	0,60	0,1	F/R	M	E	C	5	B	182,40	33,90	S
8	Nil	0,60	0,1	R	L	G	G	5	B	113,51	10,81	S
9	Nil	0,40	0,1	F/R	M	G	G	3	B	94,89	46,04	M
10	Nil	0,40	0,1	F	L	H	H	9	E	141,82	10,58	N
11	Nil	1,00	0,1	L	M	F	F	6	C	110,22	8,19	M
12	Nil	0,97	0,01	F/R	M	G	F	5	C	92,33	53,23	S
13	Nil	0,97	0,01	L	M	G	G	8	E	122,76	82,00	S
14	Nil	1,08	0,2	F/R	M	H	H	8	E	88,38	111,13	S
15	Nil	1,08	0,2	F	L	H	H	9	E	60,72	109,45	S
16	Nil	1,00	0,1	R	-	-	-	-	-	230,10	37,96	S
17	Nil	1,21	0,3	F/R	M	F	F	5	B	88,25	31,31	S
18	Nil	1,21	0,3	B/L	M	G	F	5	B	67,78	48,34	S
19	0,8	1,00	0,1	F/R	M	F	F	6	C	98,57	58,97	S
20	0,8	1,00	0,1	L	M	H	H	8	E	99,83	24,59	S
21	Nil	1,00	0,1	F/L	-	-	-	-	-	149,36	37,12	S

Table F-5: Isometric Failure MTE; With Failure; Rate Command; Pilot J

Test Point	Ramp Atten.	Apparent Gain	Time Constant	Track	Data Quality	IFES		APCR		Longitudinal PAC		
						Trans.	Rec.	Rating	Descriptor	Mean Phase	Mean Aggression	Severity Detected
-	/s	-	s	-	-	-	-	-	-	°	°/s²	-
1	Nil	1,00	0,1	F/R	H	C	D	3	-	249,97	15,68	S
2	Nil	1,20	0,1	F/R	H	C	C	2	-	72,20	20,06	S
3	Nil	1,20	0,1	F	H	C	D	3	-	144,63	21,87	S
4	Nil	0,80	0,1	L	H	D	D	3	-	53,53	11,97	N
5	Nil	0,80	0,1	F/R	H	C	D	3	-	97,51	14,05	M
6	Nil	1,00	0,1	F	H	C	D	3	-	86,98	12,65	N
7	Nil	0,60	0,1	F/R	H	C	D	3	-	-	-	-
8	Nil	0,60	0,1	F	H	C	C	2	-	91,52	9,44	N
9	Nil	0,40	0,1	F/R	H	C	C	2	-	87,80	6,21	N
10	Nil	0,40	0,1	R	H	C	C	2	-	359,69	3,95	N
11	Nil	1,00	0,1	F	H	C	C	2	-	102,82	19,29	M
12	Nil	0,97	0,01	L	H	C	C	2	-	23,80	12,17	N
13	Nil	0,97	0,01	F/R	H	B	C	2	-	69,27	9,90	N
14	Nil	1,08	0,2	R	H	B	C	2	-	103,29	13,54	M
15	Nil	1,08	0,2	F/R	H	B	C	2	-	142,43	13,69	M
16	Nil	1,00	0,1	-	-	-	-	-	-	-	-	-
17	Nil	1,21	0,3	R	H	D	D	3	-	193,34	17,11	S
18	Nil	1,21	0,3	F	H	D	C	2	-	102,40	26,48	S
19	0,8	1,00	0,1	R	H	B	C	2	-	166,83	10,44	N
20	0,8	1,00	0,1	F/R	H	B	C	2	-	315,68	23,08	M
21	Nil	1,00	0,1	F/R	H	C	C	2	-	124,05	13,39	M
22	0,4	1,00	0,1	F	L	C	F	7	A	159,36	21,41	M
23	0,4	1,00	0,1	F/R	H	C	C	2	-	138,60	13,23	M
24	0,27	1,00	0,1	F/R	H	C	C	2	-	96,95	17,18	S
25	0,27	1,00	0,1	F	H	E	C	6	B	148,06	21,58	N

Test Point	Ramp Atten.	Apparent Gain	Time Constant	Track	Data Quality	IFES		APCR		Longitudinal PAC		
						Trans.	Rec.	Rating	Descriptor	Mean Phase	Mean Aggression	Severity Detected
-	/s	-	s	-	-	-	-	-	-	°	°/s²	-
26	Nil	1,00	0,1	F	M	E	D	3	-	102,55	13,03	M
27	Nil	1,16	0,01	F/R	M	C	D	3	-	112,72	21,99	S
28	Nil	1,16	0,01	F	H	D	D	2	-	113,84	15,85	S
29	Nil	0,59	0,01	F	H	C	D	3	-	111,43	9,13	M
30	Nil	0,59	0,01	L	H	C	D	3	-	42,73	19,95	N
31	Nil	1,00	0,1	-	-	-	-	-	-	-	-	-
32	Nil	0,65	0,2	F/R	H	C	D	3	-	55,58	7,09	M
33	Nil	0,65	0,2	F	H	C	D	3	-	81,05	12,98	M
34	Nil	1,30	0,2	F	H	C	D	3	-	168,48	21,68	S
35	Nil	1,30	0,2	F/R	H	C	D	3	-	115,78	28,37	S
44	Nil	1,21	0,4	F	H	B	C	2	-	205,93	15,86	S

Table F-6: Isometric Failure MTE; With Failure; Rate Command; Pilot K

Test Point	Ramp Atten.	Apparent Gain	Time Constant	Track	Data Quality	IFES		APCR		Longitudinal PAC		
						Trans.	Rec.	Rating	Descriptor	Mean Phase	Mean Aggression	Severity Detected
-	/s	-	s	-	-	-	-	-	-	°	°/s²	-
1	Nil	1,00	0,1	R	M	D	D	5	C	271,68	12,63	N
2	Nil	1,20	0,1	F/R	M	E	E	6	D	79,78	30,12	S
3	Nil	1,20	0,1	F	M	E	D	6	C	63,30	13,98	M
4	Nil	0,80	0,1	R	H	B	A	1	-	77,51	4,47	N
5	Nil	0,80	0,1	F/R	H	C	B	4	A	106,43	6,79	N
6	Nil	1,00	0,1	F	M	C	C	5	A	82,80	11,20	M
7	Nil	0,60	0,1	F	M	B	A	2	-	91,41	4,28	N
8	Nil	0,60	0,1	F/R	M	C	C	-	-	63,11	6,84	N
9	Nil	0,40	0,1	F	M	A	B	1	-	159,00	3,58	N
10	Nil	0,40	0,1	F/R	H	B	B	2	-	55,50	2,57	N
11	Nil	1,00	0,1	R	M	C	C	5	A	93,30	24,91	S
12	Nil	0,97	0,01	F	M	E	E	7	D	74,21	28,25	M
13	Nil	0,97	0,01	F/R	M	E	D	6	C	58,36	22,59	M
14	Nil	1,08	0,2	F	M	D	D	5	B	161,78	16,16	M
15	Nil	1,08	0,2	F/R	M	D	C	5	A	80,13	13,28	M
16	Nil	1,00	0,1	R	M	D	C	5	B	188,64	27,37	S
17	Nil	1,21	0,3	R	M	E	D	6	D	83,30	34,20	S
18	Nil	1,21	0,3	F/R	M	D	D	5	C	100,56	28,56	S
19	0,8	1,00	0,1	F	M	C	D	5	C	92,02	20,50	S
20	0,8	1,00	0,1	F/R	H	D	D	5	C	214,55	15,91	M
21	Nil	1,00	0,1	F/R	-	-	-	-	-	87,11	10,66	N
22	0,4	1,00	0,1	F	M	D	C	5	B	79,76	22,05	S
23	0,4	1,00	0,1	F/R	M	E	E	7	D	93,78	27,65	S
24	0,27	1,00	0,1	R	M	D	D	5	C	87,01	9,73	M
25	0,27	1,00	0,1	F/R	M	C	C	5	B	96,79	21,07	S

Table F-7: Isometric Failure MTE; With Failure; Rate Command; Pilot L

Test Point	Ramp Atten.	Apparent Gain	Time Constant	Track	Data Quality	IFES		APCR		Longitudinal PAC		
						Trans.	Rec.	Rating	Descriptor	Mean Phase	Mean Aggression	Severity Detected
-	/s	-	s	-	-	-	-	-	-	°	°/s²	-
51	Nil	1,00	0,1	F/R	L	F	F	5	B	62,44	36,35	M
52	Nil	1,20	0,1	F	M	C	C	5	A	84,60	51,49	S
53	Nil	1,20	0,1	F/R	H	C	C	5	A	89,55	24,94	S
54	Nil	0,80	0,1	R	M	B	C	4	A	143,47	16,24	M
55	Nil	0,80	0,1	F/R	H	C	C	5	A	198,80	17,37	M
56	Nil	1,00	0,1	R	H	D	C	5	B	99,03	26,14	M
57	Nil	0,60	0,1	F	L	B	C	4	A	65,83	5,70	N
58	Nil	0,60	0,1	F/R	H	C	C	5	A	49,27	15,02	N
59	Nil	0,40	0,1	F	M	C	C	2	-	189,29	4,39	N
60	Nil	0,40	0,1	F/R	H	C	C	2	-	48,98	4,45	N
61	Nil	1,00	0,1	R	H	C	C	5	A	76,60	18,08	M
62	Nil	0,97	0,01	F	H	C	D	5	A	91,72	23,30	M
63	Nil	0,97	0,01	F/R	H	C	C	5	B	96,98	9,42	N
64	Nil	1,08	0,2	F	H	C	C	5	B	61,72	17,98	M
65	Nil	1,08	0,2	F/R	H	C	C	5	B	176,96	17,62	M
66	Nil	1,00	0,1	R	H	C	C	5	A	58,73	21,48	M
67	Nil	1,21	0,3	R	H	C	D	5	A	80,25	34,25	M
68	Nil	1,21	0,3	F/R	H	C	D	5	A	58,04	30,56	M
69	0,8	1,00	0,1	F	M	C	C	5	A	60,68	12,52	N
70	0,8	1,00	0,1	F/R	H	C	C	5	A	94,72	14,60	M
71	Nil	1,00	0,1	R	-	-	-	5	-	80,58	13,80	N
72	0,4	1,00	0,1	R	H	C	C	5	A	64,05	20,45	M
73	0,4	1,00	0,1	F/R	M	C	C	5	A	97,82	19,26	M
74	0,27	1,00	0,1	R	H	C	D	5	B	285,88	40,63	M
75	0,27	1,00	0,1	F/R	M	D	D	5	B	77,47	28,55	M

Table F-8: Isometric Failure MTE; With Failure; Attitude Command; Pilot H

Test Point	Ramp Atten.	Apparent Gain	Time Constant	Track	Data Quality	IFES		APCR		Longitudinal PAC		
						Trans.	Rec.	Rating	Descriptor	Mean Phase	Mean Aggression	Severity Detected
-	/s	-	s	-	-	-	-	-	-	°	°/s²	-
51	Nil	1,00	0,1	F/R	L	E	D	5	B	165,79	40,68	S
52	Nil	1,20	0,1	F/R	M	E	C	6	B	77,28	48,89	S
53	Nil	1,20	0,1	F	L	H	H	9	E	67,56	96,12	S
54	Nil	0,80	0,1	F/R	H	D	C	4	B	70,04	32,80	M
55	Nil	0,80	0,1	R	H	D	C	4	B	68,03	29,18	S
56	Nil	1,00	0,1	F/R	H	D	C	4	B	76,89	29,17	M
57	Nil	0,60	0,1	F/R	H	D	C	4	B	82,14	12,01	M
58	Nil	0,60	0,1	F	H	D	B	4	A	191,6	17,53	M
59	Nil	0,40	0,1	F/R	H	D	B	4	A	187,58	10,31	M
60	Nil	0,40	0,1	R	H	C	C	3	-	58,84	8,38	N
61	Nil	1,00	0,1	F/R	H	D	C	4	B	81,31	27,28	S
62	Nil	0,97	0,01	R	M	D	C	5	B	117,52	17,93	M
63	Nil	0,97	0,01	F/R	H	D	C	4	B	70,41	23,49	S
64	Nil	1,08	0,2	F/R	H	E	D	6	B	70,08	34,30	S
65	Nil	1,08	0,2	R	H	C	C	4	B	101,03	17,53	M
66	Nil	1,00	0,1	F	-	-	-	6	B	68,33	36,34	S
67	Nil	1,21	0,3	F/R	M	G	G	7	E	96,30	39,98	S
68	Nil	1,21	0,3	R	M	E	E	6	C	83,89	34,72	S

Table F-9: Isometric Failure MTE; With Failure; Attitude Command; Pilot J

Test Point	Ramp Atten.	Apparent Gain	Time Constant	Track	Data Quality	IFES		APCR		Longitudinal PAC		
						Trans.	Rec.	Rating	Descriptor	Mean Phase	Mean Aggression	Severity Detected
-	/s	-	s	-	-	-	-	-	-	°	°/s²	-
51	Nil	1,00	0,1	F/R	H	C	C	2	-	-	-	-
52	Nil	1,20	0,1	R	L	B	B	2	-	104,48	8,92	N
53	Nil	1,20	0,1	F/R	H	C	B	2	-	31,64	19,37	M
54	Nil	0,80	0,1	R	H	C	B	2	-	128,01	10,06	N
55	Nil	0,80	0,1	F/R	H	B	B	2	-	118,75	12,92	N
56	Nil	1,00	0,1	F/R	H	B	B	2	-	16,99	9,57	N
57	Nil	0,60	0,1	F	H	D	C	3	-	193,18	12,10	N
58	Nil	0,60	0,1	F/R	H	B	B	2	-	161,91	5,70	N
59	Nil	0,40	0,1	F	H	C	B	3	-	91,90	6,15	N
60	Nil	0,40	0,1	F/R	H	B	B	3	-	83,90	4,43	N
61	Nil	1,00	0,1	F	M	B	B	3	-	86,88	10,71	N
62	Nil	0,97	0,01	F	H	E	G	7	A	96,20	37,53	S
63	Nil	0,97	0,01	F/R	M	C	B	4	A	110,40	23,60	M
64	Nil	1,08	0,2	F/R	H	B	B	3	-	67,63	8,68	N
65	Nil	1,08	0,2	F	M	B	B	3	-	106,34	14,13	N
66	Nil	1,00	0,1	F/R	-	-	-	3	-	189,10	12,31	N
67	Nil	1,21	0,3	R	H	B	C	3	-	57,97	26,02	M
68	Nil	1,21	0,3	F	H	B	C	6	C	91,23	32,79	S

Table F-10: Isometric Failure MTE; With Failure; Attitude Command; Pilot K

Test Point	Ramp Atten.	Apparent Gain	Time Constant	Track	Data Quality	IFES		APCR		Longitudinal PAC		
						Trans.	Rec.	Rating	Descriptor	Mean Phase	Mean Aggression	Severity Detected
-	/s	-	s	-	-	-	-	-	-	°	°/s²	-
51	Nil	1,00	0,1	R	M	B	C	5	A	20,32	12,59	M
52	Nil	1,20	0,1	F	M	F	G	7	D	80,59	61,01	S
53	Nil	1,20	0,1	R	H	D	D	5	B	70,99	25,51	M
54	Nil	0,80	0,1	F/R	H	B	C	4	A	105,38	21,29	M
55	Nil	0,80	0,1	F	M	B	B	4	A	138,48	10,23	N
56	Nil	1,00	0,1	F/R	H	C	C	5	A	81,21	17,04	M
57	Nil	0,60	0,1	R	H	B	B	3	-	52,99	5,82	N
58	Nil	0,60	0,1	F/R	M	B	C	3	-	39,89	13,93	N
59	Nil	0,40	0,1	R	H	D	D	3	-	63,32	7,40	N
60	Nil	0,40	0,1	F	M	B	C	3	-	133,20	8,83	N
61	Nil	1,00	0,1	F/R	H	D	C	5	B	66,68	17,38	M
62	Nil	0,97	0,01	R	M	D	B	5	B	251,32	8,81	N
63	Nil	0,97	0,01	F/R	M	D	E	6	C	170,92	39,93	M
64	Nil	1,08	0,2	R	H	F	E	7	D	52,24	25,52	S
65	Nil	1,08	0,2	F/R	L	F	F	7	D	88,07	26,57	S
66	Nil	1,00	0,1	L	M	D	D	5	B	85,08	11,65	M
67	Nil	1,21	0,3	R	H	C	C	5	B	62,97	15,44	M
68	Nil	1,21	0,3	R	M	D	C	5	C	217,93	28,03	M
69	0,8	1,00	0,1	R	H	C	C	5	B	-	-	-
70	0,8	1,00	0,1	F/R	M	D	C	5	B	-	-	-
71	Nil	1,00	0,1	F	-	-	-	-	-	-	-	-
72	0,4	1,00	0,1	F	M	B	B	4	A	-	-	-
73	0,4	1,00	0,1	F/R	H	B	B	3	-	-	-	-
74	0,27	1,00	0,1	R	M	D	C	5	A	-	-	-
75	0,27	1,00	0,1	F/R	M	D	C	5	B	-	-	-

Table F-11: Isometric Failure MTE; With Failure; Attitude Command; Pilot L

Pilot		Control Force / displacement magnitude at moment of failure	Post-failure required pilot gain	Timing of Failure	Attitude / attitude rate at moment of failure	Visual references	Pre-failure required pilot gain	Cyclic control force / displacement direction from trim at moment of failure
Pilot G	Rating	5	4	4	4	1	1	2
	Rank	1	2	3	4	6	7	5
Pilot H	Rating	5	5	5	5	4	3	3
	Rank	1	4	2	3	5	7	6
Pilot J	Rating	3	3	4	4	4	4	1
	Rank	6	5	3	1	2	4	7
Pilot K	Rating	5	5	4	3	5	3	4
	Rank	1	3	5	6	2	7	4
Pilot L	Rating	5	5	3	2	3	4	3
	Rank	2	1	7	4	6	3	5

Table F-12: Influencing factors of APC severity caused by Isometric Failure; Pilots: G, H, J, K